

Mechanosensory and Sphingolipid Mediators of Inflammatory Signaling in Placental
Dysfunction
by
Yuliya Fakhr

A thesis submitted in partial fulfillment of the requirements for the degree of

Doctor of Philosophy

Medical Sciences - Obstetrics & Gynecology

University of Alberta

© Yuliya Fakhr, 2022

Abstract

Preeclampsia (PE) is a leading cause of maternal and fetal morbidity. Placental dysfunction plays a key role in PE and includes decreased syncytialization and increased inflammation and cell death. Tumor Necrosis Factor alpha (TNF- α) is a key factor in inducing this dysfunction. The controversy in using TNF- α inhibitors during pregnancy highlights the importance of identifying downstream mediators of its signaling. I investigated sphingolipids and mechanosensory mediators as potential targets. In other tissues, TNF- α signals via sphingosine kinase 1 (SphK1), a sphingosine 1-phosphate (S1P) synthesizing enzyme. TNF- α also intersects with S1P signaling by upregulating S1PR2 in other tissues. SphK1 hinders ST formation, and S1PR2 increases cell death and placental inflammation. Whether this occurs downstream of TNF- α signaling is unclear. Piezo1, a mechanosensory channel, regulates epithelial cell function via S1P. Other mechanosensory channels play a role in increasing both syncytialization and cell death. The role of Piezo1 in the placenta and the syncytium and its relationships to TNF- α and S1P remain unknown. I hypothesized that TNF- α will induce placental dysfunction by altering SphK1, S1PR2, and Piezo1 levels and activity.

The first study investigated levels of SphK1 in placental biopsies from normal pregnancies and PE and the S1P regulatory enzyme levels in response to TNF- α in cultured human villous explants and primary human trophoblasts. Placental SphK1 was increased in PE. Only S1P phosphatase 1 increased at the end of the syncytial regeneration in explants, regardless of TNF- α treatment, suggesting a role for S1P degradation at the end of syncytialization. The expression of SphK1 in trophoblasts was increased in response to TNF- α , suggesting that elevated TNF- α in PE can upregulate SphK1 in trophoblasts but other factors are involved in SphK1 upregulation at the placental level.

Next, I examined the syncytialization, cell death and syncytial shedding, and the release of inflammatory cytokines and growth factors from villous explants that were treated with TNF- α and/or the SphK1 inhibitor, PF-543. Increased cell death, shedding, interferon- α 2, IFN- γ -induced protein 10, fibroblast growth factor-2, and platelet-derived growth factor-AA release induced by TNF- α were reversed upon SphK1 inhibition. TNF- α also decreased IL-10 release, and inhibiting SphK1 reversed this effect. Inhibiting SphK1 alone decreased TNF- α release. Hence, inhibiting SphK1 can partially reverse the TNF- α -induced PE phenotype of the placenta.

The third study investigated placental levels of S1PRs in placental biopsies from women with PE and in response to TNF- α in villous explants, in primary human trophoblasts, and in a choriocarcinoma cell line, BeWo. Placental S1PR1 remained unchanged in PE and in primary trophoblasts and BeWo cells in response to TNF- α . However, TNF- α muted the surge of S1PR1 at the end of the re-syncytialization phase in explants. Since S1PR1 signaling is generally protective, this suggests that TNF- α could induce its disruptive effect by decreasing placental S1PR1. Placental S1PR2 was higher PE, and S1PR2 was increased in primary trophoblasts treated with TNF- α but was decreased in treated BeWo cells. S1PR2 and S1PR3 increased in response to TNF- α at the end of explant re-syncytialization. Hence, BeWo cells are not an appropriate model to study S1PRs. Since S1PR2 activity also decreased cell death and human placental lactogen, a marker for syncytial mass, high placental expression of S1PR2 in PE may be induced by TNF- α , and this increase in S1PR2 could be protective against TNF- α -induced placental damage.

Finally, I examined the role of Piezo1 on syncytialization, cell death, and the release of inflammatory cytokines and growth factors from cultured villous explants using Yoda1, a Piezo1

pharmacological agonist. Piezo1 interaction with TNF- α and SphK1 was also examined. Piezo1 activation increased syncytial endocrine function but at higher concentrations also increased cell damage, inflammatory cytokine, and growth factor release. Piezo1 increased TNF- α and TNF- α increased Piezo1, but co-treating with Yoda1 and TNF- α decreased syncytialization. Piezo1 increased syncytial placental alkaline phosphatase release via SphK1. Placental Piezo1 expression was higher in PE. This showed that low Piezo1 expression and activity induced syncytialization via SphK1, whereas, high levels of expression and activity, found in PE, induced placental damage via TNF- α .

This work shows the association between TNF- α , SphK1, S1PR2, and Piezo1 signaling and expression patterns in physiological placental functions and dysfunction. This provides the groundwork for sphingolipid and mechanosensory pharmaceutical targets to be investigated in lieu of TNF- α inhibitors.

Preface

This thesis is an original work by Yuliya Fakhr. The study was conducted in accordance with the Declaration of Helsinki and approved by the Health Research Ethics Board Biomedical at the University of Alberta (Pro00034274, first approved 15 November 2012, continuously approved since then with the latest one-year renewal approved 2 January 2022). Informed consent was obtained from all subjects who provided placentas and de-identified patient characteristics in the study. All data are reported as results in this thesis. Data will be shared by reasonable requests made to the corresponding author.

Components of Chapter 1 have been published as:

Fakhr Y, Brindley DN, Hemmings DG. Physiological and pathological functions of sphingolipids in pregnancy. *Cellular Signalling*. 2021 Sep 1;85:110041.

Components of Chapters 3 and 4 have been published as:

Fakhr Y, Koshti S, Habibyan YB, Webster K, Hemmings DG. Tumor Necrosis Factor- α Induces a Preeclamptic-like Phenotype in Placental Villi via Sphingosine Kinase 1 Activation. *International Journal of Molecular Sciences*. 2022 Mar 29;23(7):3750.

Acknowledgements

My Ph.D. degree has been one of the most developmental experiences for me as a thinker and as a person overall. I want to thank my supervisor, Denise Hemmings, for everything she has taught me over the last years. She has given me all the techniques, the writing skills, data analysis, presentation skills, good habits, and life outlook to be able to be the scientist and person I am today. I am so appreciative of her strong values, teamwork, patience, and endless support. I would also like to thank my committee members, Sandy Davidge, Meghan Riddell, and Venu Jain, for their advisement, encouragement, patience, and genuine support throughout my degree. Likewise, I thank my other examining committee members as well for taking the time to evaluate my work and participate in my defense. Furthermore, I would also like to thank every member of the Obstetrics and Gynecology Department for their friendship and mentorship. Not only that, but I would like to thank all my mentees, my peer reviewers, my advisors, and my lab members who have made my experience so meaningful and pleasant. I would like to thank all the undergraduate students I worked with over the years for teaching me what it takes to be a good mentor.

I want to thank my family without whom this experience would not be possible. My parents, Tanios Fakhr and Olena Burdyak, have been instrumental in getting me to this point. Thank you for all driving to afterschool education and for constantly believing in my abilities. My brother, Daniel Fakhr, was so emotionally supportive and kind and willing to take my midnight stress calls. I would like to thank my grandma, Raissa Makagon, for her constant curiosity and interest in my research project.

To my YEG friends who have become my new family, thank you so much. They have given me support that I will never be able to repay. I would like to especially thank Siju

Varghese and Carla Sosa Alvarado for their generosity and endless support. I would like to thank Austin Krausert for teaching my Microsoft Word skills and helping me with formatting.

I am also extremely grateful for all the funding that made my research possible. Thank you to the Faculty of Medicine and Dentistry (75th Anniversary Graduate Studentship, Medical Science Graduate Student Award) and the Faculty of Graduate Studies (Thesis Completion Award, Doctoral Recruitment Scholarship), the Maternal and Child Health Program, CIHR, and Women and Children's Health Research Institute. I would like to thank Donna Dawson, Maya Henriquez, the hospital delivery room staff, and the Women and Children's Health Research Institute staff at the Royal Alexandra Hospital and at the University of Alberta.

Table of Contents

1.	Introduction	1
1.1.	Overview	2
1.2.	Preeclampsia Overview	3
1.2.1.	General Characteristics of Preeclampsia	3
1.2.2.	The Placenta in PE	12
1.3.	TNF-α in Pregnancy	15
1.3.1.	TNF- α Signaling.....	15
1.3.2.	TNF- α Ligand and Receptor Expression in the Placenta	19
1.4.	S1P in Placenta	20
1.4.1.	S1P Metabolism in Pregnancy Physiology and PE.....	20
1.4.1.1.	Sphingomyelin and Ceramides	20
1.4.1.2.	S1P and its Regulatory Enzymes	23
1.4.1.2.1.	Sphingosine Kinases.....	27
1.4.1.2.2.	S1P Lyase	29
1.4.1.2.3.	S1P Phosphatases and Lipid Phosphate Phosphatases	30
1.4.2.	S1P Receptors in Physiology and PE	33
1.4.3.	S1P and Placental Development and Function	38
1.4.3.1.	Sphingolipids and Extravillous Trophoblasts	38
1.4.3.2.	S1P, CERs, and Villous Trophoblasts	41
1.4.3.3.	S1P, CERs, and Placental Vasculature	44
1.5.	Piezo1 in the Placenta	48

1.6.	Synthesis and Rationale.....	52
1.7.	Aims, Hypothesis, Significance:.....	53
2.	Chapter 2: Material and Methods	57
2.1.	General Methods.....	58
2.1.1.	Placenta Samples	58
2.1.2.	Placental Explant Culture	58
2.1.3.	Immunohistochemistry of Placental Biopsy Sections.....	61
2.1.4.	Placental Tissue RNA Isolation	62
2.1.5.	Quantitative PCR	63
2.1.6.	BCA Protein Assay	64
2.1.7.	Lactate Dehydrogenase (LDH) Quantification.....	65
2.1.8.	Quantification of the Beta-Subunit of Human Chorionic Gonadotropin (β -hCG)	65
2.1.9.	Quantification of Human Placental Lactogen (hPL)	66
2.1.10.	Quantification of Human Placental Alkaline Phosphatase Activity (PLAP) ..	66
2.1.11.	Quantification of Cytokines.....	67
2.1.12.	Statistics and Analysis	69
2.2.	Chapter 3 Specific Methods	69
2.2.1.	Treatments and Experimental Protocols	69
2.2.2.	Trophoblast Multinucleation and E-cadherin Staining	70
2.3.	Chapter 4 Specific Methods	71

2.3.1. Explant Treatments	71
2.3.2. Primary Trophoblast Isolation	71
2.3.3. Experimental Protocol Used for Plating Primary Cultured Trophoblasts	72
2.4. Chapter 5 Specific Methods	73
2.4.1. BeWo Cell Culture.....	73
2.4.2. Explant Treatments	74
2.4.3. Western Blots.....	74
2.4.4. Primary Cultured Trophoblasts Staining for S1PR1/2.....	75
2.5. Chapter 6 Specific Methods	76
2.5.1. Treatment of Villous Explants	76
2.5.2. Statistics and Analysis	76
3. Chapter 3: TNF-α Regulation of Sphingosine 1-Phosphate Regulatory Enzymes	
in the Placenta	77
3.1. Introduction.....	78
3.2. Results	81
3.2.1. SphK1 Expression in Placentas from Normal and PE Pregnancies.....	81
3.2.2. Experimental Villous Explant Model of Syncytial Self-Regeneration.....	83
3.2.3. Expression of S1P Synthesizing Enzymes in Villous Explants.....	84
3.2.4. Expression of S1P Catabolic Enzymes in Villous Explants	85
3.2.5. Expression of SphK1 in Primary Human Trophoblasts.....	86
3.3. Discussion	105

4.	Chapter 4: Tumor Necrosis Factor-α Induces a Preeclamptic-like Phenotype in Placental Villi via Sphingosine Kinase 1 Activation	113
4.1.	Introduction.....	114
4.2.	Results	116
4.2.1.	Effect of TNF- α on ST Regeneration and its Interaction with SphK1	116
4.2.2.	Effect of TNF- α on Placental Cytokine and Factor Release and its Dependence on SphK1 Activity	118
4.2.3.	PF-543 Dose Response in Villous Explants	120
4.3.	Discussion	136
5.	Chapter 5: S1P Receptors in Placental Physiology and Pathology.....	145
5.1.	Introduction.....	146
5.2.	Results	148
5.2.1.	S1P and Placental ST Function.....	148
5.2.2.	S1PR2 and Placental ST Function	148
5.2.3.	Placental S1PR Expression in PE	149
5.2.4.	S1PR Expression in BeWo Cells	150
5.2.5.	S1PR Expression in Primary Human Cytotrophoblasts.....	151
5.2.6.	S1PR Expression in Regenerating Villous Explants	151
5.2	Discussion	163
6.	Chapter 6: Piezo1 Activation Induces Syncytial Function and Cytokine Release in Human Term Placental Chorionic Explants	169
6.1.	Introduction.....	170

6.2.	Results	172
6.2.1.	Higher Levels of Piezo1 in Placental Biopsies from Women with PE.....	172
6.2.2.	Pharmacologically Activating Piezo1 with Yoda1 Increased Markers of ST Function 173	
6.2.3.	Pharmacologically Activating Piezo1 with Higher Concentrations of Yoda1 Increased Placental Cell Damage and Release of Inflammatory Cytokines and Growth Factors 174	
6.2.4.	Piezo1 and TNF- α Signaling Intersection in the Placenta	175
6.2.5.	Piezo1 and Sphk1 Signaling Intersection in the Placenta.....	175
6.3.	Discussion	192
7.	Chapter 7: General Discussion and Future Directions.....	199
7.1.	Proposed Model and Mechanisms of Placental Function	200
7.1.1.	ST Endocrine Function	200
7.1.2.	Cell Membrane Damage and ST Shedding.....	201
7.1.3.	Cytokine and Growth Release	201
7.2.	Summary and Relevance to PE	202
7.3.	Experimental Model Strengths and Limitations.....	206
7.4.	Future Directions	208
7.5.	Conclusions.....	213
Appendices.....		273
Appendix A.....		274

Appendix B 277

List of Figures

Figure 1.1: Structure and Organization of the Human Placenta	14
Figure 1.2: Sphk1 and S1P Act as Co-Factors for TNFR1 Signaling	18
Figure 1.3: Known Components of the S1P Metabolic and Signaling Pathway	26
Figure 1.4: General S1PR G-protein Coupling and Functions	37
Figure 1.5: Known Pathways of S1P and CER Signaling in Placental Function	47
Figure 1.6: Structure of Piezo1	51
Figure 2.1A-D: Structure and Organization of a Dissected Villous Explant.....	60
Figure 2.2: Placement of Villous Explants in the Insert Well	60
Figure 3.1: Sphk1 Expression was Higher in Placental Biopsies from Women with Preeclampsia (PE).....	90
Figure 3.2: Syncytial Shedding in Villous Explants was Maximal After 4 Days of Incubation	92
Figure 3.3: HPRT1 is Not Altered with Treatment or Time in Explants or in Biopsies from Women with PE.....	94
Figure 3.4: Sphk1 mRNA Expression is Constant from 0-48 Hours and is Not Significantly Affected by TNF- α in Term Villous Explants	96
Figure 3.5: SGPP1 mRNA Expression Increases in Term Villous Explants After 48 Hours of Re- Syncytialization Even After TNF- α Treatment	98
Figure 3.6: S1P Lyase (SGPL1) mRNA Expression is Constant from 0-48 Hours and is Not Affected by TNF- α in Term Villous Explants	100
Figure 3.7: LPP3 mRNA Expression is Constant from 0-48 Hours and is Not Significantly Affected by TNF- α in Term Villous Explants	102

Figure 3.8: Cultured Primary Trophoblasts Collected Via a Negative Selection Column were Sufficiently Pure from Vimentin-Positive Cells.....	103
Figure 3.9: TNF- α Treatment for 24 hrs Increased Sphk1 Protein Expression in Cultured Primary Trophoblasts from 1 to 20 Ng/MI.....	104
Figure 4.1: TNF- α Decreases β -hCG Release from Cultured Primary Trophoblasts Without Affecting Their Viability	121
Figure 4.2: Resyncytialization in Term Placental Villous Explants from Normal Pregnancies Decreased in Response to TNF- α and Sphk1 Inhibition Independently.....	123
Figure 4.3: 1 ng/mL of TNF α with or without 1 μ M PF-543 Treatment did not Affect β -hCG or LDH Release into Supernatants	124
Figure 4.4: Inhibiting SphK1 with PF-543 Diminished TNF- α Effects on LDH Release and PLAP-Positive Shed Particles but not on β -hCG Secretion at 48 Hours.....	127
Figure 4.5: Inhibiting SphK1 with PF-543 Diminished TNF- α Effects on the Release of IFN α 2 and IP-10.....	128
Figure 4.6: Inhibiting SphK1 with PF-543 Diminished TNF- α Effects on the Release of FGF2, PDGF-AA, and IL-10	131
Figure 4.7: Inhibiting SphK1 with PF-543 and/or TNF- α Treatment did not Affect the Release of Some Cytokines, Factors, or Chemokines	133
Figure 4.8: Inhibition of SphK1 Decreased Release of TNF- α	134
Figure 4.9: SphK1 Inhibition with PF-543 Increased β -hCG Secretion After 48 Hours	135
Figure 5.1: S1P Treatment Increases Secretion of β -hCG at 48 Hours but not LDH or hPL	153

Figure 5.2: Inhibiting S1PR2 with JTE-013 Treatment Increases LDH and Beta-Human Chorionic Gonadotropin (β -hCG) Secretion at 48 Hours but Decreases Human Placental Lactogen (hPL) Release	154
Figure 5.3: S1PR2 Protein Expression is Higher in Whole Placental Biopsies from Mothers with PE Compared to Placental Biopsies from Mothers with Normal Pregnancies.....	157
Figure 5.4: TNF- α Decreases S1PR2 Expression in BeWo cells without Affecting S1PR1 Expression.....	159
Figure 5.5: TNF- α Increases S1PR2 Expression in Cultured Primary Trophoblasts without Affecting S1PR1 Expression	160
Figure 5.6: S1PR1 mRNA Expression Decreases Whereas S1PR2 and S1PR3 Expression Increase After 48 Hours of TNF- α Treatment in Term Chorionic Explants.....	162
Figure 6.1: Piezo1 Levels but not mRNA Levels were Higher in Placental Biopsies from Women with PE.....	179
Figure 6.2: Yoda1 Significantly Increased Markers of Syncytial Function	181
Figure 6.3: Pharmacologically Activating Piezo1 Significantly Increased Placental Cell Membrane Damage	182
Figure 6.4: Release Of Inflammatory Cytokines and Growth Factors from Villous Explants Treated with Yoda1 for 48 Hours was Increased.....	184
Figure 6.5: Inflammatory Cytokines and Growth Factors from Villous Explants Treated with Yoda1 for 48 Hours for Which There were No Changes	186
Figure 6.6: Activation of Piezo1 Elevated TNF- α , Which in Turn Upregulated Piezo1 Transcription After 3 Hours.....	187

Figure 6.7: Pharmacologically Activating Piezo1 in the Presence of TNF- α Decreased β -hCG Release 188

Figure 6.8 Inhibiting SphK1 Decreases the Effect of Yoda1 on PLAP Activity but not β -hCG or LDH Release..... 190

Figure 7.1: Signaling Intersections Between TNF- α , SphK1, Piezo1, and S1PRs in Placentas of Women with PE 202

List of Tables

Table 1.1: Summary of the Levels of Sphingolipids, Their Metabolizing and Catabolizing Enzymes, and Their Receptors Across Normal Gestation and PE	33
Table 2.1: Primer Sequences.....	64
Table 2.2: Human Cytokine/Chemokine 42-Plex Discover Array Analytes Measured in Supernatants of Cultured Explants.....	69
Table 3.1: Table of Characteristics of Sample Donors	88
Table 5.1: Table of Characteristics of Sample Donors	155
Table 6.1: Pregnancy Characteristics.....	177

ABBREVIATIONS

ABCG2	ATP-binding cassette transporter G2
AC	Adenylyl cyclase
ACER(s)	Alkaline ceramidase(s)
Akt	Protein kinase B
cAMP	Cyclic adenosine monophosphate
CER(s)	Ceramide(s)
cIAP(s)	Cellular inhibitor of apoptosis proteins
CT(s)	Cytotrophoblast(s)
ddH ₂ O	Double-distilled water
DMEM	Dulbecco's modified eagle medium
DMSO	Dimethyl sulphoxide
dNK	Decidual natural killer cells
EGF	Epidermal growth factor
ERK	Extracellular-signal-regulated kinase
EVT	Extravillous trophoblasts
FADD	Fas-associated DD protein
FBS	Fetal bovine serum
FCS	Fetal calf serum
FGF-2	Fibroblast growth factor-2
Flt-3L	Fms-Related Tyrosine Kinase 3 Ligand
GCM-1	Glial cells missing-1
G-CSF	Granulocyte Colony-Stimulating Factor

GM-CSF	Granulocyte-Macrophage Colony-Stimulating Factor
GRO- α	Growth Regulated Oncogene alpha
hCG	Human chorionic gonadotropin
HDL(s)	High density lipoprotein(s)
hPL	Human placental lactogen
HPRT1	Hypoxanthine-guanine phosphoribosyl transferase
HUVEC	Human umbilical vein endothelial cells
IFN(s)	Interferon(s)
IL(s)	Interleukin(s)
IL-1RA	Interleukin Receptor Antagonist
IMDM	Iscove's modified dulbecco's medium
IP-10	Interferon gamma-induced protein 10
ITS	Insulin-transferrin-sodium selenite
IUGR	Intrauterine growth restriction
LDH	Lactate dehydrogenase
LHr(s)	Luteinizing hormone receptors
LPP(s)	Lipid Phosphate Phosphatase(s)
LPS	Lipopolysaccharide
MCP	Monocyte Chemotactic Protein
MDC	Macrophage-Derived Chemokine
MFSD2B	Major facilitator superfamily transporter 2b
MIP	Macrophage Inflammatory Protein
NF- κ B	Nuclear factor kappa B

PBS	Phosphate buffered saline
PCR	Polymerase chain reaction
PDGF	Platelet-Derived Growth Factor
PE	Preeclampsia
PI3K	Phosphatidylinositol 3-kinase
PKC	Protein kinase C
PLAP	Placental alkaline phosphatase
PLC	Phospholipase C
PIGF	Placental growth factor
RANTES	Regulated on Activation, Normal T cell Expressed and Secreted
Ras	Rat sarcoma viral oncogene
RIPK1	Serine/threonine receptor interacting protein kinase 1
ROCK	Rho-associated kinases
sCD40L	Soluble Cluster of Differentiation 40 Ligand
S1P	Sphingosine 1-Phosphate
S1PR(s)	S1P Receptor(s)
SD	Standard deviation
SEM	Standard error mean
sENG	Soluble endoglin
sFlt	Soluble fms-like tyrosine kinase 1
SGPL1	Sphingosine 1-Phosphate Lyase
SGPP(s)	Sphingosine 1-Phosphate Phosphatase(s)
SODD	Silencer of death domain

SphK(s)	Sphingosine Kinase(s)
SPNS2	Protein spinster homolog 2
ST	Syncytiotrophoblast/Syncytium
TGF- β	Transforming Growth Factor beta
TGF β R	Transforming Growth Factor beta Receptor
TNF- α	Tumour necrosis factor alpha
TNFR(s)	Tumour necrosis factor alpha receptors
TRADD	TNF- α receptor-associated death domain
TRAF2	TNF- α receptor-associated factor 2
TRPV	Transient receptor potential villanoid family
VEGF	Vascular Endothelial Growth Factor A

1. Introduction

Part of this section is published in Fakhr Y, Brindley DN, Hemmings DG. Physiological and pathological functions of sphingolipids in pregnancy. Cellular Signalling. 2021 Sep 1;85:110041

1.1. Overview

Preeclampsia (PE) affects 5-8% of mothers. PE is a pregnancy disorder characterized by high blood pressure and end-organ damage. The disorder leads to 76,000 maternal and 500,000 annual deaths globally and increases the rate of preterm and low birth weight neonates (1, 2). The cause of PE remains elusive, albeit the placenta plays a major role in its initiation and progression. The placenta in PE is characterized by poor development of the syncytium, high levels of syncytial shedding and cell damage, and high levels of maternal circulating inflammatory cytokines (3). Pro-inflammatory cytokines are notorious for disrupting placental function, notably tumor necrosis factor- α (TNF- α) (4). One of the mediators of TNF- α signaling in non-placental endothelial and epithelial cells, is sphingosine kinase 1 (SphK1), the main producer of sphingosine 1-phosphate (S1P) (5-8). S1P is a bioactive sphingolipid that regulates various cellular processes by binding to one of its five S1P receptors (S1PR1-5) (9). High levels of SphK1 activity and S1P inhibit syncytialization (10). Although the individual roles that TNF- α , SphK1, and S1P play in the pathogenesis of PE have been studied, we do not know whether they interact in the placenta. Given the importance of both TNF- α and S1P on placental function and pregnancy outcomes, it is essential to understand the interaction between TNF- α and SphK1, the main producer of extracellular S1P, in the placenta. It is also important to understand the interaction between TNF- α and S1PR2, whose activation generally leads to inflammation and cell death in non-placental tissue.

Piezo1 is a mechanosensory channel that when activated can induce pro-inflammatory pathways in a variety of cell types (11, 12). Piezo1 expression also increases in response to inflammatory cytokines (11). However, little is known about whether Piezo1 signaling interweaves with TNF- α signaling or about the placental role of Piezo1 in general. Recently,

Piezo1 was shown to signal via SphK1 in epithelial cells from non-placental tissue. Whether this occurs in the placenta is unknown.

This chapter will provide the current understanding in these areas and the knowledge gaps that are important to address. I will begin with a background review of PE and the placental dysfunction observed in PE (1.2). This is then followed by the role of TNF- α in placental function and PE (1.3), the role of sphingolipids in placental signaling and PE (1.4), and the role of Piezo1 in other tissues (1.5). My current knowledge of the associations between TNF- α , S1P, and Piezo1 is discussed (1.6). Finally, the end of the chapter concludes with a summary of the rationale that leads to the thesis aims, the hypotheses, and the significance of the research (1.7)

1.2. Preeclampsia Overview

1.2.1. General Characteristics of Preeclampsia

Preeclampsia (PE) is the leading cause of maternal death, morbidity, intensive care admissions, and premature birth (SOGC, 2014). It is manifested by the new onset of high blood pressure, end-organ damage, and edema after the 20th week of gestation (13, 14). PE is the cause of 76,000 maternal and 500,000 annual deaths globally (1, 2). Maternal PE symptoms can progress to dysfunctions in vital organs, blood clotting abnormalities, seizures, and death in extreme cases (13). PE poses a major threat to fetal health because blood flow through the placenta to the fetus is compromised, which often leads to intrauterine growth restriction (IUGR) (15), premature birth (16), and fetal death in extreme cases (17). Developing PE also predisposes both the mother and the infant to chronic complications later in life. Mothers who experience PE are also at increased risk of chronic cardiovascular disorders in later life (18). These women are 3.7 times more likely to develop hypertension within 14.1 years, 2.16 times more likely to

develop ischemic heart disease in 11.7 years, and 1.81 times more likely to experience a stroke in 10.4 years (19). On the other hand, fetuses exposed to an unfavorable intrauterine environment, low in oxygen and nutrients, created by PE are at a significantly higher risk of developing Type 2 diabetes in adult life (20).

PE is currently classified into two subtypes with different proposed etiologies: early-onset and late-onset PE. Although no definitive consensus exists on distinguishing early-onset versus late-onset PE, this is generally determined based on gestational age. Most experts define early-onset PE as PE occurring at a time when the fetus is preterm, earlier than 37 weeks of gestation, or at a time when the fetus is premature, occurring earlier than 34 weeks of gestation (21). Early-onset PE is often linked to poor placental development due to insufficient spiral artery remodeling, described in 1.2.2, resulting in poor placental perfusion. Late-onset PE, often considered the less severe form of PE (22), is thought to occur due to maternal predisposing factors, with little evidence of placental stress. The dichotomous etiologies, however, are debatable since recent evidence shows the presence of maternal factors, syncytial stress, anti-angiogenic factors, and pro-inflammatory cytokine release in both subtypes of PE (21).

Several maternal factors predispose the mother to develop PE. For instance, nulliparity is a risk factor, with the risk for the development of PE decreasing from 4.1% in the first pregnancy to 1.7% in the second pregnancy (23). A multiple gestation pregnancy increases the risk from 1.8% in singleton pregnancies to 9.3% in multiple pregnancies (24). Additionally, women with a family history of chronic hypertension are 2.3 times more likely to develop PE (25). Metabolic disorders such as obesity increase the risk of PE by 3 fold (26). A previous history of PE increases the risk of PE in subsequent pregnancies. The risk for developing PE in the second pregnancy is 14.7% in women who experienced PE in their first pregnancy as opposed to a 1.1%

risk for women with no previous history of PE. This risk increases to 31.9% for women in their third pregnancy with a history of PE in both of their previous pregnancies compared to 1.1% risk of PE in mothers in their 3rd pregnancy with no history of PE (23). Women of advanced maternal age above 35 years old have a higher risk of development of PE (9.4%) as compared to younger women (6.4%) (27). Preexisting diabetes mellitus as well as gestational diabetes mellitus both increase the risk of developing PE, with a relative risk of 3.56 (28) and an odds ratio of 1.29, respectively (29). Reports also suggest a dose-dependent relationship between maternal body mass index and the development of PE. In fact, maternal obesity is highly associated with the development of PE, with an odds ratio of 2.93 (30).

PE typically develops in two stages (31, 32). The first stage manifests in the first trimester of pregnancy due to poor spiral artery remodeling. The second stage manifests after the second trimester of pregnancy as a maternal syndrome characterized by an imbalance between angiogenic and antiangiogenic factors (31, 32). Animal models and human studies have demonstrated uteroplacental ischemia, induced by poor spiral artery remodeling, as a principal driver of the hypertensive and end-organ damage phenotype observed in the mothers.

To better understand the role of the placenta in the development and progression of PE, it is important to get familiarized with the role of the placenta as a whole and the different cell types that contribute to its specific functions. In pregnancy, the mother, the placenta, and the fetus all contribute important factors for the optimum growth of the fetus and the ultimate success of the pregnancy. The placenta is often ignored, but the roles it plays are essential. The placenta is a fetal-derived organ that develops during pregnancy to act as the interface between the maternal and fetal circulations. It metabolizes carbohydrates, lipids, and proteins and transports these metabolites into the fetal circulation. It provides the fetus with water, oxygen, and nutrients. The

placenta is also responsible for transferring waste products and carbon dioxide from the fetus into the maternal circulation, to be excreted by the mother. Hormones and other mediators secreted by the placenta contribute to supporting and maintaining the pregnancy. Other critical functions include providing a protective barrier against pathogens and defending the allogeneic fetus against maternal immune rejection (33).

The placenta is a complex organ with numerous cell types that interact with each other and are part of each other's signaling cascades (Figure 1.1). It is composed of endothelial and vascular smooth muscle cells that are involved in the transport of blood and contribute to the regulation of placental vascular tone (34). Fibroblasts produce structural components and regulate cell processes like angiogenesis (35, 36). Moreover, fetal macrophages, more specifically Hofbauer cells, are functionally polarized M2-like cells that reside in the placenta. These cells promote angiogenesis and vasculogenesis and thus support placental development (37); whereas, maternal macrophages outside the placenta can be on the M1 and M2 continuum and induce a myriad of cellular responses (38), summarized in the following review (39). A unique and key cell type only found in the placenta is the stem-like cytotrophoblast (CT) that can differentiate into two major cell lineages: extravillous trophoblasts (EVTs) or villous CTs.

EVTs migrate and invade into the maternal decidua to anchor the placenta into the uterine wall and to remodel uterine spiral arteries to establish a fetal-maternal blood flow (40). These trophoblasts are mainly important during the early stages of pregnancy when the placenta is embedding into the maternal decidua. The differentiation of CTs into EVTs occurs in the early first trimester of pregnancy, and the initial stages of differentiation are stimulated by hypoxia-inducible factor, whose expression is induced in the presence of a physiologically hypoxic (normoxic for this process) cell microenvironment (41). Hypoxia also induces the expression of

Notch1, a key regulator of CT differentiation into the EVT lineage. Notch1 represses CT proliferation, inhibits the differentiation into a ST, and favors the cell survival and the proliferative capacity of EVTs (42). In later stages of EVT differentiation, EVTs migrate distally in villi, thereby losing their proliferative capacity, modifying their cytoskeletal organization, losing epithelial cell markers, and beginning to express some mesenchymal markers (43). As EVTs differentiate further, they start acquiring a vascular phenotype, evidenced by their expression of vascular markers such as VE-cadherin and platelet endothelial cell adhesion molecule (44). In the late stages of EVT signaling, Wnt signaling is turned on to further induce EVT maturation and motility (45).

CTs also differentiate into villous trophoblasts. These cells fuse, by a process called syncytialization, to form the ST, a multinucleated barrier that protects the fetus and also controls the bidirectional transport between the separate circulatory systems of the mother and fetus (46). The syncytium transports nutrients, water, amino acids, glucose, vitamins, minerals, and antibodies from the mother to the fetus (47, 48). The syncytium is also the major producer of placental hormones such as human chorionic gonadotropin (hCG) hormone, human placental lactogen (hPL), and placental growth factor (PlGF) (46, 49). PlGF (discussed in later paragraphs), hPL, and hCG have critical roles in pregnancy maintenance.

During the first trimester, a hyperglycosylated isoform of hCG, hCG-H is produced by EVTs (50, 51). During the first trimester, low levels of hCG-H are produced by EVTs in PE(52). hCG-H exerts its effects by binding to TGF- β receptors (TGF β R) or luteinizing hormone receptors (LHr). hCG-H binds TGF β Rs on endothelial cells to promote angiogenesis in the uterus and in the placenta (53). hCG-H also binds TGF β R and LHrs on EVTs, thereby signaling

in an autocrine manner. This signaling induces the invasive capacity of EVT_s and promotes their survival (50).

Regular or normally glycosylated hCG, is produced by the ST, and exerts its effects by binding LHr in various cell types. Similar to the low levels of hCG-H found in PE, low levels of hCG are also found in term pregnancies complicated with PE (54). hCG binds LHr in corpus luteum cells to induce the production of progesterone during the first 4 weeks of pregnancy when progesterone production is dependent on the corpus luteum (55). hCG also plays a key role in maintaining pregnancy by inducing myometrial quiescence (56). Similar to hCG-H, ST-produced hCG also promotes uterine and placental angiogenesis and binds LHrs on EVT_s to promote their invasion and survival (55).

hPL is a placental hormone secreted by the ST with growth hormone-like properties. hPL is detectable in maternal circulation after 20-40 days of gestation (57). The ST produces hPL at a constantly increasing rate throughout pregnancy to 34 weeks, after which its production plateaus. This deems it an attractive proxy for assessing placental and ST mass throughout the different stages of gestation (58, 59). However, hPL is undetectable in the fetal circulation, suggesting that its role is to facilitate placental growth and to support fetal nutrient uptake. Indeed, a role for hPL was identified in mobilizing fatty acids in maternal circulation and in decreasing maternal breakdown of glucose and protein usage, thereby increasing the availability of amino acids ready for placental uptake (60).

Underlying progenitor villous CT_s contribute to the continuous turnover of the ST layer, similar to the regeneration process found in other epithelial barriers (61). The ST is formed when underlying CT_s proliferate, differentiate, and fuse into the basal side of the ST. The physiological hypoxic uterine environment and low levels of reactive oxygen species stimulate

CT differentiation via cyclic adenosine monophosphate (cAMP) and glial cells missing-1 (GCM-1), a transcription factor (62, 63). GCM-1 induces the transcription of the fusogenic proteins, Syncytin-1 and Syncytin-2, which are the key regulators of CT cell-cell fusion (64). The roles of Syncytin-1 in syncytialization are better understood than that of Syncytin-2. Syncytin-1 increases the expression of cell-cycle regulators including cyclin dependent kinase 4, transcription factor E2F1, and c-myc, leading to increased CT proliferation (65). As the CT fuses into its overlying ST layer, expression of E-cadherin, an epithelial adherens junction protein, is downregulated in CT and ST to accompany the fusion event. Syncytin-1 also functions as an inhibitor of trophoblast apoptosis (66).

As the ST matures, clustering of nuclei in the ST forms syncytial knots, which are shed into the placental circulation while undergoing apoptosis (67). This apoptotic pathway is mainly regulated by calpain-1, which cleaves apoptotic inducer factor. The cleaved factor is translocated into the mitochondria where it initiates the caspase-dependent apoptotic pathway (68). The mature ST also releases microparticles and extracellular vesicles, rich in soluble fms-like tyrosine kinase 1 (sFlt) and soluble endoglin (sEng) (69-71). Recent reports might suggest, however, that extracellular vesicles act as cargo for sEng but not sFlt (72), suggesting that sFlt might be directly released into the maternal circulation.

Reports from human studies suggest up to a 50% reduction in uteroplacental blood flow in patients with PE, and an even higher reduction of flow in those with severe PE (73). Animal models support poor placental perfusion as the origin of the maternal syndrome since physically constricting uterine arteries on gestational day 14 in the mouse model often results in hypertension and the occurrence of proteinuria (74). The poor perfusion mouse model also highlights the subsequent increase in circulating antiangiogenic factors, sEng and sFlt, and the

increase of circulating pro-inflammatory cytokines like TNF- α (74). The increase in these factors leads to the systemic inflammation and endothelial dysfunction observed in mothers with PE.

In normal pregnancies, physiological levels of vascular endothelial growth factor (VEGF), transforming growth factor beta (TGF- β), and placental growth factor (PlGF), are necessary for healthy vascular function and angiogenesis. These factors contribute to vascular adaptations that occur in healthy pregnancies, such as enhanced vasodilation capacity. VEGF exerts its effects by binding to its receptor, which is coupled to endothelial nitric oxide synthase (75, 76), leading to the release of nitric oxide. Nitric oxide release is critical for vasodilation and angiogenesis. Similarly, PlGF, expressed by the ST (77) and the endothelium (78), regulates the development and function of placental vasculature (79). TGF- β is a cytokine that exerts its effects by binding to membrane-bound endoglin, which is highly expressed in endothelial cells and the ST. TGF- β signaling is critical for angiogenesis (80), and for the regulation of vasoconstriction and vasodilation of arteries in the mother (81). TGF- β also acts as an anti-inflammatory cytokine. For instance, it improves dermatitis by lowering TNF- α levels (82).

In PE, reduced placental perfusion leads to placental hypoxia and oxidative stress and its release of anti-angiogenic factors, sFlt and sEng. sFlt is a scavenger receptor that binds VEGF and PlGF, thus preventing them from binding their membrane-bound receptors and exerting their functions (83). For instance, sFlt binds VEGF, and prevents VEGF-mediated production of nitric oxide, leading to an increase in systemic vasoconstriction (84, 85). This ultimately leads to increased blood pressure. sFlt also increases endothelial cell sensitivity to inflammatory cytokines, notably TNF- α (86), which leads to further exacerbation of endothelial dysfunction (87). On the other hand, sEng binds TGF- β and inhibits pro-inflammatory effects mediated by

TGF- β but also inhibits TGF- β activation of endothelial nitric oxide synthase, ultimately leading to exacerbated vasoconstriction (88, 89), which eventually clinically manifests as hypertension.

Normal pregnancies comprise a modulated inflammatory state. Wegmann et al proposed that normal pregnancy involves the shift towards a Th2 environment, where increased circulating Th2 cytokines and decreased Th1 cytokines maintain pregnancy and block fetal rejection (90). However, this notion has been challenged over the years, and new evidence suggests that although a Th2 and Th1 balance is important for pregnancy, the immunology of pregnancy is more complex and dependent on the timing and stage of the pregnancy (91).

In the first trimester, maternal macrophages, uterine or decidual natural killer (dNK) cells, dendritic cells, and regulatory T cells accumulate in the decidua to regulate placental attachment to the uterus (92, 93). dNK cells, which comprise over 70% of the decidual immune cell population (94) secrete angiogenic factors (95) and both Th1 and Th2 cytokines that regulate trophoblast invasion, spiral artery remodeling, and vasculogenesis (96). Placental cells are also activated to increase the production of inflammatory cytokines that induce physiological processes (97).

PE is well understood as a hyper-inflammatory condition in pregnancy where the concentration of pro-inflammatory and Th1 cytokines in maternal blood are elevated. Circulating levels of TNF- α and interleukin-6 (IL-6) (98-100) are increased further in PE following their excessive release from the placenta (97, 101-104). Cultured CTs isolated from women with PE show an increased release of IL-1 β , IL-2, IL-4, IL-6, IL-8, IL-10, IL-12, IL-18, TGF- β , interferon gamma (IFN- γ), IFN- γ inducible protein 10 (IP-10), and monocyte chemoattractant protein 1 (MCP-1), many of which promote the PE pathophysiology (105-108). The pathological inflammation observed in PE is attributed to an excessive release of antiangiogenic factors (109),

oxidative stress, and hypoxia, which leads to the systemic activation of maternal leukocytes (108). Increased ST particles shed from the placenta in PE are released into maternal circulation and can embed into maternal lungs, further stimulating an immune response (110). Particles shed from the ST contain high levels of sFlt and sEng and can further trigger maternal peripheral blood mononuclear cells, leading to a further release of pro-inflammatory cytokines (111, 112). This increased production of circulating pro-inflammatory cytokines follows with detrimental impacts on maternal blood pressure, fluid homeostasis, and in severe cases, death (31).

IL-10, a potent anti-inflammatory cytokine, is believed to play a prominent role in neutralizing the hyper-inflammatory state in PE. Supplementing rat models of placental ischemia with IL-10 alleviates the increase in pro-inflammatory cytokines, reactive oxygen species, and hypertension (113). A decrease in circulating IL-10 levels in women with PE has been reported in numerous studies (114-117). Additionally, maternal lymphocytes in the systemic circulation of women with PE express lower levels of IL-10 (115). Trophoblasts (118) and placentas (119) of women with PE also express lower levels of IL-10.

1.2.2. The Placenta in PE

Part of the pathophysiology that occurs in early-onset PE is the shallow invasion of EVT's into the maternal decidua that leads to inadequate remodeling of the maternal spiral uterine arteries. The purpose of this remodeling is to reduce uteroplacental resistance, allowing an increase in blood flow into the intervillous space that bathes the ST, the fetoplacental barrier. Mature distal EVT's with a vascular phenotype invade the maternal decidua, disrupt the smooth muscle in the blood vessel wall of the spiral arteries, and replace the endothelium (120). This process is mediated by several growth factors, cytokines, and dNK interactions in the microenvironment of the invading EVT. The disruption in signaling or the balance of these

factors leads to poor invasion and then poor remodeling (120). Poor remodeling often results in poor placental perfusion, discussed in 1.2.2, leading to a low oxygen environment for the fetus (121-123) and all the subsequent placental, fetal, and maternal damages discussed above.

The placenta in PE is typically characterized by low levels of CT proliferation, high levels of ST shedding, high levels of placental autophagy, and low levels of CT differentiation and fusion (124-126). However, it is important to note that Redline et al reported a high level of CT proliferation in placentas of mothers with PE. The authors propose that a high proliferative capacity in combination with an immature and undifferentiated phenotype of CTs could in fact be contributing to the placental dysfunction observed in PE (127). Placentas of mothers with PE also exhibit low expressions of GCM-1 and Syncytin-1 (128, 129). One mechanism that can lead to this downregulation in PE is enhanced hypoxia greater than that seen normally in the placenta. Indeed, a hypoxic environment leads to the inhibition of the phosphatidylinositol 3-kinase (PI3K)-protein kinase B (Akt) signaling pathway. This inhibition activates glycogen synthase kinase 3 beta, which phosphorylates GCM-1 and leads to its ubiquitin-based degradation (129). This decrease in GCM-1 levels would subsequently decrease the expression of the Syncytin fusogenic proteins. Evidence has shown that a high level of reactive oxygen species, extreme hypoxia, and maternal predispositions can often lead to Syncytin-1 promoter hypermethylation, deeming it inaccessible for GCM-1 binding (130, 131). This decrease in GCM-1 and Syncytin-1 would then lead to increased trophoblast apoptosis, decreased CT proliferative capacity, and decreased CT differentiation and fusion. This altered balance in turnover would lead to a ST with gaps, reduced barrier function, and increased fetal protein leakage into the maternal circulation (132). This would also lead to decreased endocrine function of the ST, and decreased release of ST-produced hormones, like hPL and hCG, further contributing to pregnancy dysfunction.

Placentas in PE are characterized by higher levels of ST shedding and higher rates of ST knot apoptosis (124). The high levels of membrane vesicle shedding further stimulate pro-inflammatory responses and inhibition of angiogenic signaling, as described in the above sections (133).

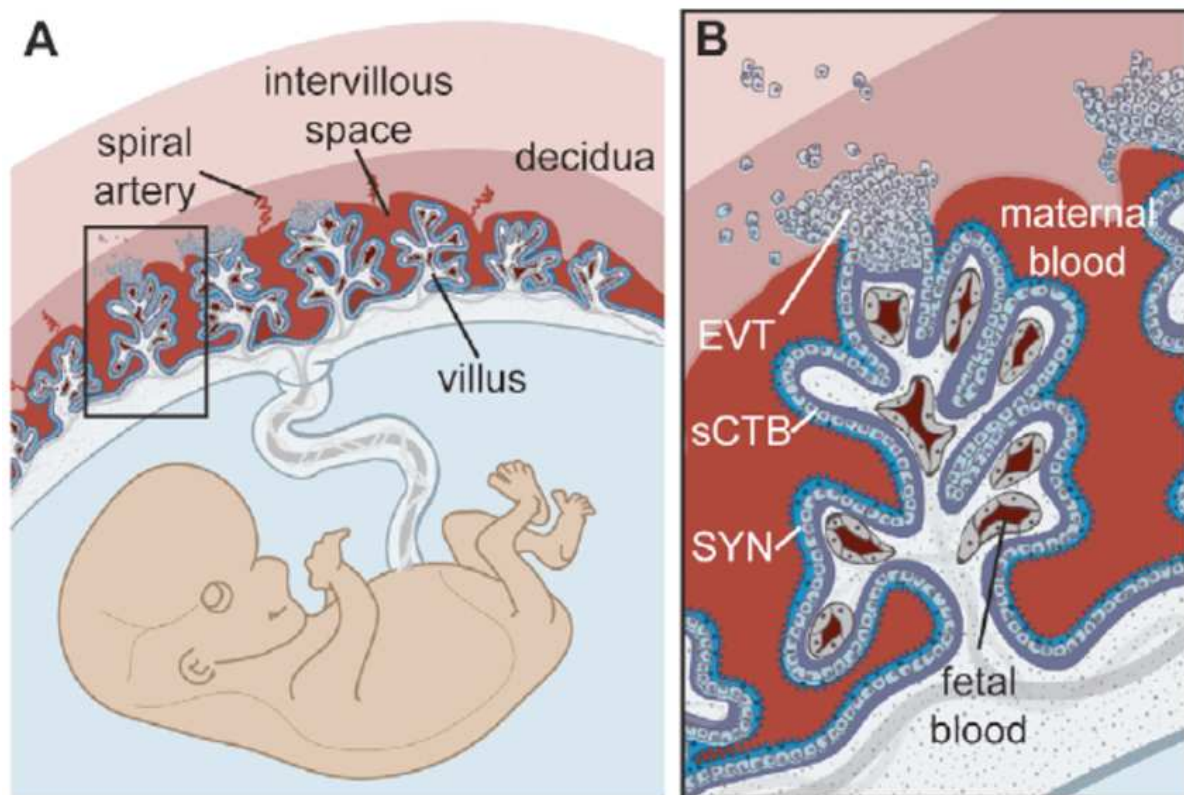


Figure 1.1: Structure and Organization of the Human Placenta

(A): Spatial representation of the fetus attached to the placenta which is embedded into the decidua. (B): The organization of the placenta into villous structures comprised of extravillous trophoblasts (EVT) invading the decidua and the underlying stem-like cytotrophoblast (sCTB) which forms the multinucleated syncytium (SYN) in direct contact with maternal blood (134).

This figure is reused under the Creative Commons Attribution (CC- BY) license.

1.3. TNF- α in Pregnancy

Pro-inflammatory cytokines are notorious for disrupting placental function, notably TNF- α (4). Elevated TNF- α is linked to pregnancy complications including recurrent spontaneous abortions (135), preterm labor (136), and PE (137). Injecting TNF- α alone into pregnant non-human primates leads to the development of PE symptoms (138). Moreover, elevated TNF- α causes a PE-like placental phenotype that includes poor ST function, high ST shedding, and high inflammation (139, 140). TNF- α also increases trophoblast apoptosis and hinders ST formation and endocrine function (139). Despite its blatant role in inducing a PE phenotype, high levels of circulating TNF- α are not reliable diagnostic markers for PE, with little correlation observed between TNF- α levels and late-onset PE (141). However, TNF- α levels are positively associated with the severity of the diagnosis (142).

Physiological levels of TNF- α have pregnancy enhancing roles like inducing mucin 1 shedding from uterine epithelial cells, a major feature of embryo implantation (143). Normal levels of TNF- α also regulate the fate (144, 145), proliferation (146-148), and differentiation (149, 150) of various cells, including CTs (4, 139). TNF- α maintains normal levels of apoptosis that are necessary for fetal development (151). This deems market available TNF- α inhibitors controversial for use during pregnancy (152).

1.3.1. TNF- α Signaling

TNF- α (TNF, cachexin, or cachectin) is a pro-inflammatory cytokine. It is mainly produced by macrophages and monocytes, although most endothelial, epithelial, and stromal cells also produce TNF- α . The protein is generated as a type II transmembrane protein and can be later cleaved into its soluble form (sTNF- α) by TNF Alpha Converting Enzyme (TACE or

ADAM17) (153).

TNF- α induces a diverse range of cell regenerative (survival, proliferation, differentiation) and destructive (apoptosis, pro-inflammatory, cell death) effects. These differential effects are dependent on cell type, the concentration of TNF- α , and the balance of signaling between both receptors.

TNF- α transduces its cellular effects by activating membrane-bound TNF receptor 1 (mTNFR1, TNFRSF1A, CD120a, p55) or TNF receptor 2 (mTNFR2, TNFRSF1B, CD120b, p75). TNF- α binds to its membrane receptors either in its mTNF- α form via cell-to-cell contact (154), or in a paracrine manner through sTNF- α . While both sTNF- α and mTNF- α activate TNFR1, mTNF- α is the primary activator of TNFR2 (155). In fact, the rapid dissociation of sTNF- α from TNFR2 brought forth a notion of TNFR2 serving as a TNF- α ligand passing receptor (156). TNFRs are also cleaved by proteolytic enzymes to form sTNFRs which serve to neutralize TNF- α (157), albeit binding to it with a lower affinity than mTNFRs.

TNFR1 and TNFR2 have common and separate downstream pathways which lead to their overlapping and distinct biological functions. Both TNFRs lack intrinsic enzyme activity and thus recruit cytosolic enzymes to promote their signaling cascade. TNFR1 intracellular signaling is currently better understood. In the absence of ligand activation, TNFR1 constitutive activation is prevented through the binding of a silencer of death domain (SODD) to the DD (158). Upon ligand activation, TNFR1 DD favors the binding of the DD of the cytosolic adaptor protein, TNF receptor-associated death domain (TRADD), which displaces SODD. After binding TNFR1, TRADD undergoes a conformational change and binds TNF receptor-associated factor 2 (TRAF2) (159) along with the serine/threonine receptor interacting protein kinase 1 (RIPK1)

and cellular inhibitor of apoptosis proteins 1 and 2 (cIAP1/2), forming complex 1. SphK1 and SIP both bind TRAF2 and act as co-factors for the TNFR1 Complex 1 (Figure 1.2) (5).

TNFR1 Complex 1 can activate various pathways. One signaling pathway is the activation of mitogen activated protein kinase kinases which ultimately lead to the translocation of NF- κ B into the nucleus to act as a transcription factor for a myriad of genes coding for enzymes, receptors, and cytokines, ultimately regulating processes like apoptosis, cell proliferation, and inflammation. A second pathway is activated when Complex 1 dissociates from TNFR1 and Fas-associated DD protein (FADD) (159) binds TRADD and forms Complex II by recruiting and activating caspase-8 (151). This ultimately leads to the activation of caspase 3 and the induction of apoptosis. A third pathway is activated when Complex 1 recruits apoptosis signaling kinase-1 which activates mitogen activated protein kinase kinases which phosphorylate c-Jun N-terminal kinases and p38 mitogen activated protein kinase (160), the latter leading to apoptosis. C-Jun N-terminal kinases activate activating protein 1, a transcription factor that regulates inflammation and cell fate (160). TNFR1 Complex 1 can also induce cell growth and proliferation by inducing extracellular-signal-regulated kinases (ERK) that lead to the activation of Akt (161).

Contrary to TNFR1, mechanisms of TNFR2 signal transduction are less defined. Yet, TNFR2-mediated pathways often overlap with those of TNFR1. Despite not having a DD, TNFR2 is still able to bind TRAF2 and induce the NF- κ B, c-Jun N-terminal kinases, FADD, and Akt pathways. These pathways ultimately lead to a range of biological effects, including inflammation, apoptosis, and proliferation.

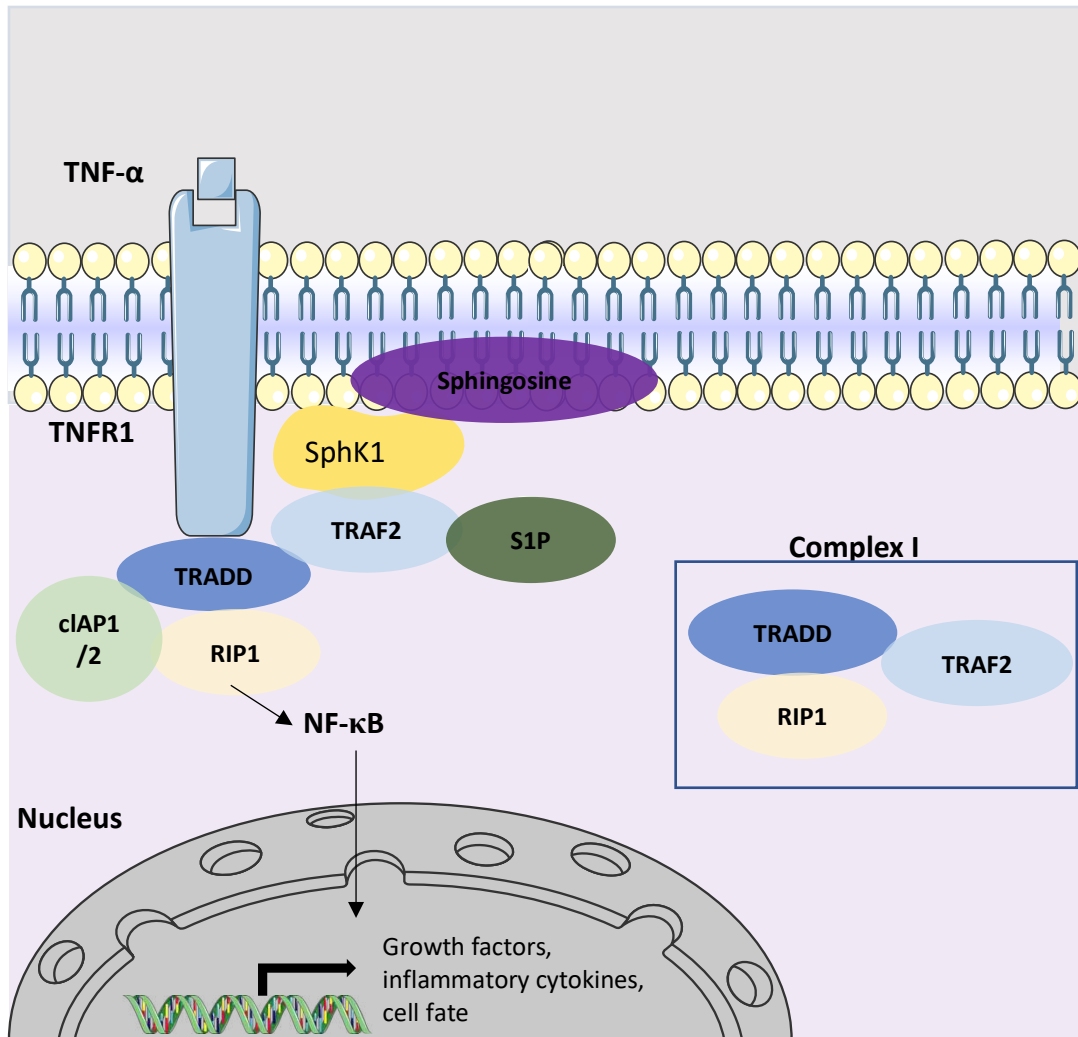


Figure 1.2: Sphk1 and S1P Act as Co-Factors for TNFR1 Signaling

Tumor Necrosis Factor-alpha (TNF- α) binds TNF- α Receptor 1 (TNFR1) and activates TNFR1 Complex 1, comprised of TNF- α receptor associated death domain (TRADD), serine/threonine receptor interacting protein kinase 1 (RIP1), which together with TRADD binds cellular inhibitor of apoptosis proteins 1 and 2 (cIAP1 and cIAP2), and TNF- α receptor associated factor 2 (TRAF2) which binds Sphingosine kinase 1 (SphK1) and Sphingosine 1-Phosphate (S1P) as cofactors. This signaling pathway activates the transcription factor NF- κ B, which subsequently leads to the upregulation of growth factors, inflammatory cytokines, and cell death or cell survival (162). The figure was created by Servier Medical Art by Servier and is licensed under a

1.3.2. TNF- α Ligand and Receptor Expression in the Placenta

TNF- α expression and the expression of its receptors changes in the placenta throughout pregnancy. In placentas of first trimester pregnancies, TNF- α is highly expressed and mainly localized in the trophoblast layers: the CTs and ST. TNFR1 mRNA is mainly expressed in the ST, with underlying CTs and stromal cells exhibiting low expression (163). The mRNA expression of TNFR2 is low, with the first trimester placenta intermittently expressing TNFR2 mRNA throughout the syncytium and with null expression in the villous core (163). This suggests that in the early first trimester when CT is differentiating into its various lineages, TNF- α may have an active role in regulating part of this process through TNFR1. Term placentas display decreased TNF- α levels in trophoblast layers, and increased expression in the villous core. TNFR1 mRNA expression in term placentas exhibits a similar expression pattern compared to that in the first trimester but with an increased overall expression, suggesting an increase in TNFR1 signaling in term placentas (163). Similar to TNF- α , stromal TNFR2 expression is higher in term placentas, whereas the syncytium expresses low levels of TNFR2 (163). Since TNFR2 can be involved in cell growth and proliferation, it can be expected that its expression, and perhaps signaling, is decreased in the ST with the increase in gestational age as the placenta reaches its maturity.

1.4. S1P in Placenta

1.4.1. S1P Metabolism in Pregnancy Physiology and PE

Table 1.1 summarizes the differences in sphingomyelin, ceramides (CERs), sphingosine, S1P, and S1P synthesizing and catabolizing enzymes in normal pregnancies and those complicated with PE.

1.4.1.1. Sphingomyelin and Ceramides

Sphingomyelin in the plasma membrane is cleaved by families of sphingomyelinases to produce CERs. CERs are also produced through *de novo* synthesis in the endoplasmic reticulum. CER can be phosphorylated by CER kinase to form CER 1-phosphate, which is pro-inflammatory through its activation of phospholipase A2 (164). CER can also be metabolized by acid, alkaline, and neutral ceramidases to yield sphingosine (165, 166), which is then phosphorylated by SphK1 and SphK2 to produce S1P. The S1P: CER ratio determines cell fate because S1P is protective as opposed to long-chain CERs (C16:0-C24:0) that are generally cytotoxic and pro-apoptotic (167, 168). Since S1P is formed as a product of CER metabolism and cannot be synthesized *de novo*, the S1P: CER rheostat is heavily dependent on the levels and activity of the enzymes that regulate S1P and CER turnover.

Sphingomyelin is also the second most abundant circulating phospholipid, with the majority bound to high density lipoproteins (HDL) (169). Its physiological roles in the circulation are not fully explored and sphingomyelin levels in plasma and placentas throughout normal gestation remain unknown. However, circulating levels of C16:0- and C18:0- sphingomyelin are elevated in women who later develop PE, but only in the first trimester of pregnancy (170). Total sphingomyelin levels are elevated in placental arteries of women with PE

(171), and C16:0 and C24:0-sphingomyelin are elevated in placental chorionic arteries in PE (Table 1.1) (172). Total levels of sphingomyelin secreted from cultured placental villous explants isolated from placentas of mothers with PE are also elevated. However, lipid profiling of ST microvesicles that are released from the syncytium into the circulation of mothers with PE does not show any significant differences in the concentrations of sphingomyelin and CER species when compared to samples obtained from healthy pregnancies (173). Recently, however, another study shows a higher level of sphingomyelin-C18:0 in extracellular vesicles shed from placentas of women with PE (72).

Sphingomyelinases, the family of enzymes that convert sphingomyelin into CERs, have not been extensively studied in the context of pregnancy. Among acid, alkaline, and neutral sphingomyelinases, acid sphingomyelinase has been studied the most. Mammalian expression of the acid sphingomyelinase gene results in two forms of the enzyme: lysosomal acid sphingomyelinase and a secretory form, located in the extracellular space. Secretory acid sphingomyelinase levels are increased in the plasma of women in their first trimester of pregnancy who later develop early or late-onset PE (174). These high levels are also positively correlated with an increase in plasma endoglin and soluble vascular cell adhesion molecule 1, markers of endothelial dysfunction, in the late-onset but not in the early-onset PE group. This indicates that elevated sphingomyelinase could play a role in the development of PE by inducing endothelial dysfunction (174). Similarly, the protein expression of placental acid sphingomyelinase was higher in samples from women with PE compared to those from a gestational age-matched control group. The patterns of glycosylation of the enzyme were also altered in placentas from PE pregnancies, leading to lower enzymatic activity in the PE group. Albeit, total sphingomyelin was unchanged in PE samples which could be explained by elevated

levels of sphingomyelin synthase. These levels, however, were not tested (175).

The levels of C16:0-CER, C18:0-CER, and C24:0-CER increase in maternal plasma as normal pregnancy progresses into the third trimester, suggesting a role for pro-inflammatory CERs in parturition as observed with pro-inflammatory cytokines (170, 176). This increase in late pregnancy could just reflect the increased concentration of pro-apoptotic CERs in the placental syncytial knots that are released into maternal blood (175). The release of apoptotic syncytial knots is part of the crucial turnover process of normal placental trophoblasts and this is elevated in PE.

The concentrations of C14:0-CER and C24:0-CER species are higher in the plasma of women who develop PE in the third trimester (170, 176). Additionally, another study showed that elevated levels of CERs in maternal plasma, but not in the placenta, are associated with a more severe PE phenotype including the HELLP (Hemolysis Elevated Liver enzymes Low Platelet) syndrome, proteinuria, and preterm delivery, but not hypertension (177). By contrast, Melland-Smith et al. showed that the levels of C16:0-CER, C18:0-CER, C20:0-CER, and C24:0-CER, but not C22:0-CER are higher in both maternal blood and placentas from women with PE when compared to levels in samples obtained from women without PE who delivered gestationally matched preterm infants (175). This is explained by decreased mRNA, protein expression, and activity of placental acid ceramidase-1, the enzyme that metabolizes CER into sphingosine. This reduces CER degradation and leads to its systemic and placental accumulation. Furthermore, CERs in placentas from women in both groups are mainly confined to trophoblast cell subtypes and syncytial knots (175), which are undergoing apoptosis and are shed into the maternal bloodstream. In addition, arteries isolated from placentas of women with PE contain high levels of total CERs (171). More research is needed to understand the role of CERs in

syncytial shedding under physiological conditions and the consequences of elevated placental CERs on this process in the development of pregnancy disorders.

The role and expression of alkaline ceramidases (ACER), which cleave CERs to sphingosine, in human and mouse placentas are explained well in a recent review (178). Briefly, ACER1-3 are expressed in the human placenta with both ACER-2 (179, 180) and ACER-3 being the main enzymes as shown by the Obeid group (181). In mice, ACER-2 is highly expressed between E9.5 and E12.5 (180), the critical window for vascular development. Moreover, this enzyme is expressed in major placental cell types at E11.5, including fetal endothelial cells, spongiotrophoblasts, and trophoblast giant cells (180). Crossing double knockout (KO) mothers of ACER-2 and wild-type fathers leads to the death of 50% of embryos at E12.5 with hemorrhages occurring in the junctional and labyrinth zones of the mouse placenta. Additionally, both hemorrhaged and non-hemorrhaged ACER-2 deficient placentas display a decrease in placental vascularization in the labyrinth zone. Similarly, ACER-2 deficient placentas show a decrease in placental sphingosine and S1P levels, without altering CER levels. This shows that ACER-2 deficiency in both the mother and the fetus leads to defects in placental vascularization that may result in pregnancy loss, potentially by decreasing S1P and sphingosine-mediated inhibition of protein kinase C (PKC) (182). This study also shows that ACER-3 only increases in the placentas of non-hemorrhaged Acer-2 deficient mice (180). This implies that ACER-3 increases in response to Acer-2 deficiency and alleviates some of the detrimental effects with overlapping signaling responses.

1.4.1.2. S1P and its Regulatory Enzymes

The majority of circulating S1P is released from erythrocytes (183-186) that act as a reservoir (186), but activated platelets also produce a significant amount of S1P in response to

thrombotic stimuli from adenosine diphosphate, thrombin, or collagen (187). Erythrocytes and platelets are both distinguished by high SphK activity and low levels of S1P degrading enzymes (187-189). Circulating S1P levels in plasma range from 100 to 400 nM (187, 190-198) to as high as 1 μ M (199, 200) depending on the population characteristics and the efficiency of the techniques used for plasma isolation. Some technical differences could result in partial platelet activation and the release of S1P. S1P in the blood is bound to lipoproteins and serum albumin with more than 60% bound to HDL (201, 202). Apolipoprotein M is the main binding protein in the S1P-HDL complex (203).

In normal human pregnancies, plasma S1P concentrations range between 170 to 330 nM, but they do not change throughout gestation (170, 176). Circulating levels of S1P in women with PE were similar to the normal group across all three trimesters (170, 176). One study, however, shows an increase in S1P, sphingomyelin, and C18:0-CER produced by placental explants collected from mothers with severe PE who were treated with aspirin, when compared to those from normal healthy pregnancies (204), (Table 1.1). In this study, the authors cultured minced placental tissue rather than intact villous explants, potentially releasing some CERs due to cell damage. Although the authors report minimal cell damage, results from the disruption of tissues should, however, be interpreted with caution. On the other hand, a recent study shows that the levels of S1P specifically bound to HDL decrease in women with PE (205). S1P has distinct effects depending on the binding to different protein carriers. For instance, S1P bound to HDL has longer-lived effects on strengthening the endothelial barrier than does S1P bound to albumin (206). However, the presence of albumin facilitates the release of S1P from erythrocytes and this albumin-bound S1P can reduce permeability in rat venules (207). Hence, low levels of HDL-S1P in PE could contribute to endothelial barrier dysfunction as seen in patients with sepsis (208).

Measuring S1P levels bound to different protein carriers in healthy and at-risk pregnancies could serve as a better predictor of the onset of pregnancy disorders.

Another mechanism by which plasma S1P could contribute to cellular responses is through its dephosphorylation by lipid phosphate phosphatases (LPPs) ectoenzymes. Sphingosine is then taken up by cells and rephosphorylated by SPHKs (209, 210). This can increase intracellular S1P levels or the S1P can be exported outside of the cells through transporters such as SPNS2 to act on cell surface receptors or be transferred to erythrocytes for storage. This regulation has not been studied in relation to the fetoplacental interface, which contacts maternal erythrocytes directly. The contribution of trophoblasts to S1P levels in either the maternal or fetal circulation is unknown.

Measuring the levels and activities of enzymes involved in S1P metabolism provides a better understanding of how sphingolipid signaling is regulated in various reproductive tissues. Studying S1P metabolism also provides information on the state of the S1P: CER rheostat because S1P metabolic enzymes are often expressed in non-overlapping intracellular locations (Figure 1.3). Emerging evidence also suggests that the effects of some enzymes extend beyond sphingolipid metabolism. For instance, as previously noted, SphK1 binds to TRAF2 to mediate TNF- α effects through TNFR1 (Figure 1.2) (211). It is important to study changes in the levels of enzymes involved in sphingolipid metabolism over the course of normal and complicated pregnancies to determine dynamic changes, in addition to the changes in steady state concentrations of S1P and CER. S1P is synthesized by phosphorylation of sphingosine by SphK1 and SphK2. The lipid is degraded by S1P lyase, S1P phosphatases (SGPPs) or LPPs (Figure 1.3).

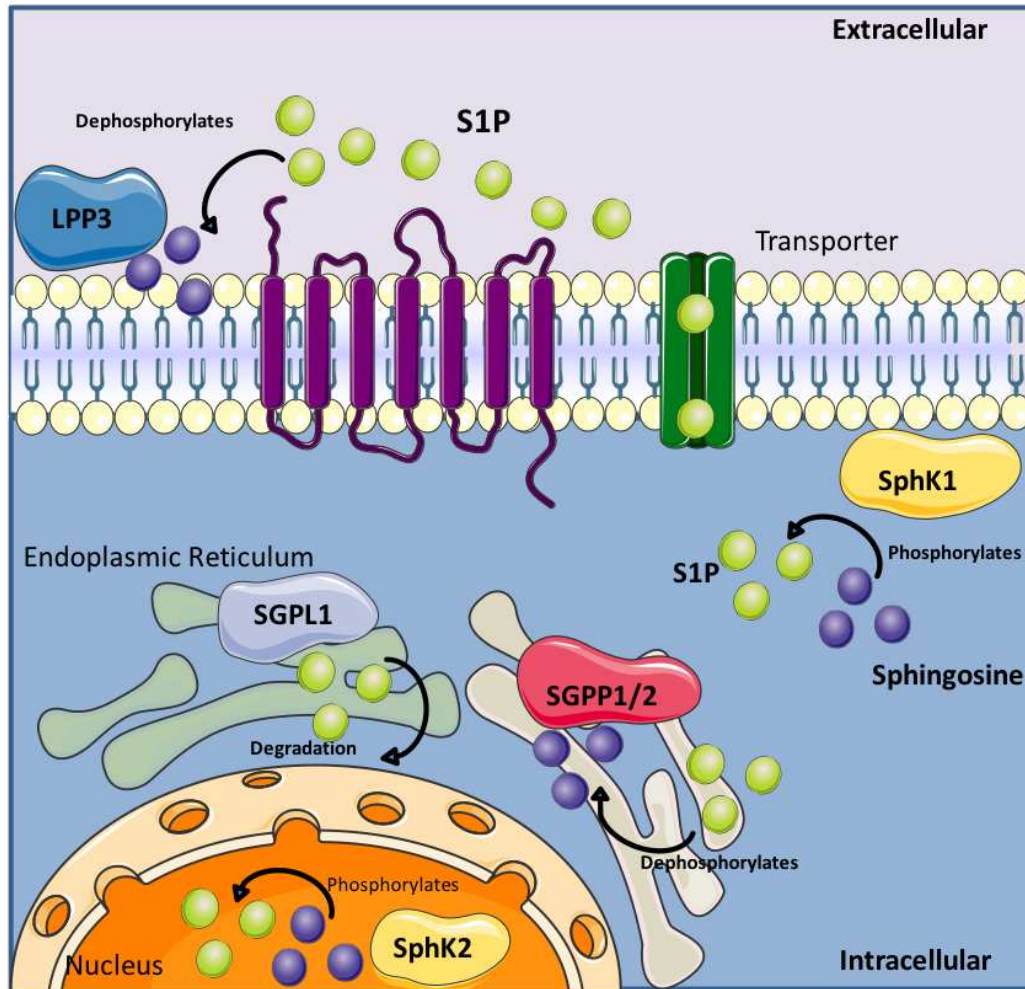


Figure 1.3: Known Components of the S1P Metabolic and Signaling Pathway

SphK1 is a kinase that phosphorylates sphingosine to produce S1P at the intracellular cell membrane. S1P can then exit the cell and act in a paracrine or autocrine manner by interacting with one of its five G protein-coupled receptors (S1PR1-5). Lipid phosphate phosphatase 3 (LPP3) is an integral membrane protein that dephosphorylates extracellular S1P. Sphingosine 1-phosphate phosphatase (SGPP1) dephosphorylates intracellular S1P. While the actions of LPP3 and SGPP1 are reversible, S1P lyase (SGPL1) degrades intracellular S1P in an irreversible reaction. The figure was created by Servier Medical Art by Servier and is licensed under a Creative Commons Attribution 3.0 Unported License.

1.4.1.2.1. Sphingosine Kinases

SphK1 and SphK2 synthesize S1P through the ATP-dependent phosphorylation of sphingosine. Double KO of *SphK1* and *SphK2* are lethal in mice, whereas KO of either *SphK1* or *SphK2* produces viable mice with minor phenotypic changes. This implies that SphK1 and SphK2 exhibit redundancy in functions, at least for viability, and can compensate for each other (212).

SphK1 is mainly cytosolic (213), whereas its substrate, sphingosine, is associated with the plasma membrane (214). Thus SphK1 activation includes its translocation from the cytosol to the cell membrane (215). This translocation requires phosphorylation of the enzyme through ERK-1 or ERK-2. SphK1 is the major source of extracellular S1P (216) because S1P produced by SphK1 is normally actively transported outside the cell (217, 218) via membrane-associated ATP-binding cassette transporter G2 (ABCG2) (219, 220), major facilitator superfamily transporter 2b (MFSD2B) and protein spinster homolog 2 (SPNS2) (221). The differences in expression and activity of the S1P transporters, ABCG2, MFSD2B, and SPNS2 in normal and pathological pregnancies have not been explored. Activation of SphK1 generates a well-established anti-apoptotic effect, which is upregulated in cancer cells and inhibits their apoptosis (222). Extracellular S1P signaling is generally regarded as pro-survival and anti-apoptotic (223, 224). However, whether the anti-apoptotic effects of SphK1 are due to its production of S1P and the release of S1P and S1P signaling through cell surface receptors, a role for SphK1 as a signaling molecule in its own right is not well understood. As mentioned, SphK1 and S1P have recently been identified as co-factors for TRAF2 which ultimately leads to NF- κ B activation (211).

SphK2 is located mainly in the nucleus and sometimes in the rough endoplasmic reticulum. It contributes to intracellular S1P signaling mechanisms as discussed in later sections. However, SphK2 is also located in the cytosol and the mitochondria (225), suggesting that in addition to regulating gene transcription, S1P produced specifically by SphK2 could have important roles in mitochondrial and cytosolic signaling. SphK2 activation, contrary to SphK1, induces apoptosis and inhibits cell proliferation in several cell types (226-228).

We showed that the protein expression of SphK1 and its activity increase from the late second trimester to term in human decidua while SphK2 activity does not change (229). Studies in sheep revealed that the intensity of staining for SphK1 rises from day 20 to 120 of a 152-day pregnancy in the caruncular (maternal) region of the placentome, the trophoctoderm, uterine and placental vasculature, and in the syncytium (230). Steady increases in the expression of SphK1 are also seen in uterine and decidua throughout pregnancy in rodents (231-233). The increases in similar tissues in several species demonstrate the critical maternal and fetal roles of SphK1 in pregnancy. The importance of SphK1 in the progression of healthy pregnancies is emphasized by the finding of decreased SphK1 mRNA, protein expression, and activity in placentas of pregnancies complicated by PE (234).

The mechanisms behind changes in placental SphK1 expression and activity during pregnancy have been investigated using cultured placental trophoblast cells or chorionic villous explant cultures. SphK1 mRNA and protein expression in human term chorionic explants and JAR cells, a cell line used as a model for second trimester trophoblasts, is higher when cultured under hypoxic conditions (1% O₂) compared to standard culture conditions (21% O₂). Under conditions that are normoxic for these cells and tissues (8% O₂), SphK1 expression was similar to that found at 21% O₂ (234). This suggests that trophoblasts upregulate their SphK1 levels in

response to hypoxia, a condition that often accompanies disorders like PE. However, these results in isolated placental cells and tissues are in contrast to the decreased SphK1 expression found in term placental biopsies from women with PE compared to those from women with normal births (234). Factors such as increased inflammation and oxidative stress that are often elevated in PE should increase SphK1 expression (235, 236). The discrepancy between the *in vitro* and *ex vivo* studies could be due to the multifaceted nature of PE since PE can be grouped into several categories based on placental and maternal factors. Importantly, the study showing decreased SphK1 expression (234) did not distinguish cell types since whole thickness biopsies were used to measure SphK1 mRNA and protein. Hence, more research is required to determine the SphK1 responses of individual cell types to hypoxia and the cell-specific SphK1 levels in the placentas of women with pregnancy disorders. Additionally, the fluctuation of SphK2 levels across normal pregnancy and its levels in pregnancy disorders have not yet been explored.

1.4.1.2.2. S1P Lyase

S1P lyase (SGPL1) irreversibly degrades S1P into delta2-hexadecenal and phosphoethanolamine (237). SPGL1 can also degrade dihydro-S1P into hexadecenal and phosphoethanolamine. SGPL1 is an integral membrane protein located mainly on the cytosolic side of the endoplasmic reticulum (238). From current evidence, we know that fetal SGPL1 deficiencies lead to a myriad of dysfunctions likely resulting from greatly elevated levels of sphingolipids. These include nephrosis, neurological, and immunological defects that define a novel disorder called SGPL1 insufficiency syndrome (239). In severe cases, this syndrome can result in abnormal fluid accumulation and ultimately perinatal death (239). Similarly, global KO of *SGPL1* in mice results in death before eight weeks of age (240).

Mouse trophoblasts in the decidual layer display high cytoplasmic and perinuclear SGPL1 expression on day 8 of pregnancy, when chorionic villi and vasculature begin developing (241). Labyrinth-zone spongiotrophoblasts and maternal endothelial cells within the labyrinth display a much weaker level of SGPL1. While the role of spongiotrophoblasts remains poorly understood, some roles in developing the villous labyrinth have been described (242, 243). The expression of SGPL1 in fetal endothelial cells is undetectable. The changes in SGPL1 expression in the normal mouse placenta across gestation remains unknown. SGPL1 expression in the sheep placenta decreases from day 20, the commencement of sheep placental development, and remains low through the last day examined, day 120, when the placenta is fully developed (230).

Our studies on human decidua revealed that SGPL1 mRNA expression increases over time from the late second trimester through to term and that both mRNA and protein expressions are higher in decidual tissues collected from mothers with a term pregnancy compared to those from a preterm pregnancy (229). This indicates a role for SGPL1 during the parturition process. These disparate results suggest species-specific roles for SGPL1 in decidual and placental tissues throughout pregnancy. However, the limited number of studies on SGPL1 in these tissues restricts our understanding of the effect of SGPL1 on S1P levels in normal and abnormal pregnancies.

1.4.1.2.3. S1P Phosphatases and Lipid Phosphate Phosphatases

S1P phosphatases (SGPP1-2) dephosphorylate S1P into sphingosine (244, 245). SGPPs are part of the lipid phosphate phosphatase (LPP) super-family. In mammals, both SGPPs and SGPL1 are found on the cytosolic face of the endoplasmic reticulum (244-246) and they cannot degrade extracellular S1P. SGPP1 mRNA is expressed in all human tissues but occurs at high concentrations in human kidneys and the placenta (247), the latter suggesting an important role

for SGPP1 in normal placental development and/or function. SGPP1 expression in the sheep placenta increases throughout pregnancy (230) (Table 1.1). However, this does not imply similar regulation in human pregnancy, as seen with the species-specific regulation of SGPL1. We found that decidual SGPP1 but not SGPP2 mRNA expression is higher in term compared to preterm pregnancy, although there were no differences in protein expression for either enzyme (229). SGPP1 and SGPP2 expression in the placenta of pregnancies complicated with PE have not yet been studied. The high expression of SGPP1 in normal placentas suggests an unexplored key function for SGPP1 in dephosphorylating intracellular S1P. We know little about the patterns of SGPP2 expression and its role in pregnancy.

LPP1-3 also dephosphorylate S1P. LPP3, notably, is known for modulating S1P extracellular levels (210, 248, 249). This is because LPP3 is present on the plasma membrane with its active site outside of the cell and thus it functions as an ectoenzyme to degrade circulating lipid phosphates such as S1P (244, 248-251). We found that although both LPP1 and LPP3 mRNA levels increase in term compared to preterm decidua, the activity of these enzymes did not change (229). Little else is known about LPP3 expression in pregnancy.

	Normal Gestation	Preeclampsia
Sphingomyelin	↓ C30:1, C32:1 sphingomyelin in decidua during labor (252)	<ul style="list-style-type: none"> • ↑ circulating C16:0- and C18:0-sphingomyelin in th first trimester (170) • No change in syncytial microvesicles (173) • ↑ placental arteries (171) and chorionic arteries (172) • ↑ C16-SM and C24-SM in chorionic arteries (172) • ↑ secretion from villous explant cultures in severe preeclampsia (204)
Ceramides (CERs)	<ul style="list-style-type: none"> • ↑ circulating C16:0-CER, C18:0-CER, and C24:0-CER in the third trimester (176) • ↓ long-chain CERs in decidua during labor (252) 	<ul style="list-style-type: none"> • No change in syncytial microvesicles (173) • ↑ plasma C14:0-CER and C24:0-CER in the third trimester (176, 253) • ↑ plasma but not placenta CERs in HELLP phenotype (177) • ↑ plasma and placental C16:0 -CER, C18:0-CER, C20:0-CER, and C24:0-CER, but not C22:0-CER (175) • ↑ placental arteries (171) • ↑ C18:0-CER secretion from villous explant cultures in severe preeclampsia (204) • No change in placental chorionic arteries (172)
Sphingosine	Unknown	No change in placental chorionic arteries (172)
Sphingosine 1-Phosphate (S1P)	No change in circulating levels throughout gestation (176, 253)	<ul style="list-style-type: none"> • No change in circulating levels across all three trimesters (253) • ↑ in plasma during the third trimester (176) • ↓ HDL-bound plasma S1P (205) • ↑ secretion from villous explant cultures in severe preeclampsia (204) • No change in placental chorionic arteries (172)
Sphingosine Kinase 1 (SphK1)	<ul style="list-style-type: none"> • ↑ expression across gestation in human decidua (229), sheep placentome (230), rodent uterus, and decidua (231-233) • ↑ activity in human decidua across gestation (229) 	<ul style="list-style-type: none"> • ↓ expression and activity in maternal plasma and placentas (234) • No mRNA change in placental chorionic arteries (172)
Sphingosine Kinase 2 (SphK2)	No change across gestation in human decidua (229)	No mRNA change in placental chorionic arteries (172)
S1P lyase (SGPL1)	• ↓ expression in sheep placentome across gestation (230)	• ↑ in placental chorionic arteries (172)

	<ul style="list-style-type: none"> • ↑ expression across gestation in human decidua (229) 	
S1P phosphatases (SGPP1, 2) and Lipid phosphate phosphatases (LPP)	<ul style="list-style-type: none"> • ↑ LPP1, SGPP1, and LPP3 mRNA levels but not activity at term (229) • ↑ SGPP1 in sheep placentome across pregnancy (230) 	<ul style="list-style-type: none"> • ↑ SGPP1 mRNA placental chorionic arteries (172), no change in SGPP2 mRNA
S1P Receptors (S1PR)	<ul style="list-style-type: none"> • S1PR1 peaks in sheep placentome at day 80 of gestation and gradually decreases after (230) • S1PR1,2 is not changed across gestation in decidua (229) • ↑ decidual S1PR3 across gestation (229) 	<ul style="list-style-type: none"> • ↓ placental S1PR1 in the basal (maternal) side (254) • ↓ S1PR1 mRNA levels in the placenta (234) • ↓ S1PR1,3 mRNA levels in the placenta in severe preeclampsia (234) • No change in placental S1PR2 mRNA (234) • ↓ S1PR1 mRNA in placental chorionic arteries (172) • ↑ S1PR2 mRNA in placental chorionic arteries (172) • No change in S1PR3 in placental chorionic arteries (172)

Table 1.1: Summary of the Levels of Sphingolipids, Their Metabolizing and Catabolizing Enzymes, and Their Receptors Across Normal Gestation and PE

The Table summarizes changes in sphingomyelin, ceramides (CERs), sphingosine, and sphingosine 1-phosphate (S1P) levels across normal gestation, as well as in preeclampsia (PE). The Table also summarizes the changes in levels and activity of various S1P regulatory enzymes and receptors.

1.4.2. S1P Receptors in Physiology and PE

S1P mediates its cellular effects by signaling intracellularly through mechanisms that continue to be elucidated or extracellularly as a ligand for cell surface receptors. Intracellular S1P controls gene transcription in the nucleus and also regulates the assembly of the cytochrome oxidase complex in the mitochondria (255). Nuclear SphK2 produces S1P which inhibits histone deacetylases (256), thus favoring histone acetylation and the epigenetic control of gene

expression, e.g. p21 (256). S1P also binds and interacts with prohibitin-2 and localizes in the mitochondria (255). This interaction is important for mitochondrial respiration, which has important implications for oxidative stress and aging. Little is currently known about the intracellular roles of S1P in pregnancy.

S1P exerts its extracellular responses by signaling through five specific G protein-coupled receptors, S1PR1-5, formerly called endothelial differentiation genes (Figure 1.4). As a result, there are a vast array of studies on the pharmacological applications of modulating S1P signaling by utilizing different receptor agonists and antagonists. S1PR1 and S1PR3 are expressed in most cell types (257). S1PR1 and S1PR3 have similar functions and thus are often grouped. They both increase the production of nitric oxide by endothelial cells and this induces vasodilation. S1PR1 and S1PR3 have important roles in neural cell function and migration (258) and induce lymphocyte trafficking and migration (259-261). However, these two receptors also have independent functions that will be described below. Globally knocking out S1PR1 is embryonically lethal due to hemorrhage and incomplete vascular maturation (262), whereas knocking out S1PR3 produces only minor alterations in phenotype (263).

S1PR2 KO mice are viable. They do not exhibit major abnormalities, but they have an increased risk of seizures between 3 and 7 weeks of age (264). S1PR4 and S1PR5 have restricted expression profiles and are mainly concentrated in neuronal and immune cells (265, 266). S1PR4 activation maintains dendrocyte function and triggers lymphocyte differentiation (267). S1PR5 activation induces natural killer cell trafficking (266) and neuronal cell migration (268).

S1PR1 couples mainly with G_i , but S1PR2-5 can also couple with G_i or $G_{12/13}$. G_i activation can inhibit adenylyl cyclase (AC) formation of cAMP. G_i activation can also induce ERK-1/2 activation through rat sarcoma viral oncogene (Ras) activation, which increases ERK-

1/2 activities. Moreover, G_i activation induces PI3K to activate Akt, which induces cell survival and migration, and the Rac pathway. Only S1PR2 and S1PR3 can couple with G_q. G_q signaling activates phospholipase C (PLC), which produces diacylglycerol with a release of Ca²⁺ along with activation of the classic PKC. S1PR2-5 can also couple with G_{12/13} and this activates Rho-associated kinases (ROCK). S1PR2-G_{12/13} coupling induces jun amino terminal kinase through ROCK, a pathway often leading to cell survival signaling. These signaling pathways have been well-studied in non-pregnancy conditions (269, 270). However, more research is needed to identify the balance of pathways that are activated during gestation in non-reproductive tissues and those that are involved in mediating the function of reproductive organs and the placenta during pregnancy. Examining the expression of different S1PRs is important because of these overlapping signaling properties and because the binding affinities of S1P at normal circulating concentrations to S1PR1, S1PR2, and S1PR3 are similar (271). Moreover, differences in signaling by S1P bound to different protein carriers are just being elucidated (206, 207). Finally, it is critical to understand the conditions that change the balance of S1PR expression to favor different pregnancy outcomes.

S1PR1 mRNA is mainly expressed in sheep blood vessels of the cotyledon and the caruncular region underlying the syncytium. This expression peaks at day 80 after which it gradually decreases (230). Although not measured across pregnancy, pregnant mice on day 14.5 express S1PR1 and S1PR2 in vascular regions of the placenta (272).

In human decidua, we found that expressions of mRNA for S1PR1, S1PR2, and S1PR3 are not altered with gestational age (229). However, decidual S1PR3 protein expression is positively correlated with gestational age (229). Table 1.1 summarizes the differences in S1PRs in normal pregnancies and those complicated with PE. S1PR1 expression is lower in placental

biopsies of patients with severe PE, but this was only observed in the basal plate (maternal side) of the placenta (254). This result is supported by another study where S1PR1 mRNA expression was lower in whole placental lysates from women with PE while both S1PR1 and S1PR3 mRNA expressions were lower in women with severe PE (234). In this same study, no difference in S1PR2 mRNA expression was detected among placentas from women with normal, PE, or severe PE pregnancies. Finally, placental chorionic arteries of women with PE show lower S1PR1 expression and higher SGPP1, SGPL1, and S1PR2 expression compared to women with normal pregnancies (172). These results highlight the importance of studying the mechanisms of decreased signaling along the S1P-S1PR1 and S1P-S1PR3 axes, increased S1P-S1PR2 signaling, and the regulation of S1P levels in mediating placental dysfunction in PE, specifically in the chorionic arteries.

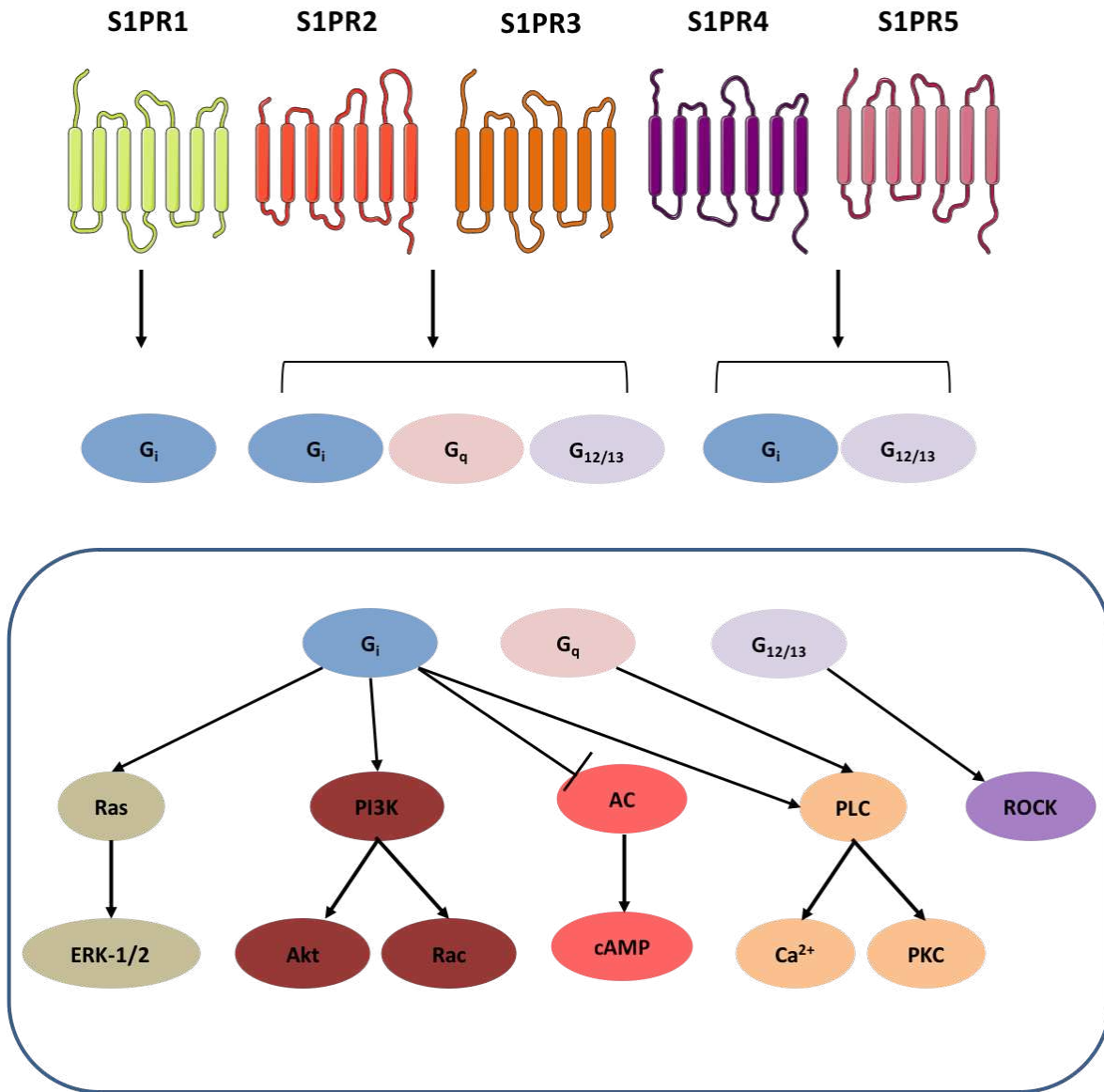


Figure 1.4: General S1PR G-protein Coupling and Functions

S1PR1-5 can couple with G_i which leads to the activation of phospholipase C (PLC) and Ca²⁺ release, PLC-protein kinase C (PKC), rat sarcoma virus (Ras)-extracellular-signal-regulated kinases (ERK), phosphoinositide 3-kinase (PI3K)-protein kinase B (Akt), PI3K-Rac, or AC-cyclic adenosine monophosphate (cAMP) interactions. S1PR2 and S1PR3 couple with G_q, leading to PLC pathways activation. S1PR2,3,4,5 couple with G_{12/13} leading to rho-associated kinase (ROCK) activation. These pathways regulate basic cellular functions such as

proliferation, survival, migration, vascular tone, endothelial barrier function, and neural cell communication.

1.4.3. S1P and Placental Development and Function

1.4.3.1. Sphingolipids and Extravillous Trophoblasts

EVTs migrate and invade the maternal decidua to anchor the placenta into the uterine wall and to remodel uterine spiral arteries and establish a fetal-maternal blood flow during the early stages of pregnancy (40). Poor EVT migration and invasion are at the core of the pathophysiology of PE. Hence, studying sphingolipid signaling in EVT function introduces an arsenal of potential targets to improve placental health in pregnancy complications.

The roles of sphingolipid signaling in EVTs have been studied in primary trophoblasts isolated from placentas as well as EVT cell lines such as Swan-71, SGHLP-4, HTR8/SVneo, and JEG-3 cells. These cell lines were isolated from placentas at different gestational ages. It is therefore important to note the differences in their sphingolipid signaling profiles when conducting studies and to interpret experimental results with caution. S1PR1-3 are expressed in Swan-71 and SGHPL-4 cells (273). HTR8/SVneo cells express S1PR1-5 mRNA with S1PR4 and S1PR5 mRNAs reported as the most abundantly expressed (274).

Treating JEG-3 cells with TGF- β upregulates SPHK1 production by activation of the activin receptor-like kinase-1/mothers against decapentaplegic homolog-1 pathway (275). Treating JEG-3 cells or first trimester placental explant cultures with sodium nitroprusside to induce oxidative stress increases C16:0-CER, C18:0-CER, C20:0-CER, C24:0-CER, and sphingomyelin, but not C22:0-CER (175). Further testing reveals that elevated CER levels in JEG-3, in accordance with other cell types (276), increase mitochondrial fission, disposing of

non-functional organelles, and autophagy as evidenced by the upregulation of the universal autophagy marker, LC3B-11 (175). Consistent with the literature on other cell types, high CER levels increase trophoblast autophagy. Moreover, treating JEG-3 cells and primary trophoblasts with C16:0-CER in the presence of QVDOPh, a caspase-8 inhibitor, increases necroptosis (277).

The adaptation of trophoblast mitochondria to the placental microenvironment occurs through the processes of fusion, biogenesis, fission, and mitophagy. These events contribute to mitochondrial recycling and repair, critical events for placental health (278). Recent studies show that placentas from pregnancies complicated by PE exhibit increased mitochondrial fission (279, 280) accompanied by increased CERs. This phenotype can be induced by treating primary CTs or JEG-3 cells with C16:0-CER (280). Furthermore, inhibiting acid ceramidase-1 in JEG-3 cells or *in vivo* in pregnant mice leads to an increase in the pro-apoptotic factor, Bcl-2-related ovarian killer, which mediates mitochondrial fission. Mitochondrial fission occurs during the initial phases of apoptosis, prior to caspase activation and membrane blebbing. Increased fission enables increased mitochondrial fragmentation, an essential step for outer membrane permeabilization and cytochrome C release (281). Increased fission in PE can explain the high level of CT apoptosis and hence the hindrance of syncytial formation and function.

Treating co-cultures of first trimester dNK and HTR8/SVneo cells with FTY720 reduces dNK-mediated EVT migration in a wound-healing assay (282). FTY720 is a sphingosine analog that gets phosphorylated by SphK1 or SphK2 (283) to form FTY720-P, which activates all S1PRs except for S1PR2. FTY720-P binds to S1PR1 with the highest affinity causing internalization of the receptor by recruiting β -arrestin (284). Hence, FTY720 results could be interpreted based on its initial role as an S1PR1 agonist or a functional antagonist upon longer exposures, leading to internalization (284). Treatment with FTY720 is often utilized in animal

studies in lieu of S1P because of the longer half-life of FTY720-P (285). Treatment of decidual leukocytes with FTY720 followed by co-culture with first trimester placental explants from the same mother led to reduced EVT outgrowth area (282). dNK cells migrate to and accumulate in the decidua at the beginning of pregnancy and secrete cytokines, enzymes, and other signaling molecules that prime EVTs for invasion. dNK cells also interact with EVTs to remodel spiral arteries. dNK cells predominantly express S1PR5 (282), assuming primer efficiencies were similar, highlighting a role of S1P-S1PR5 signaling in pregnancy. Notably, FTY720 treatment also decreases dNK migration and downregulates S1PR5 and VEGF expression, the main inducer of placental angiogenesis. These outcomes occur without changing IL-8 expression, an inducer of leukocyte migration and placental angiogenesis (282, 286). This means that FTY720 signaling induces leukocyte migration independent of IL-8 signaling. However, the mechanism for this outcome remains unclear. Treating HTR8/SVneo cells, a cell line used to model villous trophoblasts from the second trimester, but not BeWo cells, with S1P leads to a 6.5-fold increase of IL-8 secretion by increasing its transcription (Figure 1.5) (286). This suggests that S1PR1 activation decreases EVT migration and IL-8 release (Figure 1.5), but whether the decrease in migration is mediated through IL-8 secretion is debatable. Whether the effects of FTY720 are due to its phosphorylation leading to its high-affinity binding and internalization of S1PR1 was not tested in the study.

Treating JEG-3, Swan-71, SGHPL-4, and human first trimester explants with 100 nM S1P decreases cell migration or EVT outgrowth in villous explants by >50%. This occurs by activating the $G_{12/13}$ /Rho/ROCK signaling pathway downstream of S1PR2 (Figure 1.5), but this does not affect proliferation or cell viability (273). Treating Swan-71 cells with 1 or 10 nM 1,25-dihydroxyvitamin D decreases mRNA expression for S1PR2 and reverses the decrease in EVT

migration by S1P (273). Therefore, studying negative regulators of S1PR2 expression can shed light on factors inducing migration with potential therapeutic applications. EVT migration depends on cAMP production, which S1P inhibits through S1PR1/G_i coupling and not through S1PR2 (273). Both FTY720 and S1P decrease EVT migration; this suggests similar mechanisms of action. However, the downstream pathway of FTY720-hindrance of EVT migration is not fully understood.

HTR8/SVneo cells increase IL-8 secretion in response to the activation of S1PR1 and S1PR3 that subsequently activate Rho/Rho-kinase and Rac1 signaling pathways, although their effects on EVT migration were not studied (286). Activating S1PR1, but not S1PR3, in these cells increases trophoblast invasion. This outcome is mediated through ERK-1/2 (Figure 1.5) and increased MMP-2 mRNA expression (287). Alternatively, treating HTR8/SVneo cells with miR-125b-1-3p reduces EVT invasion by decreasing S1PR1 expression (254). These studies suggest that specific activation of S1PR1 induces EVT migration and invasion. Hence, investigating specific activators of S1PR1 and testing induction of EVT migration could lead to effective therapeutics.

1.4.3.2. S1P, CERs, and Villous Trophoblasts

Brunnert et al. reported that BeWo cells express S1PR2 mRNA more abundantly compared to other S1P receptors (274). Primary human trophoblasts isolated from term placentas express S1PR1-3 with minimal to almost no expression of S1PR4 and S1PR5. S1PR5 is, however, expressed in placental biopsies where all cell types are present, albeit at minimal levels (288). Another study revealed that primary human CTs, ST, and EVTs from the early first trimester express S1PR1 and S1PR2 predominantly, with some expression of S1PR3 (273).

Treating CTs with epidermal growth factor (EGF), which promotes syncytialization and trophoblast viability, increases SphK1 activity partially through the actions of PI3K (289). Inhibiting SphK1 with N,N-dimethylsphingosine (DMS), a dual SphK1 and SphK2 inhibitor, induces cytotoxicity and apoptosis, confirming the importance of these enzymes for trophoblast viability (289). EGF treatment also decreases intracellular levels of CER and independently inhibits the DNA nicking induced by C16:0-CER (290). This implies that EGF promotes trophoblast survival by altering the S1P: CER rheostat by decreasing CER levels and increasing S1P levels by increasing SphK1 activity. Moreover, upon treating cultures with alkaline or acid ceramidase inhibitors, only acid ceramidase inhibitors induce apoptosis of trophoblasts despite an increase in CER levels in the presence of either inhibitor. Treating trophoblast cultures with EGF in the presence of an ACER inhibitor is unable to rescue trophoblasts from IFN- γ induced apoptosis (290). Treating primary trophoblasts with C16:0-CER in the presence of QVDOPh, a caspase-8 inhibitor, also decreases cell fusion (277). Hence, C16:0-CER, which is increased in mothers with PE (170), increases apoptosis and decreases cell fusion of placental trophoblasts. Alternatively, treating primary human trophoblasts with C8:0-CER increases hCG secretion without affecting trophoblast fusion or viability (291). Hence, sphingolipids are important factors that contribute to the disordered placental phenotype seen in pregnancy pathologies like PE, and more investigation into the S1P: CER rheostat is warranted.

According to the Human Protein Atlas, the transporters that carry S1P outside of the cell, ABCG2, SPNS2, and MFSD2B are expressed in the placenta. Notably, inhibiting ABCG2 with Ko143 in BeWo cells or primary trophoblasts increases apoptosis, but only in the presence of TNF- α and IFN- γ (292). In this study, siRNA knockdown of this transporter in BeWo cells in the presence of these cytokines or C2:0- or C8:0-CERs also increases apoptosis. This highlights the

protective role of extracellular S1P signaling against trophoblast apoptosis and can provide a mechanism to explain the increased inflammatory-mediated apoptosis of trophoblasts in PE pregnancies.

Primary human CTs express high levels of SphK1 protein prior to spontaneous fusion that occurs after three days in culture. Once the cells become terminally differentiated to form ST, SphK1 expression drops to 80% of its original value. In contrast, the levels of SphK2 are below the level of detection in CTs and ST (46). SGPP2 protein expression does not fluctuate throughout differentiation (46). In keeping with the reduced SphK1 levels in differentiated cultures, S1P levels in supernatants decrease by 10-fold after three days of culture. Sphingosine, the precursor of S1P, also decreases by 30% at this same time (46). This decrease in SphK1 and S1P levels that is associated with an increase in differentiation highlights an inhibitory role for SphK1 and S1P in the syncytialization process.

Treatment of trophoblasts with S1P, but not sphingosine, decreases the expression of GCM-1, a transcription factor for syncytin-1 (46). Syncytin-1 is a commonly used marker for syncytium formation because it is only expressed by ST and thus GCM-1 is a marker of increased syncytialization. S1P, but not sphingosine, decreases cell fusion rates, potentially by increasing Akt phosphorylation. Inhibiting SphK1 produces the opposite effect. Contradictory with other syncytialization markers, S1P treatment increases placental alkaline phosphatase activity (PLAP), a marker for differentiation (46). Another study showed that S1PR-G_i coupling lowers cAMP levels, hCG secretion, and PLAP levels but not fusion of primary human trophoblasts (293). Inhibiting SphK1 in primary CTs with the non-specific inhibitor, N,N-dimethylsphingosine, decreases cell viability and increases apoptosis (289). This indicates that

trophoblast syncytialization is a multi-faceted process and that S1P is a negative regulator of some aspects of differentiation (Figure 1.5), but not of cell fusion.

Treating pregnant mice at gestational day 15.5 with SKI II, an SphK1 inhibitor, decreases the cytokine storm induced by lipopolysaccharide (LPS). SKI II decreases the expression of TNF- α , IL-1 β , IL-10, and IL-6 and also decreases neutrophil infiltration into the placental labyrinth, the site of maternal-fetal exchange in the mouse placenta (294). S1P plays a role in stimulating inflammation (295). Blocking SphK1 activity and decreasing S1P levels should reduce inflammatory cytokine release and neutrophil migration into human placental villi.

1.4.3.3. S1P, CERs, and Placental Vasculature

About 80% of embryos and placentas from *Sphk1*^{-/-}*Sphk2*^{+/-} mice at gestational day 8.5 of pregnancy are absorbed. Uteri from gestational days 9.5 and 10.5 from these mice are intensely dark red, indicative of hemorrhaging (231). Treating pregnant ewes with FTY720 decreases blood vessel density in the placenta (230). Although not tested in the ewe study, FTY720 can act as a functional antagonist for S1PR1. This means that decreased S1P-S1PR1 signaling can impede blood vessel development. This highlights the important role of S1P and S1PR1 in angiogenesis during pregnancy.

Globally knocking out S1PR1 is embryonically lethal due to inadequate vascularization and hemorrhage (262). In contrast, S1PR2 or S1PR3 KO mice show only minor alterations in phenotype. However, S1PR2 KO mice have an increased risk of seizures between 3 and 7 weeks of age (263, 264). LPP3 KO in mice is lethal and results in pregnancy loss between embryonic days 7.5 to 9, the period in which vascular development peaks. Mouse embryos with an LPP3

deficiency fail to form a placenta in part through poor vasculogenesis throughout the yolk sac (296).

The Hemmings lab showed that human placental arteries express S1PR1-5 with the highest levels for S1PR3 and S1PR5 (34). S1P acts as a vasoconstrictor in arteries from the human placental chorionic plate and the stem villi. However, modulation by S1P-induced nitric oxide only occurs in arteries from the stem villi. Using Y27632, a ROCK inhibitor, our lab elucidated that S1P-mediated vasoconstriction is in part mediated by ROCK activation. This vasoconstriction occurred due to an increase in Ca^{2+} -sensitization (Figure 1.5) (34). There is a crucial role for S1P bound to HDL in fetal cord blood to reorganize actin filaments in endothelial cells and thus conserve the arterial endothelial cell barrier of the fetal placental vasculature through the activation of S1PR1 (172). Moreover, HDL-bound S1P activates S1PR1 in the placental vasculature and reduces the formation of reactive oxygen species, the release of the pro-inflammatory cytokines, IL-1 β and IL-8, and the mRNA levels of downstream effectors for TNFR1 (297). This indicates that HDL-bound S1P, which is decreased in PE (205), exerts its protective effects on placental vasculature by signaling through S1PR1. Since blocking S1P synthesis also showed a decrease in inflammation (294), it is important to decipher the effect of differential S1PR signaling, S1P carriers, and cell type in determining the effect of S1P.

Notably, the levels of total sphingomyelin species, dihydrosphingosine, and mRNA expressions for S1PR1 and SGPL1 increase in placental chorionic arteries of women with PE (172). On the other hand, C20:0-CER and S1PR1 mRNA and protein levels decrease in chorionic arteries of women with PE. Total CERs, total sphingosine, S1P metabolic enzymes, and S1PR3 levels remain unchanged. However, mRNA expression for S1PR2 and SGPPL are increased in isolated endothelial cells from fetal placental arteries obtained from PE pregnancies

(172). This is in discordance with other literature that indicates a decrease in S1PR1 expression and an increase in S1PR2 expression in PE (234) and can be explained by the heterogeneity of placental tissue. Moreover, this raises important objectives for future studies to test the roles of S1PR1/2 in the vascular dysfunction found in women with PE (172). Finally, treating mice at gestational day 7.5 with acid ceramidase-1 inhibitors, Ceranib-2 and D-NMAPPD, leads to a decrease in placental and fetal weight, potentially due to the accumulation of CER species, which promote trophoblast autophagy. This inhibition also increases the accumulation of long-chain CERs and disruption of placental morphology, including reduced placental vascularization, labyrinth zone branching, and area of the junctional zone (175).

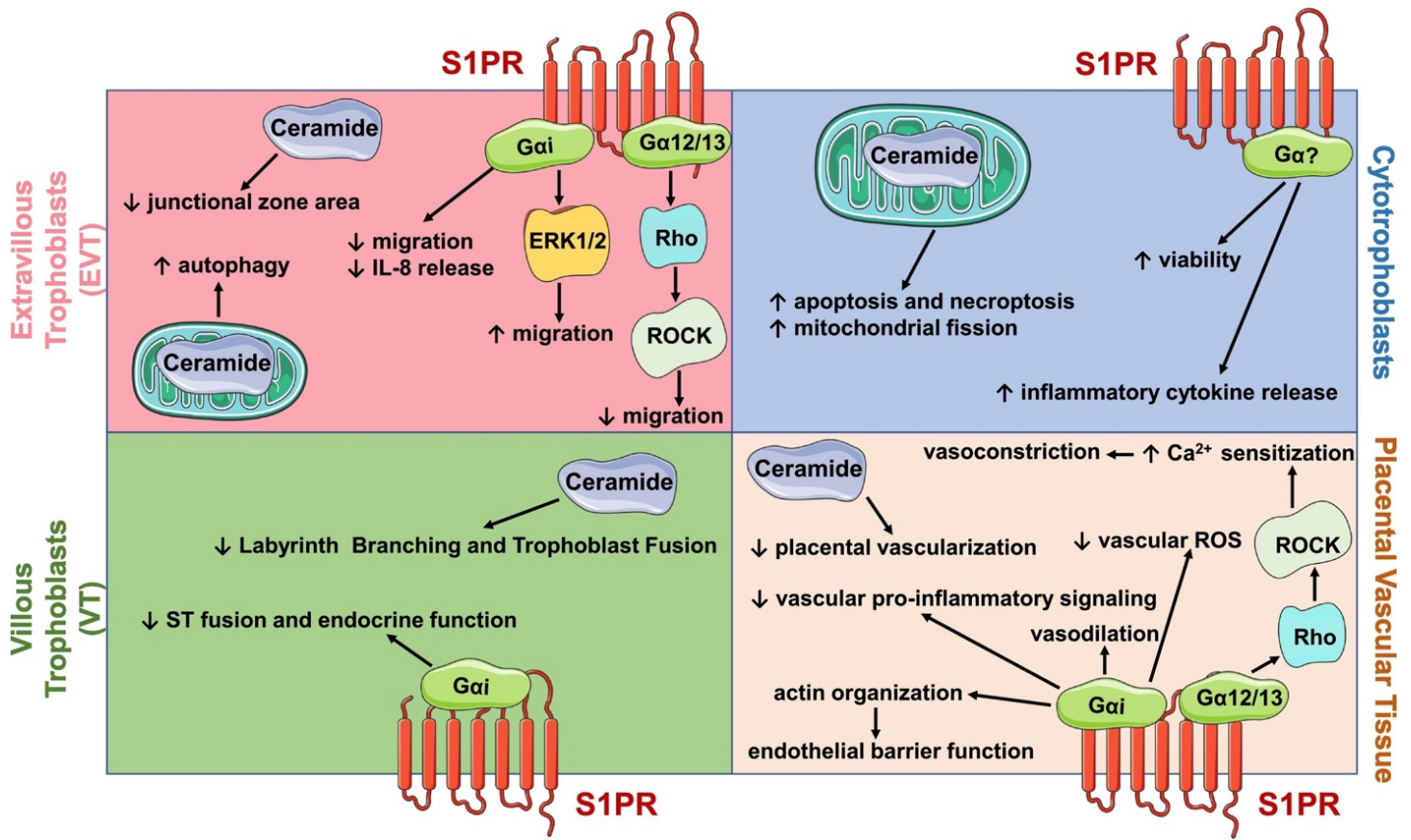


Figure 1.5: Known Pathways of S1P and CER Signaling in Placental Function

In the placenta, sphingosine 1-phosphate (S1P) generally mediates protective cellular processes whereas ceramide (CER) induces destructive processes. In normal physiology, these processes occur within the right balance to conserve the structure and function of the various cells that compose the placenta. S1P increases cytotrophoblast (CT) viability and pro-inflammatory cytokine release. Depending on the cell line used, S1P decreases or increases EVT migration by activating S1PR1 and S1PR2. S1P decreases villous trophoblast syncytialization, albeit the mechanisms of this action remain unexplored. S1P generally acts as a vasodilator. S1P can also induce vasoconstriction and maintains endothelial barrier function potentially by decreasing vascular reactive oxygen species (ROS) and pro-inflammatory signaling. On the other hand,

CER increases trophoblast death. More specifically, CER species increase EVT autophagy, and CT apoptosis and necroptosis. CERs decrease junctional zone areas in murine pregnancies as well as labyrinth branching. CERs inhibit the syncytialization or fusion of the placental barrier, increase CT mitochondrial fission, and disrupt placental vascularization. This image is from (9).

1.5. Piezo1 in the Placenta

As previously mentioned, circulating S1P levels are elevated in PE (170, 176). Since TNF- α can activate SphK1 and increase S1P levels in non-placental endothelial cells (162, 298-300), elevated TNF- α could be one of the factors that could explain this increase in circulating S1P in PE (4). However, another mechanism for this S1P increase can be through the activation of Piezo1, a transmembrane mechanosensitive cation channel (Figure 1.6). Recently, a study showed that Piezo1 inhibition or knockout in zebrafish embryos decreases epithelial barrier apoptotic cell extrusion, resulting in epithelial mass formation (301). Eisenhoffer and colleagues illustrated that Piezo1 activation due to overcrowding increases the release of S1P, and the Piezo1-induced cell extrusion is mediated via S1P release (302).

Activation of Piezo1 induces the influx of Ca²⁺ and other cations into cells (303). In endothelial cells, Piezo1 channels can be activated with a force-by-lipids mechanism, occurring through mechanical changes in the membrane due to factors such as shear stress (304). Piezo1 activation can result in the downstream activation of G proteins. For instance, the activation of Piezo1 by mechanical forces such as shear stress results in the release of ATP and activation of the G_q/G₁₁ signaling cascade (305). Another pathway involves the shear stress mediated activation of Piezo1 and subsequent release of adrenomedullin, thus activating its G_s-coupled receptor cascade (305). However, controversy remains on the exact mechanism of Piezo1 signaling with some investigators suggesting that G_q/G₁₁ activation by shear stress is independent

of Piezo1 (306). The interaction between Piezo1 and G protein-coupled receptors suggests a possible interaction between Piezo1 and S1P, which signals through G protein-coupled receptors, S1PR1-5. Hence, an unexplored pathway through which S1P levels and signaling are altered in the placenta is through Piezo1.

Two mechanisms for Piezo1 activation have been proposed: the lateral membrane tension model, which is explained by changes in the lipid membrane activating the mechanosensitive channel; and the tethered spring model which is explained by changes in the extracellular matrix or cytoskeleton activating mechanosensitive channels (307, 308). Piezo1, then, can be activated by membrane tensions resulting from membrane stretching and crowding (302). Using these sensing mechanisms, increased signaling through Piezo1 channels maintains homeostasis among epithelial cells by regulating cell proliferation and cell apoptosis (302, 309). During the syncytialization process in placental development, a balance of proliferation and apoptosis is required to maintain healthy syncytium function (61). Increased trophoblast death and decreased proliferation, differentiation, and fusion result in a weakened syncytium which is observed in PE (310); however, it is unknown whether Piezo1 regulates this balance in the placenta. It is also unknown whether a change in Piezo1 expression can explain the resulting imbalance between trophoblast death and proliferation that is seen in placentas of women with PE. Piezo1 induces differentiation of various cell types, such as mesenchymal stem cells (311). However, its role in trophoblast differentiation has not been investigated.

Alternatively, membrane lipid metabolism, such as membrane sphingolipid cleavage, may lead to changes in membrane tension. Piezo1 can also be activated by high flow or shear stress conditions (312). Piezo1 has been found in vascular endothelial cells, chondrocytes, astrocytes, human fetal endothelial cells, and rat uterine arteries (304, 312, 313). Piezo1 function

has been mainly investigated due to its Ca^{2+} -mediated effects on vasodilation of blood vessels; however, it has recently been shown to regulate epithelial cell proliferation and apoptosis.

Piezo1 is important in fetal development (314), but limited studies exist on the physiology and mechanism of the channel in pregnancy. Indeed, Piezo1 is present in uterine arteries, and expression of the protein in these arteries is higher in those of pregnant rats (312). *Piezo1*^{-/-} have extremely low survival rates past embryonic days 9.5 and 11.5, with the longest survival being E16.5. This timing of lethality coincides with the development of the placenta (315), highlighting a leading role for Piezo1 in this process. Specifically, the vasculature of *Piezo1*^{-/-} mouse embryos consists of smaller vessels with greater disorganization compared to the wild type (315). Moreover, an endothelial specific *Piezo1*^{-/-} knockout reduces the shear-stress induced intracellular Ca^{2+} current and decreases the alignment of the endothelial cells in response to shear stress (315). These findings provide evidence that Piezo1 plays a critical role in the cellular response to shear stress in development.

Piezo1 is a relatively novel mechanosensory channel and hence its mechanical inducers in the placenta remain unclear although Piezo1 responds to shear stress in uterine vascular tissue (312, 314). Optimal shear stress is necessary for syncytial function where both upper and lower ranges of shear stress are detrimental for syncytialization (316-318) but the role of Piezo1 in this is unknown. Piezo1 also responds to membrane crowding and stretching in epithelial layers (319). Recently, BeWo cells, a choriocarcinoma trophoblast cell line, was shown to respond to membrane stretch induced by cell membrane lipid remodelling (320). Recently, mechanosensory stimuli and channels were identified as key regulators of syncytialization. Sanz et al showed that high flow induces rabbit trophoblast syncytialization through a Ca^{2+} -dependent mechanism (318). Moreover, high flow reduced apoptosis in the JAR cell line and increased placental

growth factor levels from syncytia derived from primary human trophoblasts (317). With respect to mechanosensory channels, much of the focus in placental syncytialization has been on the transient receptor potential villanoid family (TRPV). For instance, activating TRPV6 on BeWo-derived syncytia with fluid shear stress induces microvilli formation, a characteristic of a mature syncytium (316). TRPV6 also induces proliferation and inhibits apoptosis of trophoblasts (321). On the other hand, TRPV1 induces apoptosis and hinders syncytialization (322). This hints at a role for mechanosensory channels in placental function and their disruption in placental disorders like PE. Little is known about a role for Piezo1.

Piezo1 activation has recently been associated with the induction of pro-inflammatory pathways in a variety of cell types (12, 323-325). Piezo1 expression also increases in response to inflammatory cytokines. For instance, Piezo1 mRNA increases in chondrocytes treated with interleukin-1 alpha (IL-1 α) (326). No evidence on the role of Piezo1 in placental inflammation, a hallmark of PE, is available.

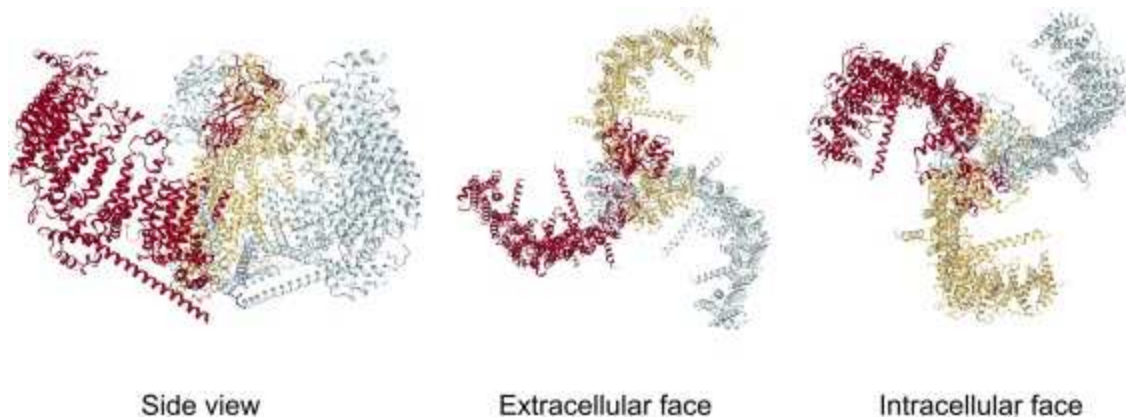


Figure 1.6: Structure of Piezo1

The structure of the transmembrane Piezo1 mechanosensory channel is depicted from the side view, the extracellular face, and the intracellular face. Piezo1 channel is a mechanosensory

nonselective homotrimeric channel activated by shear stress and fluid flow. Permission was sought and granted from the primary author and the journal as outlined in Appendix A (327).

1.6. Synthesis and Rationale

SphK1 and S1P are implicated in downstream signaling pathways of multiple pro-inflammatory cytokines, including TNF- α (162). In endothelial cells, the TNFR signaling pathway involves S1P as a cofactor and the binding of SphK1 to TRAF (298-300). The addition of TNF- α to human umbilical vein endothelial cells (HUVECs) (6, 7), hepatocytes (328), lung cell line (329), fibroblast cell line (329), cochlear cells (330), and neutrophils (331) activates SphK1 leading to S1P secretion. *In vivo* models demonstrate that some of the TNF- α -induced responses may in fact be through the S1P signaling system, as in cases of inflammatory pathologies like atherosclerosis and rheumatoid arthritis (162). TNF- α treatment also leads to mRNA and protein upregulation of S1PR2 in cultured human microvascular endothelial cells and to increased vascular permeability, a hallmark of inflammation (332). However, in fibroblast-like human synoviocytes, the addition of TNF- α upregulates S1PR3 mRNA and protein leading to inflammatory cytokine secretion, with no effects on S1PR1,2 expression (333). Thus, TNF- α alters S1PRs expression and modifies S1P levels by affecting its regulatory enzymes' activity and this varies depending on the cell type.

No studies examining the role of S1P signaling in the detrimental effects mediated by TNF- α in the placenta have been published to this day. Given the importance of both TNF- α and S1P on placental function and pregnancy outcomes, it is essential to understand the relationship between TNF- α and S1P. Piezo1 expression increases in response to inflammatory cytokines. Astrocytes pretreated with proinflammatory LPS, a stimulator of TNF- α signaling, increased the expression of Piezo1 (12). Piezo1 mRNA also increases in chondrocytes with IL-1 α treatment

(326). It is unknown whether TNF- α induces ST dysfunction by increasing Piezo1 activation or expression in the ST.

As mentioned, Eisenhoffer et al found that Piezo1 activation increased epithelial cell extrusion via S1P release (302). Recently, mechanosensory stimuli and channels were shown to elicit a variety of responses on trophoblast differentiation, fusion, and survival (334), depending on the channels activated. Since the ST is an epithelial barrier, it is crucial to maintain the balance of CT fusion and extrusion of syncytial knots to maintain barrier integrity. It is currently unknown whether the ST expresses this channel and whether Piezo1 activity and expression may have a role in ST function.

1.7. Aims, Hypothesis, Significance:

Overall, I hypothesize that TNF- α will be dependent on S1P signaling to induce syncytial dysfunction. It will do this by activating and increasing the expression of S1P synthesizing enzymes, decreasing the expression of S1P degrading enzymes, and altering S1PR expression/activation. I also hypothesize that Piezo1 will mediate the interaction between TNF- α and S1P and their effects on the syncytium. Four studies were undertaken to better understand the contribution of S1P and Piezo1 signaling in the detrimental effects of TNF- α in placental dysfunction in PE.

The first study investigated the levels of S1P metabolic enzymes in cultured placental villous explants, isolated from term placentas of healthy pregnancies, throughout ST formation. Since SphK1 expression in primary human CTs decreases to 80% of its original value after three days of differentiation and fusion, I hypothesized that SphK1 and SphK2 expression will decrease with ST formation, and SGPP1, SGPP2, SGPL1, and LPP3 will increase with ST

formation. S1P circulating levels are increased in mothers with PE; however, whether elevated placental SphK1 is the source of this increase is unknown. In the second part of this study, I measured the difference in levels of placental SphK1 in healthy pregnancies and those complicated with PE. I hypothesized that SphK1 will be higher in the placentas of women with PE. Since PE is characterized by high levels of TNF- α , I also explored the role of TNF- α in regulating S1P synthesizing and metabolizing enzymes in cultured villous explants. I also measured the effect of high levels of TNF- α on SphK1 expression in cultured primary human CTs. Since TNF- α disrupts ST formation and SphK1 activity also disrupts ST formation, I hypothesized that treating villous explants with TNF- α will increase S1P synthesizing enzymes, SphK1 and SphK2, and decrease S1P breakdown enzymes, SGPP1/2, SGPL1, and LPP3.

The second study investigated the role of SphK1 in mediating the functions of TNF- α in cultured placental villous explants. Independent studies show that TNF- α and S1P decrease syncytialization. Moreover, TNF- α activates SphK1 leading to S1P release in various cell types. SphK1 is a cofactor in TNF- α -TNFR1 signaling which activates NF- κ B, leading to the increase in inflammatory cytokines and growth factors and the induction of cell death. I hypothesized that blocking SphK1 activity will block TNF- α -induced ST shedding, placental cell membrane damage, placental inflammatory cytokine release, and syncytialization.

The third study investigated the role of S1PR2 in ST formation and TNF- α regulation of S1PRs in villous explants, a trophoblast cell line, and primary human CTs. The study also explored the levels of S1PRs in placentas from normal pregnancies and those complicated with PE. Studies in various cell types suggest that S1PR2 signaling is involved in cell differentiation, inflammatory cytokine release, and apoptosis. The role of S1PR2 was examined in syncytialization and placental cell membrane damage of explants. TNF- α increases S1PR2

expression in non-placental microvascular cells. For those reasons, I predicted that it is the main receptor affected by TNF- α signaling in the placenta. I also examined the effect of TNF- α on S1PR1 expression, as S1PR1 has protective properties, as summarized above. Hence, I examined whether placental S1PR1 and S1PR2 expression are altered in PE and whether that correlated with altered expression of these receptors in response to TNF- α in villous explants, a BeWo cell line model, and in primary CTs. I hypothesized that activation of S1PR2 will decrease ST function and increase cell death. I also hypothesized that TNF- α will decrease S1PR1 expression and increase S1PR2 expression in all listed models.

The final study explored the role of Piezo1 activation in placental cell death, ST formation, and inflammation as well as the intersection of Piezo1 signaling with TNF- α and SphK1. Piezo1 was recently identified in the rat placenta, but its expression is unclear in human placentas. Other mechanosensory channels are implicated as regulators of trophoblast syncytialization. Piezo1 exerts its effects on epithelial extrusion by releasing S1P. Moreover, inflammatory cytokines increase Piezo1 expression. However, the effect of TNF- α on Piezo1 expression and activity in the placenta and specifically in trophoblasts is unclear. Moreover, Piezo1 induces cell damage and apoptosis in other cell types by stimulating inflammatory cytokine release. So, this study investigated the placental expression of Piezo1 in healthy pregnancies and in those complicated with PE. It also investigated the interaction of Piezo1 with TNF- α and SphK1 on placental function. I hypothesized that Piezo1 activity will increase ST formation, inflammatory cytokine release, and placental cell death. TNF- α will enhance Piezo1 functions. Piezo1 functions will be dependent on SphK1 activation.

Understanding the interactions between TNF- α , S1P signaling, and Piezo1 in the placenta will aid in understanding the mechanisms of placental dysfunction in PE. Despite TNF- α playing

a key role in the development and exacerbation of the PE phenotype, market available TNF- α inhibitors are still controversial for usage during pregnancy due to potential off-target effects (335). TNF- α plays key roles in the early stages of pregnancy and in later stages during fetal development. TNF- α is a multifaceted and pleiotropic molecule involved in multiple signaling pathways. The aim of my thesis was to identify potential secondary targets in the TNF- α -induced dysfunction found in PE. In my studies, I explored various S1P pathway components, enzymes and receptors, as well as Piezo1, a mechanosensory channel that can signal through S1P, as downstream components of TNF- α detrimental signaling. Identifying S1P pathway components and Piezo1 as downstream factors in the TNF- α signaling pathway will help identify an arsenal of more specific pharmaceutical targets that can improve placental function and alleviate the PE phenotype. Additionally, understanding the interactions between TNF- α , Piezo1, and S1P pathway components can help identify off-target effects resulting from the market-available drugs that target these molecules.

2. Chapter 2: Material and Methods

2.1. General Methods

2.1.1. Placenta Samples

Women were recruited and provided written informed consent. The study was approved by the University of Alberta Health Research Ethics Board (Pro00034274, continuously approved since November 15, 2012, continuously approved since then with the latest renewal approved on January 2, 2022) and conformed to the standards set by the Declaration of Helsinki. Term placentae were collected immediately after elective caesarean section deliveries at the Royal Alexandra Hospital (Alberta, Canada) from women with no health complications and from women with PE. Women with multiple pregnancies, metabolic comorbidities (thyroid, diabetes, obesity) or of advanced maternal age were excluded from the study to minimize confounding variables. Women with PE were defined as those who had blood pressures above 140/90 mmHg on two occasions measured 6 hours apart and at least 30 mg/dL proteinuria in a 24-hour collection. Three evenly spaced 6 mm² placental biopsies were obtained from term placentas in the area between the umbilical cord and the edge of the placenta. Biopsies were taken at least 1 cm way from the umbilical cord or the edge of the placenta. Samples were collected within 2 hours of delivery. In total, 17 and 12 placentas were obtained from women with healthy pregnancies and PE, respectively.

2.1.2. Placental Explant Culture

Placental chorionic villi were dissected within 1-2 hours following delivery and washed 3 times with gentle shaking using Hanks' Balanced Salt Solution (Hyclone Laboratories Inc, ThermoFisher Scientific). A diagram of a dissected villous explant structure and organization is shown in Figure 2.1. A self-regenerating explant culture method was adapted from Siman et al

and Trowell (336, 337) by culturing explants at the gas-liquid interface. Briefly, three x 2 mm³ blocks of chorionic villi were placed onto inserts with 8 µm pore polyethylene terephthalate membranes (353182, ThermoFisher Scientific), as shown in Figure 2.2. Inserts were placed into wells in a companion 12-well plate. 550 µL of Iscove's Modified Dulbecco's Media (IMDM, Hyclone Laboratories Inc, ThermoFisher Scientific) with 1% Penicillin-Streptomycin, 1% antibacterial/antimycotic, and 1% ITS+1 Liquid Media Supplement (MilliporeSigma, Toronto, ON, Canada) was added to the wells in the companion plates. The plates were incubated at 37°C in 5% CO₂ and the media was changed every 48 hours.

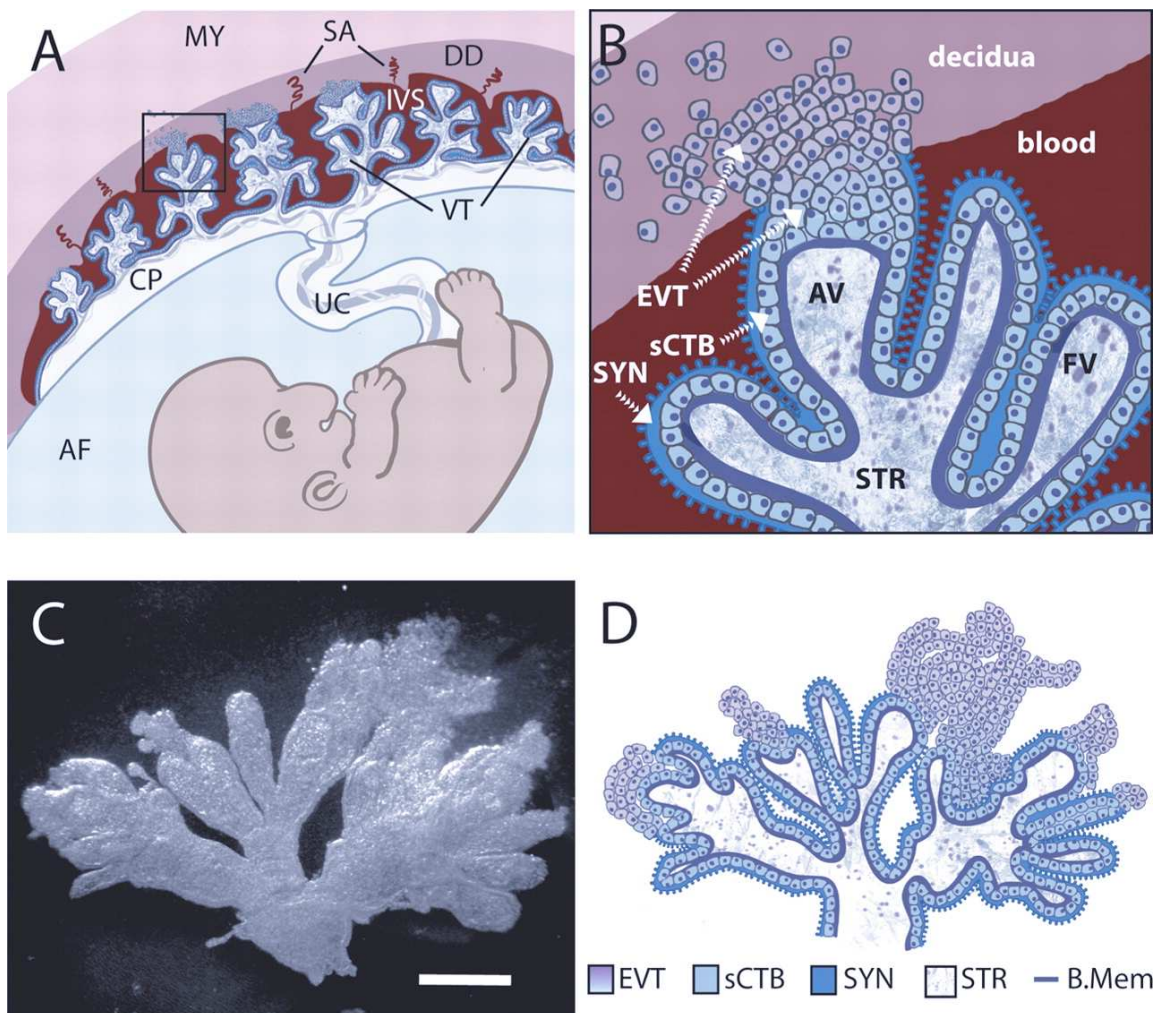


Figure 2.1A-D: Structure and Organization of a Dissected Villous Explant

Placental villi include anchoring villi (AV) and floating villi (FV). Placental villi are composed of villous trees (VT), extravillous trophoblasts (EVT), stem-like cytotrophoblasts (sCTB), the multinucleated syncytium (SYN), villous stroma (STR), and the basement membrane (Mem). The myometrium (MY), spiral arteries (SA), decidua (DD), intervillous space (IVS), chorionic plate (CP), umbilical cord (UC), and amniotic fluid (AF) are the placental and villous surrounding structures. Villi in the figure represent those of a 6-week pregnancy. This image is from (338). Permission was sought and granted from the primary author and the journal as outlined in Appendix B.

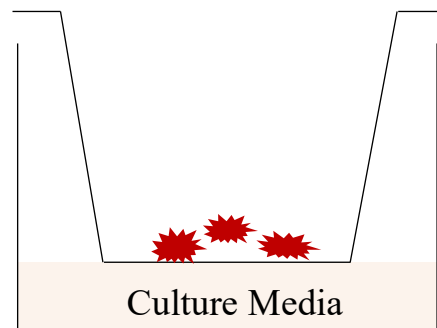


Figure 2.2: Placement of Villous Explants in the Insert Well

Three villi were placed per insert. Villous explants were placed in a manner where they had no contact with the insert walls and no contact with each other. Culture media was added to the well of the companion plate, such that the explants were cultured on the gas-liquid interface.

2.1.3. Immunohistochemistry of Placental Biopsy Sections

Placental biopsies were collected from placentas within 2 hours of delivery from the area between the umbilical cord and the placental edge. Three evenly spaced 6 mm² biopsies from each patient were embedded into one mold with Tissue-Tek® O.C.T. (#4583, ThermoFisher Scientific, Waltham, MA, USA). Three 8 µm sections from varying depths of 1 mold were cut on a cryostat and these sections were placed on a Superfrost slide (ThermoFisher Scientific). The sections were fixed with 100% ice-cold methanol for 20 minutes at -20°C and blocked for 1 hour with 10% normal goat serum. The sections were then incubated in a moist chamber simultaneously with a rabbit anti-SphK1 primary antibody (1:80, ab46719, Abcam, Cambridge, England) or a Piezo1 primary rabbit antibody (1:200, Proteintech 15939, Rosemont, IL, USA) in addition to a mouse anti-E-cadherin primary antibody (1:200, 55413, R&D Systems, Minneapolis, MN, USA) in 1xPBS overnight. SphK1 specificity was confirmed using protein-protein blast with a 100% query coverage (National Library of Medicine, National Center for Biotechnology Information). E-cadherin and Piezo1 antibodies were validated in the following papers, respectively (339, 340). E-cadherin localizes at the apical membrane of the CT layer which fuses into the basal membrane of the syncytial region. Syncytialized portions were defined as nuclei external to the E-cadherin demarcation. Slides were washed 3 times with 1xPBS for two minutes per wash. AlexaFluor goat anti-rabbit 488 and goat anti-mouse 594 (1:200, A32731 and A11032, Invitrogen, Waltham, MA, USA) secondary antibodies were added simultaneously and incubated in the dark for 1 hour at room temperature. After washing 3 times with 1xPBS, the sections were incubated for 10 minutes in the dark with DAPI (4',6-diamidino-2-phenylindole, 1:100, D1306, Invitrogen). The slides were washed again and mounted with PermaFluor Aqueous Mounting Medium (TA-030-FM, ThermoFisher Scientific). Three randomly selected

areas from each section were imaged using the 20x objective on Zeiss Axio Observer (Zeiss, Oberkochen, Germany) and Zen Black software (Zeiss, Toronto, ON, Canada). Images were analyzed using ImageJ software (U.S. National Institutes of Health, Bethesda, MD, USA). Briefly, images were set to a consistent threshold value, and mean integrated density was calculated. Integrated density values were normalized to the number of nuclei in the image, calculated through the “Analyze particles” function on ImageJ. Normalized values for each sample were averaged and the standard error of the mean was determined.

2.1.4. Placental Tissue RNA Isolation

Placental tissue was collected in a similar manner as described above and was placed into liquid nitrogen. The frozen samples were wrapped into aluminum foil, re-submerged in liquid nitrogen, and crushed using a mortar and pestle until the tissues were in powder form. Next, each sample was transferred into a 2 mL PCR tube containing a single steel bead (QIAGEN, Toronto, ON, Canada). Each tube was then filled with 1 mL of TRIzol reagent (Life Technologies, Fisher Scientific Company). The samples were lysed using a TissueLyser II (QIAGEN) at a setting of 25.00 frequency/s for 2 minutes, repeated 3 times. 200 μ L of chloroform was then added to each sample before vigorously shaking for 1 minute, followed by a 5-minute incubation at room temperature. Samples were then centrifuged for 15 minutes at 15,000 rcf at 4°C. Following this step, the RNA layer (aqueous top layer) was extracted and transferred to a new 2 mL tube and the Invitrogen RNA isolation kit was used to purify the isolated RNA. Finally, quantification of the RNA in these samples was carried out using the Nanodrop Spectrophotometer (ThermoFisher Scientific). Samples that were below a 260/280 ratio of 1.7 were discarded, but this was very uncommon with the isolation kit that was used.

2.1.5. Quantitative PCR

Purified RNA was reverse transcribed into cDNA using 500 ng of total RNA, 4 μ L of ABM 5x all-in-one RT MasterMix (AT6490, ABM Life Sciences, Vancouver, BC, Canada), and Ultra PureTM Distilled Water (110977-015, Invitrogen) as needed to reach a final volume of 20 μ L. The primer sequences for the genes of interest and the housekeeping gene, hypoxanthine-guanine phosphoribosyl transferase (HPRT1), were designed using OligoPerfect Designer (Integrated DNA Technologies, Coralville, IA, USA) and listed in Table 2.1 below. The PCR reaction was carried out using Applied Biosystems Power UpTM SYBR[®] Green MasterMix (100029284, Life Technologies), 0.6 μ L of primers (10 μ M), 6.3 μ L of Ultra PureTM Distilled Water, and 2.5 μ L of cDNA from each sample. The $\Delta\Delta$ CT method of relative quantification was used to analyze the results in Chapter 3. In the remaining chapters, the primer pair amplification efficiency was calculated using the slope of the standard curve with the following equation $E=10^{(-1/\text{slope})}$. Threshold cycle means were averaged from duplicate reaction wells. The means were corrected with the reaction efficiency and an internal sample control. The corrected values were then expressed relative to the housekeeping gene, HPRT1. The mathematical equation used for the relative qRT-PCR calculations was: Ratio = $[E_{\text{Piezo1}}^{\Delta\text{Ct}(\text{Control-Sample})}] / [E_{\text{HPRT1}}^{\Delta\text{Ct}(\text{Control-Sample})}]$

Gene	Forward Primer	Reverse Primer
HPRT1	5'-GAC CAG TCA ACA GGG GAC ATA A-3'	5'-AAG CTT GCG ACC TTG ACC-3'
SphK1	5'-CTG GCA GCT TCC TTG AAC CAT-3'	5'-TGT GCA GAG ACA GCA GGT TCA-3'
SphK2	5'-CCA GTG TTG GAG AGC TGA AGG T-3'	5'-GTC CAT TCA TCT GCT GGT CCT C-3'
SGPP1	5'-GGC CAG TGC ACC AAG GAC AT-3'	5'-TAC TGC CAG CGG CCA TAG GT-3'
SGPP2	5'-CAT TTG TGT TGG GAC TGG TG-3'	5'-TAT GAC ACA CAC GGG GAA GA-3'
SGPL1	5'-CCC ATT TGA TTT CCG GGT GA-3'	5'-ATG CCA CCC TGC CAA TCT GT-3'
LPP3	5'-CCC GGC GCT CAA CAA CAA CC-3'	5'-TCT CGA TGA TGA GGA AGG G-3'
S1PR1	5'- ACC CCA TCA TTT ACA CTC TGA CC-3'	5'-GGT TGT CCC CTT CGT CTT TCT-3'
S1PR2	5'-CCA ATA CCT TGC TCT CGG C-3'	5'-CAG AAG GAG GAT GCT GAA GG-3'
S1PR3	5'-TCA GGG AGG GCA GTA TGT TC-3'	5'-CTG AGC CTT GAA GAG GAT GG-3'
Piezo1	5'-TGA AGC GGG AGC TCT ACA AC-3'	5'-TCT CGT TGG CAT ACT CCA CA-3'

Table 2.1: Primer Sequences

2.1.6. BCA Protein Assay

Cells or tissues were placed in lysis buffer (20 mM Tris, 5 mM EDTA, 10 mM Na₄P₂O₇, 100 mM NaF, 1% NP-40) with a protease inhibitor cocktail (Sigma-Aldrich, St. Louis, MO, USA) mixed in a 100:1 ratio in a tube with a metal bead. Samples were lysed using the Qiagen Tissue Lyser III (Qiagen, Hilden, Germany) through three cycles of 25 shakes/s, with 2 minutes per cycle. Total protein was quantified using the Pierce BCA Protein Assay Kit (ThermoFisher Scientific) with an albumin standard following manufacturer recommendations. Samples were run in duplicates at a 1:10 dilution. Absorbance was measured with a Synergy HTX spectrophotometer (Agilent Technologies, Santa Clara, CA, USA) at a 562 nm wavelength.

2.1.7. Lactate Dehydrogenase (LDH) Quantification

Lactate dehydrogenase (LDH) is released from all cell types as a result of cell membrane damage and is a marker for cell death. Experimental supernatants were centrifuged at 15000 rpm for 15 mins, and supernatant LDH levels were measured with the CytoTox 96® Non-Radioactive Cytotoxicity Assay following the manufacturer's protocol (Promega, Madison, WI, USA). If LDH was present, then it would result in a color change to red due to the formation of Formazan, and the absorbance was read at 562 nm using a Synergy HTX spectrophotometer. Samples were run at a 1:2 dilution in duplicates. Culture media alone was used as a negative control and subtracted from the experimental sample absorbance values. Values were normalized to total protein mass and calculated as a ratio of the no-treatment control. Duplicate wells for each treatment were averaged.

2.1.8. Quantification of the Beta-Subunit of Human Chorionic Gonadotropin (β -hCG)

β -hCG is secreted by the ST and is a marker of a functional ST. β -hCG concentration from experimental supernatants was measured using an enzyme-linked immunosorbent assay (ELISA) with the ELISA 1911 kit (DRG Diagnostics, Marburg, Germany) following the manufacturer's instructions. After centrifuging the samples at 15000 rpm for 15 mins, the supernatant was collected and run at a 1:5 dilution with the manufacturer's supplied buffer. Absorbance was measured using the Synergy HTX spectrophotometer at a wavelength of 450 nm. The values from each assay obtained from the culture medium alone were subtracted from experimental sample values. β -hCG concentrations were extrapolated using spectrophotometer measurements compared to those from a standard curve. Measured concentrations were

normalized to total protein mass per well and calculated as a ratio of the no-treatment control. Duplicate wells for each treatment were averaged.

2.1.9. Quantification of Human Placental Lactogen (hPL)

hPL released into experimental supernatants was quantified using an ELISA EIA 1283 (DRG Diagnostics) following the manufacturer's instructions. Supernatants from explant cultures were centrifuged at 15000 rpm for 15 mins and the pellet was discarded. Samples were diluted 10-fold. A wavelength of 450 nm was used on the Synergy HTX spectrophotometer to measure the absorbance of the samples. Culture media alone was used as a negative control and subtracted from experimental sample values. The concentrations of hPL in samples were extrapolated using spectrophotometer measurements compared to those from a standard curve. Values were normalized to total protein per well and calculated as a ratio of the no treatment or vehicle control.

2.1.10. Quantification of Human Placental Alkaline Phosphatase Activity (PLAP)

PLAP activity was measured in both supernatants and tissues of villous explants. PLAP activity was measured from villous particles shed into the bottom wells of the insert cultures to estimate the amount of ST shedding in response to various treatments. All particles reaching the bottom well were less than the 8 μ M pore size. Experimental supernatants were diluted 10 times in manufacturer supplied buffer. Villous tissue was lysed in manufacturer supplied buffer and samples were diluted 80-fold. All samples were analyzed following the manufacturer's protocol (ab83369, Abcam, Cambridge, England). Briefly, phosphorylated p-Nitrophenol was added to the samples as a substrate. The alkaline phosphatase in the samples converts the substrate into the non-phosphorylated p-Nitrophenol, ultimately leading to a change in color. Absorbance was

measured with a Synergy HTX spectrophotometer at a 405 nm wavelength. The values from each assay obtained from the culture medium alone were subtracted from experimental sample values. PLAP activity of samples was extrapolated using spectrophotometer measurements compared to those from a standard curve. Measured concentrations were normalized to total protein mass per well and calculated as a ratio of the no-treatment control. Duplicate wells for each treatment were averaged.

2.1.11. Quantification of Cytokines

Supernatants from cultured explants were tested for 42 cytokines/chemokines in duplicate. Tests were performed by Eve Technologies (Calgary, Alberta, Canada) using a Luminex array with a Bio-Plex™ 200 system (Bio-Rad Laboratories Inc., Hercules, CA, USA) and a (HD42) kit (Millipore, St. Charles, MO, USA). All analytes analyzed and their full names are listed in Table 2.2 below.

Analyte	Full Name
EGF	Epithelial Growth Factor
Eotaxin-1 (CCL-11)	Eotaxin-1
FGF-2	Fibroblast Growth Factor-2
Flt-3L	Fms-Related Tyrosine Kinase 3 Ligand
CX3CL1	Fractalkine
G-CSF	Granulocyte Colony-Stimulating Factor
GM-CSF	Granulocyte-Macrophage Colony-Stimulating Factor
GRO- α (CXCL1)	Growth Regulated Oncogene alpha
IFN- α 2	Interferon alpha 2
IFN- γ	Interferon gamma
IL-1 α	Interleukin 1-alpha

IL-1 β	Interleukin 1-beta
IL-1RA	Interleukin Receptor Antagonist
IL-2	Interleukin 2
IL-3	Interleukin
IL-4	Interleukin 4
IL-5	Interleukin 5
IL-6	Interleukin 6
IL-7	Interleukin 7
IL-8	Interleukin 8
IL-9	Interleukin 9
IL-10	Interleukin 10
IL-11	Interleukin 11
IL-12(p40)	Interleukin 12 p40 subunit
IL-12(p70)	Interleukin 12 p70 subunit
IL-13	Interleukin 13
IL-15	Interleukin 15
IL-17A	Interleukin 17A
IL-18	Interleukin 18
IP-10 (CXCL10)	Interferon gamma-induced protein 10
MCP-1	Monocyte Chemotactic Protein 1
MCP-3	Monocyte Chemotactic Protein 3
MDC	Macrophage-Derived Chemokine
MIP-1 α (CCL3)	Macrophage Inflammatory Protein 1-alpha
MIP-1 β (CCL4)	Macrophage Inflammatory Protein 1-beta
PDGF-AA	Platelet-Derived Growth Factor AA
PDGF-AB/BB	Platelet-Derived Growth Factor AB/BB
RANTES (CCL5)	Regulated on Activation, Normal T cell Expressed and Secreted

sCD40L	Soluble Cluster of Differentiation 40 Ligand
TGF- β	Transforming Growth Factor beta
TNF- α	Tumor Necrosis Factor alpha
VEGF-A	Vascular Endothelial Growth Factor A

Table 2.2: Human Cytokine/Chemokine 42-Plex Discover Array Analytes Measured in Supernatants of Cultured Explants

2.1.12. Statistics and Analysis

Results were analyzed using GraphPad Prism (GraphPad Software, San Diego, CA, USA). Results from imaging and Western Blots were analyzed using a Student's T-test. Normalized fusion, β -hCG, LDH, PLAP, and cytokine/chemokine results from cultured explant experiments were analyzed using a two-way ANOVA and two-stage linear step-up procedure of Benjamini, Krieger, and Yuketieli post-hoc test to control for the false discovery rate. Dose-response experiments were analyzed using a non-parametric Kruskal-Wallis test and two-stage linear step-up procedure of Benjamini, Krieger, and Yuketieli post-hoc. A p value less than 0.05 was considered significant. All groups were subjected to post-hoc analyses. Only significant post-hoc p-values are shown in the figures.

2.2. Chapter 3 Specific Methods

2.2.1. Treatments and Experimental Protocols

Explants were pre-incubated for 4 days to allow the shedding of the original syncytium and all experimental treatments began on day 4 of culture at the start of the ST regeneration phase, as shown in Figure 3.1. Explants were treated with either TNF- α (1 or 10 ng/mL, a kind gift from Hoffmann-La Roche) alone or with 0-20 μ M PF-543 (PZ0234, MilliporeSigma), a

specific inhibitor that binds SphK1 at its active site (341). To test if inhibition of SphK1 could impact TNF- α effects, explants were pretreated with PF-543 (1 μ M) for 30 minutes before TNF- α (1 or 10 ng/mL) administration. Treatments were done in duplicates for 24 or 48 hrs prior to supernatant and tissue collection. Trophoblast fusion (described in 2.2.2), LDH release (described in 2.1.7), β -hCG release (described in 2.1.8), and PLAP-positive shed particles (described in 2.1.10), and cytokine and growth factor release (described in 2.1.11) were assessed.

2.2.2. Trophoblast Multinucleation and E-cadherin Staining

As a morphological assessment of syncytialization, multinucleated trophoblast areas were measured to assess CT fusion into the multinucleated ST. Cultured explants from duplicate wells (3 explants/well) were fixed in 1% Paraformaldehyde in PBS, embedded, and sectioned as described above. The 3 villi from each well were placed in 1 mold that was sectioned at 3 varying depths and these sections were placed onto 1 slide. Similar blocking and washing procedures were followed as described above. Samples were then incubated with the E-cadherin primary antibody (1:200) overnight. AlexaFluor-488 goat anti-mouse secondary antibody (1:200) and DAPI (1:100) were used as described above. Slides were similarly mounted as before and 20 Z-stacks of each image were captured with a confocal Zeiss LSM 700 microscope and Zen Black software (Zeiss, Toronto, ON, Canada). Three randomly selected fluorescent images were captured per section with the 20x objective and analyzed using ImageJ software. Syncytialized portions were defined as nuclei external to the E-cadherin demarcation. The total area of the syncytialized portions of the explants was measured and normalized against the total surface area of the villi.

2.3. Chapter 4 Specific Methods

2.3.1. Explant Treatments

Explants were incubated for 4 days to allow the shedding of the original syncytium and all experimental treatments began on day 4 of culture at the start of the ST regeneration phase. Explants from the same placenta were cultured in duplicates for various time points in a time course from 0 to 48 hours. Explants were either in the no treatment control group or treated with TNF- α (1 ng/mL). Villi were collected at the designated time points and processed for qRT-PCR to detect S1P metabolic and catabolic enzyme expression. Primer sequences are listed in Table 2.1.

2.3.2. Primary Trophoblast Isolation

Primary human CTs were isolated using a negative-selection column method previously developed by our lab (342). Placentas collected from healthy term pregnancies as described above were processed within 1 hour of delivery. Briefly, placental cotyledons were dissected, and maternal decidua and fetal membranes were trimmed. The remaining tissue was washed in 2% IMDM with fetal calf serum (FCS, Gibco, Grand Island, NY) to remove excess blood. Placental tissue was then scraped with a blunt blade to remove vascular and connective tissue. The remaining 100 mL of tissue was then digested with 2.5 μ g/mL of trypsin (272750-018, Gibco) and azide-free 0.1 μ g/mL DNase (Sigma) in 200 mL of Locke Ringer's Buffer Solution (pH=7.8, 0.154 M NaCl, 5.63 mM KCl, 8.33 mM D-glucose, 2.38 mM NaHCO₃). Digestions were completed at 37°C for a total of seven times, with the first two rounds of trypsinized cells discarded. The cells collected at the end of the other rounds of trypsinization were pooled and then cleared of red blood cells using a lysis buffer (150 mM NH₄Cl, 10mM NaHCO₃, 0.1 mM

Disodium EDTA) with gentle rotation for 2-8 mins. After washing, the remaining cells were incubated for 30 minutes with 10% NGS to prevent non-specific binding to the secondary antibody. After that cells were then incubated with mouse anti-human primary antibodies to CD9 (clone 50H.19, made in house, binds placental stromal cells), MHC Class I (clone w6/32, Harlan Sera-Lab, Crawley Down, Sussex, UK, binds all nucleated placental cells except for CTs, which do not express MHC Class I), and MHC Class II (clone 7H3, made in house, primarily binds cells of immune origin). After incubation, cells were pelleted, resuspended in 2% FCS in PBS, and run through columns containing glass beads coated with mouse IgG, the secondary antibody that all the primary antibodies would bind to once they are bound to the cells that are to be eliminated (Sigma). 1×10^6 cells were run per column at the drop rate of 1 drop per 7 seconds. Fibroblasts, white blood cells, endothelial cells, and smooth muscle cells adhere to the glass beads in the column, whereas CTs pass through the column and are collected. Collected cells were pelleted and frozen in a 10% Dimethyl Sulfoxide (DMSO) in FCS solution. Collected CTs were tested for purity by seeding 2×10^5 trophoblasts in fibronectin-coated 96-well plates (167008, ThermoFisher Scientific). After 24 hours of culture, trophoblasts were stained with mouse anti-human vimentin (1:200, MilliporeSigma) to quantify contaminating mesenchymal cells, most importantly fibroblasts. Trophoblast batches that had more than 4 contaminating cells per well were not used in these studies.

2.3.3. Experimental Protocol Used for Plating Primary Cultured Trophoblasts

The primary trophoblast cells were thawed into 10% FBS IMDM (MilliporeSigma), plated on fibronectin-coated (1:100, 33016015, ThermoFisher Scientific) Nunc Lab-Tek Chamber Slides (MilliporeSigma) and incubated under standard culture conditions. After 24 hours, the cells were washed three times with PBS. Next, the media was switched to 2% FBS

IMDM and the 24-hour treatment phase for the cells began. The cells were treated with different concentrations of recombinant TNF- α (0 ng/mL, 1 ng/mL, 10 ng/mL, and 20 ng/ml). At the end of the treatment phase after 24 hours, the cells were washed three times with 1xPBS. The cells were then fixed with 100% methanol for 20 mins at -20°C. The cells were blocked for one hour in 10% normal goat serum. The sections were then incubated in a moist chamber with a rabbit anti-SphK1 primary antibody (1:80, ab46719, Abcam, Cambridge, England) in 1xPBS overnight. Slides were washed 3 times with 1xPBS for two minutes per wash. AlexaFluor goat anti-rabbit 488 (1:200, A32731, Invitrogen, Waltham, MA, USA) secondary antibody was added and incubated in the dark for 1 hour at room temperature. The slides were then incubated with DAPI (Invitrogen) for 10 minutes and washed 3 times with 1xPBS for two minutes each wash. The negative control was the sample incubated only with the secondary antibody and not the primary antibody. A small drop of PermaFluor Mountant (TA-030-FM, ThermoFisher Scientific) was added to each sample before coverslips were placed. The slides were stored at 4°C in the dark before being visualized with the fluorescent microscope (Zeiss Axio Observer, Zeiss, Oberkochen, Germany) with the 20x objective.

2.4. Chapter 5 Specific Methods

2.4.1. BeWo Cell Culture

BeWo cells were cultured in DMEM: F12 medium (Gibco) with 10% FBS and 1% Penicillin-Streptomycin in 6-well plates (140675, ThermoFisher Scientific). When cells reached around 80% confluency, treatment began with 0-20 ng/mL of TNF- α or 20 μ g/mL of LPS as a positive control for 24 hours.

2.4.2. Explant Treatments

Explants were incubated for 4 days to allow the shedding of the original syncytium and all experimental treatments began on day 4 of culture at the start of the ST regeneration phase. Explants from the same placenta were cultured in duplicates for 48 hours with S1P or a S1PR2 inhibitor. S1P (0-10 μ M) was administered in 0.1% fatty-acid free bovine serum albumin in the regular explant media. To determine the role of S1PR2, explants were treated with 10 μ M of JTE-013, a potent S1PR2 inhibitor, for 48 hours. LDH release (described in 2.1.7), β -hCG release (described in 2.1.8), and hPL release (described in 2.1.9) were assessed.

For the time course explant experiments, explants from the same placenta were cultured in duplicates for various time points in a time course from 0 to 48 hours. Explants were either in the no treatment control groups or treated with TNF- α (1 ng/mL). Villi were collected at the designated time points and processed for qRT-PCR to measure mRNA expression of S1PR1, S1PR2, and S1PR3. Primer sequences are listed in Table 2.1.

2.4.3. Western Blots

Total protein concentration of lysed placental biopsies or homogenates of cultured BeWo cells were measured using the BCA assay described above. 50 μ g of sample protein was loaded for quantification of S1PR1 expression and 100 μ g was loaded for quantification of S1PR2 expression. Samples were mixed with 5x Laemmli sample buffer, containing 2-ME, and heated for 3 minutes at 90°C prior to loading. SDS-PAGE with a 12% gel was performed at 110 V (Mini-Protein II gel system, Bio-Rad Laboratories, Hercules, CA). After electrophoresis, gel proteins were transferred onto a nitrocellulose membrane for 90 minutes at 400 mA in transfer buffer (20% methanol, 25 mM Tris, 190 mM Glycine). After transfer, the membrane was

blocked for 1 hour at room temperature with 50% blocking buffer (LI-COR Biosciences, Lincoln, NE) in 1xPBS. After blocking, membranes were incubated overnight at 4°C with a rabbit polyclonal antibody against S1PR1 (1:500, ab11424, Abcam) combined with a mouse monoclonal α -Tubulin (1:1000, ab7291, Abcam) antibody to control for protein loading. Alternatively, membranes were incubated with a S1PR2 mouse monoclonal antibody (1:500, sc-365589, Santa Cruz Biotechnology, Inc., Dallas, TX, USA) and with a mouse β -actin (1:2000, sc-4778, Santa Cruz Biotechnology, Inc.) to control for protein loading control. Loading controls were carefully chosen to avoid overlap in molecular weights between the protein of interest and the loading protein. The next day, membranes were washed with 1xPBS, and incubated with goat anti-rabbit or goat anti-mouse IRDye 800CW or IRDye 600CW (LI-COR Biosciences) on a shaker at room temperature for 1 hour in the dark. Blots were then washed with 1xPBS-Tween 20 three times with a 20-minute wash each and imaged using the Odyssey infrared imaging system (LI-COR Biosciences). Blots were analyzed by densitometry using Image Studio Lite (LI-COR Biosciences) and genes of interest were normalized against their corresponding loading controls.

2.4.4. Primary Cultured Trophoblasts Staining for S1PR1/2

Cells were cultured and stained as described in 2.3.3. The antibody used for staining S1PR1 is a rabbit polyclonal antibody (1:100, ab11424, Abcam) and for S1PR2 is a mouse monoclonal antibody (1:100, sc-365589, Santa Cruz Biotechnology, Inc., Dallas, TX, USA). The secondary antibodies used were AlexaFluor goat anti-rabbit 594 and goat anti-mouse 488 (1:200, A32740 and A28175, Invitrogen).

2.5. Chapter 6 Specific Methods

2.5.1. Treatment of Villous Explants

On day 4 of incubation, which corresponded to the beginning of the ST regeneration phase, Yoda1, a pharmacological Piezo1 agonist (Millipore Sigma) was added to insert wells in a dose response (0-20 μ M). Co-treatment experiments were performed with 1 ng/mL TNF- α + 10 μ M Yoda1, 1ng/mL TNF- α alone, 10 μ M Yoda1 alone, or the no treatment control + vehicle control (DMSO, Sigma Aldrich). Villous explants and supernatants were collected and frozen at times 0-48 hours after treatment. LDH release (described in 2.1.7), β -hCG release (described in 2.1.8), hPL release (described in 2.1.9) villous PLAP activity (described in 2.1.10), and cytokine and growth factor release (described in 2.1.11) were assessed.

2.5.2. Statistics and Analysis

Results were analyzed using the methods described in the general section above. For publication purposes and journal requirements, all values are displayed as mean +/- standard deviation (SD).

3. Chapter 3: TNF- α Regulation of Sphingosine 1-Phosphate Regulatory Enzymes in the Placenta

A version of Figure 3.1, Figure 3.2, and Table 3.1 was published in: Fakhr Y, Koshti S, Habibyan YB, Webster K, Hemmings DG. Tumor Necrosis Factor- α Induces a Preeclamptic-like Phenotype in Placental Villi via Sphingosine Kinase 1 Activation. *International Journal of Molecular Sciences*. 2022; 23(7):3750. <https://doi.org/10.3390/ijms23073750>.

3.1. Introduction

Intracellular and extracellular S1P levels are regulated by several enzymes. SphK1 phosphorylates sphingosine at the inner cell membrane to produce S1P. S1P can then exit the cell via active transport and act in a paracrine or autocrine manner by interacting with one of its five G protein-coupled receptors (S1PR1-5). LPP1-3 are broad-specificity integral membrane proteins that can dephosphorylate S1P. LPP3 is the predominant LPP that acts on S1P and can function as an ectoenzyme, primarily dephosphorylating extracellular S1P (343). SphK1 and LPP3 hence mainly regulate extracellular S1P availability.

SphK2 is typically located in the nucleus and synthesizes S1P that partakes in intracellular signaling (9). SGPP1,2 are S1P-specific phosphatases that generally dephosphorylate intracellular S1P. SGPP1, however, is also reported to exit into the extracellular space via ABC transporters, and hence may also regulate extracellular S1P (344). While the actions of LPPs and SGPPs are reversible, the degradation of intracellular S1P by SGPL1 is an irreversible reaction.

S1P synthesizing and catabolic enzyme expression is regulated by various growth factors, endocrine factors, and inflammatory cytokines or stimuli (345-349), including TNF- α (347, 350). Elevated TNF- α is linked to pregnancy complications such as recurrent spontaneous abortions (135), preterm labour (136), and PE (137). Injecting TNF- α alone into pregnant non-human primates leads to the development of PE symptoms (138). Moreover, elevated TNF- α causes a PE-like placental phenotype that includes poor ST function, high ST shedding, and high inflammation (139, 140).

TNF- α increases SphK1 expression in MDA-MB-231 epithelial breast adenocarcinoma cells but not in MCF-7 breast cancer cells (351). In HUVEC cells, SphK2, SGPP1, and SGPP2 mRNA expression decreases in response to TNF- α (347). However, the levels of S1P synthesizing and catabolic enzymes in response to TNF- α treatment have not been assessed in placental tissue yet. Because circulating S1P levels are increased in PE, a disorder with high levels of circulating TNF- α , it is important to measure the levels of all S1P metabolic enzymes in response to TNF- α . This will provide a better understanding of sphingolipid metabolism and the production of S1P in different intracellular and extracellular compartments. In this chapter, I will be using the villous explant model to understand TNF- α regulation of the enzyme levels over the entirety of the ST regeneration period.

The placental ST is the epithelial barrier that separates maternal and fetal circulations and facilitates the exchange of materials between the mother and fetus (65). To maintain its integrity, ST formation is in constant turnover during pregnancy with a tight balance between ST generation and ST shedding. The ST is formed when the underlying CT proliferates, differentiates, and fuses into the basal membrane of the ST. When the ST reaches maturation, nuclear aggregates (also known as syncytial knots) form and egress from the barrier while undergoing apoptosis (65, 352). These multinucleated syncytial knots are normally shed into the maternal circulation, but are increased in PE. To better understand the regulatory role of SphK1 in the ST regeneration cycle on proliferation, differentiation, and fusion, I investigated its levels throughout this phase. I also measured the response of SphK1 and other S1P regulatory enzymes in response to TNF- α treatment during ST formation. Altered S1P enzyme levels will likely lead to changes in S1P levels in various cellular compartments, leading to altered cellular responses.

S1P circulating levels are increased in mothers with PE (170, 176). Whether SphK1 placental levels change in PE remains unclear, since conflicting trends have been reported (234, 353). S1P and SphK1 activation regulate ST formation (46). While high levels of S1P inhibit syncytialization (10), inhibiting SphK1, which would decrease S1P production, increases trophoblast fusion (46). This suggests that SphK1-mediated regulation of ST formation might be due to the production of S1P that partakes in extracellular signaling. Since S1P enzymes are localized in specific cell compartments, it is important to understand the fluctuation of all S1P regulatory enzymes as a proxy to S1P levels in specific subcellular compartments. Since both S1P and SphK1 play independent roles in ST formation, it is important to measure the fluctuation of all S1P regulatory enzymes throughout ST formation on a gross tissue level as well as a cell-specific level.

In this study, I investigated SphK1 levels in placental biopsies of women with PE and healthy controls using two different methods to confirm its change in expression in PE. Next, I investigated the physiological regulation of S1P enzymes, most importantly SphK1, in placental villi, the functional structural unit of the placenta, throughout the syncytialization process. I also determined the effect of TNF- α treatment on S1P regulatory enzyme expression in villous explants throughout the syncytialization cycle. Since TNF- α regulates S1P enzymes in a cell-specific manner (354-356), I also investigated whether TNF- α alters SphK1 levels in primary human CTs, the key functional cell in the human placenta.

My hypothesis was that SphK1 expression would be higher in placental biopsies of women with PE. I further hypothesized that SphK1 expression would remain consistent during the first 24 hours of regeneration but increase at the end of regeneration, potentially to allow the ST endocrine function to occur after fusion. Since TNF- α mediates its effects by increasing S1P

in other tissues, I also hypothesized that placental SphK1 expression would increase whereas LPP3, SGPP1, and SGPL1 expression would decrease to allow for the increased levels of S1P, in response to TNF- α treatment. I discovered that the overall placental expression of SphK1 was increased in the placentas of women with PE. In contrast, I found that the overall placental expression of S1P regulatory enzymes was not altered in response to TNF- α treatment in villous explants. However, TNF- α increased SphK1 expression in cultures of differentiating CTs. This implies that SphK1 regulation by TNF- α only occurs in trophoblasts but not in the whole placental villi. SGPP1 expression increased at the end of ST regeneration in explants, regardless of TNF- α treatment. This suggests that reduced S1P levels might signal the start of ST shedding.

3.2. Results

3.2.1. SphK1 Expression in Placentas from Normal and PE Pregnancies

17 women with healthy pregnancies and 12 women with PE were enrolled in the study and their clinical characteristics are summarized in Table 3.1. Women with PE had higher systolic (155.3 ± 7.6 versus 113.8 ± 3.7 mmHg; $p < 0.0001$) and diastolic (107.9 ± 15.6 versus 71.4 ± 3.6 ; $p = 0.008$) blood pressures compared to those in the healthy control group. All participants in the PE group were positive for proteinuria. Infants born to mothers in the PE group had lower gestational ages (37.2 ± 0.3) compared to those from healthy control mothers (38.9 ± 0.3 ; $p = 0.005$). There were no significant differences in maternal parity, infant birth weight, or fetal sex between groups. All samples in the PE group were collected from mothers who developed PE after 34 weeks of gestation and were categorized as displaying mild PE.

Previous studies show that dysregulated SphK1-S1P levels are observed in the placentas of women with PE, and high levels of S1P or SphK1 activity are inhibitory to ST development

(46). I investigated whether cell-specific expression of SphK1 differed in placental biopsies from women with PE compared to those from normal pregnancies. To visualize expression differences in placental layers and cell types, I used immunohistochemistry. SphK1 was expressed throughout the villi and in trophoblastic layers (Figure 3.1A). This enzyme was expressed in both CTs and the multinucleated ST, as shown in the magnified images C1 and PE3, respectively (Figure 3.1A). In both healthy control and PE groups, SphK1 expression rarely overlapped with the nuclear stain, and SphK1 exhibited a strong overlap with the E-cadherin staining, as identified with white arrows. This implies that in trophoblastic layers, SphK1 is mainly localized to the cytoplasm and in close proximity to the cell membrane. Overall, no overt qualitative differences in SphK1 expression between the PE (n=12) and the healthy control (n=17) groups were observed in trophoblastic layers (Figure 3.1A), but SphK1 expression appeared higher in the villous core of biopsies from the PE group, as shown in samples PE2 and PE3. Quantitative analysis of whole sample images demonstrated increased SphK1 overall in placental biopsies from women with PE ($p=0.02$; Figure 3.1B). In Figure 3.1B, there were 3 samples in the healthy group that displayed much higher levels of SphK1 staining. Upon comparing the clinical characteristics of these samples with the rest of the group, I did not see any differences in the clinical characteristics, such as blood pressure, gestational age, or infant birth weight, that would suggest a resemblance to those characteristics seen in a PE phenotype.

Quantitative analysis of SphK1 mRNA expression using the $\bar{\Delta}\Delta C_t$ method demonstrated increased SphK1 in placental biopsies from women with PE ($p=0.03$; Figure 3.1C; n=9). There were 3 samples in the PE group that displayed much higher levels of SphK1 mRNA expression. Upon comparing the clinical characteristics of these samples with the rest of the PE group, I did not see any differences in systolic or diastolic blood pressure, gestational age, infant birth

weight, or fetal sex with the other samples in this group. PE is a highly clinically heterogeneous disorder that can be caused by distinct factors. Benton et al report subtypes of PE based on placental gene expression clusters (357). This heterogeneity and the various presentations of placental dysfunction in PE can explain the heterogeneity that I saw in SphK1 expression, specifically the mRNA expression.

3.2.2. Experimental Villous Explant Model of Syncytial Self-Regeneration

The self-regenerating explant model was chosen for this part of the study as it closely resembles the state of the placenta in the second trimester of pregnancy. In this model, the explant undergoes high levels of syncytial regeneration, and the placenta has the highest degree of syncytial regeneration during the second trimester. This is evidenced by the increase in the secretion of hPL, a marker of syncytial mass, at the start of the second trimester (358). PE manifests after the second trimester of pregnancy (31), sometimes as late as the third trimester in cases of late-onset PE. Even though early-onset PE starts developing during the first trimester, the poor development and function of the placenta during the second trimester exacerbates the disorder to clinically detectable levels. During the second trimester, the ST is characterized by high levels of regeneration to form an intact placental barrier.

To characterize the time in culture needed for the ST to be fully shed prior to regeneration, explants were incubated for varying timepoints from dissection (0 days) up to 8 days and then assessed for the presence of ST using immunohistochemistry (Figure 3.2; n=3). E-cadherin is an epithelial adherens junction protein, which is found in both CTs and the ST in the placenta since trophoblasts are epithelial cells. High E-cadherin expression was saturated at the basal ST membrane where the apical side of the CT fuses into the ST. Since ST differentiation involves downregulating E-cadherin expression, the apical side of the ST expresses E-cadherin at

low levels and is often not visualized with the microscope parameters optimal for the signal on the basal membrane of the ST. Any nuclei present on the apical side of the heavy E-cadherin demarcation belong to the multinucleated ST layer. Explants incubated for 0, 1, 6, and 8 days after initiation of culture showed multiple nuclear clusters towards the apical side of the strong E-cadherin demarcation that define numerous areas of multinucleated ST (Figure 3.2A, white arrows). Explants incubated for 2 or 3 days showed progressively fewer nuclei outside the E-cadherin staining than seen at 0 and 1 days, implying a lower syncytial area. By day 4 of incubation, the ST was almost fully shed (Figure 3.2A, red arrow). Day 4 of culture was then used as the first day of treatment for all further experiments. Multiple areas of multinucleated ST reappeared on days 6-8 (Figure 3.2A, white arrows) of culture showing evidence for regeneration of the ST layer. LDH levels peaked on day 2 of culture and dropped again on day 4 of culture, showing evidence of ST sloughing before day 4 of culture (Figure 3.2B).

3.2.3. Expression of S1P Synthesizing Enzymes in Villous Explants

To determine the effect of TNF- α on the expression of various components of the S1P regulatory pathway during ST regeneration, explants were cultured for 4 days in media to allow for shedding of the present ST, then treated with TNF- α over the next 2 days. For each gene, the results were analyzed as follows: A) mRNA expression without treatment normalized to HPRT1 expression, a commonly used housekeeping gene, and then relative to time 0; B) mRNA expression following treatment with TNF- α normalized to HPRT1 expression and then relative to time 0, and C) normalized mRNA expression following treatment of TNF- α relative to the normalized no treatment control. HPRT1 was chosen as the housekeeping gene as my analysis indicated that its expression did not vary in explants in response to TNF- α or over time of culture (Figure 3.3A-C) or between normal and PE placental biopsies (Figure 3.3D). The discrepancies

in sample size in some timepoints are due to the exclusion of outliers, as measured by ROUT's test, or exclusion of wells due to culture contamination.

SphK1 expression in term placental villous explants from normal pregnancies undergoing ST regeneration in no treatment conditions did not change across 0-48 hours relative to HPRT1 (Figure 3.4A, n=4, 5). Similarly, SphK1 expression remained unchanged across 0-48 hours with 1 ng/mL of TNF- α treatment (Figure 3.4B, n=4, 5). Upon comparing treated explants with untreated control explants from individual experiments at each timepoint, I also saw that the expression of SphK1 remains similar, indicating that SphK1 did not change in response to TNF- α treatment at any of the timepoints measured (Figure 3.4C, n=4, 5). This shows that overall placental SphK1 levels are not regulated during ST formation. Overall placental SphK1 levels also do not change in response to TNF- α treatment in cultured villous explants.

3.2.4. Expression of S1P Catabolic Enzymes in Villous Explants

The expression of SGPP1 in term placental villous explants from normal pregnancies increased in both the no treatment control and the TNF- α treatment group after 48 hours (Figure 3.5A, 3.5B, respectively, n=3-5). Moreover, SGPP1 expression in the TNF- α -treated groups was unchanged compared to the untreated control groups at all measured timepoints (Figure 3.5C, n=3-5). This suggests that SGPP1 is normally upregulated at the end of ST regeneration and TNF- α did not change this.

SGPL1 expression in term placental villous explants from normal pregnancies undergoing ST regeneration in no treatment conditions did not change across 0-48 hours relative to HPRT1 (Figure 3.6A, n=3-5). Similarly, SGPL1 expression remained unchanged across 0-48 hours with 1 ng/mL of TNF- α treatment (Figure 3.6B, n=3-5). Upon comparing treated explants

with untreated control explants from individual experiments at each timepoint, I also saw that the expression of SGPL1 remains similar, indicating that SGPL1 did not change in response to TNF- α treatment at any of the timepoints measured (Figure 3.6C, n=3-5). This shows that SGPL1 levels in whole placental tissues are not regulated during ST formation. Overall placental SGPL1 levels also do not change in response to TNF- α .

Similarly, LPP3 mRNA expression in term placental villous explants from normal pregnancies undergoing ST regeneration in no treatment conditions did not change across 0-48 hours (Figure 3.7A, n=3-6). LPP3 expression also remained unchanged across 0-48 hours with 1 ng/mL of TNF- α treatment (Figure 3.7B, n=3-6). Upon comparing treated explants with untreated control explants from individual experiments at each timepoint, it is clear that the expression of LPP3 remains similar, indicating that LPP3 did not change in response to TNF- α treatment at any of the timepoints measured (Figure 3.7C, n=3-6). This shows that LPP3 levels in whole placental tissues are unchanged during ST formation. Overall placental LPP3 levels also do not change in response to TNF- α .

3.2.5. Expression of SphK1 in Primary Human Trophoblasts

Since SphK1 often responds to inflammatory stimuli in a cell-specific manner (359) (349), I aimed to investigate whether SphK1 levels were changed in differentiating trophoblasts in response to TNF- α . For this part of the study, cultured primary human trophoblasts isolated from term uncomplicated pregnancies were plated overnight and then were treated with different concentrations of TNF- α for 24 hours. Figure 3.8 confirms the purity of the isolated CTs after 24 hours of culture. A high number of contaminating vimentin-positive cells, stained in red, were found in the pre-purified culture, as shown in Figure 3.8A. Post purification, cultured

trophoblasts displayed above 99% purity with fewer than 4 contaminating vimentin-positive cells per 2×10^5 plated CTs (Figure 3.8B).

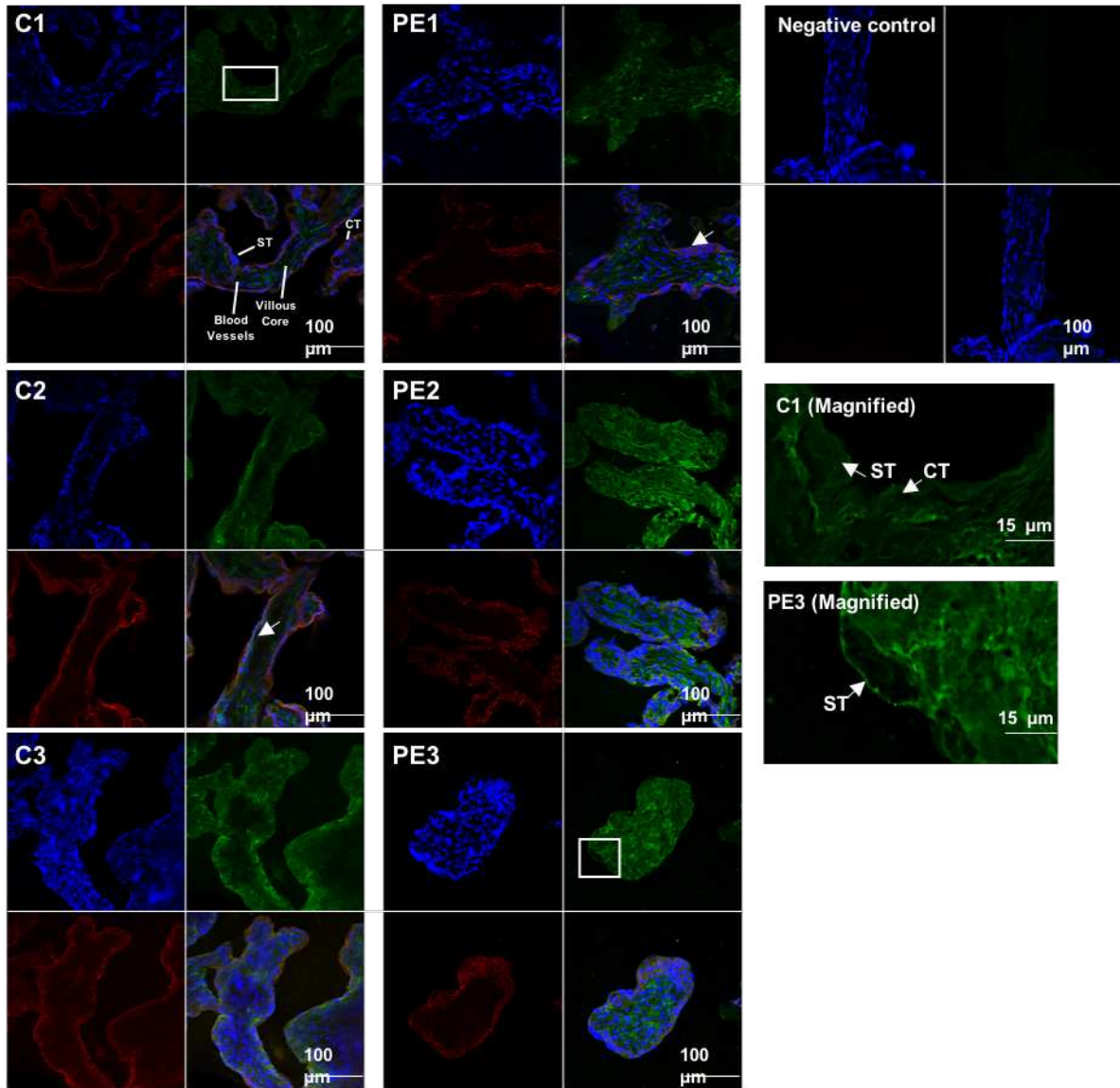
Next, I measured the effect of different concentrations of TNF- α on SphK1 levels and mRNA expression in trophoblast cultures. The SphK1 mean intensity/total nuclei was calculated for each treatment group and this was then analyzed in a ratio to the SphK1 mean intensity/total nuclei of the control group (0 ng/ml TNF- α). SphK1 mean intensity in cultured primary trophoblasts was increased in response to 1 (p=0.04), 10 (p=0.02), and 20 ng/mL (p=0.006) of TNF- α after 24 hours of treatment (Figure 3.9A). Qualitatively, SphK1 expression in the cultured trophoblasts in the no treatment control group was low, especially when compared to SphK1 expression in trophoblast layers of whole placental biopsies (Figure 3.1). SphK1 was mainly expressed in the cytoplasm of trophoblasts with little nuclear localization. Next, I analyzed SphK1 mRNA expression in response to the minimal dose of TNF- α that showed a significant increase in SphK1 staining expression, 1 ng/mL. I also treated villous explants with a lower dose of TNF- α , 0.1 ng/mL, to investigate whether TNF- α treatment would lead to a different response at lower levels. My findings showed no significant differences in SphK1 mRNA expression at either TNF- α concentration when compared to the no treatment control (n=3. Figure 3.9B). Interestingly, however, trophoblasts isolated from two placentas showed no response, whereas trophoblasts from the third placenta showed a gradual increase in SphK1 levels in response to increasing levels of TNF- α . While the clinical characteristics of infants and women who provided the samples were not different in gestational age, fetal sex, or maternal age, it is unclear what characteristics of the 3rd placenta enabled it to respond to TNF- α treatment. Regardless, the low sample size makes it difficult to make any concrete conclusions.

Pregnancy	Gestational Age (weeks)	Infant Weight (g)	Systolic Blood Pressure (mmHg)	Diastolic Blood Pressure (mmHg)	Percent Positive for Proteinuria (%)	Fetal Sex
Normal (n=17)	38.9 ± 0.3	3074 ± 86.8	113.8 ± 3.7	71.4 ± 3.6	0	11/17 Male 6/17 Female
Preeclampsia (n=12)	37.2 ± 0.3	2967 ± 274.2	155.3 ± 7.6	107.9 ± 15.6	100	7/12 Male 5/12 Female
p-value	0.003	ns	p<0.0001	0.008	N/A	ns

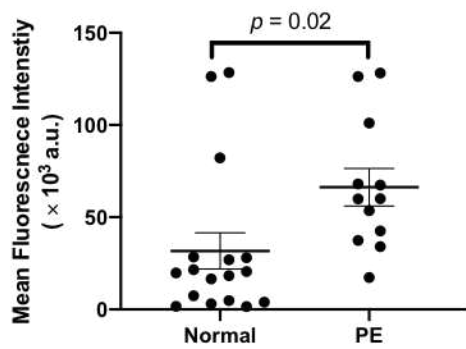
Table 3.1: Table of Characteristics of Sample Donors

Samples were analyzed using a Student's T-test or Mann-Whitney test when non-parametric (Mean +/- SEM).

A



B



C

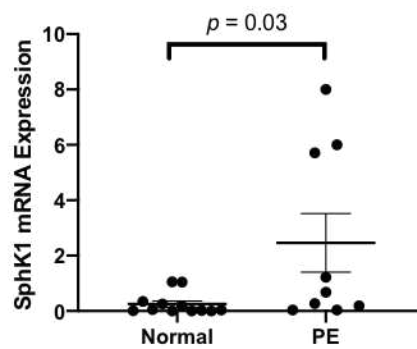
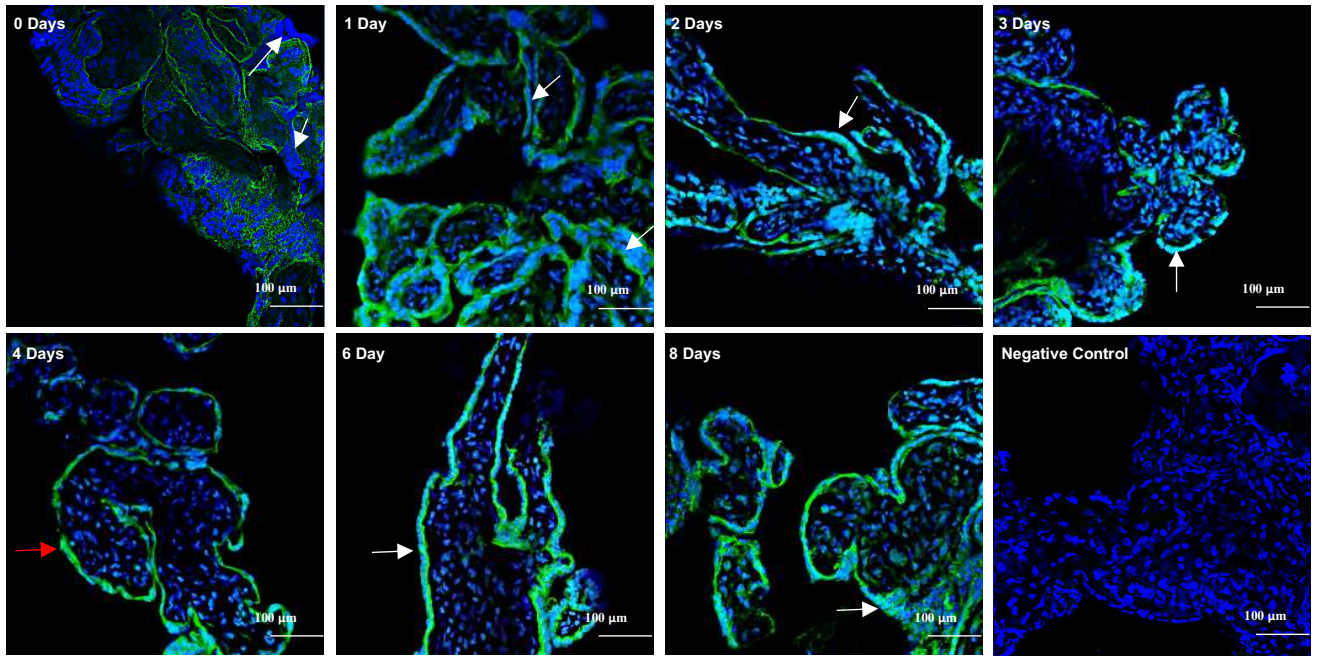


Figure 3.1: Sphk1 Expression was Higher in Placental Biopsies from Women with Preeclampsia (PE)

(A): SphK1 was expressed throughout the villi, the cytotrophoblast (CT) and syncytium (ST). Images correspond to three representative samples from healthy control pregnancies (C1, C2, C3 images) and PE (PE1, PE2, PE3 images). Whole tissue placental biopsies from women with normal or PE pregnancies were co-stained for SphK1 (AF488, green) and E-cadherin (AF594, red) expression and a nuclear stain (DAPI, blue) and visualized by confocal microscopy. For the negative control, both AF488 and AF594 secondary antibodies were used in the absence of primary antibodies. White arrows show examples of overlap between E-cadherin and SphK1 (B): Whole sample image analysis normalized to total nuclear count showed higher SphK1 fluorescence in placental biopsies from women with PE compared to healthy control pregnancies. Student's T-test ($n = 17$ normal, $n = 12$ PE, Mean \pm SEM). (C): Fold change in SphK1 mRNA expression in placental biopsies from women with PE relative to healthy control pregnancies using the $\Delta\Delta C_t$ method. Student's T-test ($n = 13$ normal, $n = 9$ PE, Mean \pm SEM).

A



B

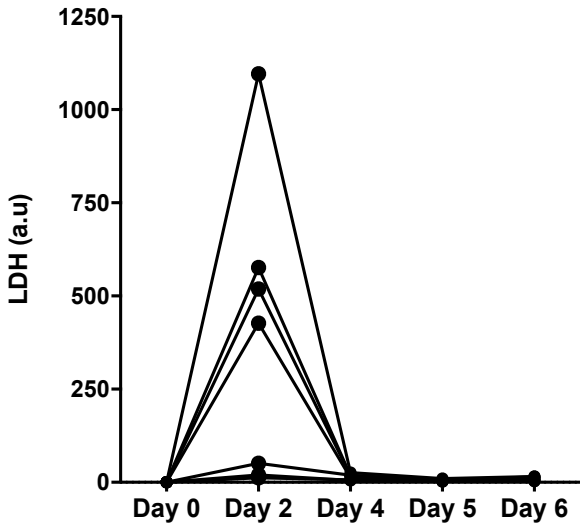


Figure 3.2: Syncytial Shedding in Villous Explants was Maximal After 4 Days of Incubation

(A): Confocal fluorescence microscopy was used to analyze the shedding of syncytium (ST) and resyncytialization of term explants after incubation for 0–8 days. DAPI stained nuclei blue and E-cadherin (AF488) stained epithelial cadherin junctions in cytotrophoblast (CT) and ST cell membranes green ($n = 5$). High areas of multinucleated ST are demarcated with white arrows and low areas of multinucleated ST are demarcated with red arrows. For the negative control, AF488 secondary antibodies were used in the absence of primary antibodies. (B): Lactate Dehydrogenase (LDH) released into supernatants from explants was measured across various timepoints. Linked data points correspond to individual experiments ($n = 6$) and each data point represents the average of duplicate wells. Measurements correspond to LDH release in the last 24 h prior to every displayed time point. Values were plotted as a change from day 0. All values are relative to total protein mass in each culture well.

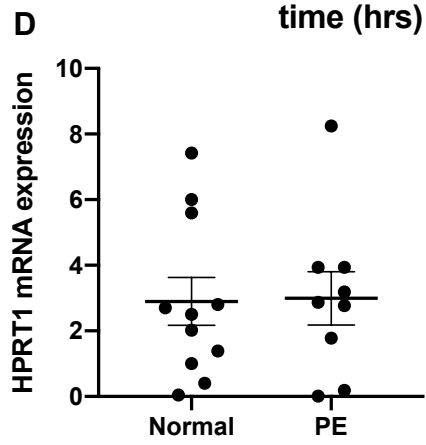
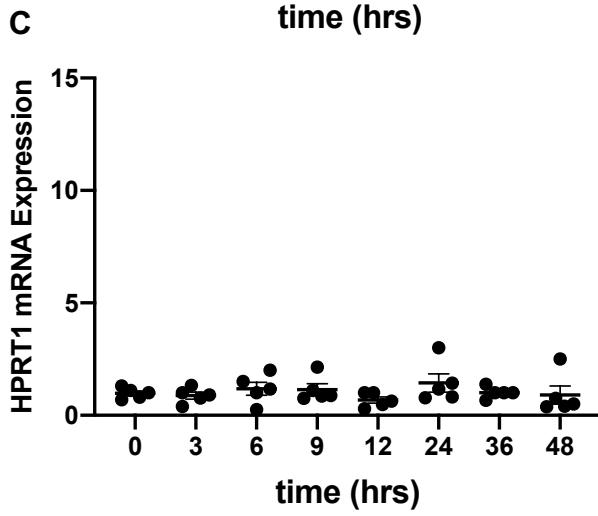
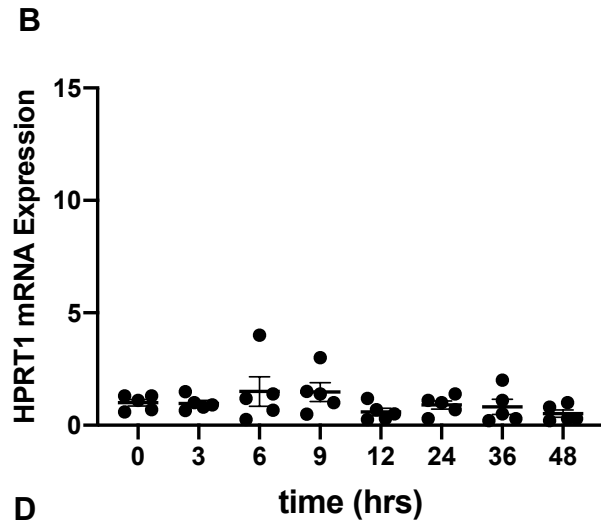
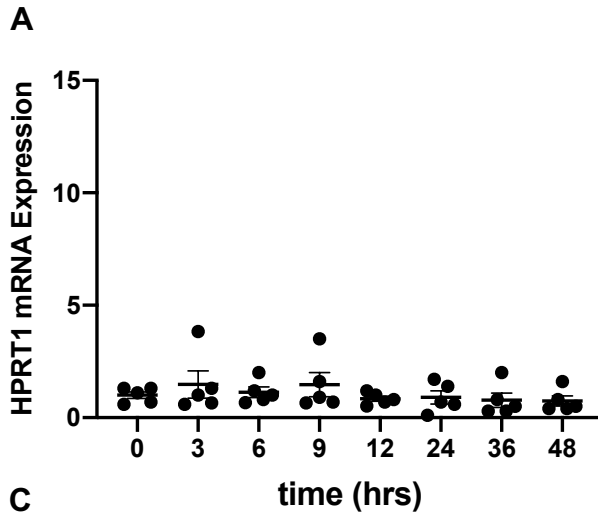
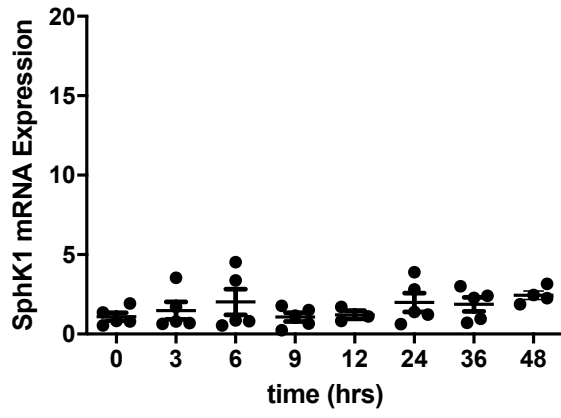


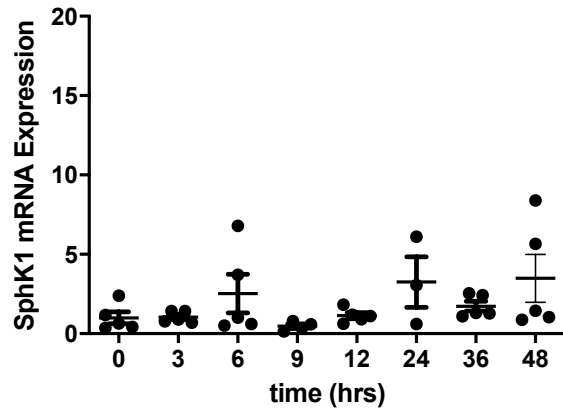
Figure 3.3: HPRT1 is Not Altered with Treatment or Time in Explants or in Biopsies from Women with PE

After 4 days of incubation, explants were treated with 0 **(A)** or 1 ng/mL of TNF- α **(B)** for 0-48 hours. HPRT1 mRNA expression was calculated relative to an internal control and then to its expression at time 0 hours. Corresponding values for cultures treated with TNF- α were calculated relative to the no treatment control **(C)**. **(A)** HPRT1 mRNA expression did not significantly change from 0-48 hours in the no treatment cultures. **(B)** HPRT1 mRNA expression did not significantly change from 0-48 hours when treated with 1 ng/mL of TNF- α . **(C)** HPRT1 mRNA expression was not significantly affected by treatment with TNF- α across times. Results were analyzed using the mixed effects model with the two-stage linear step-up procedure of Benjamini, Krieger, and Yekutieli post-hoc test ($n = 5$, Mean \pm SEM). **(D)** HPRT1 mRNA expression was not altered in placental biopsies of mothers with PE when compared to those of healthy pregnancies. Results were analyzed using a Student's T-test ($n = 11$ normal, $n = 9$ PE, Mean \pm SEM).

A



B



C

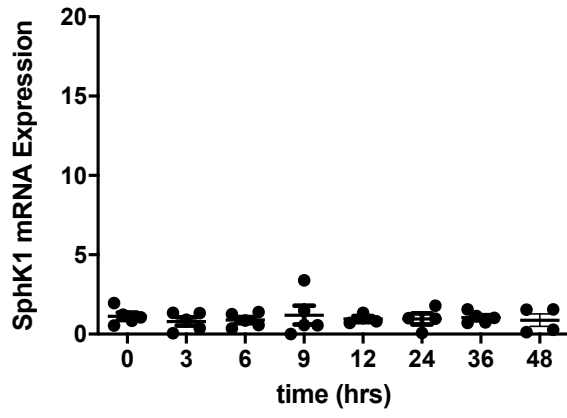


Figure 3.4: Sphk1 mRNA Expression is Constant from 0-48 Hours and is Not Significantly Affected by TNF- α in Term Villous Explants

After 4 days of incubation, explants were treated with 0 (A) or 1 ng/mL of TNF- α (B) for 0-48 hours. SphK1 mRNA expression was calculated relative to HPRT1 mRNA expression and then to its expression at time 0 hours. Corresponding values for cultures treated with TNF- α were calculated relative to the no treatment control (C). (A) SphK1 mRNA expression did not significantly change from 0-48 hours in the no treatment cultures. (B) SphK1 mRNA expression did not significantly change from 0-48 hours when treated with 1 ng/mL of TNF- α . (C) SphK1 mRNA expression was not significantly affected by treatment with TNF- α . Results were analyzed using the mixed effects model with the two-stage linear step-up procedure of Benjamini, Krieger, and Yekutieli post-hoc test ($n = 4$, Mean \pm SEM).

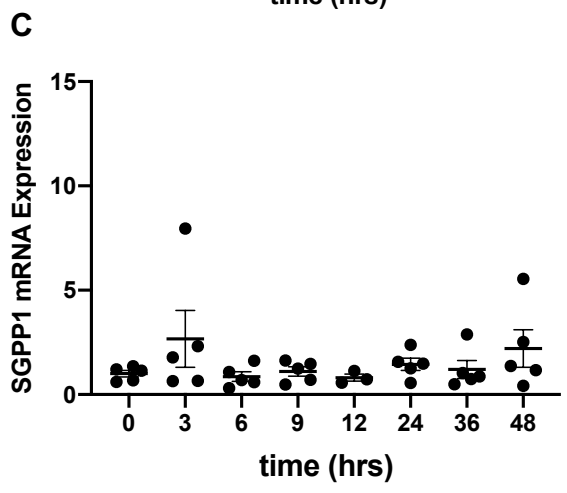
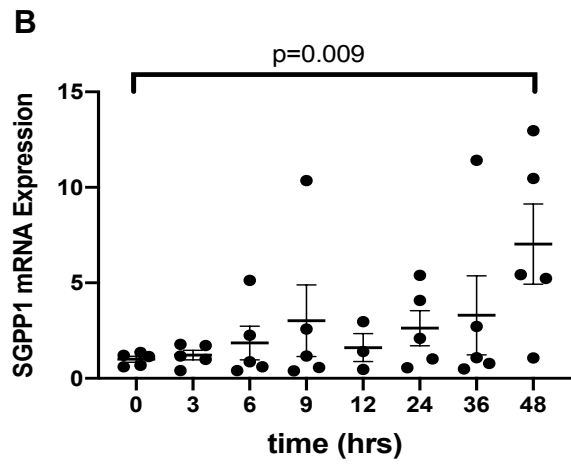
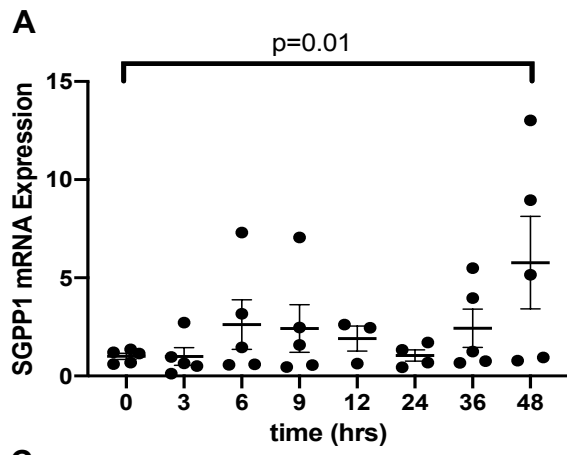


Figure 3.5: SGPP1 mRNA Expression Increases in Term Villous Explants After 48 Hours of Re-Syncytialization Even After TNF- α Treatment

After 4 days of incubation, explants were treated with 0 (**A**) or 1 ng/mL (**B**) of TNF- α for 0-48 hours. SGPP1 mRNA expression was calculated relative to HPRT1 mRNA expression and then to its expression at time 0 hours. Corresponding values for cultures treated with TNF- α were calculated relative to the no treatment control (**C**). (**A**) SGPP1 mRNA expression increased after 48 hours without treatment ($p=0.04$ by mixed effects model, 0.01 by post-hoc test). (**B**) SGPP1 mRNA increased at 48 hours when treated with 1 ng/mL of TNF- α ($p=0.04$, 0.009 by post-hoc test). (**C**) SGPP1 mRNA expression was not affected by treatment with TNF- α . Results were analyzed using the mixed effects model with the two-stage linear step-up procedure of Benjamini, Krieger, and Yekutieli post-hoc test ($n = 3-5$, Mean \pm SEM).

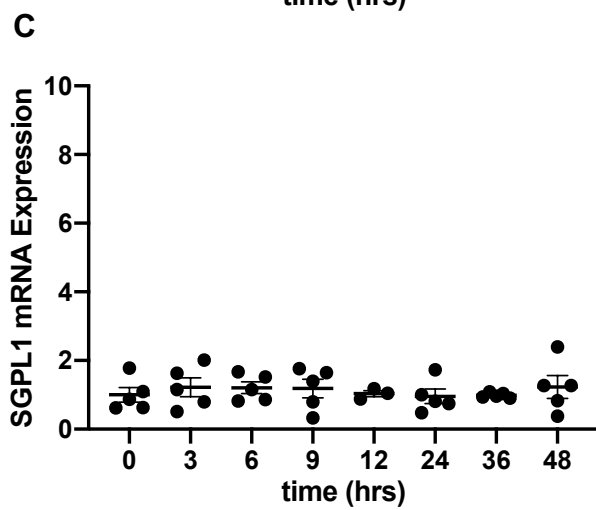
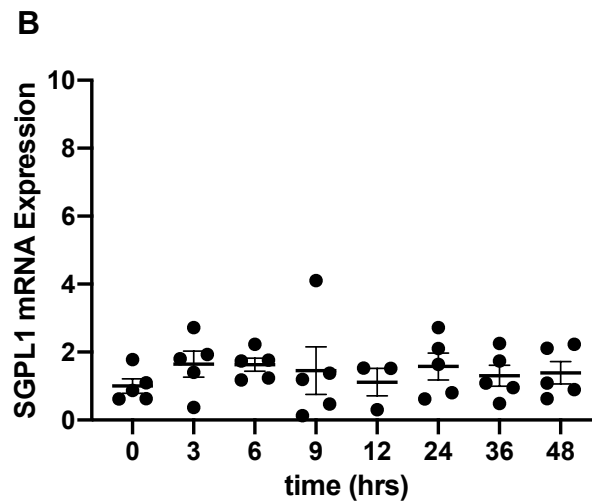
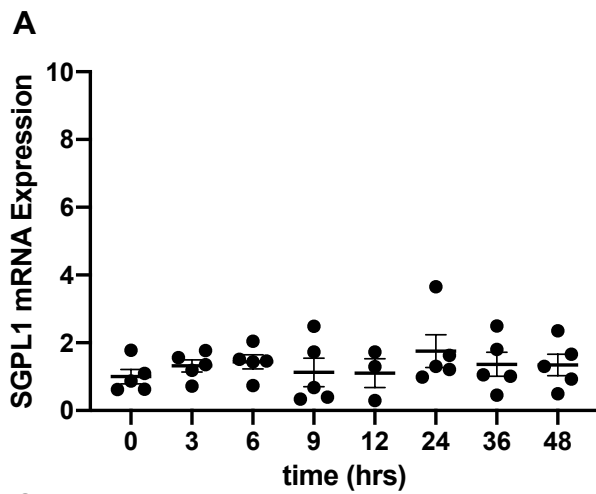


Figure 3.6: S1P Lyase (SGPL1) mRNA Expression is Constant from 0-48 Hours and is Not Affected by TNF- α in Term Villous Explants

After 4 days of incubation, explants were treated with 0 (**A**) or 1 ng/mL of TNF- α (**B**) for 0-48 hours. SGPL1 mRNA expression was calculated relative to HPRT1 mRNA expression and then to its expression at time 0 hours. Corresponding values for cultures treated with TNF- α were calculated relative to the no treatment control (**C**). (**A**) SGPL1 mRNA expression did not significantly change from 0-48 hours in the no treatment cultures. (**B**) SGPL1 mRNA expression did not significantly change from 0-48 hours when treated with 1 ng/mL of TNF. (**C**) SGPL1 mRNA expression was not significantly affected by treatment with TNF- α ($n=3-5$). Results were analyzed using the mixed effects model with the two-stage linear step-up procedure of Benjamini, Krieger, and Yekutieli post-hoc test ($n = 3-5$, Mean \pm SEM).

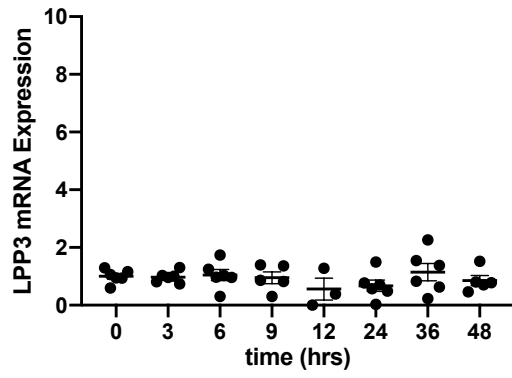
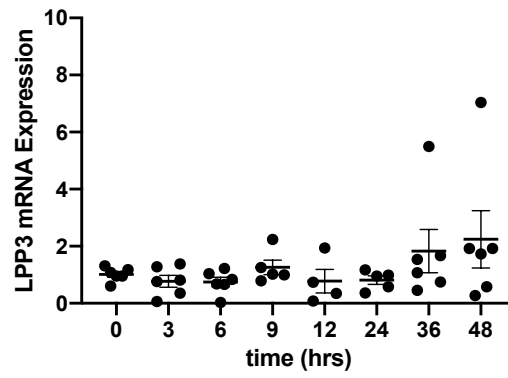
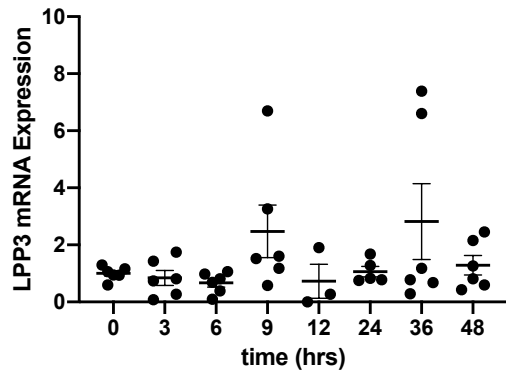
A**B****C**

Figure 3.7: LPP3 mRNA Expression is Constant from 0-48 Hours and is Not Significantly Affected by TNF- α in Term Villous Explants

After 4 days of incubation, explants were treated with 0 (A) or 1 ng/mL of TNF- α (B) for 0-48 hours. LPP3 mRNA expression was calculated relative to HPRT1 mRNA expression and then to its expression at time 0 hours. Corresponding values for cultures treated with TNF- α were calculated relative to the no treatment control (C). (A) LPP3 mRNA expression did not significantly change from 0-48 hours in the no treatment cultures. (B) LPP3 mRNA expression did not significantly change from 0-48 hours when treated with 1 ng/mL of TNF- α . (C) LPP3 mRNA expression was not significantly affected by treatment of TNF- α . Results were analyzed using the mixed effects model with the two-stage linear step-up procedure of Benjamini, Krieger, and Yekutieli post-hoc test ($n = 3-6$, Mean \pm SEM).

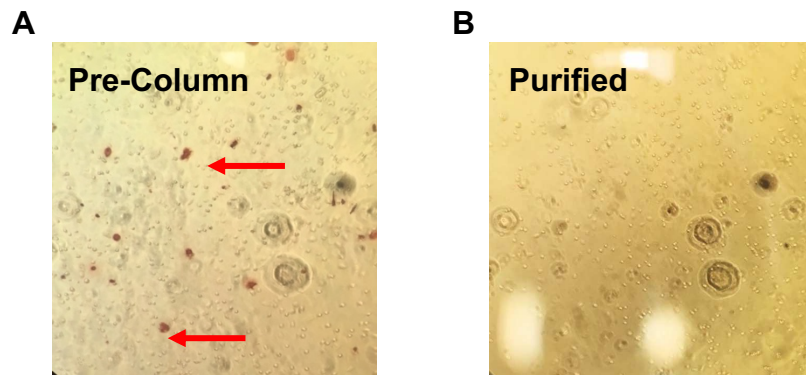


Figure 3.8: Cultured Primary Trophoblasts Collected Via a Negative Selection Column were Sufficiently Pure from Vimentin-Positive Cells

Primary cytotrophoblasts (CTs) were cultured for 24 hours and stained for vimentin (a marker of mesenchymal cells, in red) before (A) and after (B) column purification. Placental cotyledons were dissected and trypsinized, and a mixture of cells was collected. Red blood cells in the mixture were lysed with a lysis buffer. MHC Class I, MHC Class II, and CD9-positive cells were removed using a negative selection column. Trophoblast cells were collected. Trophoblast isolations were considered sufficiently pure when there were less than 4 contaminating cells per 2×10^5 cells.

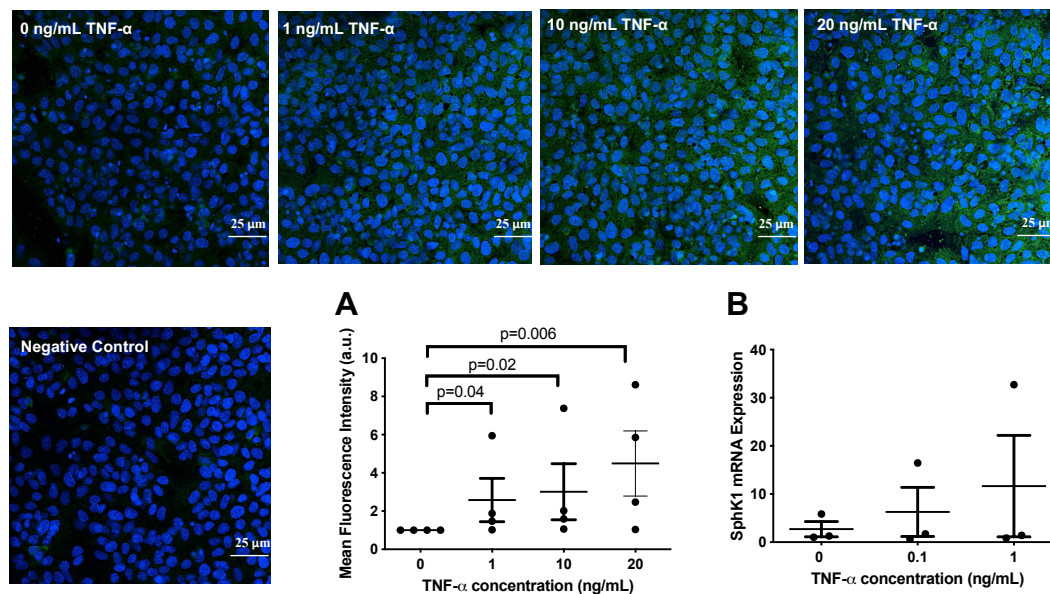


Figure 3.9: TNF- α Treatment for 24 hrs Increased Sphk1 Protein Expression in Cultured Primary Trophoblasts from 1 to 20 Ng/MI

(A) Immunofluorescence staining was analyzed using ImageJ. The images displayed are representative of cells isolated from three different placentas and two replicates. The negative control was generated by adding the fluorescent secondary antibody in the absence of the primary antibody. All values are a ratio of total nuclei. The background was subtracted using the negative control and results were plotted relative to the no treatment control. Results were analyzed using the non-parametric Kruskal-Wallis test ($p=0.01$) and the two-stage linear step-up procedure of Benjamini, Krieger, and Yekutieli post-hoc test. (B) TNF- α treatment for 24 hrs did not significantly affect SphK1 mRNA expression in cultured primary trophoblasts from 0.1 to 1 ng/mL. mRNA expression was measured by qRT-PCR using HPRT1 as the housekeeping gene and calculated relative to an internal control. Results were analyzed using the non-parametric Kruskal-Wallis test and the two-stage linear step-up procedure of Benjamini, Krieger, and Yekutieli post-hoc test. ($n = 3-4$, Mean \pm SEM).

3.3. Discussion

The objective of this study was to examine the alterations in S1P synthesizing and catabolic enzyme levels, especially SphK1, in placental explants during ST regeneration and to determine whether their expression is changed in response to high levels of TNF- α or in PE. I found that SphK1 levels were higher in the placentas of women with PE. However, I also found that TNF- α treatment did not alter S1P synthesizing and catabolic enzyme levels for SphK1, SGPP1, SGPL1, or LPP3, in placental villi as a whole in the ST regenerating villous explant model. However, it increased SphK1 expression in primary human differentiating CTs. This suggests that the elevated circulating and placental TNF- α levels in PE (4) could increase trophoblast SphK1 expression and contribute to an increase in extracellular release of S1P, which is elevated in PE (170). Even though TNF- α alone did not lead to an increase in placental SphK1, as seen in the explants, it might increase SphK1 expression in conjunction with other factors elevated in PE. The finding that SphK1 expression in placentas from mothers with PE was higher than in those without PE highlights the placenta as a potential contributor to the elevated levels of circulating S1P in PE (170). I also found that SGPP1 expression increased at the end of CT fusion and differentiation in the explant model, and this was unaffected by TNF- α treatment. This highlights a role for S1P downregulation in the progression of syncytialization from ST formation to ST shedding.

S1P is a bioactive sphingolipid involved in many physiological processes and it is produced by all cells in the placenta (9). S1P is produced when SphK1 or SphK2 phosphorylates sphingosine (9). SphK1 mRNA and protein expression are highly regulated at both the transcriptional and translational levels (360). SphK1 can be permanently degraded via ubiquitin-

mediated proteolysis (361). Another mechanism of regulating intracellular SphK1 levels is by transporting it into the extracellular space via ABC transporters (362).

S1P is elevated in the plasma of mothers with PE (170, 176). However, one study reports by qRT-PCR and Western Blot data that SphK1 mRNA and protein levels decrease in placental explants from women with PE compared to women with normal pregnancies (234). In contrast, using immunofluorescence, I observed that SphK1 levels were higher overall in placental sections from PE compared to normal pregnancies. This discrepancy could be attributed to distinct epitopes recognized by different antibodies using different methods. However, I confirmed these staining results using qRT-PCR. Recently, however, an article by Liao et al shows a lower level of SphK1 protein levels in placental villi from PE pregnancies, also measured by immunofluorescence (353). While maternal characteristics and sample size were comparable to those described in Section 3.2.1, the study by Liao et al used paraformaldehyde fixation that can result in lower levels of fluorescence and poor preservation of the cytoplasm (363) and most likely the villous core. Indeed, in my study, the staining showed a strong signal for SphK1 in the villous core, whereas the images from Liao et al show almost no expression aside from the outermost trophoblast layers. Liao et al also show that placental SphK1 activity is decreased in the PE group, however, the method utilized does not discriminate between SphK1 and SphK2 (364). Although S1P is elevated in the plasma of women with PE (170, 176), it is unknown whether the placenta is the source of this surge. Liao et al show that placental S1P levels are lower in mothers with PE (353) but did not measure circulating S1P in the mother. Since S1P is constantly transported to the extracellular space, it is unclear whether this decrease is due to increased transport, decreased synthesis, or increased lyase or phosphatase activity.

The women in the healthy control group had newborns with higher gestational ages than those in the PE group. However, it is unlikely that the differences in SphK1 expression can be explained by gestational age differences. In my recent extensive review on sphingolipids in pregnancy I note that circulating S1P levels remain constant throughout normal pregnancy, and are therefore independent of gestational age (9). Previous studies in the Hemmings lab also show that SphK1 levels in the decidua are higher with increasing gestational age (365). For these reasons, I believe it is unlikely that higher levels of SphK1 in the placentas of mothers with PE are due to lower gestational ages.

One of the interesting findings was that only SGPP1 expression was increased at the time the ST was fully reformed in villous explants. No other S1P synthesizing or catabolic enzymes that I tested were altered throughout the ST regeneration phase in untreated villous explants. While this increase in SGPP1 has not been found in other studies to date, it is in line with S1P levels decreasing in CTs as they differentiate to a final 10-fold decrease when compared to their expression in undifferentiated cells (46). This suggests a high level of S1P dephosphorylation at the end of ST formation, which can be explained by the increase in SGPP1 levels observed in this study. Reducing S1P levels at the end of syncytial regeneration could be important to remove the protective ability of S1P in order for sloughing and apoptosis to occur. This, however, remains to be investigated.

SphK1 expression in primary human CTs decreases to 80% of its original value after three days of differentiation and fusion (46). In this study, however, I found that SphK1 levels remained constant in villous explants throughout differentiation. This discrepancy highlights the advantages and disadvantages of using the villous explant model. On one hand, the CTs in villous explants are in context with the extracellular matrix and the surrounding cell types, so the

model mimics a more physiological condition. Additionally, as SphK1 can be translocated into the extracellular space (362), it is important to know the overall levels in the whole tissue. Moreover, as SphK1 is the main producer of extracellular S1P, understanding the fluctuations in SphK1 expression can predict the levels of extracellular SphK1-produced S1P circulating in placental tissues. On the other hand, small differences in cell-specific expression can be masked by the overall trend of the enzyme expression in the whole tissue.

SphK1 expression is regulated by various growth factors, endocrine factors, and inflammatory cytokines or stimuli (345-349). For instance, TGF- β 1 upregulates SphK1 in hepatic stellate cells (348). Moreover, LPS-treated mice display increased SphK1 and SphK2 levels in bronchoalveolar lavage fluids (349). Additionally, growth factors such as EGF (346, 347) and PDGF (345) upregulate SphK1 expression. Notably, TNF- α increases SphK1 expression in MDA-MB-231 epithelial breast adenocarcinoma cells but not in MCF-7 breast cancer cells (351). Interestingly, another study found that TNF- α decreases SphK1 expression in MCF-7 cells via cathepsin B cleavage of SphK1 (359). HUVEC cells, however, do not alter their SphK1 expression in response to TNF- α but increase their SphK1 mRNA expression in response to LPS (347). In this study, SphK1 expression was unaltered in response to TNF- α treatment in villous explants and only increased in cultured differentiating CTs. This further confirms that SphK1 regulation by TNF- α occurs in a cell-specific or tissue-specific manner. My results, however, also showed that 1-20 ng/mL of TNF- α hinders this syncytialization, and hence differences in SphK1 expression in response to TNF- α could be a direct effect of the cytokine or a response of hindered syncytialization.

Due to its subcellular localization, SphK1 is the main producer of extracellular S1P. Whereas since SphK2 is primarily present in the nuclei, S1P produced by SphK2 mainly

contributes to intracellular signaling. SphK2 regulation is poorly understood, but as mentioned above it is upregulated in response to inflammatory stimuli such as LPS in bronchoalveolar lavage fluids (349). In HUVEC cells, however, SphK2 mRNA expression decreases in response to TNF- α and LPS (347). Contrary to SphK1, evidence suggests that SphK2 has signaling properties independent of S1P production. For instance, SphK2 directly binds and inhibits Bcl-xL leading to apoptosis (366). Since SphK2 expression is regulated by inflammatory stimuli and controls processes crucial for maintaining placental function, it is important to investigate SphK2 expression in response to TNF- α . However, in my study, I could not detect SphK2 mRNA expression in villous explants, due to its low expression in placental tissue. This is not surprising as a previous study from our lab shows extremely low levels of SphK2 in human decidua as well (365). Moreover, a study by Singh et al also could not detect SphK2 mRNA expression in CTs and STs (46).

S1P can be dephosphorylated into sphingosine by SGPP1 or SGPP2 and LPP1-3, all enzymes belonging to the lipid phosphate phosphatase family. SGPP1/2 are S1P-specific enzymes located intracellularly at the endoplasmic reticulum. Similar to SphK1, SGPP1 can be transported into the extracellular space by ABC transporters (344). This can contribute to the regulation of extracellular S1P levels in the systemic circulation and signaling through cell surface S1PRs.

The regulation of SGPP1 and 2 expression is only partially understood. One study shows that growth factor independence 1, a transcription factor, directly suppresses SGPP1 transcription in multiple myeloma cell lines (367). SGPP1 mRNA expression but not protein expression in dendritic cells decreases in response to LPS stimulation (368). SGPP1 mRNA expression also decreases in response to LPS and TNF- α treatments in HUVECs (347). In

dendritic cells, SGPP1 translocates from the nucleus to the endoplasmic reticulum in response to inflammatory stimuli and dephosphorylates cytoplasmic S1P (368). In my study, SGPP1 expression was not altered in response to TNF- α . However, whether its transport or localization is altered warrants further investigation.

On the other hand, SGPP2 is increased in response to LPS treatment in HUVECs and neutrophils and to TNF- α treatment in HUVECs (347). SGPP2 is also upregulated in response to IL-1 β treatment in A549 cells, an alveolar epithelial choriocarcinoma cell line (347). Similar to the Hemmings' lab's previous study on the decidua (365), I was unable to detect SGPP2 levels in placental tissue by qRT-PCR. Singh et al, on the other hand, detected SGPP2 expression in CTs and STs (291).

While SGPP1, SGPP2, and S1P lyase (SGPL1) work intracellularly, LPP1-3 dephosphorylate extracellular S1P. LPP1-3 are transmembrane proteins that can have their active sites located in the inner leaflet of the cell membrane, but they also function as ectoenzymes, which dephosphorylate extracellular S1P, when their active site is on the outer leaflet of the cell membrane (369). LPP1-3 are non-specific for S1P and bind other substrates like CER and lysophosphatidate. As previously mentioned, LPP3 is the predominant ectoenzyme that acts on extracellular S1P (343). LPP3 mouse knockouts are embryonically lethal and do not form a placenta, in part due to poor vasculogenesis (370). To this date, there are no studies on LPP1 and LPP2 in the placenta. For this reason, I only examined LPP3 expression in response to TNF- α in villous explants. I found that LPP3 levels in the placenta were unchanged in response to TNF- α treatment.

S1P can be irreversibly degraded by S1P lyase (SGPL1) into delta2-hexadecenal and ethanolamine 1-phosphate. SPGL1 can also degrade dihydro S1P into hexadecenal and

phosphoethanolamine. SGPL1 is an integral membrane protein located mainly on the cytosolic side of the endoplasmic reticulum (9). From current evidence, fetal SGPL1 deficiencies lead to a myriad of dysfunctions likely resulting from greatly elevated levels of sphingolipids. SGPL1 mRNA and protein expression in addition to enzyme activity in dendritic cells decreases in response to LPS stimulation (368). I found that SGPL1 levels in the placenta were unchanged in response to TNF- α .

The results from the villous explant model did not confirm my hypotheses as S1P regulatory enzymes were unaffected by treatment with TNF- α . This lack of effect that is contrary to previous published studies could be due to the high concentrations of TNF- α used in those previous studies. For example, a study examining the impact of TNF- α on SphK1 expression in breast cancer cells showed significant results at 50 ng/mL (351). Similarly, a study published in 2012 showed significant changes in S1PR expression in human dermal microvascular endothelial cells using 50 and 100 ng/mL of TNF- α (332). It is possible that these very high concentrations of TNF- α caused mass cell death, and did not act through the S1P pathway, as is possible with treatments done for at least 24 hours. It is also possible that somewhat higher concentrations of TNF- α are necessary to produce a clear result in *in vitro* experiments. This can occur due to the three-dimensional nature of the explant models, where drugs or factors can potentially bind proteins, get metabolized, or sequester within the tissue, thereby losing some potency. This could suggest that 1 ng/mL of TNF- α was not a high enough concentration to lead to effects in sphingolipid enzyme regulation. Alternatively, villous explants could also be producing sTNFR to neutralize the effects of TNF- α treatment, thereby reducing its potency (4).

Overall, this study showed that SphK1 levels were higher in the placentas of women with PE, which implies that the placenta could be a primary contributor of the elevated systemic S1P

levels in the mother. SGPP1 expression was increased at the end of ST regeneration regardless of TNF- α treatment, highlighting the importance of decreased S1P at the end of ST regeneration and before ST shedding. This shows the importance of S1P levels in regulating trophoblast turnover. The increase in only SGPP1 as opposed to other enzymes, like LPP3 or SGPL1, suggests an importance for dephosphorylating cytosolic S1P, leading to the production of sphingosine, at this phase of turnover. TNF- α did not alter S1P enzyme expression in placental tissues but led to SphK1 upregulation in differentiating CTs. This implies the cell-specific TNF- α regulation of S1P synthesizing and catabolic enzymes. The TNF- α -induced expression of SphK1 in differentiating CTs can be a mechanism to amplify TNF- α signaling (371) or can lead to the increase of extracellular S1P which would then signal through its S1PRs. This study proposes that the elevated TNF- α levels in PE can partially explain the elevated placental SphK1 expression that is observed in my study, particularly in the CTs. TNF- α and SphK1 activity (46) independently inhibit CT fusion, a step in the syncytialization process. Since my study showed altered SphK1 levels in the placenta in PE and in response to TNF- α , it is important to investigate whether these molecules belong to the same signaling pathway that leads to the disruption of placental function in PE.

4. Chapter 4: Tumor Necrosis Factor- α Induces a Preeclamptic-like Phenotype in Placental Villi via Sphingosine Kinase 1 Activation

A version of this article was published in: Fakhr Y, Koshti S, Habibyan YB, Webster K, Hemmings DG. Tumor Necrosis Factor- α Induces a Preeclamptic-like Phenotype in Placental Villi via Sphingosine Kinase 1 Activation. *International Journal of Molecular Sciences*. 2022; 23(7):3750. <https://doi.org/10.3390/ijms23073750>. The study was conceptualized and administered by Yuliya Fakhr and Denise Hemmings. Data were collected and analyzed by Yuliya Fakhr, Saloni Koshti, Yasaman Habibyan, and Kirsten Webster. Yuliya Fakhr wrote the first draft. Yuliya Fakhr and Denise Hemmings performed all revisions and edits of the manuscript.

4.1. Introduction

The placenta in PE is characterized by poor development of the ST, high levels of shedding and cell damage, and high levels of inflammatory cytokines (3). In PE, low CT proliferation leads to impaired differentiation and reduced fusion to ST, disrupting syncytial formation and thus, function. Abnormally high levels of placental cell death and ST shedding in PE (65) lead to a variety of pro-inflammatory responses (372) which further worsen the PE phenotype (373).

Elevated TNF- α is a strong hinderer of syncytialization. TNF- α decreases trophoblast proliferation, trophoblast fusion, and the release of placental hormones by the ST (4). TNF- α also leads to high levels of placental cell death and CT cell death, particularly by signaling through TNFR1 (374). TNFR1 activation requires SphK1 activation as a co-factor (5). TNF- α also leads to the release of pro-inflammatory cytokines from the placenta (4). TNF- α -TNFR1 signaling activates NF- κ B (211), which leads to the release of multiple cytokines and growth factors (375). Since TNFR1 signaling requires SphK1 activation, TNF- α could potentially induce its damaging effects on the placenta through SphK1 activation.

Despite the established role for TNF- α in placental damage, physiological levels of TNF- α have pregnancy-enhancing roles like inducing mucin 1 shedding from uterine epithelial cells, a major feature of embryo implantation (143). Normal levels of TNF- α also regulate the fate (144, 145), proliferation (146-148), and differentiation (149, 150) of various cells, including CTs (4, 139). TNF- α maintains normal levels of apoptosis that are necessary for fetal development (151). This deems market available TNF- α inhibitors controversial for use during pregnancy (152). My aim was to explore alternative factors downstream of TNF- α signaling that can be targeted.

The addition of TNF- α to HUVECs (6, 7), hepatocytes (328), lung, or fibroblast cell lines (376) activates SphK1, the main producer of S1P. Circulating levels of S1P are higher in women with PE (170, 176), where inflammation plays a role. I showed in Chapter 3 that SphK1 levels were higher in the placentas of women with PE. While high levels of S1P inhibit syncytialization (10), inhibiting SphK1, which would decrease S1P production, increases trophoblast fusion (46). Although the individual roles that TNF- α and S1P play in the pathogenesis of PE have been studied, we do not know whether TNF- α mediates its effects in the placenta through S1P by affecting SphK1 expression or activity. In Chapter 3, I showed that TNF- α did not alter the expression of S1P synthesizing and catabolic enzymes in whole placental villi in the explant model. However, in cultured primary CTs specifically, I showed that SphK1 levels were increased in response to TNF- α treatment.

Given the importance of both TNF- α and S1P on placental function and pregnancy outcomes, it is essential to understand the interaction between TNF- α and SphK1, the main producer of extracellular S1P, in the placenta. In this study, I investigated the interaction of TNF- α and SphK1 and their effects on ST formation and function, cell death, and cytokine and factor release during ST regeneration using the placental explant model. I hypothesized that high levels of TNF- α would decrease syncytialization, increase ST shedding, and increase placental cytokine release through activation of SphK1. This study showed that blocking SphK1 blocked TNF- α -induced placental damage, ST shedding, and cytokine release. However, at lower concentrations, TNF- α decreased CT fusion independently of SphK1 activation.

4.2. Results

4.2.1. Effect of TNF- α on ST Regeneration and its Interaction with SphK1

SphK1 expression and activity are increased in response to proinflammatory stimuli (377, 378) and S1P increases epithelial cell extrusion (302). Epithelial cell extrusion can be construed as a form of epithelial cell turnover, a process crucial for the maintenance of the ST. For these reasons, I investigated the effects of SphK1 inhibition using PF-543, a SphK1 inhibitor, on ST formation, function, and shedding in normal and proinflammatory conditions. To determine the functional and cytotoxic impact of TNF- α treatment in purified trophoblast cultures, I assessed β -hCG secretion and LDH release, respectively, after 24 hours of treatment at different concentrations of TNF- α . 1 ($p < 0.0001$), 10 ($p < 0.0001$), and 20 ng/mL ($p < 0.0001$) of TNF- α decreased β -hCG secretion (Figure 4.1A) without affecting cell viability, as evidenced by stable levels of LDH released in response to each concentration of TNF- α (Figure 4.1B). This suggested that 1 ng/mL of TNF- α was sufficient to induce decreased ST regeneration.

I then confirmed the concentration of TNF- α with maximum effects on resyncytialization in the explant model. After the initial 4-day culture to allow syncytial shedding, the explants were treated with TNF- α for 24 or 48 hours ($n=3$). As shown in Figure 3.2A, resyncytialization of term placental villous explants from normal pregnancies increased from 24 to 48 hours in the no treatment control. After 48 hours of incubation without TNF- α , the ST was relatively thick and consistent around the villi (white arrow). There were no overt differences seen with TNF- α treatment after 24 hours among the different TNF- α concentrations and the no treatment control. However, 48 hours of treatment with 0.1, 1, and 10 ng/mL of TNF- α resulted in reduced ST (red arrows). Treatment with 1 ng/mL or 10 ng/mL of TNF- α for 48 hours led to the most consistent

and reproducible hindrance of resyncytialization compared to the no treatment control, and hence were the chosen concentrations for further experiments.

TNF- α treatment (1 ng/mL) decreased the area of multinucleated ST after 48 hours ($p=0.003$, $n=4$, Figure 4.2), regardless of PF-543 treatment. SphK1 inhibition with PF-543 (1 μ M) also decreased the area of the multinucleated ST after 48 hours ($p=0.02$, $n=4$, Figure 4.2), regardless of TNF- α treatment. The area of multinucleated ST was not different after co-treatment of the explants with TNF- α and PF-543 when compared to individual TNF- α or PF-543 treatments ($n=4$). I analyzed samples after 24 hours of treatment as well, but there were no significant differences among the groups. Levels of β -hCG released into the supernatant were measured in explants treated with 1 ng/mL TNF- α , 1 μ M PF-543, or a combined treatment of 1 ng/mL TNF- α and 1 μ M PF-543 after 24 or 48 hours of treatment. None of these treatments affected β -hCG ($n=6$) or LDH ($n=8$) levels released by the explants (Figure 4.3).

Since 1 ng/mL TNF- α had no significant effects on β -hCG and LDH release after 24 or 48 hours of treatment, I tested whether a higher TNF- α concentration could hinder explant resyncytialization and increase cell death by acting through SphK1. Explants were treated with 10 ng/mL TNF- α , 1 μ M PF-543, or the combination of 10 ng/mL TNF- α and 1 μ M PF-543 ($n=6$). No significant changes were observed in β -hCG levels compared to controls in any of the groups at 24 hours post-treatment (Figure 4.4). At 48 hours post-treatment, however, 10 ng/mL TNF- α decreased β -hCG release ($p=0.008$). However, inhibiting SphK1 (1 μ M PF-543) did not rescue this decrease (Figure 4.4). Furthermore, administration of 10 ng/mL TNF- α in explants with 1 μ M PF543 significantly decreased β -hCG levels to control levels compared to 1 μ M PF-543 treatment alone ($p=0.05$). This is likely due to the inhibitory effects of TNF- α as the treatment interaction was not significant. As well, β -hCG levels after co-treatment with PF-543

and TNF- α compared to TNF- α alone were not significant. This all indicates that SphK1 activity did not mediate TNF- α effects on this ST endocrine function.

No significant changes were observed in LDH levels compared to controls in any of the groups at 24 hours post-treatment (Figure 4.4). However, TNF- α increased cell membrane damage as detected by increased LDH release at 48 hours (10 ng/mL, $p=0.01$, Figure 4.4) that was inhibited by co-treatment with PF-543 (1 μM) with an interaction of $p=0.006$. Post-hoc tests further confirmed this interaction as TNF- α increased LDH levels ($p=0.0005$) and inhibiting SphK1 in the presence of TNF- α decreased LDH levels from TNF- α -induced levels ($p=0.02$). Since the 24-hour treatment showed no differences in LDH release, I measured ST shedding only at 48 hours. ST shedding, demarcated by positive PLAP activity in the culture supernatant, was elevated in response to TNF- α treatment (10 ng/mL, $p=0.03$, Figure 4.4, $n=5$). This effect was diminished upon Sphk1 inhibition (1 μM) with a treatment interaction of $p=0.02$.

4.2.2. Effect of TNF- α on Placental Cytokine and Factor Release and its Dependence on SphK1 Activity

Treating explants with 10 ng/mL of TNF- α increased the release of the inflammatory cytokines Eotaxin ($p=0.03$) and MIP-1 β ($p=0.001$) after 48 hours (Figure 4.5, $n=5$). The treatment also increased the release of sCD40L ($p=0.01$), RANTES ($p<0.0001$), GM-CSF ($p=0.06$), IL-18 ($p=0.0002$), MCP-3 ($p=0.0006$), MIP-1 α ($p=0.009$), IL-6 ($p=0.055$), IL-12p40 ($p=0.02$), IL-12p70 ($p=0.002$), IL-2 ($p=0.007$), IL-15 ($p=0.004$), and IL-1RA ($p=0.006$), cytokines whose circulating levels are elevated in PE (Figure 4.5). The increased release of these factors in response to TNF- α was independent of SphK1 activation. TNF- α also increased the

release of IFN α 2 (p=0.0006) and IP-10 (p=0.02). The increase in these cytokines was reversed by SphK1 inhibition with a treatment interaction of p=0.06 and p=0.03, respectively (Figure 4.5).

TNF- α also increased the release of the following growth factors (Figure 4.6, n=5): fractalkine (p=0.009), IL-7 (p=0.01), EGF (p<0.0001), and Flt3L (p<0.0001). Two interleukins that are decreased in PE, IL-4 (p=0.002) and IL-9 (p=0.02), were also increased by this treatment. The increased release of these factors was independent of SphK1 activation. TNF- α increased the release of FGF2 (p=0.02) and PDGF-AA (p=0.01) (Figure 4.6) which was dependent on SphK1 since co-treatment of TNF- α with PF-543 decreased this release (p=0.02 and p=0.01, respectively) with treatment interactions of p=0.06 and p=0.05, respectively. Post-hoc tests further confirmed this interaction as TNF- α increased FGF2 (p=0.004) and PDGF-AA (p=0.003) and inhibiting SphK1 in the presence of TNF- α decreased FGF2 (p=0.02) and PDGF-AA (p=0.01) levels from TNF- α -induced levels. PF-543 treatment showed an overall change in FGF2 levels (p=0.05). This change, however, was most likely due to its interaction with TNF- α , since post-hoc tests showed no difference between PF-543 treated groups and the no treatment control. The only cytokine tested that was decreased by TNF- α treatment alone was IL-10 (p=0.05). PF-543 treatment in combination with TNF- α not only reversed this decrease but further increased IL-10 release to 44.7 \pm 20.6% higher than the no treatment control with a treatment interaction of p=0.003. This highlights the PF-543 treatment effect (p=0.02). Inhibiting SphK1 with PF-543 increased GRO- α release (p=0.01, Figure 4.6) but TNF- α had no effect on this cytokine. GRO- α was not detected in some samples and these were designated as 0 on the graph, and were excluded from statistical analysis. Neither TNF- α nor PF-543 treatments had any effect on IFN γ , IL-1- α , IL-1 β , IL-5, IL-8, MCP-1, G-CSF or PDGF-BB (Figure 4.7). Inhibiting SphK1 in the absence of TNF- α treatment decreased TNF- α release (p=0.008, Figure

4.8). TNF- α and GRO- α were the only factors affected by PF-543 treatment alone.

4.2.3. PF-543 Dose Response in Villous Explants

The dosage of 1 μ M PF-543 to inhibit SphK1 was established based on effective dosages in other cell types that examined different outcome measures. However, the effects of PF-543 on placental explant resyncytialization or cell death have not been investigated. I, therefore, wanted to determine whether higher doses of PF-543 that are still highly specific for inhibiting SphK1, would lead to enhanced effects. Thus, a PF-543 dose-response was performed. Explants were treated with 0 μ M, 1 μ M, 10 μ M, or 20 μ M of PF-543 (n=4) on Day 4 of explant culture. β -hCG and LDH levels were measured. With respect to ST endocrine function, no significant changes were observed in β -hCG at any PF-543 concentration after 24 hours of treatment (Figure 4.9A). However, inhibiting SphK1 activity with 10 or 20 μ M of PF-543 for 48 hours increased β -hCG secretion (p=0.04, p=0.02, respectively; Figure 4.9B). No significant changes in LDH levels were observed at any concentration of PF-543 at either time point (Figures 4.10C, 4.10D).

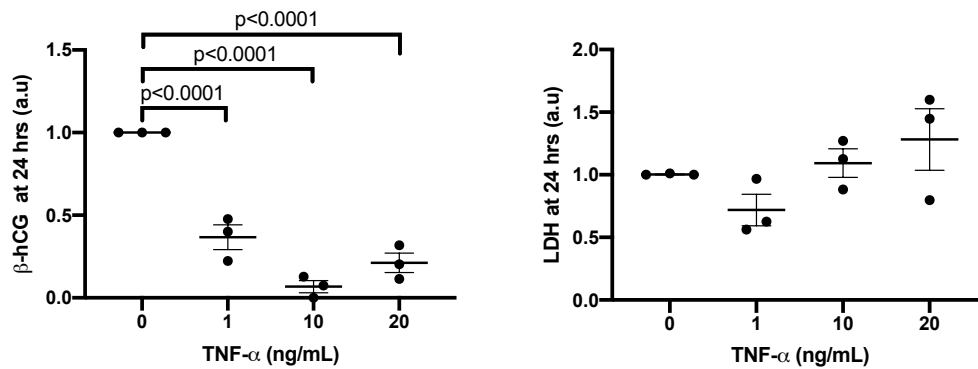


Figure 4.1: TNF- α Decreases β -hCG Release from Cultured Primary Trophoblasts Without Affecting Their Viability

Primary CTs were cultured for 24 hours after which supernatants and cell lysates were collected.

(A) TNF- α decreased β -hCG secretion from cultured trophoblast cells in a dose-dependent manner from 1 ng/mL to 10 ng/mL ($p=0.0008$). **(B)** TNF- α treatment for 24 hrs did not appear to affect the cytotoxicity of primary cultured trophoblast cells from 1 to 20 ng/mL. All results were calculated as a ratio of total protein in the well. These results were then calculated as a ratio relative to the no treatment control from the same experimental replicate and depicted as a fold-change difference within their own experimental subset. The arbitrary units (a.u) reflect the relative nature of the results that were calculated as a ratio of the chosen reference. All results were analyzed using a one-way ANOVA, two-stage linear step-up procedure of Benjamini, Krieger, and Yekutieli post-hoc test and linear trend post-hoc analysis ($n = 3$, Mean \pm SEM).

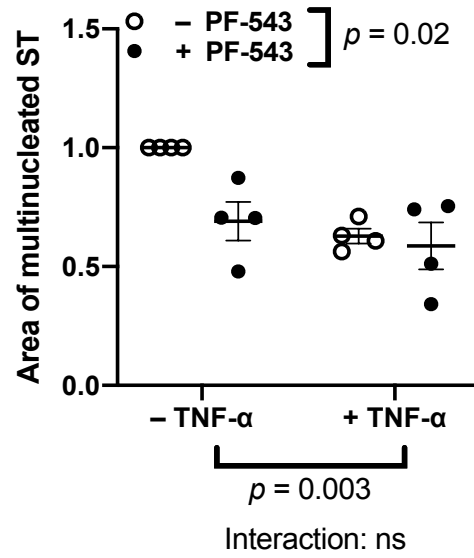
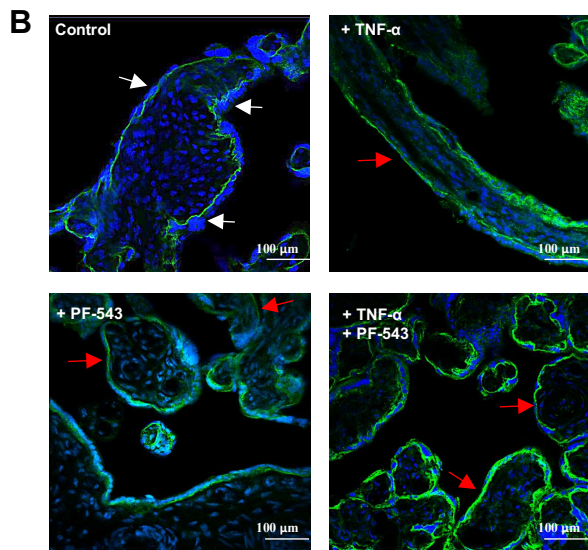
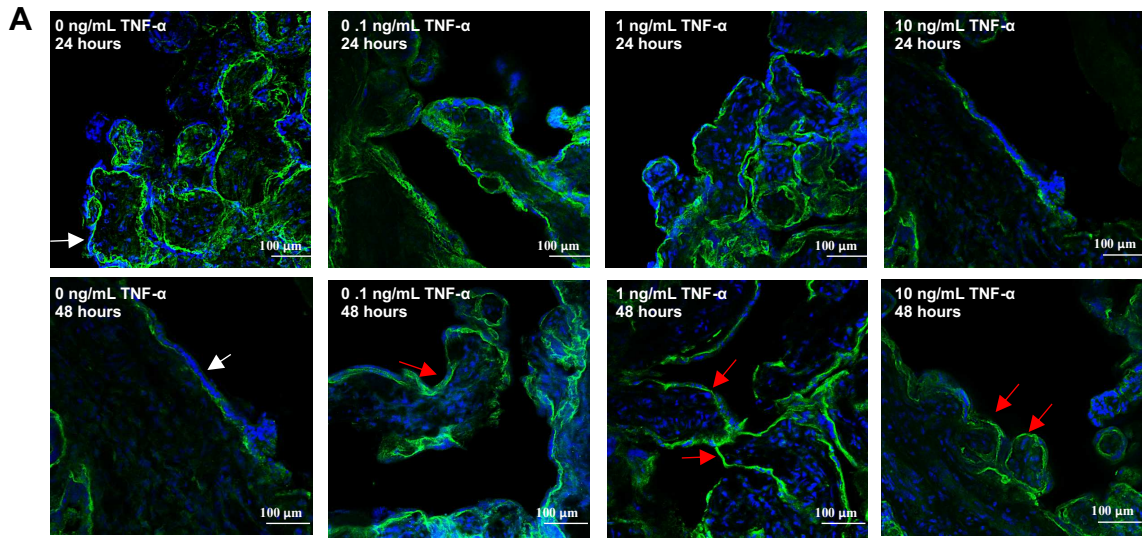


Figure 4.2: Resyncytialization in Term Placental Villous Explants from Normal Pregnancies Decreased in Response to TNF- α and Sphk1 Inhibition Independently

(A): Explants were cultured for 4 days prior to treatment to induce syncytial shedding.

Resyncytialization of term villous explants following treatment with 0–10 ng/mL of TNF- α after 24 or 48 hours of treatment was analyzed using confocal fluorescence microscopy. DAPI stained nuclei blue and E-cadherin (AF488) stained adherens junctions green ($n = 3$). **(B):** Explants were pre-cultured for 4 days prior to treatment with 1 ng/mL of TNF- α , 1 μ M PF-543, a co-treatment of both or a no treatment control for 48 hours. Results were analyzed by measuring the total area of the ST and normalizing it to the total surface area of the explant. Results are presented as relative to the no treatment control and analyzed using a two-way ANOVA with the two-stage linear step-up procedure of Benjamini, Krieger, and Yekutieli post-hoc test ($n = 4$, Mean \pm SEM).

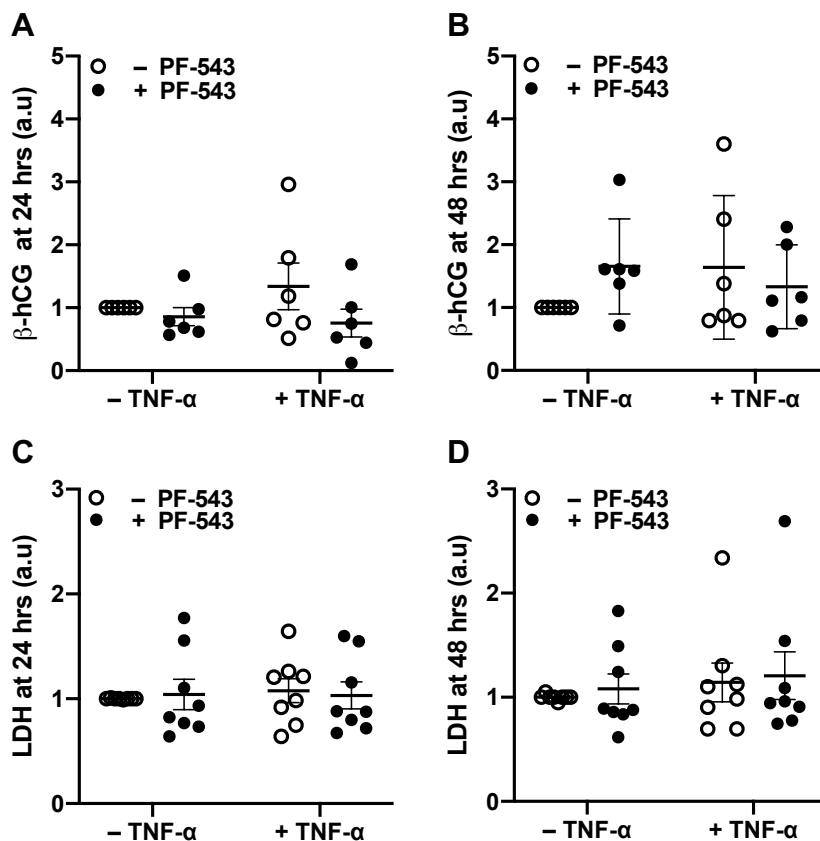


Figure 4.3: 1 ng/mL of TNF α with or without 1 μ M PF-543 Treatment did not Affect β -hCG or LDH Release into Supernatants

Explants were cultured for 4 days prior to treatment with 1 ng/mL of TNF- α , 1 μ M PF-543, a co-treatment of both or a no treatment control for 24 or 48 hours. Supernatants were centrifuged at 15000 RPM for 15 mins prior to quantification of β -hCG and LDH. **(A)** and **(B)** represent β -hCG released into supernatants after 24 and 48 hours, respectively, as measured by ELISA ($n = 6$). **(C)** and **(D)** represent LDH released into supernatants after 24 and 48 hours, respectively, as measured with a colorimetric assay ($n = 8$). Results were normalized against total protein mass. Normalized values were then calculated as a ratio relative to the no treatment control from the same experimental replicate and depicted as a fold-change difference within their own experimental subset. The arbitrary units (a.u) reflect the relative nature of the results that were

calculated as a ratio of the chosen reference. Results were analyzed using a two-way ANOVA with the two-stage linear step-up procedure of Benjamini, Krieger, and Yekutieli post-hoc test (Mean \pm SEM).

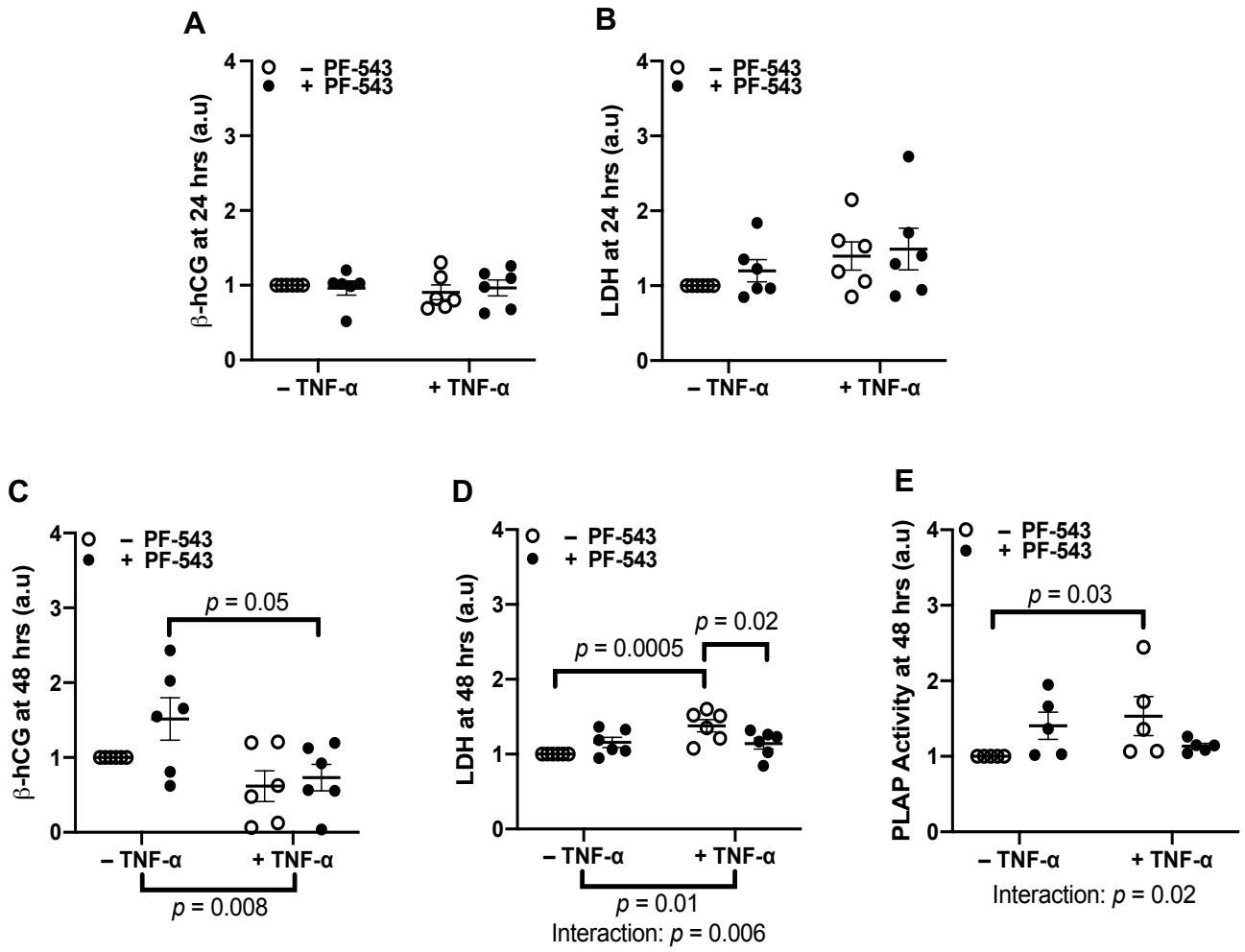


Figure 4.4: Inhibiting SphK1 with PF-543 Diminished TNF- α Effects on LDH Release and PLAP-Positive Shed Particles but not on β -hCG Secretion at 48 Hours

Explants were pre-cultured for 4 days prior to treatment with 10 ng/mL of TNF- α , 1 μ M PF-543, a co-treatment of both or a no treatment control for 48 hours. Supernatants were centrifuged at 15,000 RPM for 15 min prior to analysis. (A) β -hCG released after 24 hours or (C) 48 hours was measured by ELISA. (B) LDH released into the supernatant after 24 hours or (D) 48 hours was measured with a colorimetric assay. (E) Non-centrifuged supernatants were analyzed for PLAP activity using an alkaline phosphatase activity assay. Results were normalized against total protein mass. Normalized values were then calculated as a ratio relative to the no treatment control from the same experimental replicate and depicted as a fold-change difference within their own experimental subset. The arbitrary units (a.u) reflect the relative nature of the results that were calculated as a ratio of the chosen reference. Results were analyzed using a two-way ANOVA with the two-stage linear step-up procedure of Benjamini, Krieger, and Yekutieli post-hoc test ($n = 6$ or $n = 5$, Mean \pm SEM).

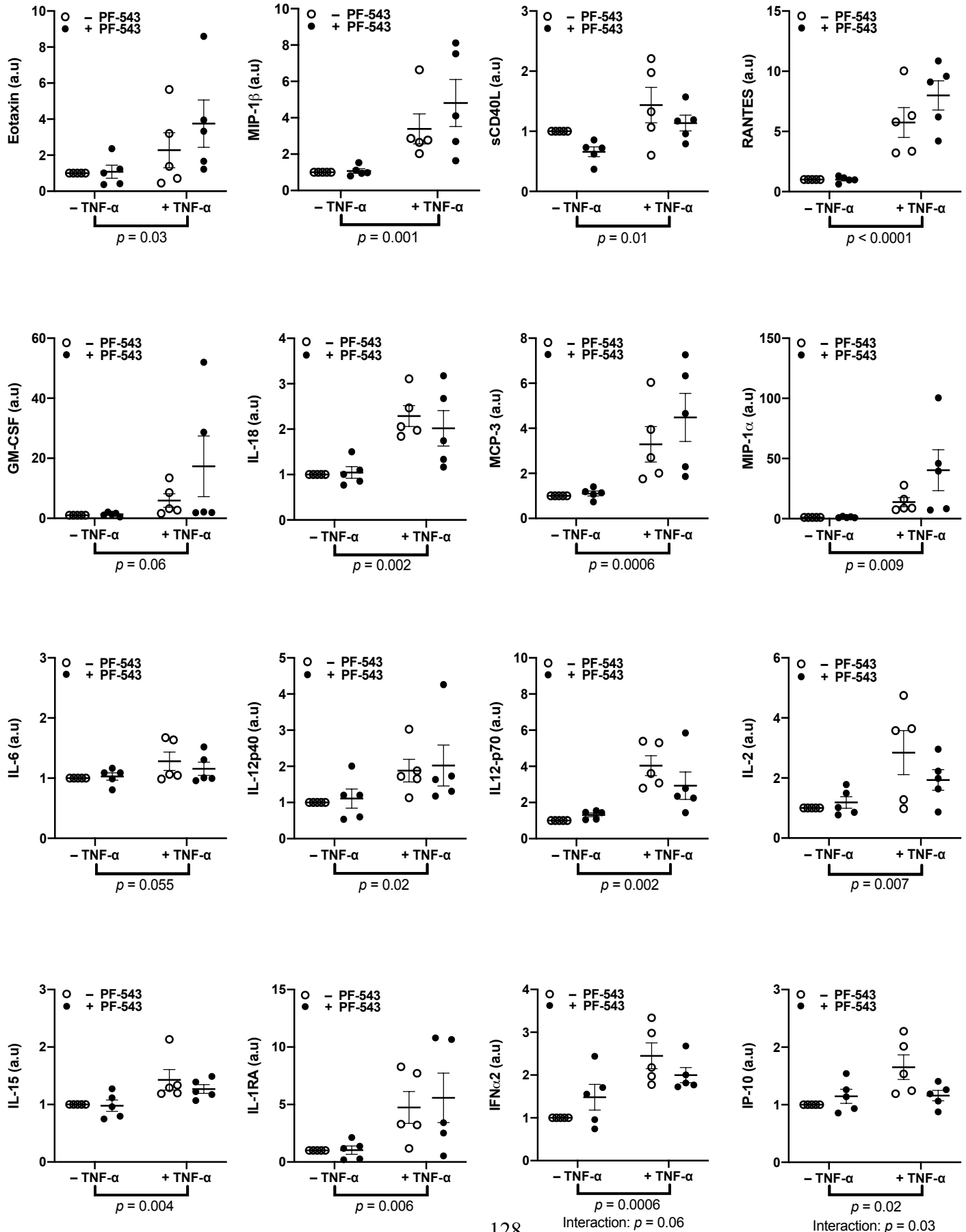


Figure 4.5: Inhibiting SphK1 with PF-543 Diminished TNF- α Effects on the Release of IFN α 2 and IP-10

Explants were cultured for 4 days prior to treatment with 10 ng/mL of TNF- α , 1 μ M PF-543, a co-treatment of both, or a no treatment control for 48 hours. Supernatants were centrifuged at 15,000 RPM for 15 min prior to quantification of pro-inflammatory cytokines and chemokines using a multiplex array. Results were normalized against total protein mass. Normalized values were then calculated as a ratio relative to the no treatment control from the same experimental replicate and depicted as a fold-change difference within their own experimental subset. The arbitrary units (a.u) reflect the relative nature of the results that were calculated as a ratio of the chosen reference. Results were analyzed using a two-way ANOVA with the two-stage linear step-up procedure of Benjamini, Krieger, and Yekutieli post-hoc test ($n = 5$, Mean \pm SEM).

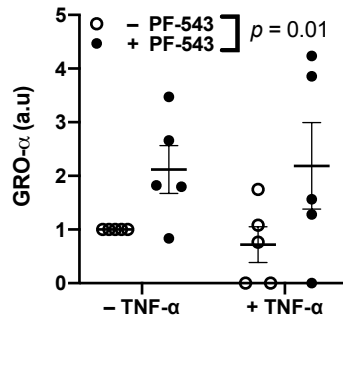
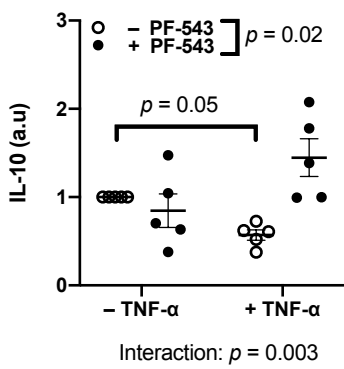
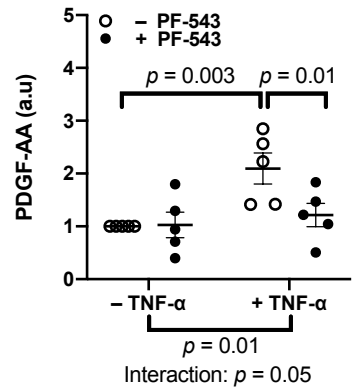
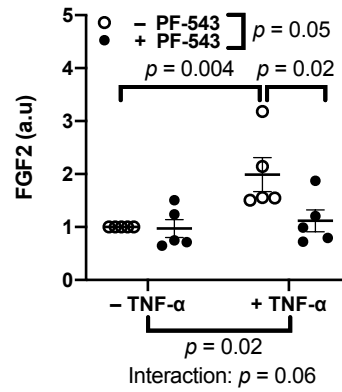
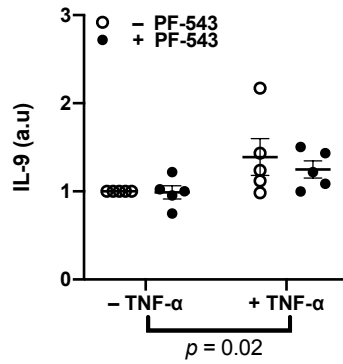
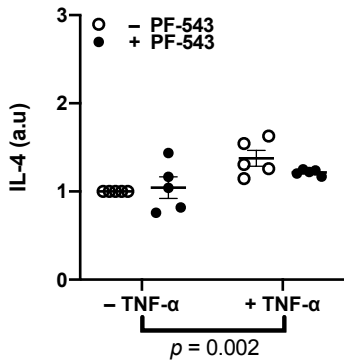
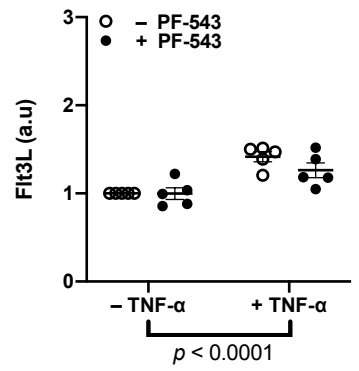
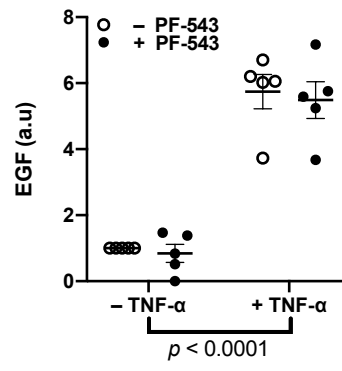
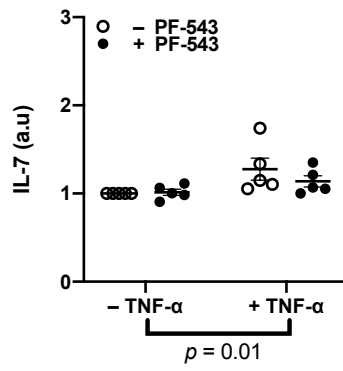
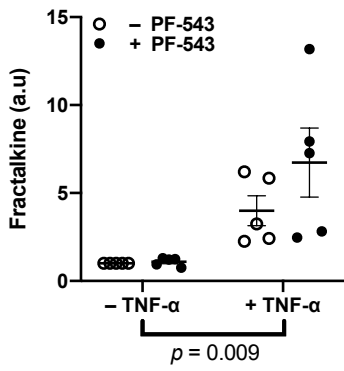


Figure 4.6: Inhibiting SphK1 with PF-543 Diminished TNF- α Effects on the Release of FGF2, PDGF-AA, and IL-10

Explants were cultured for 4 days prior to treatment with 10 ng/mL of TNF- α , 1 μ M PF-543, a co-treatment of both, or a no treatment control for 48 h. Supernatants were centrifuged at 15,000 RPM for 15 min prior to quantification of growth factors and chemokines using a multiplex array. Results were normalized against total protein mass. Normalized values were then calculated as a ratio relative to the no treatment control from the same experimental replicate and therefore depicted as a fold-change difference within their own experimental subset. The arbitrary units (a.u) reflect the relative nature of the results that were calculated as a ratio of the chosen reference. Results were analyzed using a two-way ANOVA with the two-stage linear step-up procedure of Benjamini, Krieger, and Yekutieli post-hoc test ($n = 5$, Mean \pm SEM).

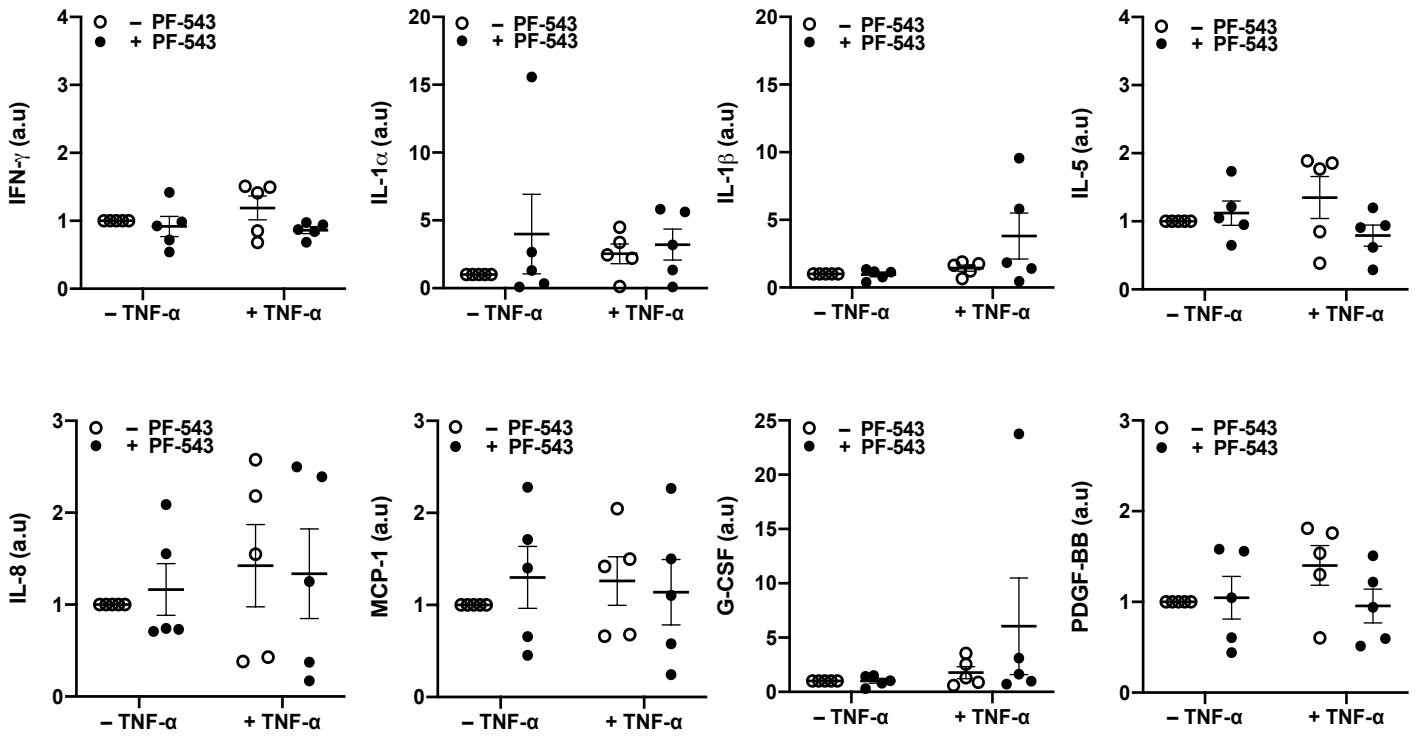


Figure 4.7: Inhibiting SphK1 with PF-543 and/or TNF- α Treatment did not Affect the Release of Some Cytokines, Factors, or Chemokines

Explants were cultured for 4 days prior to treatment with 10 ng/mL of TNF- α , 1 μ M PF-543, a co-treatment of both or a no treatment control for 48 hours. Supernatants were centrifuged at 15000 RPM for 15 mins prior to quantification of inflammatory cytokines, growth factors, and chemokines on a multiplex array. Results were normalized against total protein mass.

Normalized values were then calculated as a ratio relative to the no treatment control from the same experimental replicate and depicted as a fold-change difference within their own experimental subset. The arbitrary units (a.u) reflect the relative nature of the results that were calculated as a ratio of the chosen reference. Results were analyzed using a two-way ANOVA with the two-stage linear step-up procedure of Benjamini, Krieger, and Yekutieli post-hoc test ($n = 5$, Mean \pm SEM).

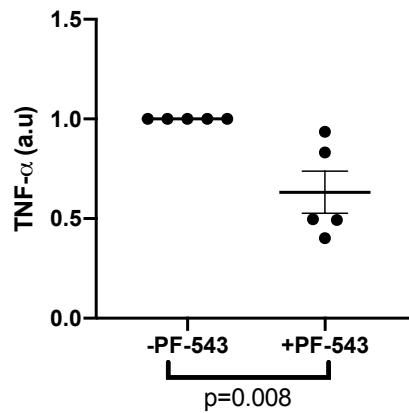


Figure 4.8: Inhibition of SphK1 Decreased Release of TNF- α

Explants were cultured for 4 days prior to treatment with 1 μ M PF-543 or a no treatment control for 48 hours. Supernatants were centrifuged at 15000 RPM for 15 mins prior to quantification of TNF- α using a multiplex array. Results were normalized against total protein mass. Normalized values were then calculated as a ratio relative to the no treatment control from the same experimental replicate and depicted as a fold-change difference within their own experimental subset. The arbitrary units (a.u) reflect the relative nature of the results that were calculated as a ratio of the chosen reference. Results were analyzed using a Mann-Whitney test ($n = 5$, Mean \pm SEM).

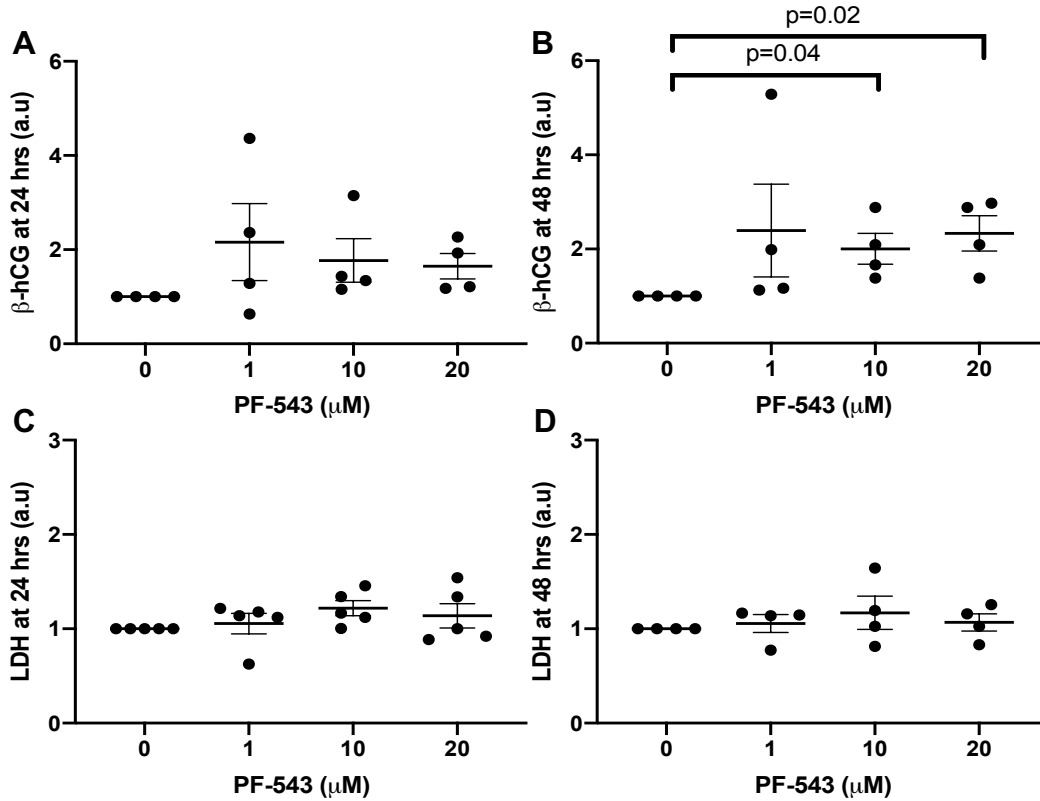


Figure 4.9: SphK1 Inhibition with PF-543 Increased β-hCG Secretion After 48 Hours

Explants were cultured for 4 days prior to treatment with a PF-543 dose response (0-20 μM). Supernatants were centrifuged at 15000 RPM for 15 mins prior to quantification of β-hCG and LDH. (A) and (B) represent β-hCG released into the supernatant after 24 and 48 hours, respectively, as measured by ELISA. (C) and (D) represent LDH released into the supernatant after 24 and 48 hours, respectively, as measured with a colorimetric assay. Results were normalized against total protein mass. Normalized values were then calculated as a ratio relative to the no-treatment control from the same experimental replicate and depicted as a fold-change difference within their own experimental subset. The arbitrary units (a.u) reflect the relative nature of the results that were calculated as a ratio of the chosen reference. Results were analyzed using the non-parametric Kruskal-Wallis test with the two-stage linear step-up procedure of Benjamini, Krieger, and Yekutieli post-hoc test ($n = 4-5$, Mean ± SEM).

4.3. Discussion

The focus of this study was to determine whether the effects of elevated TNF- α , which induces a PE-like placental phenotype, characterized by poor ST function, high ST shedding, and high inflammation (139, 140), are mediated through changes in SphK1 activity in placental explants. TNF- α (4, 138, 379) and S1P (9, 176), which is produced by SphK1, are already each independently associated with PE pathophysiology by inhibiting ST formation (10, 46, 139). TNF- α increases SphK1 activation in HUVECs (6, 7), hepatocytes (328), lung or fibroblast cell lines (376). In the current study, TNF- α effects on syncytial hormone production and CT fusion were found to be independent of SphK1 activation. However, placental cell death and ST shedding induced by TNF- α were dependent of SphK1 activation. TNF- α also increased the release of 16 pro-inflammatory cytokines and 9 growth factors from cultured placental explants. However, TNF- α -induced changes were dependent on SphK1 activation for only five of these factors: IFN α 2, IP-10, FGF2, and PDGF-AA were decreased while IL-10 was increased after inhibiting SphK1. Overall, I show that elevated TNF- α induced a PE-like placental phenotype, that was mediated in part through SphK1 activation.

TNF- α acts through two receptors: TNFR1 and 2 (4). The signaling pathway through TNFR1 leads to cytotoxic effects in trophoblasts (374, 380). Recently, both S1P and SphK1 were deemed essential to the signaling cascade of TNF- α through TNFR1 in HEK293T and HeLa cell lines (5). S1P and SphK1 act as cofactors for TNFR1 signaling by interacting with TNFR1 (5) and ultimately leading to NF- κ B activation (211). However, there is a knowledge gap in understanding the relationship between TNF- α and SphK1 signaling in inducing placental malfunction.

Hence, I aimed to decipher the independent role of SphK1 activation and its impact on TNF- α signaling in the placenta. Based on the existing knowledge regarding the role of SphK1 as an essential factor for TNF- α signaling (8), it was expected that inhibiting SphK1 would inhibit all the effects of TNF- α . However, I found that some effects of TNF- α on placental function were independent of SphK1 activation. Although TNF- α decreased re-syncytialization of the explants as expected, this decrease was not affected when SphK1 activity was inhibited during treatment. This implies that TNF- α hindrance of ST formation is independent of SphK1 activation. TNF- α decreased ST release of β -hCG independently of SphK1 activation but increased ST shedding was dependent on SphK1 activation. TNF- α decreased the area of multinucleated ST independently of SphK1 activation. This implies that the low amount of multinucleation is due to poor CT fusion into the ST rather than high levels of ST degradation. This can be inferred because the TNF- α -induced decrease in multinucleation was not dependent on SphK1, similar to the lack of dependence in β -hCG release. On the other hand, TNF- α -induced ST shedding was dependent on SphK1. Nonetheless, my study showed that TNF- α hinders ST development by both decreasing its formation and differentiation and by increasing its degradation.

On the other hand, only inhibiting SphK1 with PF-543 hindered fusion as well, suggesting an important role for this kinase and its product, S1P in the fusion process. This is contrary to what Singh et al. showed by using DMS to inhibit SphK1 (291). One explanation for this disparity is that DMS has many off-target effects, especially on trophoblast metabolism (46). Additionally, DMS inhibits both SphK1 and SphK2 and is a PKC inhibitor, which is downstream of S1PR2-3 signaling (381). PF-543, however, is reported to be specific and efficient, inhibiting over 95% of SphK1 activity at 1 μ M with a 134-fold selectivity for the SphK1 isoform over

SphK2 (382). Moreover, these experiments were done in villous explant cultures where the CT is in context with the surrounding tissue and extracellular matrix as opposed to those done by Singh et al. which used cultured primary trophoblasts only. In a different study using BeWo choriocarcinoma cells, Singh and colleagues show that SphK1 levels decrease as cells fuse into a multinucleated ST (46). This could imply the importance of SphK1 in inducing CT fusion and its downregulation once fusion is complete.

In contrast to the important role SphK1 may play in CT fusion, inhibiting SphK1 activity alone increased β -hCG release from cultured placental explants. The seemingly contradictory effects of SphK1 inhibition on syncytial function versus CT fusion in these findings might point to differential effects of SphK1 inhibition depending on the cell type, CT versus ST. This, however, remains to be investigated. While CT fusion and β -hCG release are both used as markers for syncytial differentiation, it is important to remember that these processes occur through separate signaling pathways and in different cell types. A differential effect on fusion versus endocrine function was also seen by Singh et al when using DMS to inhibit SphK; however, these results are opposite to mine where they found increased CT fusion and decreased β -hCG release.

Although β -hCG release was decreased with treatment of 1 and 10 ng/mL of TNF- α in primary CT cultures, the effects on β -hCG release were only observed with 10 ng/mL of TNF- α in the explant model. The need for a higher dosage in explants compared to primary cells can be explained by the complex nature of explants, which often leads to degradation or sequestration of exogenous ligands, leading to a decrease in their potency. TNF- α was previously established to have pro-apoptotic effects in the ST and to decrease β -hCG release at 10 ng/mL in villous explants (139), whereas, 1 ng/mL of TNF- α had no effect on β -hCG release (139). Thus, my

results are in agreement with this previous literature. My results also showed that TNF- α at the lower concentration of 1 ng/mL did, however, decrease trophoblast fusion. This decrease, as mentioned, had no consequences on β -hCG release. This could have occurred because minimal ST could be sufficient to produce β -hCG at healthy levels even in the presence of 1 ng/mL of TNF- α ; however, 10 ng/mL of TNF- α overcomes this compensating response by ST.

The ST is maintained by a balance of trophoblast fusion/differentiation and syncytial shedding. Since cell damage and syncytial shedding are increased in PE, I assessed the levels of LDH release and PLAP-positive shed particles, respectively. Inhibiting SphK1 alone had no effect on placental cell membrane damage or syncytial shedding. However, these measures were increased in explants treated with TNF- α alone, reflecting increased cell death. Inhibiting SphK1 while treating with TNF- α blocked the TNF- α -induced decrease in cell death and syncytial shedding. This indicates that TNF- α exerts its effects on cell death and shedding through SphK1. Since LDH is a cytosolic enzyme, the type of cell death that is most likely occurring in these experiments is necrosis, which involves releasing the contents of the cytoplasm due to cell membrane damage. However, another form of cell death that might be occurring is autophagy (383). While autophagy involves the secretion of autolysosomes that contain LDH (384), it is possible that these autolysosomes were lysed during supernatant collection and the freeze-thaw process. In this case, the LDH that was measured in the assay would have included autolysosomal LDH. For this reason, it would be important in the future to evaluate autophagy-specific markers, such as LC3-II (microtubule-associated protein light chain 3) and WD repeat domain phosphoinositide-interacting family protein 2, or WIPI2 (385).

Interestingly, LDH is a cytosolic enzyme that can induce autophagy in tumor cells (386). TNF- α (387) as well as SphK1 activation (388) increase autophagy. In fact, CER, a precursor of

S1P, increases autophagy in a trophoblast cell line (175). Autophagy is increased in the placental villi of women with PE (387), but the regulators of this process in the placenta are still unclear. My results showed that TNF- α -induced LDH release is dependent on SphK1 activity. Further research would investigate whether the TNF- α -SphK1-LDH release pathway regulates autophagy in the placenta.

Studies in epithelial and endothelial cells show that TNF- α administration increases the activity and expression of SphK1 levels (5-8). Indeed, my study showed that TNF- α is dependent on SphK1 activity to induce cell death and syncytial shedding in the placenta. Potentially, this could occur through TNF- α -induced activation of NF- κ B mediated cell death pathways (5). NF- κ B is a known activator of cell fate pathways as well as pro-inflammatory and growth factor production. Thus, SphK1-mediated TNF- α activation of IFN α 2, IP-10, FGF2, and PDGF-AA release could in fact be occurring due to NF- κ B activation. While the role of IFN α 2 is not yet clear in the placenta, this type I interferon is expressed by epithelial cells and is responsible for upregulating genes of proteins involved in immune responses in the bovine endometrium (389). IFN α 2 also increases choriocarcinoma trophoblast cell resistance to methotrexate by regulating cell viability (390). On the other hand, IP-10 inhibits angiogenesis by reducing endothelial cell viability and proliferation in various cell types, including human vascular endothelial cells. IP-10, however, also stimulates vascular smooth muscle cell motility and hence differentiation (391, 392). This step is critical for spiral artery remodeling in early pregnancy. Improper spiral artery remodeling is strongly associated with the development of PE. FGF2 and PDGF-AA are also upregulated in response to cell damage (393, 394), as a compensatory response. PDGF-AA particularly, rescues trophoblasts from TNF- α -induced cell death (298). Thus, this interaction might be occurring downstream of the cell death pathway induced by TNF- α , which is dependent

on SphK1 activation.

In my study, the only factor that TNF- α treatment of placental explants decreased was IL-10, and inhibiting SphK1 activation not only reversed this effect but led to increased levels above the control. Siwetz et al show that IL-10 levels are unchanged in response to TNF- α in first trimester villous explants (140). However, IL-10 circulating levels are lower in PE in second and third trimester pregnancies (395). This supports the idea that high levels of TNF- α in PE could be the reason behind the drop in circulating IL-10 levels. The TNF- α -induced decrease in IL-10 release was dependent on SphK1 activation. As summarized by Kalkunte S et al, IL-10 is an anti-inflammatory cytokine that is crucial for pregnancy maintenance (396). Its levels are normally decreased at term to allow the rise in inflammation necessary for the induction of labor. Hence, high levels of TNF- α lead to a further decrease in IL-10 which would skew the balance towards a hyperinflammatory state. IL-10 serves a protective role in pregnant women exposed to hypoxia, a characteristic of PE. Pregnant IL-10 knockout mice exposed to a hypoxic environment developed placental damage and PE symptoms. Treating these mice with recombinant IL-10 reversed the PE symptoms induced by hypoxia. IL-10 is also protective in other aspects of the disorder, such as inflammation and vascular function, which are all summarized in the following review (396). Interestingly, IL-10 acts as a strong protector against autophagic activity (387). Hence, the SphK1-dependent TNF- α decrease of IL-10 could be a potential mechanism of TNF- α -induced autophagy in the placenta.

TNF- α induced the release of a wide variety of inflammatory and growth cytokines but the majority of these were independent of SphK1 activation. This could be because TNF- α acts on specific cell types in the placenta that release some cytokines and not others. Hence, TNF- α could be dependent on SphK1 activation only in specific cell types. Alternatively, TNF- α could

be inducing certain cytokines through TNFR1 and some through TNFR2, whose signaling and interaction with SphK1 are yet to be investigated. Interestingly, inhibiting SphK1 led to a decrease in TNF- α release implying that SphK1 activity induces TNF- α release from the placenta. This release could be a normal physiological response when SphK1 activation levels are within normal ranges and could lead to the release of TNF- α to increase normal processes like angiogenesis and proliferation (4). However, high levels of TNF- α in pathological conditions such as PE could contribute to high levels of SphK1 activation in the placenta, which would further amplify TNF- α levels and exacerbate the PE-like phenotype. SphK1 activation induced by TNF- α was involved in syncytial shedding, membrane damage, secretion of proliferation and pro-survival factors, and secretion of proinflammatory factors IFN α 2 and IP-10. SphK1 also increased TNF- α itself suggesting a feed-forward loop. The role of SphK1 activity in mediating the TNF- α -induced decrease in IL-10 as well as the decrease in TNF- α itself has important translational implications in other inflammatory disorders as well, particularly autoimmune diseases, such as inflammatory bowel disease (397). My findings propose investigating whether SphK1 inhibitors or agonists/antagonists regulating S1P signaling, in general, could be synergistic with TNF- α -targeted antibodies for the treatment of these disorders.

Finally, only GRO- α increased in response to SphK1 inhibition. In this model, TNF- α had no effect on GRO- α . This is contrary to existing literature which shows that TNF- α increases GRO- α expression in airway smooth muscle cells (398), HUVECs (399) and keratocytes (400). However, in corneal epithelial cells, TNF- α has no effect on GRO- α expression, suggesting a cell-dependent differential response to TNF- α . The cell composition of the villous explants could have led to the lack of responsiveness to TNF- α with regards to GRO- α levels. Moreover, it is important to note that only secretion of the chemokine, and not expression, was measured in my

study. TNF- α can have different roles in regulation the transcription versus the secretion of GRO- α . In non-placental cells, GRO- α induces angiogenesis and plays a multifaceted role in tumor progression (401). While the role of GRO- α in placental and trophoblast function throughout pregnancy has not been extensively investigated, GRO- α is commonly secreted from trophoblasts in response to cell damage (402). In my study, inhibiting SphK1 could have led to a specific damage-induced signaling pathway, that was not triggered by TNF- α , that led to the increase in this cytokine.

The explant model is a complex three-dimensional culture with multiple cell types, matrices, and cell-cell interactions. Hence, potent inhibitors, like PF-543, can potentially bind proteins, get degraded, or sequester within the tissue, thereby losing some potency. To investigate if increasing concentrations of PF-543 could have distinguishable effects on explant syncytialization, I exposed explants to increasing PF-543 concentrations that were still within the specific range (382). PF-543 treatment at 10 and 20 μ M increased the release of β -hCG from villous explants without affecting cell viability. An article shows that 10 μ M of PF-543 in a monolayer cell culture did not bind any off-target kinases from the kinase profiling panel (382). Moreover, it had a 132-fold selectivity for SphK1 over SphK2 (382). As mentioned, PF-543 has not been tested in trophoblasts or in placental explants previously. Nonetheless, 1 μ M (403, 404) and even 10 μ M (405) of PF-543 are commonly used concentrations in a monolayer culture of cells isolated from other tissues.

Certain studies show a difference in function for S1P produced by SphK1 or SphK2 (406). SphK1 is the cytoplasmic isoform which contributes mainly to extracellular S1P that signals through its receptors. SphK2 is located in the nucleus and the rough endoplasmic

reticulum and is the main producer of S1P that signals intracellularly (407). SphK2 is poorly studied in the placenta and its interaction with TNF- α on placental function is unknown.

Currently, there are no definitive treatments for PE except for delivery of the fetus which often leads to preterm birth (408). This study showed that TNF- α induced its effects on several aspects of placental function by activating SphK1 and identifies the S1P signaling pathway as a potential treatable target. However, since blocking SphK1 activity also inhibited trophoblast fusion (291) and since S1P has many diverse protective functions, the market available SphK1 inhibitors (409) may pose off-target effects that will impact placental health and potentially fetal health through placental programming. Moreover, inhibition of SphK1 activity will reduce the synthesis of S1P which is protective and anti-apoptotic at normal levels (9). One way to mitigate this is to target specific S1P receptors. For instance, S1PR1 is a key player in counteracting TNF- α induced release of MCP-1 and IL-8 in placental vascular tissues (9). S1PR2 activation induces IL-6 secretion from trophoblasts (9). Hence, my next chapter will explore the role of S1PRs in the placenta as well as placental S1PR expression in PE and in response to TNF- α .

5. Chapter 5: S1P Receptors in Placental Physiology and Pathology

5.1. Introduction

Increased proinflammatory cytokines alter placental growth and function, contributing to the pathophysiology of the disorder. As reviewed in Haider et al (4), TNF- α hinders the formation and function of the placental ST, the site of hormone production and maternofetal exchange of nutrients, water, and gases. In Chapter 3 (371), I showed that TNF- α induced a placental PE-like phenotype via SphK1 activation, specifically in the case of ST shedding, IL-10 inhibition, and specific cytokine release. Currently, SphK1 inhibitors are strong pharmaceutical contenders for their therapeutic potential in inflammatory disorders, with some like Safingol entering the clinical trial stage (409). However, the total inhibition of SphK1 will affect overall S1P production and pose off-target effects (409). These effects are particularly concerning during pregnancy since S1P regulates pregnancy-enhancing functions such as regulating the balance between vasoconstriction and vasodilation, endothelial barrier function, trophoblast function, and inflammatory cytokine release in the placenta (9). For this reason, investigating S1PRs and understanding their function in the placenta might lead to a more targeted manipulation of dysfunctional S1P signaling.

S1P is a bioactive lipid that regulates multiple physiological processes by signaling through its five specific receptors, S1PR1-5. These S1PRs are differentially expressed in different placental cell types and regulate different responses. In most cases, S1PR1 and S1PR3 signaling is protective and anti-apoptotic (9). Whereas, S1PR2 signaling induces secretion of proinflammatory cytokines from trophoblast cell lines (286). In HUVECs and rat hepatocytes, treatment with S1PR2 antagonists reduces apoptosis (410, 411), implying a pro-apoptotic effect upon S1PR2 activation. The role of S1PR2 signaling in the placenta, however, is poorly understood.

Placental S1PR expression in PE may be altered in a manner that promotes destructive physiological signaling. For instance, S1PR1 and S1PR3 mRNA expression is lower in human placental samples from women with PE, while S1PR2 expression is higher in placentas of women with severe PE (234). Since placental S1PR2 is overexpressed in severe PE, it is important to decipher the role of S1PR2 in placental signaling, specifically in ST formation.

Altered placental S1PR expression as seen in PE can be the result of numerous factors. TNF- α is implicated in regulating S1PR expression in various cell types. TNF- α treatment leads to mRNA and protein upregulation of S1PR2 in cultured human microvascular endothelial cells and to increased vascular permeability, a hallmark of inflammation (332). However, in fibroblast-like human synoviocytes, that are located inside joints, the addition of TNF- α upregulates S1PR3 mRNA and protein leading to inflammatory cytokine secretion, with no effects on S1PR1 or S1PR2 expression (333). This variation in regulation of S1PR expression appears to be cell-specific and warrants investigation in the placenta in general and in the trophoblast specifically.

In summary, studies in various cell types suggest that S1PR2 signaling is involved in inflammatory cytokine release and apoptosis. S1PR1 signaling is often protective and therefore can counterbalance the detrimental S1PR2-mediated signaling. Additionally, TNF- α increases S1PR2 expression in non-placental microvascular cells. S1PR2 is also increased in severe PE. Hence, I hypothesized that inhibiting S1PR2 will increase placental ST function and decrease cell membrane damage. I further hypothesized that TNF- α will increase S1PR2 expression and decrease S1PR1 expression in BeWo cells, primary trophoblasts, and villous explants. I will also confirm that S1PR2 is higher in placentas of women with PE using a different method than that published, Western Blots.

My study showed that S1PR2 inhibition in the absence of any other treatment altered ST endocrine secretion in a hormone-specific manner and also led to an increase in cell membrane damage. S1PR2 was increased in placentas of women with mild PE. S1PR2, however, was decreased in response to TNF- α in BeWo cells, but it was increased in cultured primary human CTs. The overall expression of S1PR2 and S1PR3 in villous explants from normal term placentas increased in response to TNF- α , and TNF- α muted the S1PR1 surge that was seen in untreated cultures at the end of ST regeneration.

5.2. Results

5.2.1. S1P and Placental ST Function

I first aimed to test the effect of S1P treatment alone on the placental release of β -hCG and hPL, two prominent markers of ST function. Villous explants were cultured for 4 days to induce spontaneous ST shedding, as was described in Chapter 3 (371). On day 4, when the ST was maximally shed, explants were treated with 1 or 10 μ M of S1P in a solution containing bovine serum albumin as the lipid carrier. In Chapter 4, explants needed 48 hours of treatment to show a response in β -hCG release. So, I only examined the effects of S1P after 48 hours of treatment. My results showed that 1 and 10 μ M of S1P did not affect LDH, a marker of cell membrane damage or cell death (Figure 5.1A). However, 10 μ M of S1P increased β -hCG release from villous explants ($p=0.03$) after 48 hours of treatment. On the other hand, neither concentration of S1P altered hPL levels after 48 hours of treatment.

5.2.2. S1PR2 and Placental ST Function

Next, I aimed to identify the importance of S1PR2 signaling in unstimulated cultures on LDH release as S1PR2 signaling is a strong inducer of various forms of cell death in other cell

types. I also aimed to identify the effects of S1PR2 signaling on β -hCG and hPL release since placental S1PR2 is increased in severe PE, in which placental ST function is impaired. My results showed that inhibiting S1PR2 in the absence of any other treatment increased LDH release (Figure 5.2A, $p=0.005$), which suggests that S1PR2 activation might be decreasing cell membrane damage. Inhibiting S1PR2 with JTE-013 increased β -hCG release (Figure 5.2B, $p=0.01$) but decreased hPL (Figure 5.2C, $p=0.02$), suggesting that activation of S1PR2 by endogenous sources of S1P decreases β -hCG release but increases hPL release from the ST.

5.2.3. Placental S1PR Expression in PE

Thirteen women with healthy pregnancies and 4 women with PE were enrolled in this study and their clinical characteristics are summarized in Table 5.1. Women with PE had higher systolic (156.4 ± 14.35 versus 112.7 ± 4.976 mmHg; $p<0.0001$) and diastolic (111.6 ± 29.1 versus 70.98 ± 5.54 ; $p=0.038$) blood pressures compared to those in the healthy control group. All participants in the PE group were positive for proteinuria. There were no significant differences in infant birth weight and gestational age between the groups.

Previous studies report a general decrease in S1PR1 mRNA expression in placentas of women with PE, including in biopsies from the basal plate (maternal side) and in placental chorionic arteries (9). S1PR1 protein levels in the placentas of women with healthy pregnancies or those with PE have not been examined yet. My results in Figure 5.3A confirmed the lack of difference in S1PR1 protein expression in placentas from these groups of women, in agreement with the previously reported mRNA results (234). These results were confirmed by performing immunofluorescent staining of S1PR1 in placental biopsies (Figure 5.3C). Qualitatively, S1PR1 appears to be evenly expressed throughout the placentas from both the healthy and the PE groups. There were no overt differences in S1PR1 expression patterns between the groups.

Overall quantification of immunofluorescence confirmed the lack of difference in S1PR1 levels.

Reports on S1PR2 expression in placentas from women with PE vary and warrant further investigation. Some studies show no changes in expression in PE (353), and others show an increase in S1PR2 mRNA expression in severe PE (234). Other studies show increased S1PR2 mRNA expression in placental chorionic arteries (172). The protein expression, however, of this receptor has not been investigated in the placenta. In this study, I compared S1PR2 levels in placentas from normal pregnant women to those from women with PE by Western Blot. My study showed an increase in S1PR2 protein levels in placentas from women with PE (Figure 5.3B, $p=0.02$)

5.2.4. S1PR Expression in BeWo Cells

Since the disruption in placental S1PR expression is associated with the diagnosis of PE, it is important to investigate factors in PE that could lead to this imbalance. To start with, I investigated the effects of TNF- α treatment on S1PR1 and S1PR2 expression in BeWo cells, a choriocarcinoma cell line that closely mimics second trimester trophoblasts that can differentiate into a multinucleated ST with barrier-like properties (412). S1PR1 protein expression remained unchanged in response to 10 or 20 ng/mL of TNF- α after 24 hours of treatment (Figure 5.4A). S1PR2 expression, however, decreased in a dose-dependent manner ($p=0.02$) with significant decreases at 10 ng/mL ($p=0.03$) and 20 ng/mL ($p=0.02$) of TNF- α (Figure 5.4B). No changes in S1PR2 expression were observed on post-hoc testing in response to 1 or 5 ng/mL of TNF- α (Figure 5.4B). Since LPS treatment increases S1PR2 levels in other cell types, I used 20 μ g/mL of LPS as a positive control. In my study, however, LPS decreased S1PR2 expression ($p=0.01$, Figure 5.4B), similar to the TNF- α effect.

5.2.5. S1PR Expression in Primary Human Cytotrophoblasts

Since BeWo cells are a choriocarcinoma cell line and S1P signaling is altered in cancer (413), BeWo cells might not accurately mimic physiological trophoblast responses with respect to their S1PRs. For this reason, I also tested the effect of TNF- α on S1PR expression in primary human CTs. Since protein mass extracted from cultured CTs was not sufficient for S1PR detection by Western Blot, I used immunofluorescence to measure S1PR1 and S1PR2 levels. Similar to BeWo cells, S1PR1 expression did not change in response to TNF- α at 1, 5, 10, or 20 ng/mL of treatment for 24 hours (Figure 5.5A). On the other hand, S1PR2 expression increased after 24 hours of treatment with 20 ng/mL of TNF- α ($p=0.005$, Figure 5.5B), in contrast to the results in BeWo cells. Unlike the BeWo cells, S1PR1 and S1PR2 expression remained unchanged in response to 20 μ g/mL of LPS (Figure 5.5B), suggesting that the term primary human CTs lacked responsiveness to LPS in regards to S1PR expression.

5.2.6. S1PR Expression in Regenerating Villous Explants

Finally, since S1PR1 and S1PR2 expression is altered in PE in the whole placental tissue rather than trophoblasts specifically, I investigated the effect of treatment with 1 ng/mL of TNF- α on S1PR expression in villous explants isolated from healthy term pregnancies. To better understand S1PR expression during ST formation, I investigated the fluctuation of receptor mRNA expression at various time points throughout the ST regenerative process. Finally, as the role of S1PR3 is under-investigated in the placenta and S1PR3 expression is increased in response to TNF- α in synoviocytes (333), I also measured S1PR3 villous expression across ST formation in the absence and presence of 1 ng/mL of TNF- α . Treatment wells that were contaminated or identified as outliers by ROUT's test were excluded from the analysis. S1PR1 mRNA expression was constant during the initial phases of ST formation, from 0 to 36 hours,

and peaked at 48 hours, at the end of the regenerative cycle ($p=0.01$, Figure 5.6A). In contrast, TNF- α muted this increase in S1PR1 expression, and values remained constant throughout the ST formation phase (Figure 5.6B). Upon comparing S1PR1 mRNA expression in TNF- α -treated villi with that in untreated villi, I found that TNF- α decreased S1PR1 mRNA expression after 48 hours of treatment ($p=0.04$, Figure 5.6C).

Alternatively, S1PR2 and S1PR3 expression remained constant during ST formation (Figure 5.6D and 5.6G, respectively). In the presence of TNF- α , S1PR2 and S1PR3 mRNA expression was constant during the initial phases of ST formation, from 0 to 36 hours, and peaked at 48 hours, at the end of the regenerative cycle ($p=0.03$, Figure 5.6E and $p=0.007$, Figure 5.6H respectively). Upon comparing S1PR2 or S1PR3 mRNA expression in TNF- α -treated villi with that in untreated villi, I found that TNF- α increased S1PR2 and S1PR3 mRNA expression after 48 hours of treatment ($p=0.04$, Figure 5.6F and $p=0.002$, Figure 5.6I).

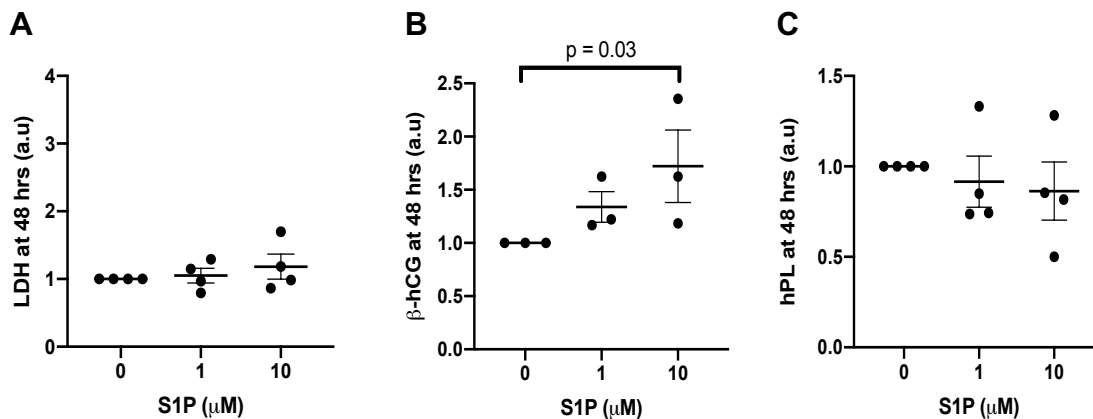


Figure 5.1: S1P Treatment Increases Secretion of β -hCG at 48 Hours but not LDH or hPL

Term chorionic villous explants were pre-cultured for 4 days prior to treatment with 0, 1, or 10 μ M of S1P. Supernatants were centrifuged at 15,000 RPM for 15 min prior to analysis. (A) LDH released after 48 h was measured with a colorimetric assay. (B) β -hCG released after 48 h was measured by ELISA. (C) hPL released after 48 h was measured by ELISA. Results were normalized against total protein mass. Normalized values were then calculated as a ratio relative to the no treatment control from the same experimental replicate and depicted as a fold-change difference within their own experimental subset. The arbitrary units (a.u) reflect the relative nature of the results that were calculated as a ratio of the chosen reference. Results were analyzed using the non-parametric Kruskal-Wallis test ($n = 3$ or $n = 4$, Mean \pm SEM).

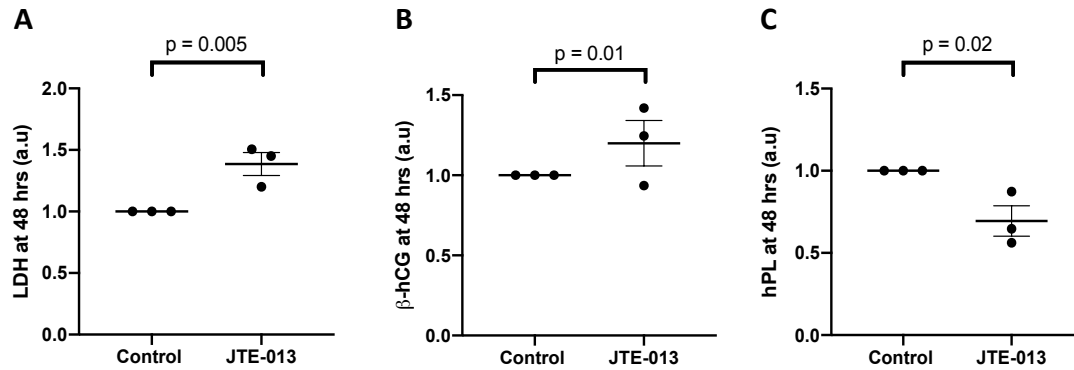


Figure 5.2: Inhibiting S1PR2 with JTE-013 Treatment Increases LDH and Beta-Human Chorionic Gonadotropin (β -hCG) Secretion at 48 Hours but Decreases Human Placental Lactogn (hPL) Release

Term chorionic villous explants were cultured for 4 days prior to treatment with 0 or 10 μ M of JTE-013. Supernatants were centrifuged at 15,000 RPM for 15 min prior to analysis. (A) LDH released into the supernatant after 48 h was measured with a colorimetric assay. (B) β -hCG released after 48 h was measured by ELISA. (C) hPL released after 48 h was measured by ELISA. Results were normalized against total protein mass. Normalized values were then calculated as a ratio relative to the no treatment control from the same experimental replicate and depicted as a fold-change difference within their own experimental subset. The arbitrary units (a.u) reflect the relative nature of the results that were calculated as a ratio of the chosen reference. Results were analyzed using the non-parametric one sample T-test. ($n = 3$, Mean \pm SEM).

Pregnancy	Gestational Age (weeks)	Infant Weight (g)	Systolic Blood Pressure (mmHg)	Diastolic Blood Pressure (mmHg)	Percent Positive for Proteinuria (%)
Normal (n=13)	38.54 ± 0.37	3175 ± 105.9	112.7 ± 4.976	70.98 ± 5.54	0
Preeclampsia (n=4)	37.2 ± 0.69	2875 ± 147.2	156.4 ± 14.35	111.6 ± 29.1	100
p-value	ns	ns	p<0.0001	0.038	N/A

Table 5.1: Table of Characteristics of Sample Donors

Samples were analyzed using a Student's T-test or Mann-Whitney test when non-parametric (Mean +/- SEM)

A

S1PR1 44 kDa
 α -Tubulin 55 kDa

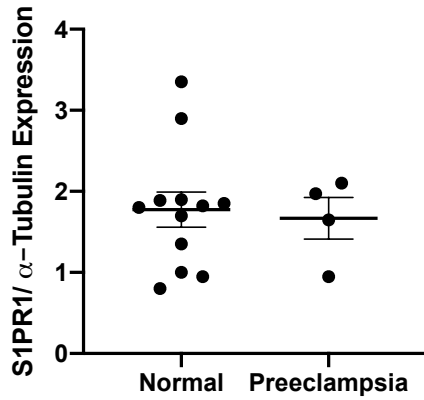
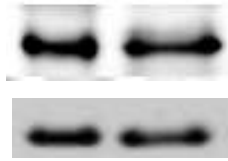
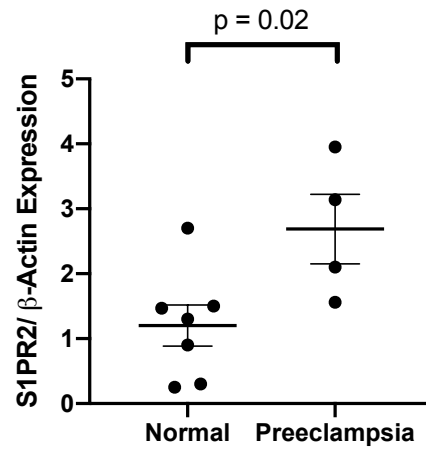
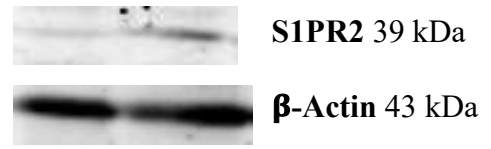
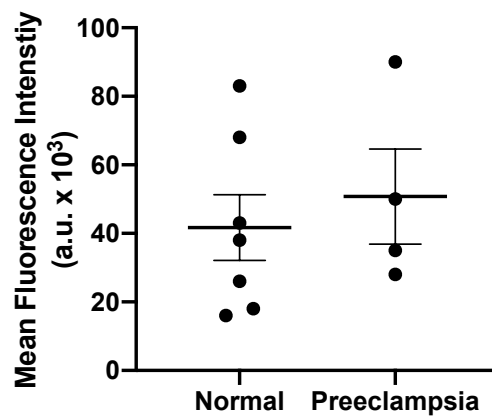
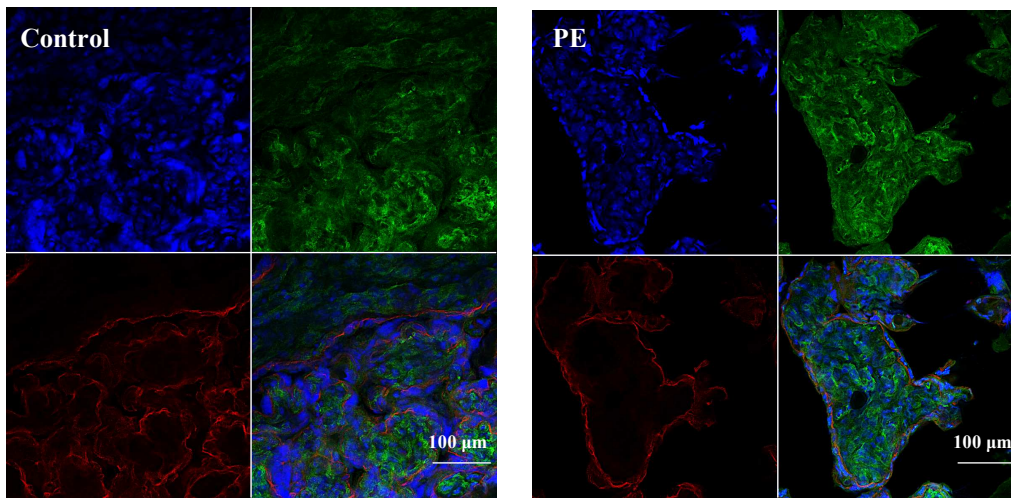
**B****C**

Figure 5.3: S1PR2 Protein Expression is Higher in Whole Placental Biopsies from Mothers with PE Compared to Placental Biopsies from Mothers with Normal Pregnancies

Placental lysates were quantified for S1PR1 (A) or S1PR2 (B) expression using Western Blot analysis with a 50 µg protein load for S1PR1 and 100 µg for S1PR2. Results were normalized to α -Tubulin expression for S1PR1 or to β -actin expression for S1PR2 and plotted as a ratio of an internal sample control to control for samples run on different blots. Results were analyzed using a Student's T-test. ($n = 4$ PE and $n = 13$ or $n = 7$ normal, Mean \pm SEM). (C) Placental biopsies were stained for S1PR1 and E-cadherin using immunofluorescent staining, visualized with secondary antibodies labelled with AF488 (shown in green) and AF594 (shown in red), respectively. DAPI was used to stain the nuclei (shown in blue) and mean fluorescence intensity for S1PR1 was normalized against total nuclei. Results were analyzed using a Student's T-test. ($n = 4$ PE and $n = 7$ healthy control, Mean \pm SEM).

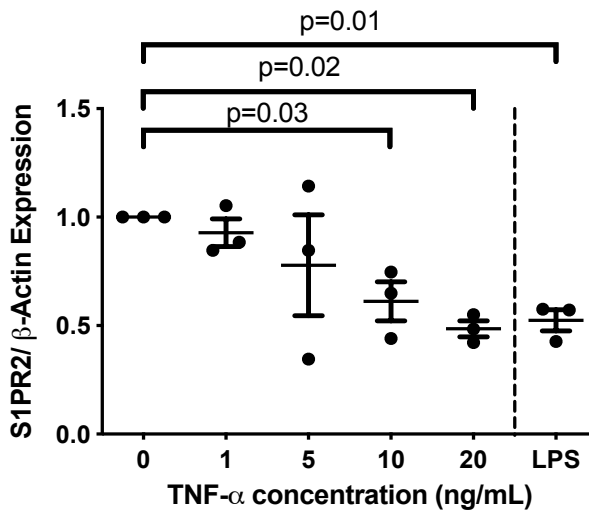
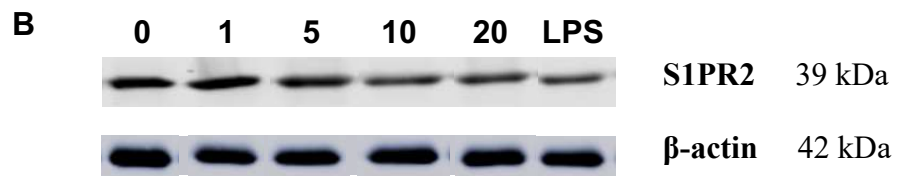
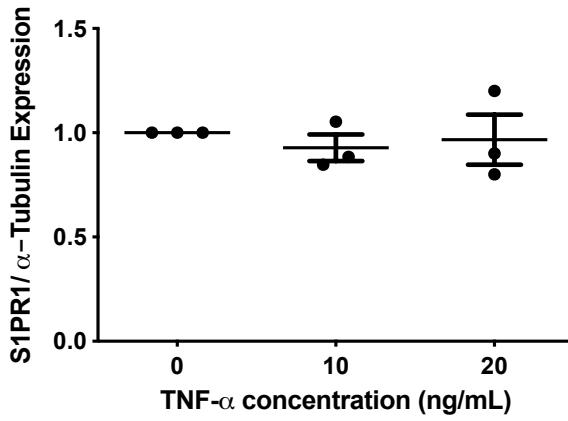
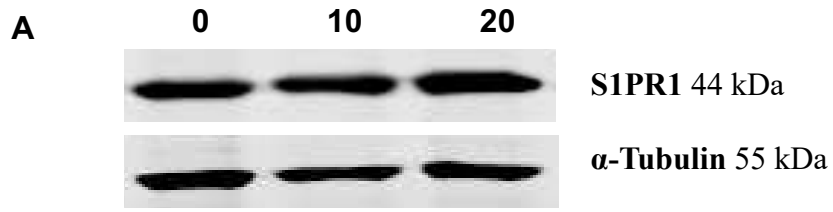


Figure 5.4: TNF- α Decreases S1PR2 Expression in BeWo cells without Affecting S1PR1 Expression

BeWo cells were cultured in 0-20 ng/mL of TNF- α or 20 μ g/mL of LPS as a positive control for 24 hrs. Lysates were analyzed for S1PR1 (A) and S1PR2 (B) protein expression by Western Blot with a 50 μ g protein load. Results were normalized to α -Tubulin expression for S1PR1 or β -actin expression for S1PR2 and plotted as a ratio of the untreated control. Results were analyzed using the non-parametric Kruskal-Wallis test with the two-stage linear step-up procedure of Benjamini, Krieger, and Yekutieli post-hoc test and a linear trend post-hoc analysis ($p=0.04$). LPS results were analyzed using a Student's T-test against the no treatment control ($n=3$, Mean \pm SEM).

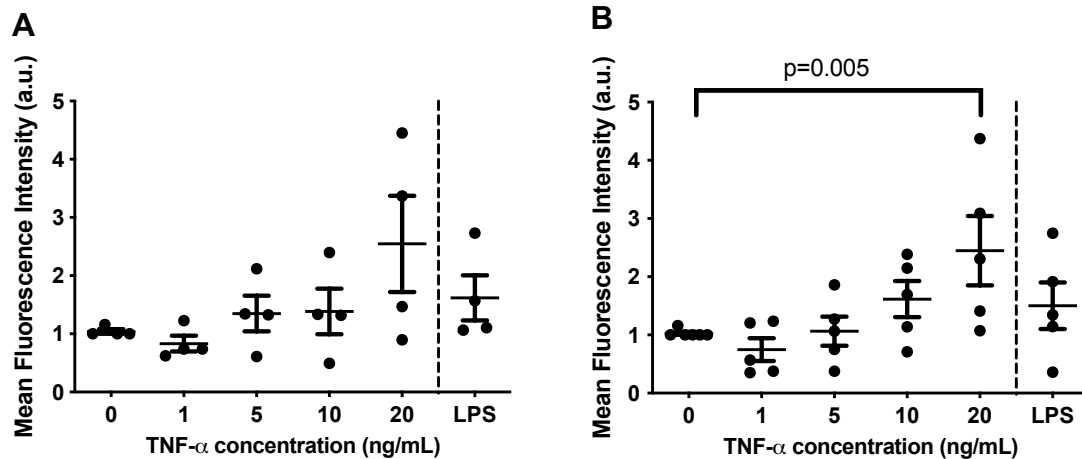
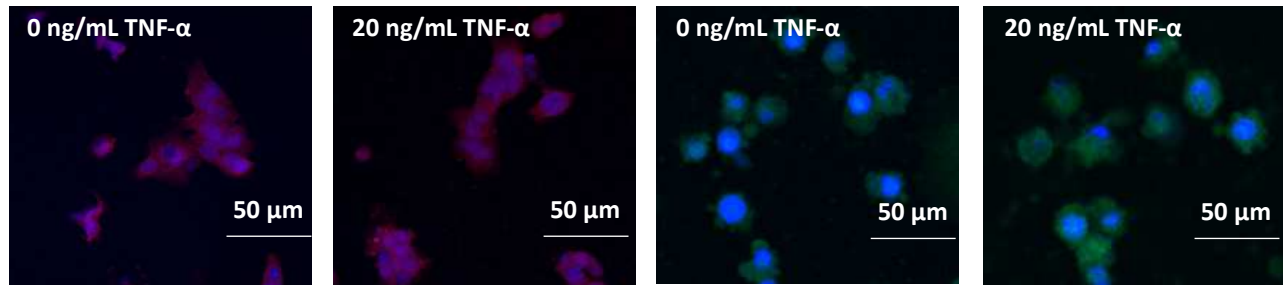


Figure 5.5: TNF- α Increases S1PR2 Expression in Cultured Primary Trophoblasts without Affecting S1PR1 Expression

Primary human cytotrophoblasts were cultured in 0-20 ng/mL of TNF- α or 20 μ g/mL of LPS as a positive control for 24 hrs. Cells were analyzed for S1PR1 (A) or S1PR2 (B) protein expression by immunofluorescent staining visualized with secondary antibodies labelled with AF594 for S1PR1 (shown in red) or AF488 for S1PR2 (shown in green), respectively. DAPI was used to stain the nuclei (shown in blue) and mean fluorescence intensity for each receptor was normalized against total nuclei. Results were analyzed using a one-way ANOVA test with the two-stage linear step-up procedure of Benjamini, Krieger, and Yekutieli post-hoc test and a linear trend post-hoc analysis. LPS results were analyzed using a Student's T-test against the no treatment control ($n = 4$ or $n = 5$, Mean \pm SEM).

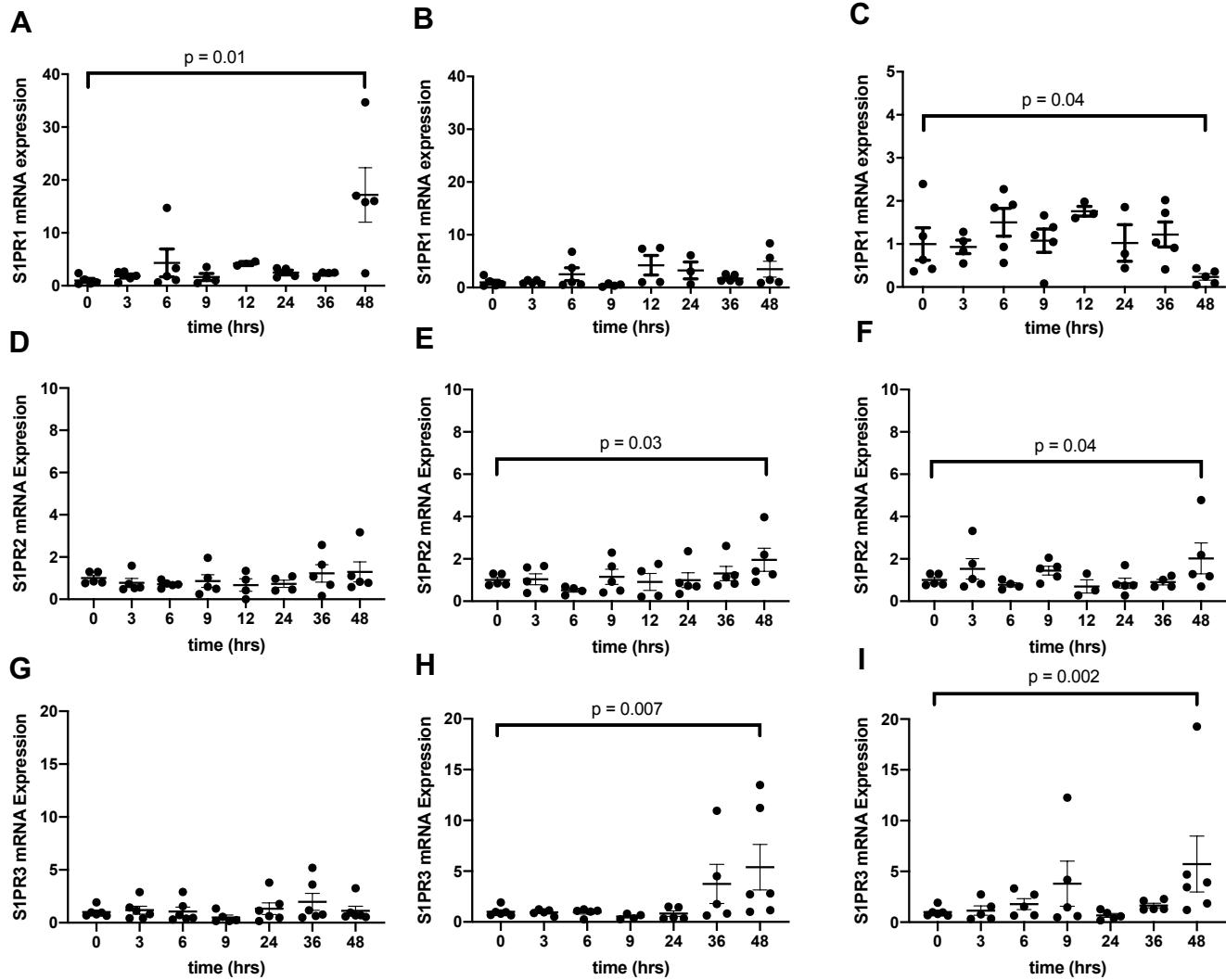


Figure 5.6: S1PR1 mRNA Expression Decreases Whereas S1PR2 and S1PR3 Expression Increase After 48 Hours of TNF- α Treatment in Term Chorionic Explants

After 4 days of incubation, explants were treated with 0 (**A, D, G**) or 1 ng/mL of TNF- α (**B, E, H**) for 0-48 hours. S1PR1-3 mRNA expression was calculated relative to HPRT1 and then time 0 hrs mRNA expression. (**A, D, G**): S1PR1, 2, 3 mRNA expression, respectively, in the no treatment control was plotted from 0-48 hours as a ratio of change from time 0. (**B, E, H**): S1PR1, 2, 3 mRNA expression, respectively, after 1 ng/mL of TNF- α treatment was plotted from 0-48 hours as a ratio of change from time 0. (**C, F, I**): Values from the TNF- α -treated group was calculated as a ratio to the no treatment control from the same placenta at each timepoint. Results were analyzed using the mixed effects model with the two-stage linear step-up procedure of Benjamini, Krieger, and Yekutieli post-hoc test ($n = 3-5$ Mean \pm SEM).

5.2 Discussion

The focus of this study was to understand the role of S1PR2 signaling in placental ST function and to investigate how the expression of S1PRs is altered in PE and in high inflammatory conditions, mimicking a PE environment. Since S1PR2 increases inflammatory cytokines in trophoblasts (286, 414), is pro-apoptotic (413), and is increased in placentas of women with severe PE (234), I hypothesized that S1PR2 activation by endogenous S1P would lead to placental cell membrane damage and would be increased in response to TNF- α in BeWo cells, primary CTs, and in cultured chorionic villi. On the contrary, the expression of S1PR1 and S1PR3, with protective S1P-mediated signaling properties (9), was predicted to decrease in response to TNF- α treatment. In this study, I found that S1PR2 activation decreased placental cell membrane damage, decreased β -hCG release, and increased hPL release. S1PR1 levels remained unaltered in placental biopsies from women with mild PE and also did not change in response to TNF- α treatment in cultures of BeWo cells or primary human CTs. In contrast, S1PR1 was decreased in response to TNF- α treatment in chorionic villi explants. Placental S1PR2 expression was higher in women with PE, and it was increased in primary CTs and in villous explants, along with S1PR3 in villous explants, in response to TNF- α treatment. BeWo cells decreased S1PR2 expression in response to TNF- α and to LPS. To my surprise, the isolated term primary human CTs were not responsive to LPS treatment in regards to S1PR expression.

My study is the first to show that S1P treatment increases β -hCG release without affecting cell viability. This finding is contrary to the previous research that showed that S1P inhibits β -hCG release from primary human CTs differentiated to ST (46). Since my experiments were done in a villous explant model, it could be argued that responses by trophoblasts are changed when these cells are in the context of their extracellular matrix and surrounding cell

types. However, this finding is also in contradiction with my previous finding in Chapter 4 that SphK1 inhibition with PF-543 increased β -hCG release from explants (371). These discrepancies have been reported previously by Singh et al (46), where SphK1 inhibition compared to S1P treatment led to contradictory results. This suggests that SphK1 inhibition effects might not be limited to decreased S1P release, but also a reorganization of the whole sphingolipid balance and possibly altering the S1P: CER rheostat and leading to alternate signaling (9). This reorganization can involve the upregulation of SphK2 to overcompensate for the loss of SphK1. This increase would potentially lead to S1P localized to different subcellular compartments that stimulates differential signaling, as noted in Chapter 1.

Inhibiting S1PR2 with JTE-013 increased cell death and β -hCG release but decreased hPL release. This implies that S1PR2 activation protects against cell death and induces hPL release, contrary to my hypothesis and existing literature. While JTE-013 is a commonly used inhibitor for S1PR2 and was previously deemed specific, a new article (415) shows that it increases CER and sphingosine levels, causing alterations in sphingolipid metabolism. Moreover, JTE-013 can also inhibit S1PR4 (415), a receptor mostly expressed in immune cells. This suggests that these results should be interpreted with caution, and that JTE-013 treatment might not strictly equate to S1PR2 inhibition but could also alter sphingolipid levels and immune responses. Recently, a new S1PR2 antagonist, GLPG2938 (1-[2-Ethoxy-6-(trifluoromethyl)-4-pyridyl]-3-[[5-methyl-6-[1-methyl-3-(trifluoromethyl)pyrazol-4-yl]pyridazin-3-yl]methyl]urea is now available (416). Hence, future studies could cross-examine the difference in responses between GLPG2938 and JTE-013. Alternatively, siRNA knockdowns of S1PR2 in villous explants or primary trophoblasts could also shed light on the role of S1PR2 in placental function.

The unexpected discrepancy between hPL and β -hCG responses was not previously seen in my other studies. However, although these hormones are used to measure ST function as a surrogate measure of ST development, each of these hormones are formed and secreted through different pathways and can be regulated differently, as seen with my S1PR2 results. As well, one study shows that cAMP treatment induces β -hCG release while inhibiting hPL release in human term trophoblasts (417).

An interesting observation is the difference in LDH, β -hCG, and hPL release in response to elevated S1P as shown in the S1P dose-response experiment and inferred from the JTE-013 inhibitor experiments. At physiological circulating levels and at levels used in this study, S1P binds S1PR1-3 at similar binding affinities, with an IC_{50} in the low nM range (271). Brunnert et al, however, shows that BeWo cells express S1PR2 more abundantly compared to other S1P receptors (274). Since I showed that primary trophoblasts behave differently than BeWo cells, it is likely that primary trophoblasts might express lower levels of S1PR2 and S1P-S1PR2 signaling would be diminished upon treatment with S1P, and S1P-S1PR1 signaling, for example, would be more prominent. Since the explant contains a variety of placental cells, each with their own differential expression of S1PRs, it is possible that inhibiting S1PR2 or treating with S1P also affected the surrounding non-trophoblast cells and potentially influenced ST maturation. It is also likely that S1P binds to other S1PRs and balances the effects of S1PR2 on LDH, β -hCG, and hPL release. Another factor that might be altering the effects seen is the differential binding affinity of albumin-bound S1P in this study. For instance, a recent article shows that HDL-bound S1P preferentially binds S1PR1 (297). Hence, in this study, albumin-bound S1P might preferentially bind and signal through S1PR1, explaining the contradiction in effects between S1P stimulation and S1PR2 signaling.

I next showed that S1PR1 expression was not changed in the placentas of mothers with mild PE compared to those of mothers with healthy pregnancies. However, S1PR2 expression was higher. This is in agreement with previous studies that show unchanged S1PR1 levels and increased S1PR2 in severe PE and increased expression of S1PR2 in placental chorionic arteries (172, 234). Although the increase in S1PR2 mRNA expression in PE has been investigated before, my study examined its protein expression, which complimented the existing evidence.

Given that placental S1PR levels were altered in PE, I aimed to investigate whether they were altered in response to TNF- α , which is increased in PE (418, 419) and plays a major role in inducing a PE phenotype, as shown in Chapter 4 (138). My study shows that S1PR1 was not altered in response to TNF- α in either BeWo cells or primary term human CTs. However, S1PR1 decreased in villous explants in response to TNF- α treatment. No changes are seen in S1PR1 expression in synoviocytes (333) or human dermal vascular endothelial cells (332), in agreement with my results in the monolayer trophoblast cultures. However, TNF- α treatment decreases S1PR1 in a human umbilical vein cell line (420), similar to the effect seen in villous explants in my study. On the other hand, TNF- α treatment increases S1PR1 expression in astrocytes (421), suggesting that S1PR1 responds to TNF- α in a cell-specific manner. My cultured explant results suggest that S1PR1 decreases in response to TNF- α in other placental cells but perhaps not in trophoblasts.

Under normal physiological conditions, S1PR1 expression in villous explants increased at 48 hours when the ST was fully matured and ready to shed. This timeline represents the villi with a fully formed mature ST, as previously shown (371), nearing shedding. This increase might occur as a protective mechanism against excessive shedding and cell damage that is activated upon the maturation of the ST. TNF- α inhibits this surge preventing cell survival

processes and leading to excessive shedding and cell death. However, to fully understand the role of S1PR1 in the syncytial cycle, further investigation using specific S1PR1 agonists and inhibitors must be completed.

My study also found that S1PR2 expression increased in response to TNF- α in primary CTs and in villous explants, which is in agreement with the higher S1PR2 levels I saw in PE and with previous literature (332). BeWo cells, however, downregulated their S1PR2 expression in response to TNF- α , in contradiction with the results I saw in other models. This suggests that BeWo cells might be a poor model for studying sphingolipid signaling in trophoblasts. In fact, recent studies highlight other reasons for the problematic use of BeWo cells as a model for human trophoblasts. First, they are near-triploid in their karyotype (422, 423) and hence do not reflect physiological signaling. Second, the heterogeneity of BeWo cells in long-term cultures can lead to non-reproducible results and inaccurate information on normal cell physiology (422).

Interestingly, cultured CTs did not respond to LPS treatment, a positive control, by altering their S1PR expression, as the BeWo cells did. This could be due to the changes in signaling as noted above between BeWo cells and primary cells. Since BeWo cells are a second trimester trophoblast model, this discrepancy could also be due to primary CTs downregulating their toll-like receptor 4 at term, since these receptors change across gestational age (424). LPS exerts its effects by binding to toll-like receptor 4. Since primary cells were isolated from placentas from term pregnancies, they might exhibit low expression for this receptor and hence exhibit diminished LPS signaling. Another explanation, although unlikely, could be that the toll-like receptors were stripped off the membrane during the trophoblast isolation process. However, the cultured cells should re-express these receptors which could be confirmed by staining.

Finally, TNF- α increased S1PR3 expression in chorionic villi, which is in agreement with its effect on synoviocytes (333). However, S1PR3 signaling in the placenta is poorly understood and warrants further investigation. Knocking out S1PR3 in mice leads to only minor alterations in phenotype (263), since S1PR3 signaling often strongly overlaps with S1PR1. For instance, S1PR1 and S1PR3 activation triggers angiogenesis in the ovine uterus. Moreover, activating S1PR1 and S1PR3 leads to the release of IL-8 from EVT_s. IL-8 is a pleiotropic pro-inflammatory cytokine that is increased in the circulation of mothers with PE (425). However, IL-8 also induces the secretion of progesterone from BeWo cells (426). Interestingly, S1PR3 activation in luteal cells, leads to the secretion of prostaglandin E₂, a strong inducer of progesterone (329). This all suggests a potential role for S1PR3 in the secretion of progesterone from the placenta. S1PR3 might also increase in response to TNF- α as a protective mechanism against the TNF- α -induced decrease in S1PR1 expression. In this case, the increase in S1PR3 would enable the placenta to rescue some of the S1PR1 signaling essential for cell viability. Nonetheless, both S1PR1 and S1PR3 expressions were lower in the placentas of women with severe PE (234). Thus, factors in addition to TNF- α are likely responsible for this change in PE.

To conclude, this study highlights the differential expression of S1PR1, S1PR2, and S1PR3 in the placenta under normal and high inflammatory conditions. Understanding the roles of these receptors in placental processes, such as ST shedding and maturation, inflammatory cytokine release, and trophoblast invasion can make them attractive targets for manipulating placental function to improve outcomes in pregnancy disorders.

6. Chapter 6: Piezo1 Activation Induces Syncytial Function and Cytokine Release in Human Term Placental Chorionic Explants

This chapter was submitted for publication as “Piezo1 Activation Induces Syncytial Function and Cytokine Release in Human Term Placental Chorionic Explants” with the following authors, Y Fakhr^{1,2}, S Koshti^{1,2}, Y Bahojb Habiby^{1,2,3}, DG Hemmings^{1,2,3}, and affiliations, ¹Obstetrics and Gynecology, ²Women and Children’s Health Research Institute, ³Medical Microbiology and Immunology and is under revision. This chapter was formatted according to specific journal requirements, which include presenting all values as Mean \pm SD and presenting all p-values with 3 significant digits.

6.1. Introduction

This study aims to identify a role for Piezo1, a mechanosensory channel, in the development of a PE placental phenotype: poor ST endocrine function, increased placental cell death and inflammatory cytokine release. In the previous chapters, I identified a connection between TNF- α and SphK1 in their signaling on the effects of placental dysfunction. Eisenhoffer et al reports that Piezo1 induces epithelial cell extrusion via SphK1 activation (301, 302). Hence, in this chapter, I will situate Piezo1 in the TNF- α and SphK1 signaling pathway by indicating its interactions with TNF- α and SphK1, separately, in placental dysfunction that is observed in PE.

PE is characterized by *de novo* hypertension and end-organ damage diagnosed by at least one of the following: proteinuria, headache/visual symptoms, chest pain, elevated white blood cell count, and/or low platelet count during the last 20 weeks of gestation or in postpartum (SOGC, 2014). In PE, circulating proinflammatory cytokines, such as TNF- α , are increased (4). The mechanism of PE etiology is still unknown; however, improper placental development due to insufficient trophoblast invasion and syncytium formation along with excessive trophoblast shedding are implicated in PE complications (427).

The placental ST is the epithelial barrier that separates maternal and fetal circulations and facilitates the exchange of materials between the mother and fetus (65). The ST also has an endocrine role, releasing hormones that maintain the pregnancy such as β -hCG, hPL, and progesterone into maternal circulation (428). To maintain ST integrity, the CTs undergo cycles of proliferation, differentiation, fusion followed by ST apoptosis and shedding throughout pregnancy (352). ST regeneration also includes the production of syncytial knots, the outgrowths of the barrier containing apoptotic ST nuclei (65). These multinucleated syncytial knots are normally shed into the maternal circulation and are increased in PE. Numerous factors have been

identified as key regulators of the syncytial cycle. Albeit, limited information is available on the role of mechanosensory channels in this process.

Piezo1 is a transmembrane mechanosensitive cation channel that when activated increases the influx of Ca^{2+} and other cations into cells (303). Piezo1 responds to mechanical stress and maintains homeostatic conditions in cells, and more specifically in a broad range of epithelial cells. Furthermore, Piezo1 channels expressed in epithelial cells can sense membrane stretching and membrane crowding (302). Using these sensing mechanisms, increased signaling through Piezo1 channels helps maintain homeostasis among epithelial cells by regulating cell proliferation and cell apoptosis (302, 309). Moreover, Piezo1 induces differentiation of various cell types, such as mesenchymal stem cells (311).

During the syncytialization process in placental development, a balance of proliferation and apoptosis is required to maintain healthy ST function (61). Increased trophoblast apoptosis and decreased proliferation, differentiation, and fusion result in a dysfunctional ST which is observed in PE (310); however, it is unknown whether Piezo1 activation regulates this balance in the placenta in physiological conditions. Additionally, it is unknown whether a change in Piezo1 expression can explain the resulting imbalance between trophoblast apoptosis and proliferation that is seen in placentas of women with PE. High flow rate, which can activate Piezo1, induces cultured rabbit trophoblast syncytialization through a Ca^{2+} -dependent mechanism (318). However, little else is known about the factors regulating Piezo1 activation and expression in the human placenta.

Piezo1 activation has recently been associated with the induction of pro-inflammatory pathways in a variety of cell types (11, 12). Piezo1 expression also increases in response to inflammatory cytokines. For instance, Piezo1 mRNA increases in chondrocytes treated with IL-

1 α (11). No evidence on the role of Piezo1 in placental inflammation, a hallmark of PE, is available. I proposed a relationship between Piezo1 and TNF- α in the placenta. TNF- α is a prominent proinflammatory cytokine that is elevated in the placenta and circulation of women with PE and is disruptive of placental syncytium formation and function (4).

Different levels of Piezo1 activation with its pharmacological agonist, Yoda1, show a dose-dependent increase in Ca²⁺ influx (314), suggesting that Piezo1 can be activated to different levels and that this can lead to distinctive effects. I hypothesized that activation of Piezo1 induces syncytialization at low levels of activation, but increases proinflammatory cytokine release and cell membrane damage at higher activation levels. I also hypothesized that Piezo1 signaling intersects with TNF- α and that levels of Piezo1 in the placenta would be higher in PE patients. This study is the first to define a role for Piezo1 in placental function using the villous explant model. Piezo1 activation increased placental endocrine function and increased cell membrane damage at higher levels of activation. Higher levels of Piezo1 activation also increased placental cytokine release, and specifically TNF- α release. Piezo1 expression was also increased in response to TNF- α and was higher in placentas of women with PE.

6.2. Results

6.2.1. Higher Levels of Piezo1 in Placental Biopsies from Women with PE

Placental biopsies were obtained from 12 women with healthy pregnancies and 9 women with PE. Women from the PE group had higher systolic and diastolic blood pressures ($p=0.0028$ and $p=0.0501$, Table 6.1) and were positive for proteinuria. Newborns from the PE group were similar in gestational age compared to those from the control group (37.00 ± 1.027 week versus

38.60 ± 1.235 weeks; p=0.0599). There were no differences in infant birth weight between groups.

Piezo1 was expressed in the vasculature and the stromal core as well as trophoblastic layers of stained placental biopsies from women with normal (n=12) pregnancies (Fig 6.1A, B). Notably, blood vessels (yellow arrows) and the syncytium (white arrows) showed a strong localization of Piezo1. E-cadherin, an adherens junction transmembrane protein, is highly expressed on the apical side of the CTs which fuses with the basal ST membrane. Nuclei expressed outside the E-cadherin demarcation represent syncytial nuclei. Piezo1 co-localized with E-cadherin at the CT apical membrane and was expressed around ST nuclei (Fig 6.1A, white arrows). This suggests that Piezo1 is expressed by both CTs and STs. Piezo1 was also expressed to a greater extent in blood vessels and trophoblast layers in placentas from PE pregnancies (Fig 6.1C, D; n=5), with a similar localization as shown in the magnified images of Fig 6.1C and 6.1D. Furthermore, quantitative analysis of whole images showed Piezo1 expression was significantly higher in sections from PE placental biopsies (p=0.0088, Fig 6.1E). However, no significant differences in Piezo1 mRNA expression was observed in whole placental biopsies from women with PE compared to normal pregnancies (p=0.95, Fig 6.1F).

6.2.2. Pharmacologically Activating Piezo1 with Yoda1 Increased Markers of ST Function

After four days of culture, the ST on explants sloughed off and then there was gradual resyncytialization after 48 hours, referred to as the regenerative phase, shown in Chapter 3, Figure 3.2 (429). Pharmacologically activating Piezo1 with 1 μM Yoda1 in villous explants at the beginning of the regenerative cycle increased β-hCG release after 48 hours of treatment (Fig 6.2A, B). Moreover, hPL secretion (Fig 6.2C) and villous PLAP activity (Fig 6.2D) increased

with 1 μ M ($p=0.0422, 0.0284$), 10 μ M ($p=0.0139, 0.0088$), and 20 μ M ($p=0.0139, 0.0103$), respectively, after 48 hours of Yoda1 treatment.

6.2.3. Pharmacologically Activating Piezo1 with Higher Concentrations of Yoda1

Increased Placental Cell Damage and Release of Inflammatory Cytokines and Growth Factors

Lower levels of Yoda1 (1 μ M) had no effects on LDH release ($p=0.181$). Activating Piezo1 with higher concentrations of Yoda1 increased LDH release from villous explants after 24 ($p=0.0325$) and 48 hours of regeneration ($p=0.0139$) with 10 μ M of Yoda1 and at 24 ($p=0.0248$) and 48 hours ($p=0.0003$) after regeneration with 20 μ M of Yoda1 (Fig 6.3A, 3B). Treating with 10 μ M Yoda1 for 48 hours during regeneration also increased the release of pro-inflammatory cytokines IL-2 ($p=0.0278$), and IFN- α 2 ($p=0.0552$) (Fig 6.4). It also increased the release of IL-1 β ($p=0.0557$), IL-7 ($p=0.0103$), IL-17 ($p=0.0058$), IL-18 ($p=0.0324$), IL-6 ($p=0.0172$), RANTES ($p=0.0604$) and IL-12p70 ($p=0.0415$), cytokines whose circulating levels are elevated in PE. Yoda1 also increased the release of growth factors EGF ($p=0.0010$), MDC ($p=0.0294$) and Flt-3L ($p=0.0115$), in addition to interleukins normally decreased in PE, IL-4 ($p=0.0168$) and IL-9 ($p=0.0226$) (Fig 6.4). Yoda1 treatment did not change the levels of the following factors: Eotaxin ($p=0.700$), IFN γ ($p=0.191$), scd40L ($p=0.0902$), FGF2 ($p=0.274$), Fractalkine ($p=0.213$), G-CSF ($p=0.153$), GM-CSF ($p=0.191$), GRO- α ($p=0.713$), IL-1 α ($p=0.190$), IL-1RA ($p=0.272$), IL-5 ($p=0.237$), IL-8 ($p=0.419$), IL-10 ($p=0.912$), IL-12p40 ($p=0.554$), IL-15 ($p=0.267$), IP-10 ($p=0.500$), MCP3 ($p=0.172$), MIP-1 α ($p=0.121$) and MIP-1 β ($p=0.228$), TGF- α ($p=0.0989$), TGF- β ($p=0.409$), PDGF-AA ($p=0.164$), and PDGF-BB ($p=0.630$) (Fig 6.5). VEGF and IL-3 levels secreted into the supernatants were undetectable.

6.2.4. Piezo1 and TNF- α Signaling Intersection in the Placenta

Since Piezo1 is increased by proinflammatory stimuli and activation of Piezo1 increased the release of markers demonstrating syncytial formation, I sought to determine whether these effects of Piezo1 activation on ST re-syncytialization and cell viability could be impacted by proinflammatory conditions, modelled by TNF- α treatment. 10 μ M Yoda1, which I showed increased LDH release, also increased TNF- α levels after 48 hours of treatment during regeneration ($p=0.0330$, Figure 6.6A). I then showed the reciprocal effect, that TNF- α treatment during regeneration increased Piezo1 mRNA expression after 3 hours compared to controls ($p=0.0263$, Figure 6.6B).

Levels of β -hCG and LDH release were measured in explants treated with 1 ng/mL TNF- α , 1 μ M Yoda1, or a combined treatment of 1 ng/mL TNF- α and 1 μ M Yoda1 ($n=6$) at 24- and 48-hours post-treatment during regeneration. 1 ng/mL of TNF- α alone had no effects on explant re-syncytialization and cell death assessed by β -hCG (Figure 6.7A, 6.7B) and LDH levels (Figure 6.7C, 6.7D), respectively. 1 μ M Yoda1 alone increased β -hCG release at 48 hours ($p=0.0286$, Fig 6.7C). Co-treating explants with 1 ng/mL TNF- α and 1 μ M Yoda1 decreased β -hCG after 48 Hours With A Significant Treatment Interaction ($P=0.0090$; Fig 6.7C).

6.2.5. Piezo1 and Sphk1 Signaling Intersection in the Placenta

Since Piezo1 exerts its some of its effects in epithelial cells by increasing S1P release (302), I investigated whether Yoda1 effects on the placenta are dependent on the activation of SphK1, an S1P synthesizing enzyme and the main producer of extracellular S1P. Pharmacologically activating Yoda1 in the presence of PF-543 did not alter β -hCG or LDH release into the supernatant (Fig 6.8A-D). Inhibiting the kinase with 1 μ M PF-543 prevents the

increase in villous PLAP activity induced by Yoda1. This is confirmed by a significant treatment interaction ($p=0.045$, Figure 6.8).

Pregnancy	Gestational Age (weeks)	Infant Weight (g)	Systolic Blood Pressure (mmHg)	Diastolic Blood Pressure (mmHg)	Percent Positive for Proteinuria (%)
Normal (n=12)	38.60 ± 1.235	3055 ± 341.5	113.8 ± 15.84	71.88 ± 14.89	0
Preeclampsia (n=9)	37.00 ± 1.027	2766 ± 511.6	157.2 ± 24.13	114.4 ± 47.10	100
p-value	0.0599	0.3814	0.0028	0.0501	N/A

Table 6.1: Pregnancy Characteristics

Results were analyzed using a Students' T-test ($n=12$ normal, $n=9$ PE, mean +/- SD).

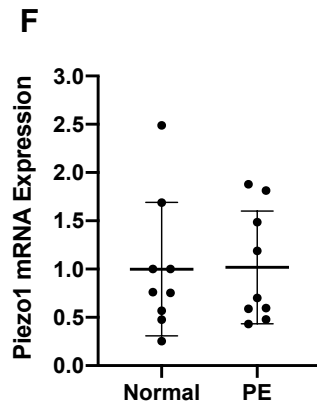
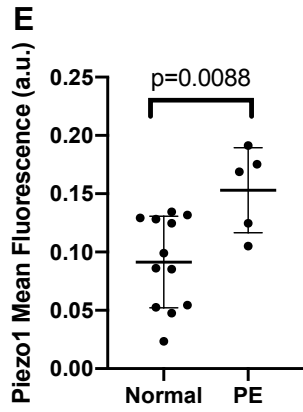
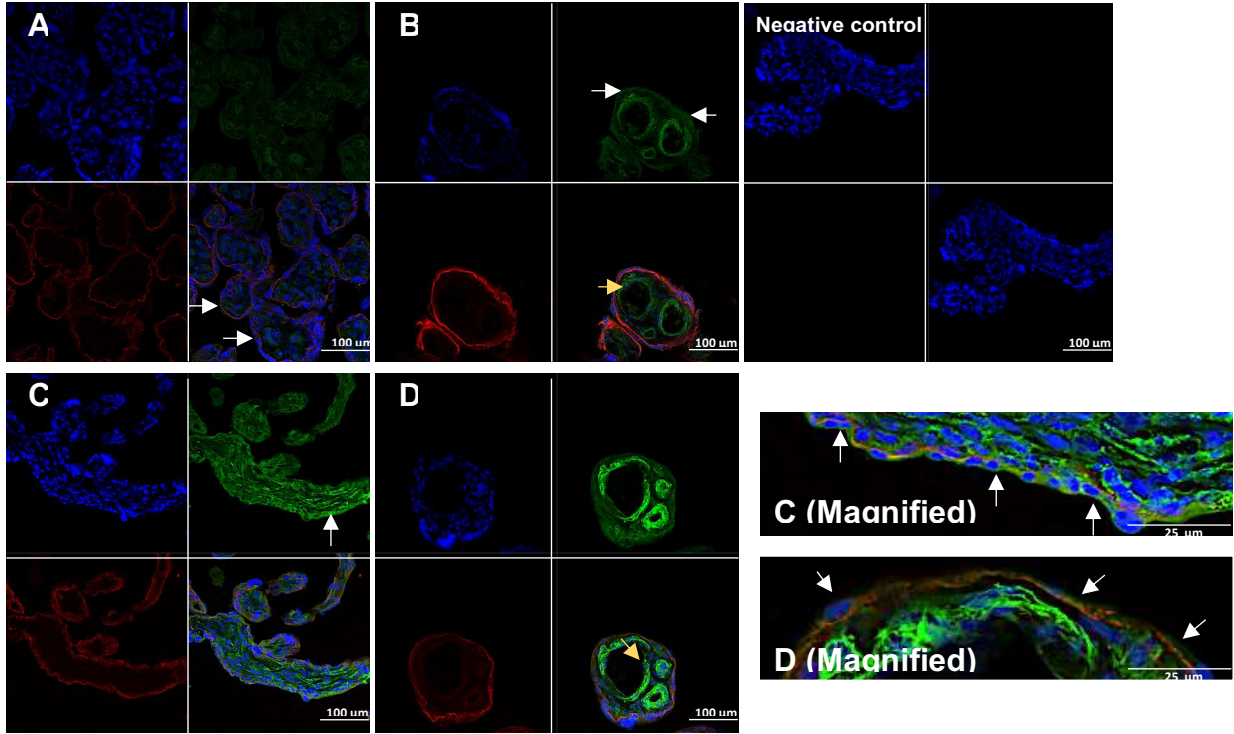


Figure 6.1: Piezo1 Levels but not mRNA Levels were Higher in Placental Biopsies from Women with PE

(A-E): A, B are representative images of two different placentas from normal pregnancies. C, D are representative images of two different placentas from PE pregnancies. Whole tissue placental biopsies from women with normal or PE pregnancies were co-stained for Piezo1 (secondary antibody tagged with AF488, green) and E-cadherin (secondary antibody tagged with AF594, red) expression and a nuclear stain, DAPI (blue) and visualized by confocal microscopy. Piezo1 was observed in the fetal blood vessels and ST in biopsies from women with normal pregnancies and PE. For the negative control, both AF488 and AF594 secondary antibodies were used in the absence of primary antibody. (E) Whole sample image analysis of sections from placental biopsies were compared between women with PE and normal pregnancies. Fluorescence was normalized to the number of nuclei. Samples were analyzed using an unpaired Students' T-test ($p=0.0088$). Values are displayed as mean \pm SD ($n = 12$ normal, $n = 5$ PE). (F) Piezo1 mRNA was measured in lysates of placental biopsies from women with normal and PE pregnancies. The housekeeping gene HPRT-1 mRNA levels were used to normalize Piezo1 levels. Samples were analyzed using an unpaired Students' T-test ($p=0.951$). Values are displayed as mean \pm SD ($n = 9$ normal, $n = 9$ PE).

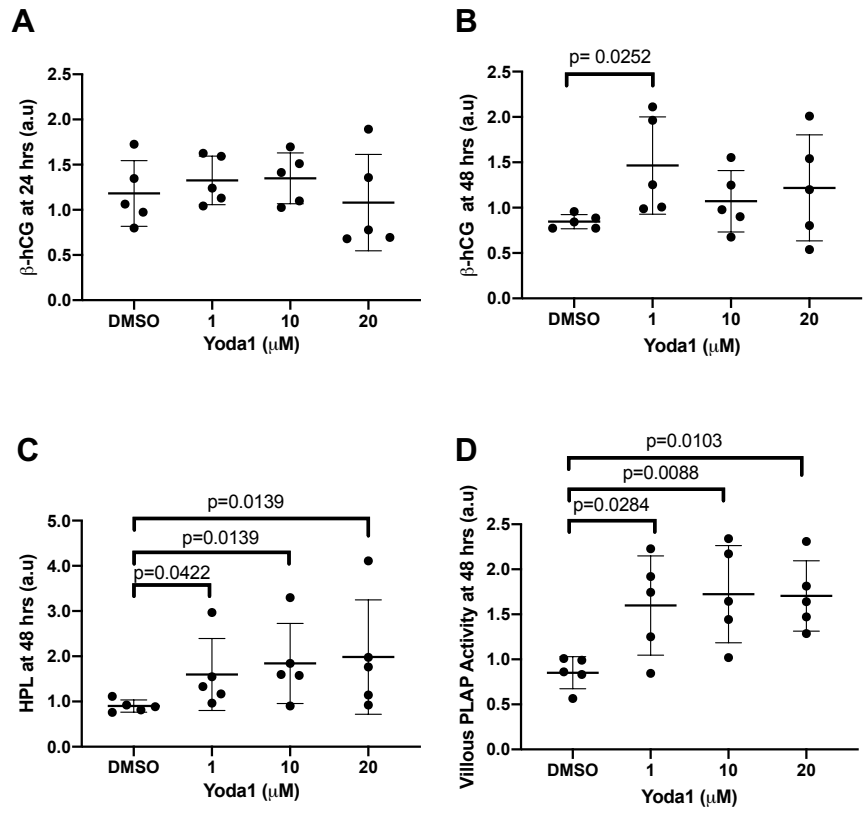


Figure 6.2: Yoda1 Significantly Increased Markers of Syncytial Function

Villous explants were pre-cultured for 4 days and then incubated with Yoda1 in a dose response (1-20 μM) or vehicle control (DMSO). (A) and (B) represent β -hCG released by the villous explants into the culture media at 24 ($p=0.555$) and 48 hours ($p=0.0963$) after treatment, respectively. (C) represents hPL released by the villous explants into the culture media after 48 hours of treatment ($p=0.0404$). (D) represents villous PLAP activity ($p=0.0257$). Explants were lysed after 48 hours of treatment and assayed for PLAP activity. All results were normalized against total protein mass of the explants per well. Normalized values were then calculated as a ratio relative to the no-treatment control from the same experimental replicate and depicted as a fold-change difference within their own experimental subset. The arbitrary units (a.u) reflect the relative nature of the results that were calculated as a ratio of the chosen reference. Results were analyzed using the non-parametric Kruskal-Wallis test and the two-stage linear step-up procedure of Benjamini, Krieger, and Yekutieli post-hoc ($n = 5$, mean \pm SD).

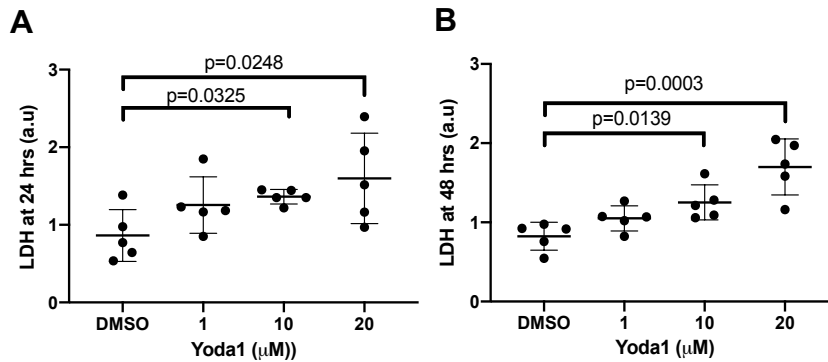


Figure 6.3: Pharmacologically Activating Piezo1 Significantly Increased Placental Cell Membrane Damage

Villous explants were pre-cultured for 4 days and incubated with Yoda1 in a dose response (1-20 μM) or vehicle control (DMSO) for 24 (A, $p=0.0911$) or 48 hours (B, $p=0.0028$). All results were normalized against total protein mass of the explants per well. Normalized values were then calculated as a ratio relative to the no treatment control from the same experimental replicate and depicted as a fold-change difference within their own experimental subset. The arbitrary units (a.u) reflect the relative nature of the results that were calculated as a ratio of the chosen reference. Results were analyzed using the non-parametric Kruskal-Wallis test and the two-stage linear step-up procedure of Benjamini, Krieger, and Yekutieli post-hoc ($n = 5$, mean \pm SD).

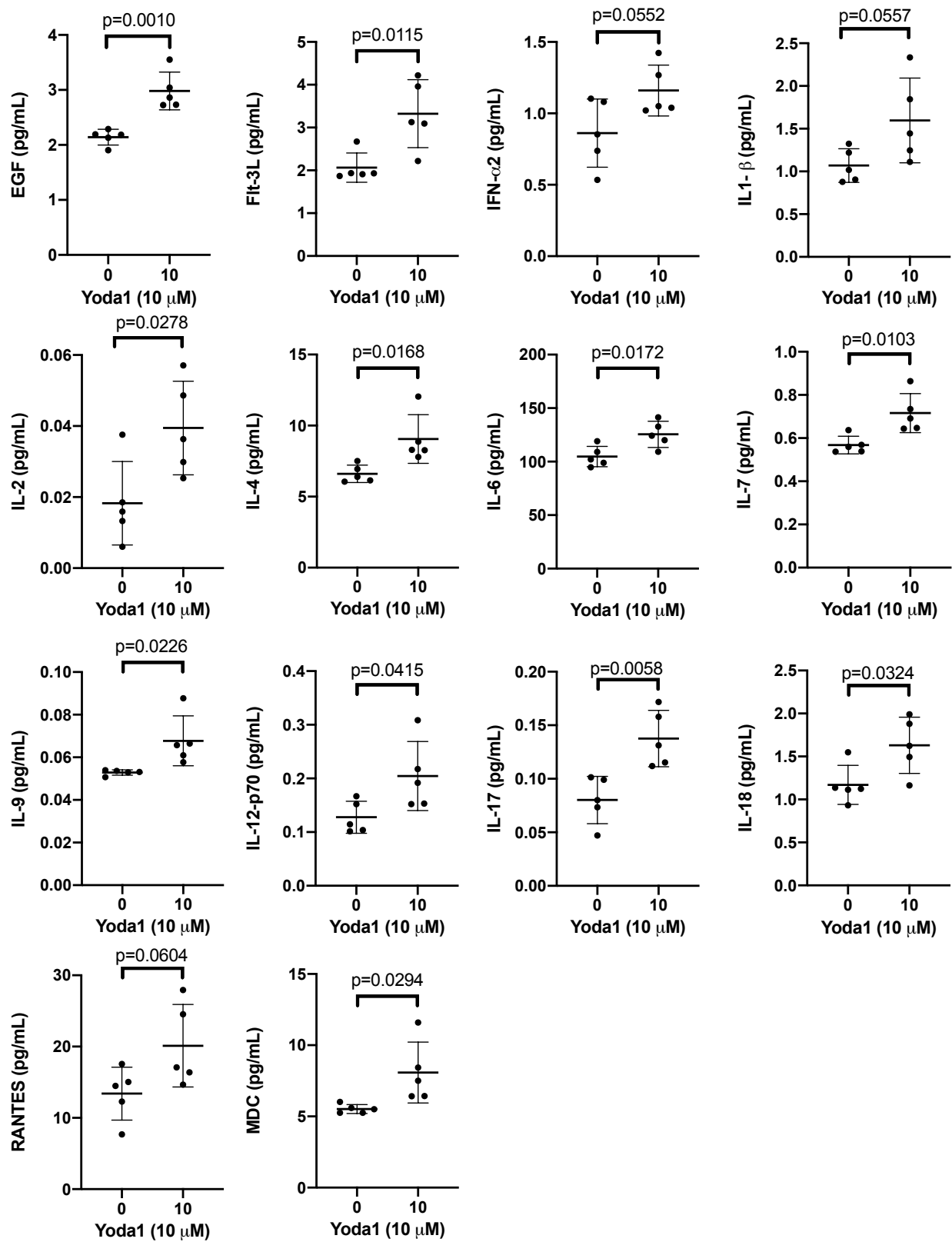


Figure 6.4: Release Of Inflammatory Cytokines and Growth Factors from Villous Explants Treated with Yoda1 for 48 Hours was Increased

Villous explants were pre-cultured for 4 days and incubated with 10 μ M Yoda1 or vehicle control (DMSO). Culture supernatants were collected, centrifuged at 15000 rpm and sent to Eve Technologies for cytokine analysis by Multiplex assays. Results were normalized against total protein mass and all displayed values are per mg of protein. Results were analyzed using an unpaired Student's T-test ($n = 5$, mean \pm SD).

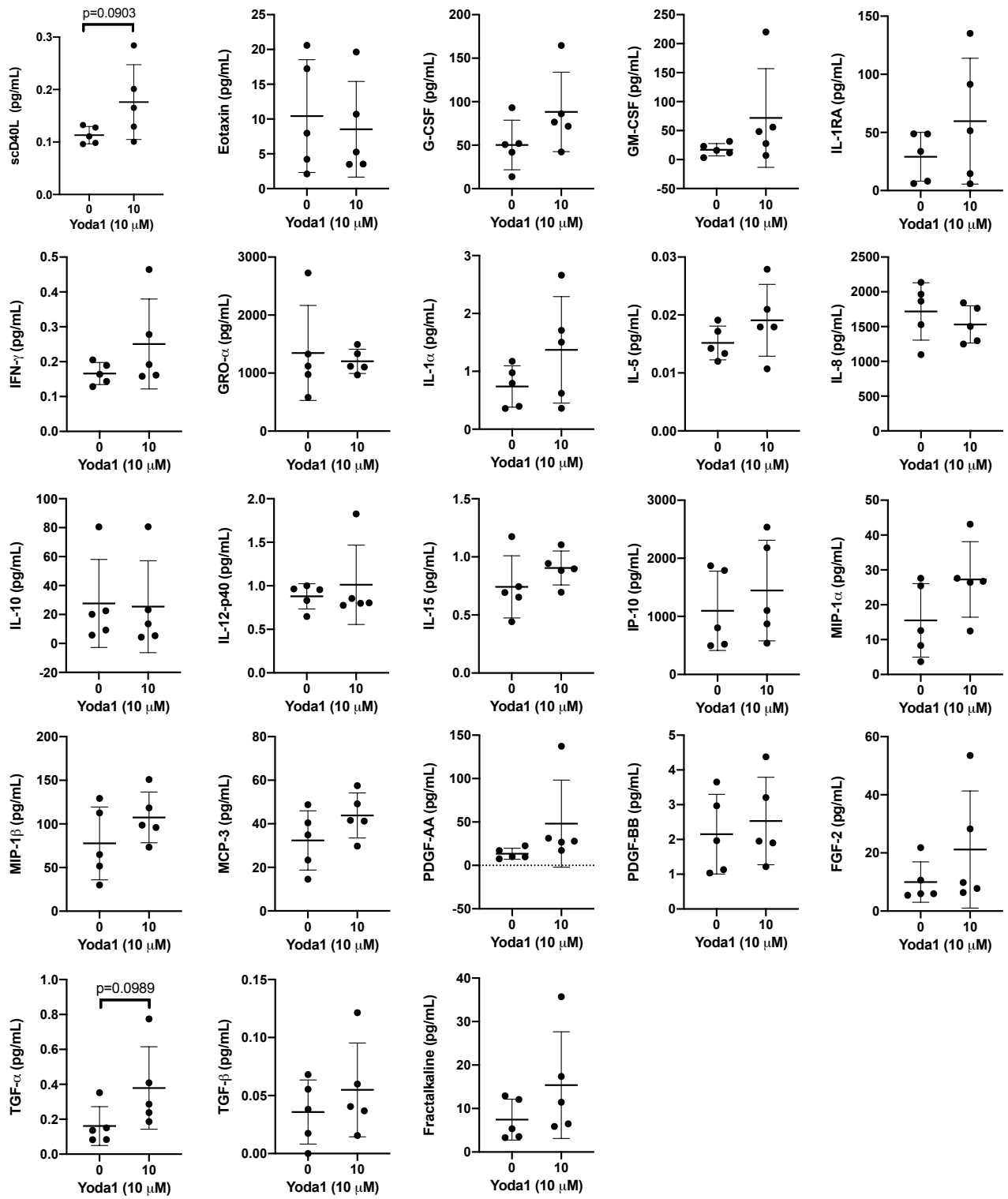


Figure 6.5: Inflammatory Cytokines and Growth Factors from Villous Explants Treated with Yoda1 for 48 Hours for Which There were No Changes

Villous explants were pre-cultured for 4 days and incubated with 10 μ M Yoda1 or vehicle control (DMSO). Culture supernatants were collected, centrifuged at 15000 rpm and sent to Eve Technologies for cytokine analysis by Multiplex assays. Results were normalized against total protein mass and all displayed values are per mg of protein. Results were analyzed using an unpaired Student's T-test ($n = 5$, mean \pm SD).

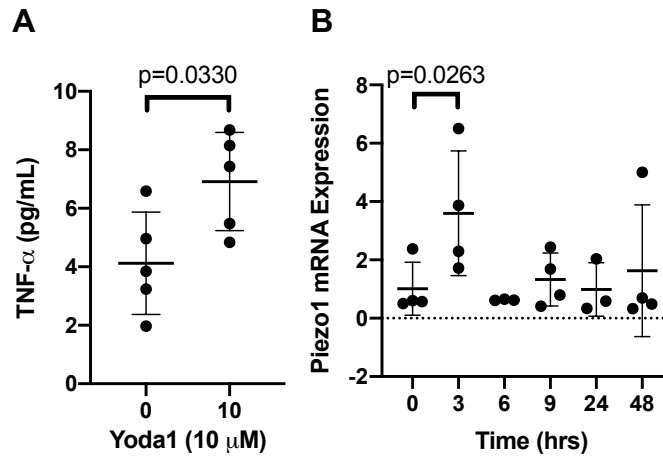


Figure 6.6: Activation of Piezo1 Elevated TNF- α , Which in Turn Upregulated Piezo1 Transcription After 3 Hours

(A) Villous explants were pre-cultured for 4 days and incubated with 10 μ M Yoda1 or vehicle control (DMSO). Results were normalized against total protein concentration and analyzed using the Student's T-test ($n = 5$, mean \pm SD). (B) Villous explants were pre-cultured for 4 days and incubated with 1 ng/mL TNF- α or no treatment control. Results were analyzed using the mixed effects model analysis ($p=0.144$), and the two-stage linear step-up procedure of Benjamini, Krieger, and Yekutieli post-hoc ($n = 3-4$, mean \pm SD).

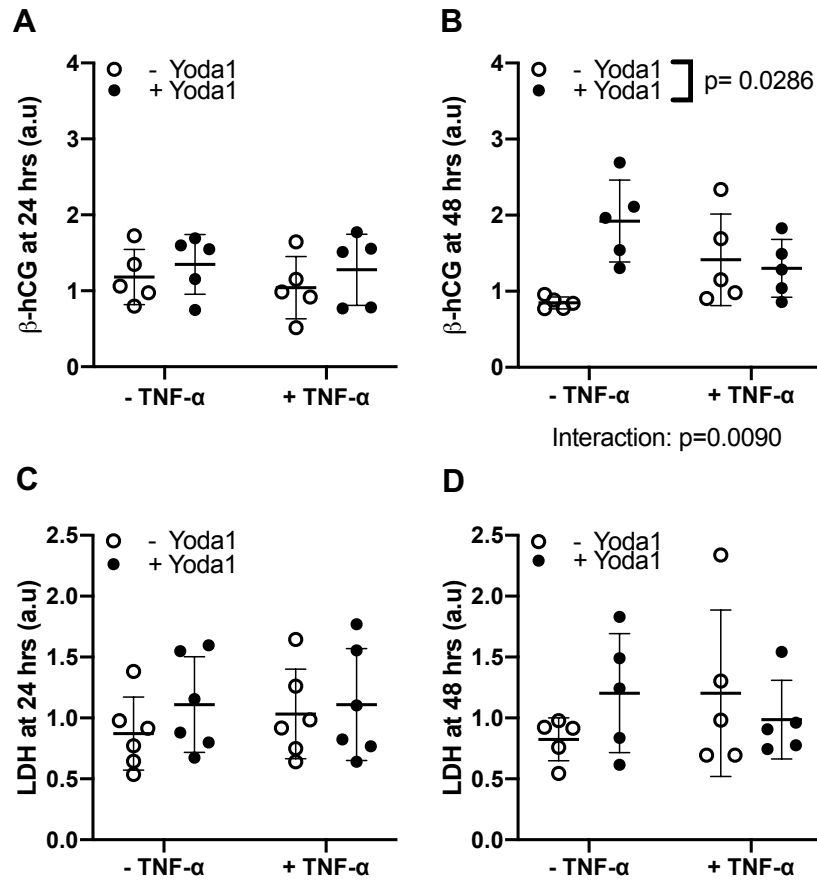


Figure 6.7: Pharmacologically Activating Piezo1 in the Presence of TNF- α Decreased β -hCG Release

Villous explants were pre-cultured for 4 days and incubated with 1 ng/mL TNF- α , 1 μ M Yoda1, TNF- α and Yoda1 co-treatment, or vehicle control (DMSO). Release of β -hCG at **(A)** 24 hours (Interaction: $p=0.854$, TNF- α Factor: $p=0.575$, Yoda1 Factor: $p=0.290$) and **(B)** 48 hours post-treatment (Interaction: $p=0.0090$, TNF- α Factor: $p=0.892$, Yoda1 Factor: $p=0.0286$). Release of LDH at **(C)** 24 hours (Interaction: $p=0.614$, TNF- α Factor: $p=0.611$, Yoda1 Factor: $p=0.327$) and **(D)** 48 hours post-treatment (Interaction: $p=0.169$, TNF- α Factor: $p=0.699$, Yoda1 Factor: $p=0.698$). All results were normalized against total protein mass. Normalized values were then calculated as a ratio relative to the no treatment control from the same experimental replicate and

depicted as a fold-change difference within their own experimental subset. The arbitrary units (a.u) reflect the relative nature of the results that were calculated as a ratio of the chosen reference. Results were analyzed using a two-way ANOVA and Tukey post-hoc test ($n = 5$, mean \pm SD).

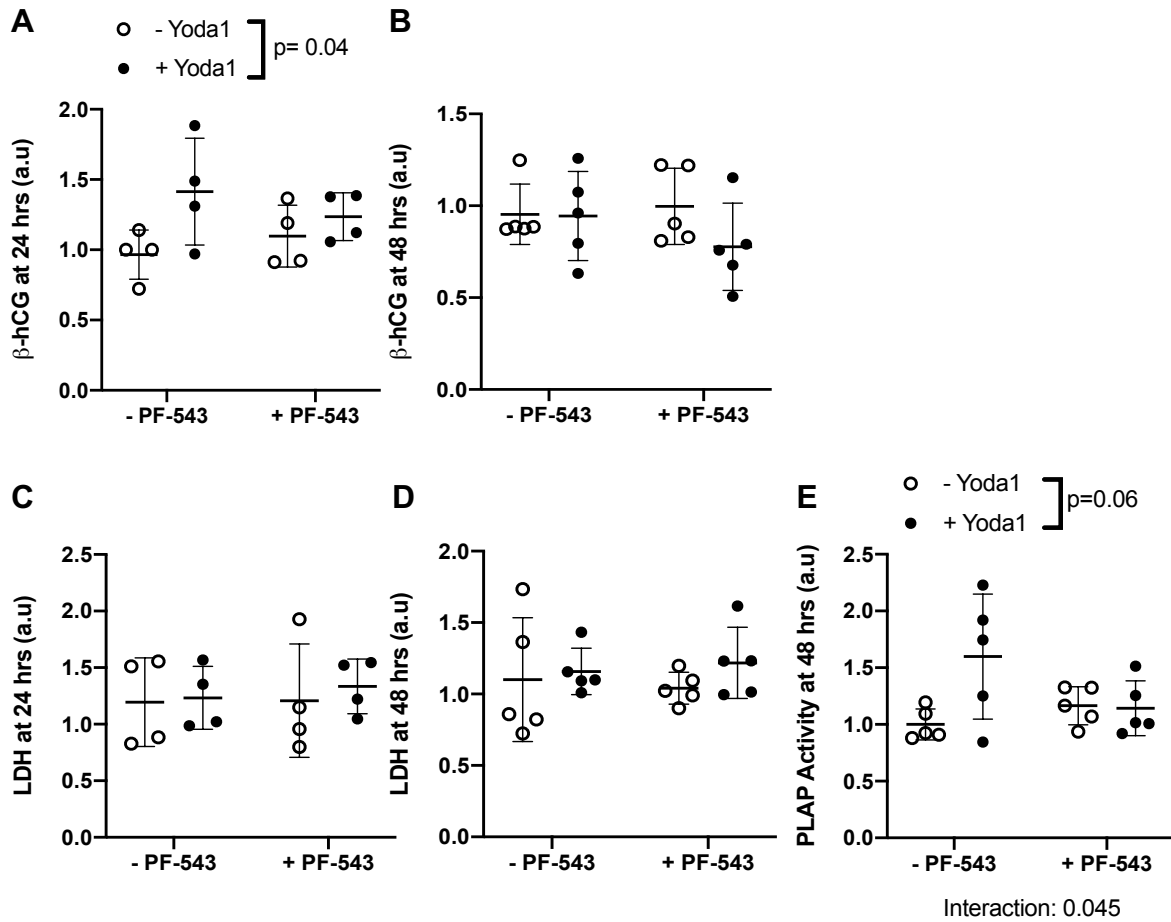


Figure 6.8 Inhibiting SphK1 Decreases the Effect of Yoda1 on PLAP Activity but not β -hCG or LDH Release

Villous explants were pre-cultured for 4 days and incubated with 1 μ M PF-543, 1 μ M Yoda1, PF-543 and Yoda1 co-treatment, or vehicle control (DMSO). Release of β -hCG at (A) 24 hours and (B) 48 hours, release of LDH at (C) 24 hours and (D) 48 hours, and (E) villous PLAP activity at 48 hours were measured post-treatment. All results were normalized against total protein mass. Normalized values were then calculated as a ratio relative to the no treatment control from the same experimental replicate and depicted as a fold-change difference within their own experimental subset. The arbitrary units (a.u) reflect the relative nature of the results

that were calculated as a ratio of the chosen reference. Results were analyzed using a two-way ANOVA and Tukey post-hoc test ($n = 4$, mean \pm SD).

6.3. Discussion

Piezo1 is a relatively novel channel, and therefore, little is known regarding its role in the placenta. I show for the first time that Piezo1 is expressed in the trophoblastic layers of the human placenta along with the blood vessels. My study also demonstrated that Piezo1 activation leads to contrasting responses: increased syncytial endocrine function and growth factor release as well as placental cell membrane damage and pro-inflammatory cytokine release. This study also revealed that Piezo1 signaling was altered in unfavorable conditions. Notably, placental Piezo1 levels were higher in PE and its signaling was altered in the presence of TNF- α , a key inducer of placental dysfunction in PE. Overall, this is the first study demonstrating that Piezo1 activation affects placental function and sheds light on the importance of investigating its signaling in healthy and diseased conditions of pregnancy.

Piezo1 has been mostly studied in the nervous and vascular system. In reproductive tissues, Piezo1 has been previously identified in mouse yolk sacs (315), rat uterine tissue (312), in isolated human fetoplacental endothelial cells, and in isolated human placental arterial endothelial cells (313). Piezo1 exhibited a strong localization in blood vessels as expected. To my knowledge, this study is the first to demonstrate Piezo1 expression in human CTs and STs. I also demonstrated that overall Piezo1 levels were elevated in placental biopsies from women with PE without any changes in mRNA expression. The mRNA expression of another mechanosensory channel, transient receptor potential vanilloid 1 (TRPV1), is downregulated in placentas from women with PE, whereas its placental protein expression is upregulated (430). This hints at the possible role of dysregulated placenta mechanosensory signaling in PE. The placenta in PE is characterized by poor invasion into the uterine wall resulting in poor uteroplacental perfusion. Other aspects of the dysregulated placental function in PE include the

malformation of the placental barrier due to high levels of CT apoptosis and low levels of CT differentiation and fusion into ST. The role of Piezo1 in pregnancy overall is understudied with only a few studies examining the role of Piezo1 in placental vascular function (313, 314). Piezo1 expression, however, is crucial for embryo viability as Piezo1 knockout mouse embryos are non-viable and die on the 8th day of gestation (313).

Recently, other mechanosensory stimuli and channels have been identified as key regulators of syncytialization. Sanz et al show that a high flow rate, which activates mechanosensory channels, induces cultured rabbit trophoblast syncytialization through a Ca²⁺-dependent mechanism (318). Moreover, a high flow rate reduces apoptosis in the JAR cell line and increases production of placental growth factor by ST derived from primary human trophoblasts (317). With respect to mechanosensory channels, the focus in placental syncytialization has been on TRPVs. For instance, activating TRPV6 with fluid shear stress induces microvilli formation, characteristic of a mature ST, in BeWo-derived syncytia (316). TRPV6 also enhances invasive EVT function by inducing proliferation and inhibiting apoptosis of HTR-8/SVneo trophoblasts (321). On the other hand, TRPV1 induces apoptosis and hinders syncytialization of primary human term CTs (322). I showed that Piezo1 activation with Yoda1 in an explant model increased β -hCG and hPL secretion, in addition to increased villous PLAP activity. β -hCG, hPL, and PLAP are commonly used as markers of functional ST. And hence, Piezo1 activation increased ST function. While β -hCG levels increased only at lower concentrations of Yoda1, hPL levels and PLAP activity increased at both lower and higher levels of activation. The increase in hPL and PLAP occurred alongside the increased placental cell membrane damage induced by the high levels of Yoda1 to activate Piezo1. This seemingly contrasting occurrence is not surprising as Piezo1 is a strong inducer of cell damage and

apoptosis (431). Inducing cell death and yet inducing the production of factors that support ST function could result from Piezo1 regulating the whole cell regeneration process, which involves a level of cell death. Alternatively, the cytotoxic effect of Piezo1 observed could be occurring due to its activation in tissues of mesenchymal origins also present in villous explants and not in trophoblast layers. Moreover, the activation of Piezo1 is unlikely to be an all or nothing event as Morley et al show a Yoda1 dose response revealing increased Ca^{2+} influx with increased doses of Yoda1 (314). This suggests that there might be dose effects of Yoda1 that can explain the differences in responses observed at 1 vs. 10 μM of Yoda1.

Increased ST apoptosis and ST aggregates have been reported in patients with PE (65). Increased ST apoptosis can result in a weak placental barrier and expose the conceptus to harmful factors present in the maternal blood, such as pathogens and immune cells. Additionally a poorly formed ST release inadequate levels of hormones, which are crucial for the maintenance of pregnancy to term. Placentas from women with PE are characterized by decreased ST formation and increased ST apoptosis, indicating that a weakened ST is a feature of PE (352). Increased inflammatory cytokines, as seen in patients with PE, can contribute to placental apoptosis (4). Piezo1 activation induces a pro-inflammatory response by endothelial cells through NF- κ B activation since these responses were decreased in endothelial-specific Piezo1 knockout mice (324). Piezo1 activation of cells from myeloid lineages increases their cytokine release (325). An intriguing study shows that adipose-specific Piezo1 knockout mice on a high fat diet have higher levels of inflammatory cytokines in their adipose tissues (323). The same study reveals that activating the channel in primary adipocytes decreases the cytokine expression, contrary to the effects seen in cells of endothelial and myeloid origins. This implies that there are differential tissue-specific effects of Piezo1 on inflammation.

I showed that pharmacologically activating Piezo1 with a higher concentration of 10 μ M Yoda1 for 48 hours in villous explants during ST regeneration increases the release of pro-inflammatory cytokines IL-2 and IL-18. It also increased the release of several other cytokines whose circulating levels are also elevated in PE (419, 432, 433). Yoda1 also increased the release of growth factors MDC, EGF, and Flt-3L, in addition to interleukins that are decreased in PE, IL-4 and IL-9 (395, 434). EGF is a strong inducer of ST differentiation (435) and the increase in EGF induced by Piezo1 activation could explain the mechanism behind Piezo1-induced ST function. IL-4 is known for its anti-inflammatory roles in the placenta and is able to counteract the pro-inflammatory effects of cytokines such as TNF- α (436). IL-4 supplementation in a reduced uterine perfusion pressure rat model of PE alleviates the pro-inflammatory and hypertensive phenotype (437). The increased production of IL-4 in response to Piezo1 could be a physiological protective mechanism to alleviate the consequences of the placental pro-inflammatory state triggered by Piezo1. Similarly, IL-9 is crucial for HTR-8/SVneo trophoblast proliferation, invasion, and tubule-formation (434). And hence the increased production of IL-9 could be a protective mechanism to counterbalance the cytokine surge in response to Piezo1.

Piezo1 increased TNF- α release from placental explants. TNF- α is a prominent proinflammatory cytokine released primarily by macrophages and other cells such as human CTs and mesenchymal cells. The cytokine is notorious for its detrimental effects on placental function, as summarized by Haider et al (4). High TNF- α protein and mRNA levels in the placenta are characteristic of PE. Exposing primary human trophoblasts to high levels of TNF- α induces apoptotic effects in the ST. Elevated TNF- α also decreases ST fusion in first-trimester human CTs (4). I sought to establish whether TNF- α also regulates the expression of Piezo1 in the placenta. The concentration of TNF- α used was similar to what Williams and colleagues

observe in patients with PE (438). TNF- α treatment upregulated Piezo1 mRNA expression after 3 hours, in support of my hypothesis and existing literature. Astrocytes pretreated with proinflammatory LPS, which induces TNF- α , increase the expression of Piezo1 (12). Piezo1 mRNA also increases in chondrocytes with IL-1 α treatment (326).

Activating Piezo1 in the presence of pathological TNF- α levels led to decreased β -hCG release that was not due to decreased cell viability. Piezo1 and TNF- α signaling pathways are interdependent. Since both these molecules upregulated each other, the decreased β -hCG release could be due to a gradual feedforward upregulation of TNF- α to a level that is detrimental to β -hCG release. Notably, Zhu and colleagues find that treatment of hepatocellular carcinoma cells with TNF- α leads to an increase of Ca²⁺ influx (439). The activation of Piezo1 channels elicits the influx of Ca²⁺ into cells (303). Hence, the interaction between TNF- α and Piezo1 is potentially Ca²⁺ mediated leading to a high level of Ca²⁺ release that is inhibitory to ST function.

Piezo1 responds to mechanical stress and maintains homeostatic conditions in a broad range of cells. Piezo1 is a relatively novel mechanosensory channel and hence its mechanical inducers in the placenta remain unclear. Piezo1 responds to shear stress in the uterine and fetoplacental vasculature (312, 314) and optimal shear stress is necessary for ST function where both upper and lower ranges of shear stress are detrimental for appropriate syncytialization (316-318). TNF- α increases Piezo1 levels, potentially to detrimental levels. This might explain the contrasting effect of Piezo1 signaling in the presence and absence of TNF- α .

I chose the explant model as the heterogeneous cell types and the microenvironment present in the explant best models the physiological environment of the villous CT. The static conditions using a specific pharmacological agent were chosen to limit mechanosensory

activation to Piezo1 alone. However, a 2021 study demonstrates the development of a promising placental explant flow model which could be used to examine further questions of Piezo1 activation and its interaction with other mechanosensory channels (440). A limitation of my study was using agonists alone without any antagonists. This choice was due to the non-specificity of the commonly used compounds to inhibit Piezo1 action. For instance, Gsmtx4 is used to inhibit Piezo family channels but also inhibits the transient receptor potential channels (441). Other inhibitors such as ruthenium red and gadolinium ions (+3) are also used in Piezo1 studies. However, these ions are potent inhibitors of Ca^{2+} channels in general (442, 443), which also deems them as non-specific inhibitors of Piezo1 since Piezo1 is a non-selective cation channel and multiple mechanosensory channels involve Ca^{2+} transport .

My experiments were timed to begin at the start of the regeneration of the ST layer. In that context, my findings suggest that Piezo1 activates multiple signaling pathways during the regenerative phase of the ST. The ST regeneration cycle is most active in the second trimester of pregnancy, during which the symptoms of PE intensify to a clinically detectable and diagnosable level. Piezo1 also regulates cell death and epithelial extrusion (302). Hence, studying Piezo1 in the shedding phase of the trophoblast cycle could increase our understanding of its effects on ST shedding in healthy and disease conditions. High levels of trophoblast death and shedding are a hallmark of PE (427) and contribute to the development and progression of the disorder in various body systems. This places Piezo1 as an important mediator of placental function, and whether its altered signaling could lead to PE pathophysiology should be investigated further. This is the first study to characterize Piezo1 expression and function in the human placenta. I show that Piezo1 increases syncytial endocrine function, placental inflammatory cytokine release, and placental cell membrane damage that is dependent on the level of Piezo1 activation.

I also reveal that Piezo1 interacts with TNF- α in a feedforward manner where my results show that TNF- α upregulates Piezo1 and Piezo1 increases TNF- α bioavailability in the villous explant model. Ultimately, Piezo1 decreases β -hCG release by ST upon activation in the presence of TNF- α .

7. Chapter 7: General Discussion and Future Directions

In this chapter, I will make connections between all four of the chapters showing my results. For interpretations, discussions, and limitations of studies belonging to a specific chapter, please refer to that chapter itself. In this chapter, I will highlight gaps that will need to be addressed to better understand the proposed model that highlights the intersections of TNF- α , SphK1, S1PR, and Piezo1 in placental dysfunction in PE. I will also highlight the strengths and limitations of my experimental models. Finally, as part of my future directions, I will propose studies that will examine TNF- α , SphK1, S1PR, and Piezo1 signaling in an animal model of PE. This study will provide answers on feasible targets that could improve overall pregnancy outcomes, including maternal, fetal, and placental health.

7.1. Proposed Model and Mechanisms of Placental Function

7.1.1. ST Endocrine Function

The summary of the intersection of TNF- α , SphK1, S1PR, and Piezo1 signaling pathways on placental function is presented in Figure 7.1. β -hCG was the only consistent marker I measured in response to TNF- α , SphK1 inhibition, Piezo1 activation, and S1PR2 inhibition. Therefore, I will use my experimental findings to describe the functional consequences in ST of each these factors alone, TNF- α , SphK1, Piezo1, and S1PR2, or in combination by assessing hCG release from the ST. The intersection of the signaling pathways of these molecules might not apply to other markers of ST function or differentiation, such as villous PLAP activity, hPL release, or even CT fusion as my results have consistently shown that these outcome measures do not necessarily all follow the same trends. Low levels of TNF- α did not affect hCG release but high TNF- α levels decreased hCG release. Low levels of SphK1 had no effect but high levels of SphK1 activation decreased hCG release. High TNF- α increased S1PR2 levels and S1PR2 activation decreased hCG release. Low levels of Piezo1 activation increased hCG release but high levels of Piezo1 activity did not affect hCG. At physiological conditions, TNF- α and SphK1 were not inhibitory of TNF- α , and Piezo1 increased hCG release independent of either. At high levels of TNF- α , which models a PE-like condition, SphK1 activity led to a decrease in hCG release through a common pathway. TNF- α also increased S1PR2 expression, which would shift the balance towards increasing S1PR2 signaling, leading to low hCG release. High levels of Piezo1 expression led to the amplification of these pathways by increasing TNF- α and decreasing hCG release.

7.1.2. Cell Membrane Damage and ST Shedding

Low levels of TNF- α led to no change in LDH release or cell membrane damage. SphK1 activity at any level did not affect LDH release on its own but mediated TNF- α -induced release. Only high levels of Piezo1 activity increased LDH release. At physiological levels, TNF- α , SphK1, and Piezo1 led to physiological levels of cell death, comparable to those of the no treatment or vehicle control. At high levels, TNF- α increased LDH release and ST shedding via SphK1 activity. Piezo1, however, was not dependent on TNF- α or SphK1 to increase LDH. This could be due to the lack of interaction in this specific pathway. Alternatively, this could be due to the Piezo1-induced increase of growth factors, not induced by TNF- α or SphK1, that can protect the placenta from TNF- α -induced cell death, and even ST shedding. S1PR2 activation decreased LDH release, but TNF- α increased S1PR2. This suggests that S1PR2 activation can also be releasing growth factors that protect the placenta from cell membrane damage.

7.1.3. Cytokine and Growth Release

TNF- α and Piezo1 activation each released similar cytokines and growth factors, including EGF, Flt-3L, IFN α 2, IL-2, IL-4, IL-6, IL-9, IL-12 p70, IL-18, and RANTES. This suggests that TNF- α and Piezo1 use similar downstream signaling pathway to mediate these effects, involving the release of these cytokines and factors. Interestingly, IFN α 2 release was stimulated by Piezo1 and its TNF- α -induced release was also dependent on SphK1 activity. This suggests that IFN α 2 might be part of the TNF- α -SphK1-Piezo1 signaling system. This, however, remains, to be experimentally confirmed.

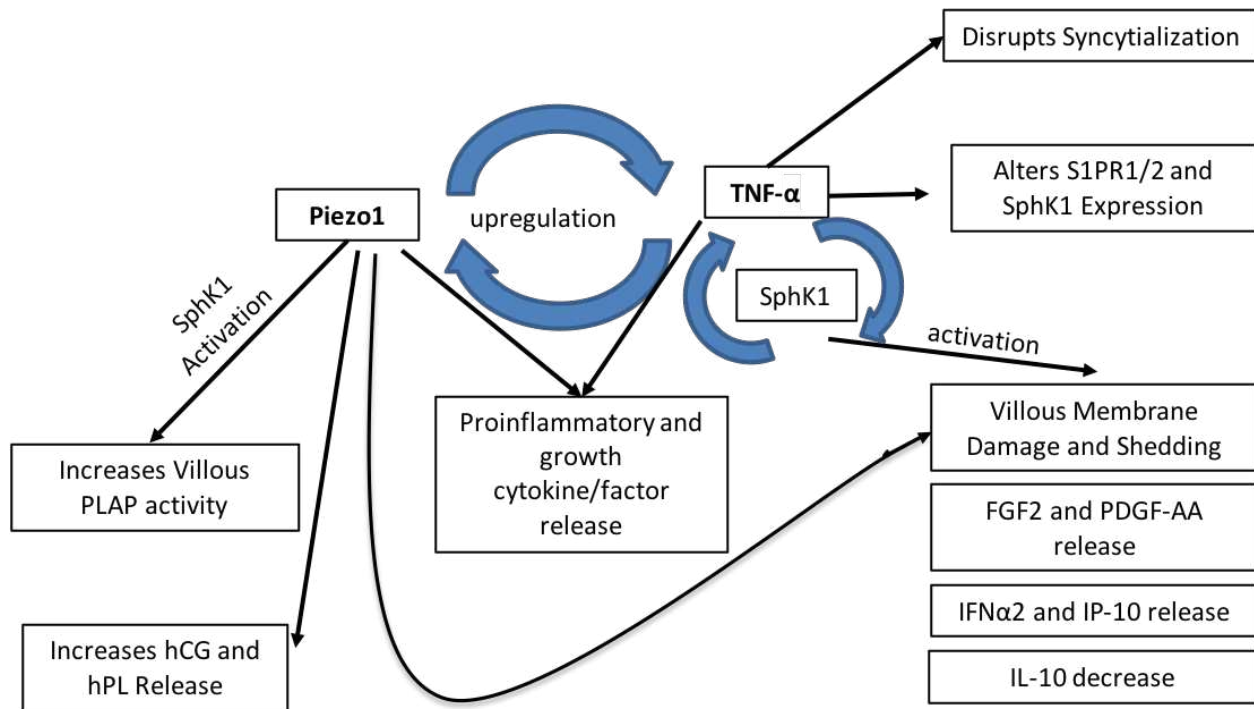


Figure 7.1: Signaling Intersections Between TNF- α , SphK1, Piezo1, and S1PRs in Placentas of Women with PE

7.2. Summary and Relevance to PE

PE is a serious pregnancy disorder and is a leading cause of fetal and maternal deaths. Mothers and newborns that survive PE are at an elevated risk of metabolic and cardiovascular disorders later in life (25, 26). Placental development and function play a key role in the pathophysiology of PE. In PE, a high level of placental cell death, pro-inflammatory cytokine release, ST shedding, and poor ST endocrine function are key characteristics of a PE phenotype (408). TNF- α is elevated in the placentas and serum of mothers with PE (444, 445). Elevated placental TNF- α leads to abnormal responses including trophoblast apoptosis (374) and inhibition of syncytialization (139). The injection of TNF- α induces PE symptoms in baboons (138) and rats (446). Despite the disruptive role of elevated TNF- α levels, TNF- α inhibitors are

controversial in pregnancy due to off-target effects such as congenital malformations (447).

Thus, my thesis aimed to identify the S1P system and Piezo1 as mediators downstream of TNF- α signaling that may be targeted to decrease pregnancy disruptive responses and retain pregnancy enhancing roles of TNF- α .

TNF- α and SphK1 activation are both implicated, separately, in disrupting ST function. TNF- α signaling is dependent on SphK1 activation in non-placental cells. In Chapter 3, I showed that increased cell death, shedding, IFN α 2, and IP-10, all of which are involved in inducing pro-inflammatory signaling and placental cell damage, were reversed upon SphK1 inhibition. FGF-2 and PDGF-AA, growth factors are released to counteract inflammatory-driven cell death. The release of these factors was induced by TNF- α and reversed upon SphK1 inhibition. TNF- α also increased the release of 26 cytokines and growth factors and hCG independently of SphK1. For instance, TNF- α increased the release of MIP-1 β , IL-6, sCD40L, RANTES, IL-2, IL-1RA, all of which are pro-inflammatory cytokines with elevated circulating levels in mothers with PE (107, 419, 448-450). The increase in these cytokines was independent of SphK1, and this suggests that SphK1 may not mediate the TNF- α -induced Th1 shift that occurs in PE. TNF- α decreased the release of hCG, a marker of ST endocrine function, and inhibiting SphK1 reversed this effect. The placenta in PE is characterized by poor ST formation and function. My results show that this phenotype can be induced by high levels of TNF- α and is dependent on SphK1 activation. TNF- α decreased the release of IL-10, whose decrease is associated with the onset of PE. Inhibiting SphK1 reversed these effects. Inhibiting SphK1 alone decreased TNF- α release. These results show that SphK1 only partially mediates the TNF- α -induced PE placental phenotype, primarily through cell damage, shedding, and specific cytokine release. The clinical implication is that

inhibiting SphK1 can be a viable option to explore to protect mothers with PE that display high circulating TNF- α from placental cell damage.

TNF- α and S1P circulating levels are elevated in mothers with PE (4, 176). However, whether elevated SphK1 levels in the placentas of women with PE are a source of high circulating S1P is unknown. It is also unknown whether elevated circulating TNF- α leads to these increased SphK1 levels in the placenta, thereby contributing to the high S1P levels. It is also unknown how TNF- α affects the levels of other placental metabolic and catabolic S1P enzymes. Chapter 3 showed that SphK1 levels were higher in placental tissue of women with PE. This hints that the placenta could be a source of the pathologically elevated circulating S1P in PE. However, TNF- α did not alter enzyme levels in whole biopsies of placental tissue. This implies that elevated TNF- α in PE alone does not lead to the elevated SphK1 seen in PE, hinting at the presence of other factors such as cytokines that might be inducing this increase in conjunction or separately from TNF- α . However, TNF- α increased SphK1 levels in differentiating primary trophoblasts. This provides an argument that the ST can be a source of S1P released into maternal circulation in response to TNF- α . When circulating or placental TNF- α levels are elevated in PE, SphK1-mediated S1P production can be increased in the ST, thereby contributing to pathological S1P levels. This suggests that targeting placental SphK1 in women with PE, that exhibit high TNF- α levels, can ameliorate the overproduction of S1P in trophoblastic layers and its release into maternal circulation. Together with Chapter 3, I show that targeting placental SphK1 in cases of increased TNF- α can in fact partially resolve the placental PE-like phenotype. For this reason, it is important to investigate S1PR signaling in placental function to potentially identify more suitable targets.

Studies in various cell types show that S1PR2 signaling is involved in cell differentiation, inflammatory cytokine release, and apoptosis (9). TNF- α increases S1PR2 expression in non-placental microvascular cells (332). However, the role of S1PR2 in the placenta is poorly understood, and the regulation of S1PR2 by TNF- α in the placenta and specifically in trophoblasts were also unknown. My work in Chapter 5 demonstrates that S1PR2 activation decreases placental cell membrane damage and decreases hCG release while increasing hPL. This suggests that S1PR2 signaling is not completely detrimental and can have varying effects on placental function, contrary to what I hypothesized. A very interesting finding in this chapter is the discrepancy of S1PR2 regulation in response to TNF- α , based on the models used. My study shows that TNF- α increases S1PR2 expression in the placenta as a whole and in differentiating primary CTs. However, in BeWo cells, S1PR2 decreases in response to TNF- α . Thus, BeWo cells, and perhaps choriocarcinoma or immortalized cell lines in general, are not an accurate model to study placental regulation of sphingolipid signaling.

Finally, I identify a secondary mediator of TNF- α and SphK1 signaling, Piezo1. In the last chapter, I identified a novel role of Piezo1 in the placenta and showed that its signaling amplifies TNF- α signaling and some of Piezo1 effects are dependent on SphK1 activation. Mechanosensory channels are recently implicated as regulators of trophoblast syncytialization (316). Moreover, Piezo1 induces cell damage and apoptosis in other cell types by stimulating inflammatory cytokine release (325). Piezo1 was recently identified in the rat placenta (314), but its expression and function are unknown in human placentas. Moreover, inflammatory cytokines increase Piezo1 expression. However, the effect of TNF- α on Piezo1 expression and activity were unclear. Piezo1 exerts its effects on epithelial extrusion by SphK1 activation and subsequent SIP release (302). However, the relationship between TNF- α , SphK1, and Piezo1 in

the placenta had not been investigated. In Chapter 6, I showed that Piezo1 expression was higher in the placentas of women with PE, suggesting that Piezo1 plays a role in the pathophysiology or is increased as a protective mechanism. I later showed that Piezo1 has distinctive functions based on the levels of activation, with increased endocrine function at lower levels and increased placental cell membrane damage and inflammatory cytokine release at higher levels of activation. This suggests that the increase in Piezo1 in placentas from women with PE can lead to more overall Piezo1 activity and the relay of its secondary messengers, ultimately leading to the detrimental effects listed. Importantly, I found that TNF- α increased Piezo1 expression and vice versa, suggesting a feedforward loop between these two factors. It also suggests that the high levels of circulating TNF- α in PE could be the leading cause of the increased Piezo1 expression seen in PE. I also showed that elevated TNF- α counteracted the endocrine function induced by low levels of Piezo1 activation. This unexpected result can be explained by the upregulated feedforward loop between TNF- α and Piezo1 levels, resulting in high TNF- α and Piezo1 levels and leading to detrimental effects. Lastly, I showed that activation of Piezo1 induced ST PLAP activity via SphK1 activation. This shows that TNF- α , S1P, and Piezo1 regulate placental functions that are important for pregnancy maintenance through overlapping pathways.

7.3. Experimental Model Strengths and Limitations

The experimental strengths and limitations pertinent to a specific chapter are discussed in that chapter's discussion. In this section, I will describe the overall strengths and limitations of the thesis. To start with, the choice of the various models throughout my thesis comes with both strengths and limitations. The choice of villous explants for assessing ST endocrine function and shedding is a very physiological model. Choosing villous explants to investigate cell death

through LDH release is physiologically relevant; however, this outcome measure does not identify the cell types experiencing cell death, nor does it identify the type of cell death. Similarly, choosing the villous explant model to study cytokine and growth factor release is physiologically relevant for addressing the state of placental health, however, this makes it hard to discern the specific cell types leading to these changes. In Chapters 4 and 5, I used both tissue cultures as well as monolayer trophoblast cultures, which highlights both tissue-level changes that are relevant on a gross physiology level, as well as trophoblast-specific changes that are relevant from a cell-specific signaling perspective. Using these different models, I showed that the SphK1 increase in expression in response to TNF- α was trophoblast-specific.

One of the biggest limitations of the monolayer cell model and the villous explant model are the culture conditions that I used. Due to resource availability, specifically the lack of low oxygen biocontainment cabinets, all culture treatments occurred in a 21% O₂ environment. Explant dissection requires 2 hours and trophoblast isolation requires over 8 hours in a biocontainment cabinet, exposed to atmospheric oxygen conditions. Although low oxygen incubators were available, the back-and-forth adjustment of tissues between different oxygen levels might lead to a shock and alter physiology. Thus, I chose to do all experiments at 21% O₂.

Numerous reports suggest that CT development and fusion occur in hypoxic conditions of 3% O₂ in early trimesters and reach 6% O₂ at term (451). The most physiological conditions to use for my models would hence be 6% O₂ since all tissues were collected from term pregnancies. However, a recent article shows that there is no difference in measures of cell death and β -hCG release from trophoblast cultures in 21% O₂ compared to 8% O₂. In fact, CTs exhibited a higher level of fusion when grown in 21% O₂ (452). This suggests that while lower oxygen levels might

be more physiologically relevant, atmospheric levels can lead to more consistent culture conditions.

Finally, another main limitation of these studies was isolating tissues and cells from placentas in the third trimester of pregnancy. All of my samples were obtained from elective Cesaerean sections of women not in labor. However, as discussed in Chapter 1, the placenta goes through various developmental stages throughout pregnancy. Additionally, the expression of S1PRs and S1P synthesizing and catabolizing enzymes in reproductive tissues changes over the progression of pregnancy, as discussed in my recent review and in Chapter 1 (9). For my particular study, using late first trimester or early second trimester placental tissue would be ideal since during those timepoints the placenta is at its peak of ST formation. This, however, was not feasible due to difficulties with setting up a reliable tissue collection system with pregnancy termination centers. Moreover, the majority of pregnancy terminations occurring in the second trimester are complicated with genetic or chromosomal anomalies and therefore would be not suitable for these studies.

7.4. Future Directions

Several further studies can be performed to strengthen the conclusions of the studies in this thesis. All the studies comparing healthy control placentas and placentas from mothers with PE measured differences in expression of SphK1 and Piezo1, but not their activity. Whereas, the experiments examining the roles of SphK1, Piezo1, and S1PR2 on the placental dysfunction in PE involved altering activity levels of these molecules, via agonists or inhibitors, but not their expression. So, there is a gap in understanding whether the change in expression of these molecules that occurs in PE correlates with the change of their activities that lead to the PE-like placental dysfunction that was observed in my studies. For future experiments, measuring

activity of the different factors in placentas and trophoblasts of women with healthy pregnancies or PE would shed light on the agreement of expression patterns and activity. In addition to that, siRNA knockdowns of SphK1, S1PRs, or Piezo1 could be performed using trophoblast cell lines or placental explants to investigate whether decreased levels of SphK1, S1PRs, or Piezo1 can affect placental physiology. Additionally, these knockdowns can be performed in conjunction with TNF- α treatment to test the dependence of TNF- α signaling on the expression rather than activation of SphK1, S1PRs, or Piezo1. Additionally, in order to investigate cell-specific interactions, these experiments should be performed in isolated primary human trophoblasts, placental endothelial cells, and placental fibroblasts.

Another aspect to investigate would be the mechanisms of activation of TNF- α , SphK1, S1PRs, and Piezo1 amongst each other, and their regulation of each other's expression. For instance, Piezo1 mediates its effects in other cell types by inducing a Ca²⁺ influx; thus, it would be beneficial to test whether TNF- α administration and SphK1 inhibition in placental explants increase intracellular Ca²⁺ in the syncytium. Testing whether SphK1 or S1PR activation or TNF- α treatment can induce a Ca²⁺ influx in the placenta would help us identify a mechanism through which TNF- α , SphK1, S1PRs, and Piezo1 pathways intersect. This can be tested by using a ratiometric fluorescent dye such as Fura-2 that binds to free Ca²⁺ or electrophysiological techniques using either a monolayer cell culture of various placental cell types or an explant model, similar to the one used in my studies. For the purpose of investigating whether signaling by these molecules intersects via Ca²⁺ influx, a monolayer cell culture model would be most appropriate, since it is a more experimentally feasible to set-up and the interpretation of the results would be easier with one cell type. However, repeating these experiments in my explant model can help make interpretations about the overall levels of intracellular and extracellular

Ca²⁺ bioavailability in response to these treatments, since extracellular Ca²⁺ can move between different cell types to mediate their signaling.

SphK1 acts as a co-factor for TNF- α -TNFR1 signaling in other cell types (9), that is mediated through NF- κ B. Hence, future experiments would utilize specific small molecule TNFR1 inhibitors (453) to block TNFR1 activation and confirm it mediates the TNF- α intersection with SphK1 and Piezo1 signaling. Additionally, testing the TNF- α -TNFR1-induced translocation of NF- κ B and its dependence on SphK1 activation would establish NF- κ B as a mediator in ST for IFN α 2, IP-10, FGF-2, PDGF-AA and IL-10 release and cell damage. TRAF-interacting protein, or TRIP, inhibits the SphK1-TRAF2 interaction during TNFR1 activation and inhibits the subsequent activation of NF- κ B (300). Using exogenous TRIP to inhibit the SphK1-dependent TNF- α effects can be a more targeted and specific approach, enabling the conservation of vital SphK1 signaling in cells. Hence, future studies examining the effects of TRIP in the presence of high TNF- α levels on placental outcomes can uncover a more specific target.

Another important aspect to investigate is the order of Piezo1 activation with respect to the activation of NF- κ B. From Chapter 6, I saw that Piezo1 induced TNF- α release, and TNF- α also increased Piezo1 levels. Thus, it becomes complicated to understand which signals are upstream when there appears to be a feedforward loop amongst the molecules. Nonetheless, assessing NF- κ B translocation in response to Piezo1 activation, using Yoda1 would be important to complete. Adding TNFR inhibitors in addition to Yoda1 and assessing NF- κ B translocation would aid in investigating the effects of Piezo1 activation on NF- κ B translocation independent of TNF- α signaling.

In this thesis, I showed that TNF- α alters the expression of S1PR1, S1PR2, and S1PR3 in the placenta and suggested using S1PR inhibitors in conjunction with TNF- α treatments. Investigating the role of Piezo1 on S1PR expression and the dependence of Piezo1 signaling in the placenta on S1PR activation would further complete our knowledge of this pathway. This could be done by measuring the various placental outcomes that were investigated in my thesis in response to S1PR1, S1PR2, or S1PR3 inhibitors in the presence or absence of Yoda1, the Piezo1 agonist. Since Piezo1 is physiologically activated by shear stress and cell crowding, placental cell models could be cultured and exposed to these conditions to investigate how Piezo1 may affect S1PR1, S1PR2, S1PR3 or SphK1 expression and activation while exposed to shear stress and cell crowding. As mentioned in Chapter 6, a recent article was published on an explant flow model (440). This model could be utilized to examine the role of shear stress-activated Piezo1 on the expression and activation of these molecules. On the other hand, examining the effects of cell-crowding induced activation of Piezo1 and its effects on S1PR1, S1PR2, S1PR3 or SphK1 expression and activation by using cell overcrowding models. Some of the available models include growing cells to confluency on an overstretched membrane and then releasing the tension, which would increase the cell density by 1.3 fold and induce an overcrowded state (302). Recently, another model emerged involving growing cells to confluency on a small petri dish, inverting the small petri dish into a large petri dish, such that the cells are in contact with the media from the large petri dish. In this study, cells were collected at the bottom of the large petri dish as an evidence of crowding-induced extrusion (454).

A big unknown in this pathway is whether SphK1 leads to mediation of TNF- α -induced placental damage via producing S1P that is mainly transported into extracellular space, where it exerts its extracellular effects through binding to S1PR1-5, or whether the effects on placental

function are independent of SphK1 production of S1P. I showed that SphK1 activity, that was inferred by using a potent SphK1 inhibitor PF-543, and S1P treatment do not lead to the same effects. This has also been observed by Singh et al (46). This complicates our understanding of the role of SphK1 in this pathway as it was previously thought to mainly function as a producer of S1P. So, a future study would examine SphK1 activity via SphK1 activity assays in response to TNF- α and Yoda1 and in response to PF-543, to determine the level of activity inhibition in the villous explant model (275, 455). The next study would examine the secretion of S1P in response to TNF- α or Piezo1 activity, in addition to examining whether S1P levels are altered in combined treatment of TNF- α with PF-543, Piezo1, and PF-543, and the three treatments combined. An important aspect to consider would be the localization of produced S1P since cytosolic, nuclear, and extracellular S1P contribute to different processes (9). S1P localization can be examined using immunodetection, as described in a recent article (456). Measuring secreted S1P by mass spectrometry has its limitations as secreted S1P immediately binds to its receptors, making it difficult to measure S1P secretion, especially if this secretion is gradual and regulated by its transporters. One way to address this would be to develop an assay with fluorescent anti-S1P antibodies (457), that do not present steric hindrance. These would be added to the culture media and the rate of these tags binding to the S1PRs on the cellular surface would be examined using live microscopy. This would help us identify how quickly S1P binds to its receptors and shed light on the appropriate window of time that S1P release should be measured within. Alternatively, developing an assay with a fluorescent antibody with a higher binding affinity than each of the S1PRs would be another way to measure S1P release.

Finally, in order to assess the feasibility of SphK1 or S1PR inhibition as viable targets to prevent the TNF- α -induced PE phenotype in the placenta, as well as pregnancy outcomes with

respect to maternal and fetal health, transitioning into animal models is required. Inducing PE with injections of TNF- α is already an established model of PE in multiple animal models (4, 138). Thus, inducing PE using this approach in rats and then treating with PF-543 or specific S1PR inhibitors/agonists such as S1PR1 agonist, SEW2871; S1PR1 inhibitor, W146; S1PR2 inhibitor, AB1; or S1PR3 inhibitor, TY-5215 would be the next steps (458). Outcomes investigated would include clinical manifestations of PE, such as proteinuria, blood pressure, any other evidence of end-organ damage, and excessive maternal weight gain, another characteristic of PE. I would also examine the balance of circulating Th1 and Th2 cytokines, and the presence of PE biomarkers throughout the different stages of pregnancy. These biomarkers would include the placental expression of placenta protein 13 and pregnancy-associated plasma protein A, which are lower in the first trimester of mothers who later develop PE. Finally, measuring common markers such as sFlt-1, sEng, VEGF, and placental growth factor would be conducted (459). Fetal outcomes such as size and cardiac function would be assessed, since fetal cardiac function is altered in PE (460). Placental morphology and function and vascular function would be assessed. Additionally, measuring placental and maternal vascular Piezo1 expression and function in animal models of healthy pregnancies and PE would clarify whether this treatment has any effects on Piezo1 signaling in placental physiology and pathophysiology.

7.5. Conclusions

In conclusion, this thesis aimed to elucidate the mechanisms through which TNF- α , Piezo1, and SphK1 could mediate placental villous explant decrease in ST function and increase placental cell death. To my knowledge, these are the first studies demonstrating Piezo1 expression in the human placenta, particularly the trophoblasts, and establishes the increased expression of Piezo1 and SphK1 in the placentas of women with normal and PE pregnancies.

These are also the first studies investigating the effects of Piezo1 on ST endocrine function in a proinflammatory state. Moreover, this is the first time investigating the novel mechanism of TNF- α acting through a SphK1 pathway in the placenta. Lastly, this thesis also showed that Piezo1 can act through a SphK1 pathway to mediate effects in ST endocrine function and TNF- α can act through a Piezo1-SphK1 mechanism to decrease resyncytialization and increase cell death. These studies are crucial to understanding the mechanisms which cause impaired syncytial development and function during PE. Moreover, determining the roles of Piezo1 and SphK1 in the TNF- α mediated effects on placental syncytialization can open novel avenues for the development of therapeutics to treat PE, which would allow for a greater range of available treatments for PE, a common pregnancy complication.

References

1. Harmon QE, Huang L, Umbach DM, Klungsøyr K, Engel SM, Magnus P, et al. Risk of Fetal Death With Preeclampsia. *Obstetrics & Gynecology*. 2015;125(3).
2. Kuklina EV, Ayala C, Callaghan WM. Hypertensive disorders and severe obstetric morbidity in the United States. *Obstetrics & Gynecology*. 2009;113(6):1299-306.
3. Keelan JA, Mitchell MD. Placental cytokines and preeclampsia. *Front Biosci*. 2007;12(605):2706-27.
4. Haider S, Knofler M. Human tumour necrosis factor: physiological and pathological roles in placenta and endometrium. *Placenta*. 2009;30(2):111-23.
5. Park ES, Choi S, Shin B, Yu J, Yu J, Hwang JM, et al. Tumor necrosis factor (TNF) receptor-associated factor (TRAF)-interacting protein (TRIP) negatively regulates the TRAF2 ubiquitin-dependent pathway by suppressing the TRAF2-sphingosine 1-phosphate (S1P) interaction. *J Biol Chem*. 2015;290(15):9660-73.
6. Xia P, Gamble JR, Rye KA, Wang L, Hii CS, Cockerill P, et al. Tumor necrosis factor-alpha induces adhesion molecule expression through the sphingosine kinase pathway. *Proc Natl Acad Sci U S A*. 1998;95(24):14196-201.
7. Xia P, Wang L, Gamble JR, Vadas MA. Activation of sphingosine kinase by tumor necrosis factor-alpha inhibits apoptosis in human endothelial cells. *J Biol Chem*. 1999;274(48):34499-505.
8. Xia P, Wang L, Moretti PA, Albanese N, Chai F, Pitson SM, et al. Sphingosine kinase interacts with TRAF2 and dissects tumor necrosis factor-alpha signaling. *J Biol Chem*. 2002;277(10):7996-8003.

9. Fakhr Y, Brindley DN, Hemmings DG. Physiological and pathological functions of sphingolipids in pregnancy. *Cell Signal*. 2021;85:110041.
10. Johnstone ED, Chan G, Sibley CP, Davidge ST, Lowen B, Guilbert LJ. Sphingosine-1-phosphate inhibition of placental trophoblast differentiation through a G(i)-coupled receptor response. *J Lipid Res*. 2005;46(9):1833-9.
11. Lee W, Nims RJ, Savadipour A, Zhang Q, Leddy HA, Liu F, et al. Inflammatory signaling sensitizes Piezo1 mechanotransduction in articular chondrocytes as a pathogenic feed-forward mechanism in osteoarthritis. *Proc Natl Acad Sci U S A*. 2021;118(13).
12. Velasco-Estevez M, Rolle SO, Mampay M, Dev KK, Sheridan GK. Piezo1 regulates calcium oscillations and cytokine release from astrocytes. *Glia*. 2020;68(1):145-60.
13. Amaral LM, Wallace K, Owens M, LaMarca B. Pathophysiology and Current Clinical Management of Preeclampsia. *Curr Hypertens Rep*. 2017;19(8):61.
14. Hypertension in pregnancy. Report of the American College of Obstetricians and Gynecologists' Task Force on Hypertension in Pregnancy. *Obstet Gynecol*. 2013;122(5):1122-31.
15. Srinivas SK, Edlow AG, Neff PM, Sammel MD, Andrela CM, Elovitz MA. Rethinking IUGR in preeclampsia: dependent or independent of maternal hypertension? *Journal of Perinatology*. 2009;29(10):680-4.
16. Sibai BM. Preeclampsia As a Cause of Preterm and Late Preterm (Near-Term) Births. *Seminars in Perinatology*. 2006;30(1):16-9.
17. Harmon QE, Huang L, Umbach DM, Klungsøyr K, Engel SM, Magnus P, et al. Risk of Fetal Death With Preeclampsia. *Obstetrics and gynecology*. 2015;125(3):628-35.

18. Melchiorre K, Thilaganathan B, Giorgione V, Ridder A, Memmo A, Khalil A. Hypertensive Disorders of Pregnancy and Future Cardiovascular Health. *Front Cardiovasc Med.* 2020;7:59-.
19. Bellamy L, Casas J-P, Hingorani AD, Williams DJ. Pre-eclampsia and risk of cardiovascular disease and cancer in later life: systematic review and meta-analysis. *BMJ (Clinical research ed).* 2007;335(7627):974-.
20. Kajantie E, Osmond C, Eriksson JG. Gestational hypertension is associated with increased risk of type 2 diabetes in adult offspring: the Helsinki Birth Cohort Study. *American Journal of Obstetrics & Gynecology.*216(3):281.e1-.e7.
21. Staff AC, Redman CWG. The Differences Between Early- and Late-Onset Pre-eclampsia. In: Saito S, editor. *Preeclampsia: Basic, Genomic, and Clinical.* Singapore: Springer Singapore; 2018. p. 157-72.
22. Obstetricians ACo, Gynecologists. Hypertension in pregnancy. Report of the American College of Obstetricians and Gynecologists' task force on hypertension in pregnancy. *Obstet Gynecol.* 2013;122(5):1122-31.
23. Hernández-Díaz S, Toh S, Cnattingius S. Risk of pre-eclampsia in first and subsequent pregnancies: prospective cohort study. *BMJ.* 2009;338.
24. Kuo HH, Yang JM, Wang KG. Preeclampsia in multiple pregnancy. *Zhonghua Yi Xue Za Zhi (Taipei).* 1995;55(5):392-6.
25. Shamsi U, Hatcher J, Shamsi A, Zuberi N, Qadri Z, Saleem S. A multicentre matched case control study of risk factors for preeclampsia in healthy women in Pakistan. *BMC Womens Health.* 2010;10:14.

26. Roberts JM, Bodnar LM, Patrick TE, Powers RW. The Role of Obesity in Preeclampsia. *Pregnancy hypertension*. 2011;1(1):6-16.
27. Lamminpaa R, Vehvilainen-Julkunen K, Gissler M, Heinonen S. Preeclampsia complicated by advanced maternal age: a registry-based study on primiparous women in Finland 1997-2008. *BMC Pregnancy Childbirth*. 2012;12:47.
28. Schneider S, Freerksen N, Röhrig S, Hoefl B, Maul H. Gestational diabetes and preeclampsia—similar risk factor profiles? *Early human development*. 2012;88(3):179-84.
29. Duckitt K, Harrington D. Risk factors for pre-eclampsia at antenatal booking: systematic review of controlled studies. *Bmj*. 2005;330(7491):565.
30. Wang Z, Wang P, Liu H, He X, Zhang J, Yan H, et al. Maternal adiposity as an independent risk factor for pre-eclampsia: a meta-analysis of prospective cohort studies. *Obesity Reviews*. 2013;14(6):508-21.
31. Burton GJ, Redman CW, Roberts JM, Moffett A. Pre-eclampsia: pathophysiology and clinical implications. *BMJ*. 2019;366:l2381.
32. Roberts JM, Hubel CA. The two stage model of preeclampsia: variations on the theme. *Placenta*. 2009;30 Suppl A(Suppl A):S32-S7.
33. Tersigni C, Meli F, Neri C, Iacoangeli A, Franco R, Lanzone A, et al. Role of Human Leukocyte Antigens at the Feto-Maternal Interface in Normal and Pathological Pregnancy: An Update. *Int J Mol Sci*. 2020;21(13):4756.
34. Hemmings DG, Hudson NK, Halliday D, O'Hara M, Baker PN, Davidge ST, et al. Sphingosine-1-phosphate acts via rho-associated kinase and nitric oxide to regulate human placental vascular tone. *Biol Reprod*. 2006;74(1):88-94.

35. Chen CP, Aplin JD. Placental extracellular matrix: gene expression, deposition by placental fibroblasts and the effect of oxygen. *Placenta*. 2003;24(4):316-25.
36. Riddell MR, Winkler-Lowen B, Jiang Y, Guilbert LJ, Davidge ST. Fibrocyte-Like Cells from Intrauterine Growth Restriction Placentas Have a Reduced Ability to Stimulate Angiogenesis. *Am J Pathol*. 2013;183(3):1025-33.
37. Reyes L, Golos TG. Hofbauer Cells: Their Role in Healthy and Complicated Pregnancy. *Frontiers in Immunology*. 2018;9(2628).
38. Tang M-X, Hu X-H, Liu Z-Z, Kwak-Kim J, Liao A-H. What are the roles of macrophages and monocytes in human pregnancy? *Journal of Reproductive Immunology*. 2015;112:73-80.
39. Mills C. M1 and M2 Macrophages: Oracles of Health and Disease. 2012;32(6):463-88.
40. Burton GJ, Woods AW, Jauniaux E, Kingdom JCP. Rheological and Physiological Consequences of Conversion of the Maternal Spiral Arteries for Uteroplacental Blood Flow during Human Pregnancy. *Placenta*. 2009;30(6):473-82.
41. Wakeland AK, Soncin F, Moretto-Zita M, Chang C-W, Horii M, Pizzo D, et al. Hypoxia directs human extravillous trophoblast differentiation in a hypoxia-inducible factor-dependent manner. *Am J Pathol*. 2017;187(4):767-80.
42. Haider S, Meinhardt G, Saleh L, Fiala C, Pollheimer J, Knöfler M. Notch1 controls development of the extravillous trophoblast lineage in the human placenta. *Proceedings of the National Academy of Sciences*. 2016;113(48):E7710-E9.
43. E. Davies J, Pollheimer J, Yong HEJ, Kokkinos MI, Kalionis B, Knöfler M, et al. Epithelial-mesenchymal transition during extravillous trophoblast differentiation. *Cell Adhesion & Migration*. 2016;10(3):310-21.

44. Zhou Y, Fisher SJ, Janatpour M, Genbacev O, Dejana E, Wheelock M, et al. Human cytotrophoblasts adopt a vascular phenotype as they differentiate. A strategy for successful endovascular invasion? *The Journal of clinical investigation*. 1997;99(9):2139-51.
45. Meinhardt G, Haider S, Haslinger P, Proestling K, Fiala C, Pollheimer J, et al. Wnt-dependent T-cell factor-4 controls human extravillous trophoblast motility. *Endocrinology*. 2014;155(5):1908-20.
46. Singh AT, Dharmarajan A, Aye IL, Keelan JA. Sphingosine-sphingosine-1-phosphate pathway regulates trophoblast differentiation and syncytialization. *Reprod Biomed Online*. 2012;24(2):224-34.
47. Coan PM, Angiolini E, Sandovici I, Burton GJ, Constância M, Fowden AL. Adaptations in placental nutrient transfer capacity to meet fetal growth demands depend on placental size in mice. *The Journal of Physiology*. 2008;586(Pt 18):4567-76.
48. Hahn T, Hahn D, Blaschitz A, Korgun ET, Desoye G, Dohr G. Hyperglycaemia-induced subcellular redistribution of GLUT1 glucose transporters in cultured human term placental trophoblast cells. *Diabetologia*. 2000;43(2):173-80.
49. Handwerger S, Freemark M. The roles of placental growth hormone and placental lactogen in the regulation of human fetal growth and development. *Journal of Pediatric Endocrinology and Metabolism*. 2000;13(4):343-56.
50. Handschuh K, Guibourdenche J, Tsatsaris V, Guesnon M, Laurendeau I, Evain-Brion D, et al. Human chorionic gonadotropin produced by the invasive trophoblast but not the villous trophoblast promotes cell invasion and is down-regulated by peroxisome proliferator-activated receptor- γ . *Endocrinology*. 2007;148(10):5011-9.

51. Evans J, Salamonsen LA, Menkhorst E, Dimitriadis E. Dynamic changes in hyperglycosylated human chorionic gonadotrophin throughout the first trimester of pregnancy and its role in early placentation. *Human Reproduction*. 2015;30(5):1029-38.
52. Keikkala E, Vuorela P, Laivuori H, Romppanen J, Heinonen S, Stenman U-H. First trimester hyperglycosylated human chorionic gonadotrophin in serum—a marker of early-onset preeclampsia. *Placenta*. 2013;34(11):1059-65.
53. Berndt S, Blacher S, Munaut C, Detilleux J, d'Hauterive SP, Huhtaniemi I, et al. Hyperglycosylated human chorionic gonadotropin stimulates angiogenesis through TGF- β receptor activation. *The FASEB Journal*. 2013;27(4):1309-21.
54. Kalkunte S, Navers T, Norris W, Banerjee P, Fazleabas A, Kuhn C, editors. Presence of non-functional hCG in preeclampsia and rescue of normal pregnancy by recombinant hCG. *Placenta*; 2010: WB SAUNDERS CO LTD 32 JAMESTOWN RD, LONDON NW1 7BY, ENGLAND.
55. Nwabuobi C, Arlier S, Schatz F, Guzeloglu-Kayisli O, Lockwood CJ, Kayisli UA. hCG: Biological Functions and Clinical Applications. *Int J Mol Sci*. 2017;18(10):2037.
56. Ambrus G, Rao CV. Novel regulation of pregnant human myometrial smooth muscle cell gap junctions by human chorionic gonadotropin. *Endocrinology*. 1994;135(6):2772-9.
57. Handwerger S, Brar A, editors. Placental lactogen, placental growth hormone, and decidual prolactin. *Seminars in reproductive endocrinology*; 1992: Copyright© 1992 by Thieme Medical Publishers, Inc.
58. Maltepe E, Penn AA. 5 - Development, Function, and Pathology of the Placenta. In: Gleason CA, Juul SE, editors. *Avery's Diseases of the Newborn (Tenth Edition)*. Philadelphia: Elsevier; 2018. p. 40-60.e8.

59. Hoshina M, Boothby M, Boime I. Cytological localization of chorionic gonadotropin alpha and placental lactogen mRNAs during development of the human placenta. *The Journal of cell biology*. 1982;93(1):190-8.
60. Eberhardt NL, Jiang S-W, Shepard AR, Arnold AM, Trujillo MA. Hormonal and cell-specific regulation of the human growth hormone and chorionic somatomammotropin genes. *Progress in nucleic acid research and molecular biology*. 1996;54:127-63.
61. Simpson RA, Mayhew TM, Barnes PR. From 13 weeks to term, the trophoblast of human placenta grows by the continuous recruitment of new proliferative units: A study of nuclear number using the disector. *Placenta*. 1992;13(5):501-12.
62. Baczyk D, Drewlo S, Proctor L, Dunk C, Lye S, Kingdom J. Glial cell missing-1 transcription factor is required for the differentiation of the human trophoblast. *Cell Death & Differentiation*. 2009;16(5):719-27.
63. Lin C, Lin M, Chen H. Biochemical characterization of the human placental transcription factor GCMA/1. *Biochemistry and cell biology*. 2005;83(2):188-95.
64. Lu X, Wang R, Zhu C, Wang H, Lin H-Y, Gu Y, et al. Fine-Tuned and Cell-Cycle-Restricted Expression of Fusogenic Protein Syncytin-2 Maintains Functional Placental Syncytia. *Cell Reports*. 2017;21(5):1150-9.
65. Roland CS, Hu J, Ren CE, Chen H, Li J, Varvoutis MS, et al. Morphological changes of placental syncytium and their implications for the pathogenesis of preeclampsia. *Cell Mol Life Sci*. 2016;73(2):365-76.
66. Knerr I, Schnare M, Hermann K, Kausler S, Lehner M, Vogler T, et al. Fusogenic endogenous-retroviral syncytin-1 exerts anti-apoptotic functions in staurosporine-challenged CHO cells. *Apoptosis*. 2006;12(1):37.

67. Mayhew TM. Turnover of human villous trophoblast in normal pregnancy: What do we know and what do we need to know? *Placenta*. 2014;35(4):229-40.
68. Huang Q, Chen H, Wang F, Brost BC, Li J, Gao Y, et al. Reduced syncytin-1 expression in choriocarcinoma BeWo cells activates the calpain1–AIF-mediated apoptosis, implication for preeclampsia. *Cellular and molecular life sciences*. 2014;71(16):3151-64.
69. Tong M, Chen Q, James JL, Stone PR, Chamley LW. Micro- and Nano-vesicles from First Trimester Human Placentae Carry Flt-1 and Levels Are Increased in Severe Preeclampsia. *Front Endocrinol (Lausanne)*. 2017;8.
70. Zhang J, Li H, Fan B, Xu W, Zhang X. Extracellular vesicles in normal pregnancy and pregnancy-related diseases. *Journal of Cellular and Molecular Medicine*. 2020;24(8):4377-88.
71. Rajakumar A, Cerdeira AS, Rana S, Zsengeller Z, Edmunds L, Jeyabalan A, et al. Transcriptionally Active Syncytial Aggregates in the Maternal Circulation May Contribute to Circulating Soluble Fms-Like Tyrosine Kinase 1 in Preeclampsia. *Hypertension*. 2012;59(2):256-64.
72. Ermini L, Ausman J, Melland-Smith M, Yeganeh B, Rolfo A, Litvack ML, et al. A Single Sphingomyelin Species Promotes Exosomal Release of Endoglin into the Maternal Circulation in Preeclampsia. *Scientific reports*. 2017;7(1):12172.
73. Lunell NO, Nylund LE, Lewander R, Sarby B, Thornström S. Uteroplacental Blood Flow in Pre-Eclampsia Measurements with Indium-113M and a Computer-Linked Gamma Camera. *Clinical and Experimental Hypertension Part B: Hypertension in Pregnancy*. 1982;1(1):105-17.
74. Alexander BT, Kassab SE, Miller MT, Abram SR, Reckelhoff JF, Bennett WA, et al. Reduced Uterine Perfusion Pressure During Pregnancy in the Rat Is Associated With Increases in Arterial Pressure and Changes in Renal Nitric Oxide. *Hypertension*. 2001;37(4):1191-5.

75. Veron D, Villegas G, Aggarwal PK, Bertuccio C, Jimenez J, Velazquez H, et al. Acute podocyte vascular endothelial growth factor (VEGF-A) knockdown disrupts α V β 3 integrin signaling in the glomerulus. *PLoS One*. 2012;7(7):e40589.
76. Bertuccio C, Veron D, Aggarwal PK, Holzman L, Tufro A. Vascular endothelial growth factor receptor 2 direct interaction with nephrin links VEGF-A signals to actin in kidney podocytes. *Journal of Biological Chemistry*. 2011;286(46):39933-44.
77. Maglione D, Guerriero V, Viglietto G, Delli-Bovi P, Persico MG. Isolation of a human placenta cDNA coding for a protein related to the vascular permeability factor. *Proceedings of the National Academy of Sciences*. 1991;88(20):9267-71.
78. Staff AC, Benton SJ, von Dadelszen P, Roberts JM, Taylor RN, Powers RW, et al. Redefining preeclampsia using placenta-derived biomarkers. *Hypertension*. 2013;61(5):932-42.
79. De Falco S. The discovery of placenta growth factor and its biological activity. *Experimental & molecular medicine*. 2012;44(1):1-9.
80. Kim SK, Henen MA, Hinck AP. Structural biology of betaglycan and endoglin, membrane-bound co-receptors of the TGF-beta family. *Experimental Biology and Medicine*. 2019;244(17):1547-58.
81. Venkatesha S, Toporsian M, Lam C, Hanai J-i, Mammoto T, Kim YM, et al. Soluble endoglin contributes to the pathogenesis of preeclampsia. *Nature medicine*. 2006;12(6):642-9.
82. Park Hh, Lee S, Yu Y, Yoo SM, Baek SY, Jung N, et al. TGF- β secreted by human umbilical cord blood-derived mesenchymal stem cells ameliorates atopic dermatitis by inhibiting secretion of TNF- α and IgE. *Stem Cells*. 2020;38(7):904-16.
83. Armaly Z, Jadaon JE, Jabbour A, Abassi ZA. Preeclampsia: Novel Mechanisms and Potential Therapeutic Approaches. *Frontiers in Physiology*. 2018;9.

84. Burke SD, Zsengellér ZK, Khankin EV, Lo AS, Rajakumar A, DuPont JJ, et al. Soluble fms-like tyrosine kinase 1 promotes angiotensin II sensitivity in preeclampsia. *The Journal of clinical investigation*. 2016;126(7):2561-74.
85. Ahmad S, Ahmed A. Elevated placental soluble vascular endothelial growth factor receptor-1 inhibits angiogenesis in preeclampsia. *Circulation research*. 2004;95(9):884-91.
86. Cindrova-Davies T, Sanders DA, Burton GJ, Charnock-Jones DS. Soluble FLT1 sensitizes endothelial cells to inflammatory cytokines by antagonizing VEGF receptor-mediated signalling. *Cardiovascular research*. 2011;89(3):671-9.
87. Llurba E, Crispi F, Verlohren S. Update on the pathophysiological implications and clinical role of angiogenic factors in pregnancy. *Fetal diagnosis and therapy*. 2015;37(2):81-92.
88. Ahmed A. New insights into the etiology of preeclampsia: identification of key elusive factors for the vascular complications. *Thrombosis research*. 2011;127:S72-S5.
89. Matsubara S, Bourdeau A, terBrugge KG, Wallace C, Letarte M. Analysis of endoglin expression in normal brain tissue and in cerebral arteriovenous malformations. *Stroke*. 2000;31(11):2653-60.
90. Wegmann TG, Lin H, Guilbert L, Mosmann TR. Bidirectional cytokine interactions in the maternal-fetal relationship: is successful pregnancy a TH2 phenomenon? *Immunology Today*. 1993;14(7):353-6.
91. Racicot K, Kwon J-Y, Aldo P, Silasi M, Mor G. Understanding the Complexity of the Immune System during Pregnancy. *American Journal of Reproductive Immunology*. 2014;72(2):107-16.

92. Shimada S, Nishida R, Takeda M, Iwabuchi K, Kishi R, Onoé K, et al. Natural killer, natural killer T, helper and cytotoxic T cells in the decidua from sporadic miscarriage. *American Journal of Reproductive Immunology*. 2006;56(3):193-200.
93. Ashkar AA, Di Santo JP, Croy BA. Interferon γ contributes to initiation of uterine vascular modification, decidual integrity, and uterine natural killer cell maturation during normal murine pregnancy. *The Journal of experimental medicine*. 2000;192(2):259-70.
94. Manaster I, Mandelboim O. The unique properties of uterine NK cells. *American journal of reproductive immunology*. 2010;63(6):434-44.
95. Burke SD, Barrette VF, Gravel J, Carter AL, Hatta K, Zhang J, et al. Uterine NK cells, spiral artery modification and the regulation of blood pressure during mouse pregnancy. *American journal of reproductive immunology*. 2010;63(6):472-81.
96. Mor G. Inflammation and pregnancy: the role of toll-like receptors in trophoblast-immune interaction. *Ann N Y Acad Sci*. 2008;1127(1):121-8.
97. Sargent IL, Germain SJ, Sacks GP, Kumar S, Redman CW. Trophoblast deportation and the maternal inflammatory response in pre-eclampsia. *J Reprod Immunol*. 2003;59(2):153-60.
98. Abell SK, De Courten B, Boyle JA, Teede HJ. Inflammatory and Other Biomarkers: Role in Pathophysiology and Prediction of Gestational Diabetes Mellitus. *Int J Mol Sci*. 2015;16(6):13442-73.
99. Harmon AC, Cornelius DC, Amaral LM, Faulkner JL, Cunningham MW, Jr., Wallace K, et al. The role of inflammation in the pathology of preeclampsia. *Clin Sci (Lond)*. 2016;130(6):409-19.

100. Bartha JL, Romero-Carmona R, Comino-Delgado R. Inflammatory cytokines in intrauterine growth retardation. *Acta Obstetrica et Gynecologica Scandinavica*. 2003;82(12):1099-102.
101. Redman CW, Sacks GP, Sargent IL. Preeclampsia: an excessive maternal inflammatory response to pregnancy. *Am J Obstet Gynecol*. 1999;180(2 Pt 1):499-506.
102. Raghupathy R, Al-Azemi M, Azizieh F. Intrauterine growth restriction: cytokine profiles of trophoblast antigen-stimulated maternal lymphocytes. *Clin Dev Immunol*. 2012;2012:734865-.
103. Fasshauer M, Blüher M, Stumvoll M. Adipokines in gestational diabetes. *Lancet Diabetes Endocrinol*. 2014;2(6):488-99.
104. Atègbo JM, Grissa O, Yessoufou A, Hichami A, Dramane KL, Moutairou K, et al. Modulation of adipokines and cytokines in gestational diabetes and macrosomia. *J Clin Endocrinol Metab*. 2006;91(10):4137-43.
105. Cornelius DC. Preeclampsia: from inflammation to immunoregulation. *Clinical medicine insights: Blood disorders*. 2018;11:1179545X17752325.
106. Roth I, Corry DB, Locksley RM, Abrams JS, Litton MJ, Fisher SJ. Human placental cytotrophoblasts produce the immunosuppressive cytokine interleukin 10. *The Journal of experimental medicine*. 1996;184(2):539-48.
107. Szarka A, Rigó J, Lázár L, Bekő G, Molvarec A. Circulating cytokines, chemokines and adhesion molecules in normal pregnancy and preeclampsia determined by multiplex suspension array. *BMC immunology*. 2010;11(1):1-9.
108. Michalczyk M, Celewicz A, Celewicz M, Woźniakowska-Gondek P, Rzepka R. The role of inflammation in the pathogenesis of preeclampsia. *Mediators of Inflammation*. 2020;2020.

109. Schaarschmidt W, Rana S, Stepan H. The course of angiogenic factors in early- vs. late-onset preeclampsia and HELLP syndrome. *Journal of perinatal medicine*. 2013;41(5):511-6.
110. Askelund K, Chamley L. Trophoblast deportation part I: review of the evidence demonstrating trophoblast shedding and deportation during human pregnancy. *Placenta*. 2011;32(10):716-23.
111. Visser N, van Rijn BB, Rijkers GT, Franx A, Bruinse HW. Inflammatory Changes in Preeclampsia: Current Understanding of the Maternal Innate and Adaptive Immune Response. *Obstetrical & Gynecological Survey*. 2007;62(3).
112. Southcombe J, Tannetta D, Redman C, Sargent I. The immunomodulatory role of syncytiotrophoblast microvesicles. *PLoS One*. 2011;6(5):e20245.
113. Harmon A, Cornelius D, Amaral L, Paige A, Herse F, Ibrahim T, et al. IL-10 supplementation increases Tregs and decreases hypertension in the RUPP rat model of preeclampsia. *Hypertension in pregnancy*. 2015;34(3):291-306.
114. Azizieh F, Raghupathy R, Makhseed Ma. Maternal Cytokine Production Patterns in Women with Pre-eclampsia. *American Journal of Reproductive Immunology*. 2005;54(1):30-7.
115. Darmochwal-Kolarz D, Rolinski J, Leszczynska-Gorzela B, Oleszczuk J. The Expressions of Intracellular Cytokines in the Lymphocytes of Preeclamptic Patients. *American Journal of Reproductive Immunology*. 2002;48(6):381-6.
116. Darmochwal-Kolarz D, Leszczynska-Gorzela B, Rolinski J, Oleszczuk J. T helper 1- and T helper 2-type cytokine imbalance in pregnant women with pre-eclampsia. *European Journal of Obstetrics & Gynecology and Reproductive Biology*. 1999;86(2):165-70.
117. Jonsson Y, Matthiesen L, Berg G, Ernerudh J, Nieminen K, Ekerfelt C. Indications of an altered immune balance in preeclampsia: A decrease in in vitro secretion of IL-5 and IL-10 from

blood mononuclear cells and in blood basophil counts compared with normal pregnancy. *Journal of Reproductive Immunology*. 2005;66(1):69-84.

118. Xu J, Gu Y, Sun J, Zhu H, Lewis DF, Wang Y. Reduced CD200 expression is associated with altered Th1/Th2 cytokine production in placental trophoblasts from preeclampsia. *American Journal of Reproductive Immunology*. 2018;79(1):e12763.

119. Peixoto AB, Araujo Júnior E, Ribeiro JU, Rodrigues DBR, Castro ECC, Caldas TMRC, et al. Evaluation of inflammatory mediators in the deciduas of pregnant women with pre-eclampsia/eclampsia. *The Journal of Maternal-Fetal & Neonatal Medicine*. 2016;29(1):75-9.

120. Sato Y. Endovascular trophoblast and spiral artery remodeling. *Molecular and Cellular Endocrinology*. 2020;503:110699.

121. Khong TY, De Wolf F, Robertson WB, Brosens I. Inadequate maternal vascular response to placentation in pregnancies complicated by pre-eclampsia and by small-for-gestational age infants. *Br J Obstet Gynaecol*. 1986;93(10):1049-59.

122. Brosens IA, Robertson WB, Dixon HG. The role of the spiral arteries in the pathogenesis of pre-eclampsia. *J Pathol*. 1970;101(4):Pvi.

123. Kaufmann P, Black S, Huppertz B. Endovascular Trophoblast Invasion: Implications for the Pathogenesis of Intrauterine Growth Retardation and Preeclampsia. *Biology of reproduction*. 2003;69(1):1-7.

124. Ishihara N, Matsuo H, Murakoshi H, Laoag-Fernandez JB, Samoto T, Maruo T. Increased apoptosis in the syncytiotrophoblast in human term placentas complicated by either preeclampsia or intrauterine growth retardation. *American Journal of Obstetrics & Gynecology*. 2002;186(1):158-66.

125. Oh S-Y, Choi S-J, Kyung Hee K, Cho E, Kim J-H, Roh C-R. Autophagy-Related Proteins, LC3 and Beclin-1, in Placentas From Pregnancies Complicated by Preeclampsia. *Reproductive Sciences*. 2008;15(9):912-20.
126. Arnholdt H, Meisel F, Fandrey K, Löhrs U. Proliferation of villous trophoblast of the human placenta in normal and abnormal pregnancies. *Virchows Archiv B*. 1991;60(1):365-72.
127. Redline RW, Patterson P. Pre-eclampsia is associated with an excess of proliferative immature intermediate trophoblast. *Hum Pathol*. 1995;26(6):594-600.
128. Lee X, Keith JC, Stumm N, Moutsatsos I, McCoy JM, Crum CP, et al. Downregulation of Placental Syncytin Expression and Abnormal Protein Localization in Pre-eclampsia. *Placenta*. 2001;22(10):808-12.
129. Chiang M-H, Liang F-Y, Chen C-P, Chang C-W, Cheong M-L, Wang L-J, et al. Mechanism of Hypoxia-induced GCM1 Degradation: IMPLICATIONS FOR THE PATHOGENESIS OF PREECLAMPSIA. *Journal of Biological Chemistry*. 2009;284(26):17411-9.
130. Gao Y, He Z, Wang Z, Luo Y, Sun H, Zhou Y, et al. Increased Expression and Altered Methylation of HERVWE1 in the Human Placentas of Smaller Fetuses from Monozygotic, Dichorionic, Discordant Twins. *PLoS One*. 2012;7(3):e33503.
131. Ruebner M, Strissel PL, Ekici AB, Stiegler E, Dammer U, Goecke TW, et al. Reduced Syncytin-1 Expression Levels in Placental Syndromes Correlates with Epigenetic Hypermethylation of the ERVW-1 Promoter Region. *PLoS One*. 2013;8(2):e56145.
132. Farah O, Nguyen C, Tekkatte C, Parast MM. Trophoblast lineage-specific differentiation and associated alterations in preeclampsia and fetal growth restriction. *Placenta*. 2020;102:4-9.

133. van der Post JA, Lok CA, Boer K, Sturk A, Sargent IL, Nieuwland R. The functions of microparticles in pre-eclampsia. *Semin Thromb Hemost.* 2011;37(2):146-52.
134. Zeldovich VB, Robbins JR, Kapidzic M, Lauer P, Bakardjiev AI. Invasive Extravillous Trophoblasts Restrict Intracellular Growth and Spread of *Listeria monocytogenes*. *PLOS Pathogens.* 2011;7(3):e1002005.
135. Shaarawy M, Nagui AR. Enhanced expression of cytokines may play a fundamental role in the mechanisms of immunologically mediated recurrent spontaneous abortion. *Acta obstetrica et gynecologica Scandinavica.* 1997;76(3):205-11.
136. Christiaens I, Zaragoza DB, Guilbert L, Robertson SA, Mitchell BF, Olson DM. Inflammatory processes in preterm and term parturition. *Journal of reproductive immunology.* 2008;79(1):50-7.
137. Alijotas-Reig J, Esteve-Valverde E, Ferrer-Oliveras R, Llurba E, Gris JM. Tumor Necrosis Factor-Alpha and Pregnancy: Focus on Biologics. An Updated and Comprehensive Review. *Clinical Reviews in Allergy & Immunology.* 2017;53(1):40-53.
138. Sunderland NS, Thomson SE, Heffernan SJ, Lim S, Thompson J, Ogle R, et al. Tumor necrosis factor alpha induces a model of preeclampsia in pregnant baboons (*Papio hamadryas*). *Cytokine.* 2011;56(2):192-9.
139. Leisser C, Saleh L, Haider S, Husslein H, Sonderegger S, Knöfler M. Tumour necrosis factor-alpha impairs chorionic gonadotrophin beta-subunit expression and cell fusion of human villous cytotrophoblast. *Mol Hum Reprod.* 2006;12(10):601-9.
140. Siwetz M, Blaschitz A, El-Heliebi A, Hiden U, Desoye G, Huppertz B, et al. TNF- α alters the inflammatory secretion profile of human first trimester placenta. *Laboratory Investigation.* 2016;96(4):428-38.

141. Jonsson Y, Rubèr M, Matthiesen L, Berg G, Nieminen K, Sharma S, et al. Cytokine mapping of sera from women with preeclampsia and normal pregnancies. *Journal of reproductive immunology*. 2006;70(1-2):83-91.
142. Peraçoli JC, Rudge MVC, Peraçoli MTS. Tumor necrosis factor-alpha in gestation and puerperium of women with gestational hypertension and pre-eclampsia. *American Journal of Reproductive Immunology*. 2007;57(3):177-85.
143. Thathiah A, Brayman M, Dharmaraj N, Julian JJ, Lagow EL, Carson DD. Tumor necrosis factor α stimulates MUC1 synthesis and ectodomain release in a human uterine epithelial cell line. *Endocrinology*. 2004;145(9):4192-203.
144. Yamashita M, Passegué E. TNF- α coordinates hematopoietic stem cell survival and myeloid regeneration. *Cell stem cell*. 2019;25(3):357-72. e7.
145. Annibaldi A, Meier P. Checkpoints in TNF-induced cell death: implications in inflammation and cancer. *Trends in molecular medicine*. 2018;24(1):49-65.
146. Lankford KL, Arroyo EJ, Kocsis JD. Chronic TNF α Exposure Induces Robust Proliferation of Olfactory Ensheathing Cells, but not Schwann Cells. *Neurochemical research*. 2017;42(9):2595-609.
147. Peng WC, Logan CY, Fish M, Anbarchian T, Aguisanda F, Álvarez-Varela A, et al. Inflammatory cytokine TNF α promotes the long-term expansion of primary hepatocytes in 3D culture. *Cell*. 2018;175(6):1607-19. e15.
148. Jiang Y, Zhou J, Zhao J, Hou D, Zhang H, Li L, et al. MiR-18a-downregulated RORA inhibits the proliferation and tumorigenesis of glioma using the TNF- α -mediated NF- κ B signaling pathway. *EBioMedicine*. 2020;52:102651.

149. Li X, Ren G, Cai C, Yang X, Nie L, Jing X, et al. TNF- α regulates the osteogenic differentiation of bone morphogenetic factor 9 adenovirus-transduced rat follicle stem cells via Wnt signaling. *Molecular Medicine Reports*. 2020;22(4):3141-50.
150. Sade-Feldman M, Kanterman J, Ish-Shalom E, Elnekave M, Horwitz E, Baniyash M. Tumor necrosis factor- α blocks differentiation and enhances suppressive activity of immature myeloid cells during chronic inflammation. *Immunity*. 2013;38(3):541-54.
151. Wang L, Du F, Wang X. TNF-alpha Induces Two Distinct Caspase-8 Activation Pathways. *Cell*. 2008;133(4):693-703.
152. Romanowska-Próchnicka K, Felis-Giemza A, Olesińska M, Wojdasiewicz P, Paradowska-Gorycka A, Szukiewicz D. The Role of TNF- α and Anti-TNF- α Agents during Preconception, Pregnancy, and Breastfeeding. *Int J Mol Sci*. 2021;22(6).
153. Black RA, Rauch CT, Kozlosky CJ, Peschon JJ, Slack JL, Wolfson MF, et al. A metalloproteinase disintegrin that releases tumour-necrosis factor- α from cells. *Nature*. 1997;385(6618):729-33.
154. Perez C, Albert I, DeFay K, Zachariades N, Gooding L, Kriegler M. A nonsecretable cell surface mutant of tumor necrosis factor (TNF) kills by cell-to-cell contact. *Cell*. 1990;63(2):251-8.
155. Grell M, Douni E, Wajant H, Löhden M, Clauss M, Maxeiner B, et al. The transmembrane form of tumor necrosis factor is the prime activating ligand of the 80 kDa tumor necrosis factor receptor. *Cell*. 1995;83(5):793-802.
156. Tartaglia LA, Pennica D, Goeddel DV. Ligand passing: the 75-kDa tumor necrosis factor (TNF) receptor recruits TNF for signaling by the 55-kDa TNF receptor. *Journal of Biological Chemistry*. 1993;268(25):18542-8.

157. Van Zee KJ, Kohno T, Fischer E, Rock CS, Moldawer LL, Lowry SF. Tumor necrosis factor soluble receptors circulate during experimental and clinical inflammation and can protect against excessive tumor necrosis factor alpha in vitro and in vivo. *Proc Natl Acad Sci U S A*. 1992;89(11):4845-9.
158. Jiang Y, Woronicz JD, Liu W, Goeddel DV. Prevention of Constitutive TNF Receptor 1 Signaling by Silencer of Death Domains. *Science*. 1999;283(5401):543.
159. Hsu H, Shu H-B, Pan M-G, Goeddel DV. TRADD-TRAF2 and TRADD-FADD Interactions Define Two Distinct TNF Receptor 1 Signal Transduction Pathways. *Cell*. 1996;84(2):299-308.
160. Tobiume K, Matsuzawa A, Takahashi T, Nishitoh H, Morita K, Takeda K, et al. ASK1 is required for sustained activations of JNK/p38 MAP kinases and apoptosis. *EMBO Rep*. 2001;2(3):222-8.
161. Rivas MA, Carnevale RP, Proietti CJ, Rosemblit C, Beguelin W, Salatino M, et al. TNF α acting on TNFR1 promotes breast cancer growth via p42/P44 MAPK, JNK, Akt and NF- κ B-dependent pathways. *Experimental Cell Research*. 2008;314(3):509-29.
162. Spiegel S, Milstien S. The outs and the ins of sphingosine-1-phosphate in immunity. *Nat Rev Immunol*. 2011;11(6):403-15.
163. Yelavarthi KK, Hunt JS. Analysis of p60 and p80 tumor necrosis factor-alpha receptor messenger RNA and protein in human placentas. *Am J Pathol*. 1993;143(4):1131-41.
164. Hoeflerlin LA, Wijesinghe DS, Chalfant CE. The role of ceramide-1-phosphate in biological functions. *Handb Exp Pharmacol*. 2013(215):153-66.
165. Hannun YA, Obeid LM. Many ceramides. *J Biol Chem*. 2011;286(32):27855-62.

166. Espaillat MP, Kew RR, Obeid LM. Sphingolipids in neutrophil function and inflammatory responses: Mechanisms and implications for intestinal immunity and inflammation in ulcerative colitis. *Adv Biol Regul.* 2017;63:140-55.
167. Pettus BJ, Chalfant CE, Hannun YA. Ceramide in apoptosis: an overview and current perspectives. *Biochimica et Biophysica Acta (BBA) - Molecular and Cell Biology of Lipids.* 2002;1585(2):114-25.
168. Perry DK, Hannun YA. The role of ceramide in cell signaling. *Biochimica et biophysica acta.* 1998;1436(1-2):233-43.
169. Jiang X-C, Li Z, Yazdanyar A. Chapter 6 - Sphingolipids and HDL Metabolism. In: Komoda T, editor. *The HDL Handbook (Second Edition)*. Boston: Academic Press; 2014. p. 133-58.
170. Dobierzewska A, Soman S, Illanes SE, Morris AJ. Plasma cross-gestational sphingolipidomic analyses reveal potential first trimester biomarkers of preeclampsia. *PLoS One.* 2017;12(4):e0175118-e.
171. Romanowicz L, Bańkowski E. Preeclampsia-associated alterations in sphingolipid composition of the umbilical cord artery. *Clin Biochem.* 2009;42(16-17):1719-24.
172. Del Gaudio I, Sasset L, Lorenzo AD, Wadsack C. Sphingolipid Signature of Human Feto-Placental Vasculature in Preeclampsia. *Int J Mol Sci.* 2020;21(3):1019.
173. Baig S, Lim JY, Fernandis AZ, Wenk MR, Kale A, Su LL, et al. Lipidomic analysis of human placental Syncytiotrophoblast microvesicles in adverse pregnancy outcomes. *Placenta.* 2013;34(5):436-42.
174. Rodríguez-Sureda V, Crovetto F, Triunfo S, Sánchez O, Crispi F, Llurba E, et al. Increased secretory sphingomyelinase activity in the first trimester of pregnancy in women later

- developing preeclampsia: a nested case-control study. *Biological Chemistry*. 2016;397(3):269-79.
175. Melland-Smith M, Ermini L, Chauvin S, Craig-Barnes H, Tagliaferro A, Todros T, et al. Disruption of sphingolipid metabolism augments ceramide-induced autophagy in preeclampsia. *Autophagy*. 2015;11(4):653-69.
176. Charkiewicz K, Goscik J, Blachnio-Zabielska A, Raba G, Sakowicz A, Kalinka J, et al. Sphingolipids as a new factor in the pathomechanism of preeclampsia - Mass spectrometry analysis. *PLoS One*. 2017;12(5):e0177601.
177. Amraoui F, Hassani Lahsinoui H, Spijkers LJA, Vogt L, Peters SLM, Wijesinghe DS, et al. Plasma ceramide is increased and associated with proteinuria in women with pre-eclampsia and HELLP syndrome. *Pregnancy Hypertens*. 2020;19:100-5.
178. Xu R, Antwi Boasiako P, Mao C. Alkaline ceramidase family: The first two decades. *Cellular Signalling*. 2021;78:109860.
179. Xu R, Wang K, Mileva I, Hannun YA, Obeid LM, Mao C. Alkaline ceramidase 2 and its bioactive product sphingosine are novel regulators of the DNA damage response. *Oncotarget*. 2016;7(14).
180. Li F, Xu R, Lin C-L, Low BE, Cai L, Li S, et al. Maternal and fetal alkaline ceramidase 2 is required for placental vascular integrity in mice. *The FASEB Journal*. 2020;34(11):15252-68.
181. Mao C, Xu R, Szulc ZM, Bielawska A, Galadari SH, Obeid LM. Cloning and Characterization of a Novel Human Alkaline Ceramidase: A Mammalian Enzyme That Hydrolyzes Phytoceramide*. *Journal of Biological Chemistry*. 2001;276(28):26577-88.

182. Hannun YA, Loomis CR, Merrill AH, Bell RM. Sphingosine inhibition of protein kinase C activity and of phorbol dibutyrate binding in vitro and in human platelets. *Journal of Biological Chemistry*. 1986;261(27):12604-9.
183. Yang L, Yatomi Y, Miura Y, Satoh K, Ozaki Y. Metabolism and functional effects of sphingolipids in blood cells. *Br J Haematol*. 1999;107(2):282-93.
184. Hänel P, Andréani P, Gräler MH. Erythrocytes store and release sphingosine 1-phosphate in blood. *Faseb j*. 2007;21(4):1202-9.
185. Ito K, Anada Y, Tani M, Ikeda M, Sano T, Kihara A, et al. Lack of sphingosine 1-phosphate-degrading enzymes in erythrocytes. *Biochem Biophys Res Commun*. 2007;357(1):212-7.
186. Bode C, Sensken SC, Peest U, Beutel G, Thol F, Levkau B, et al. Erythrocytes serve as a reservoir for cellular and extracellular sphingosine 1-phosphate. *J Cell Biochem*. 2010;109(6):1232-43.
187. Yatomi Y, Igarashi Y, Yang L, Hisano N, Qi R, Asazuma N, et al. Sphingosine 1-phosphate, a bioactive sphingolipid abundantly stored in platelets, is a normal constituent of human plasma and serum. *J Biochem*. 1997;121(5):969-73.
188. Pappu R, Schwab SR, Cornelissen I, Pereira JP, Regard JB, Xu Y, et al. Promotion of Lymphocyte Egress into Blood and Lymph by Distinct Sources of Sphingosine-1-Phosphate. *Science*. 2007;316(5822):295.
189. Yatomi Y, Ruan F, Hakomori S, Igarashi Y. Sphingosine-1-phosphate: a platelet-activating sphingolipid released from agonist-stimulated human platelets. *Blood*. 1995;86(1):193-202.

190. Hammad SM, Pierce JS, Soodavar F, Smith KJ, Al Gadban MM, Rembiesa B, et al. Blood sphingolipidomics in healthy humans: impact of sample collection methodology. *J Lipid Res.* 2010;51(10):3074-87.
191. Andréani P, Gräler MH. Comparative quantification of sphingolipids and analogs in biological samples by high-performance liquid chromatography after chloroform extraction. *Anal Biochem.* 2006;358(2):239-46.
192. Sattler KJ, Elbasan S, Keul P, Elter-Schulz M, Bode C, Gräler MH, et al. Sphingosine 1-phosphate levels in plasma and HDL are altered in coronary artery disease. *Basic Res Cardiol.* 2010;105(6):821-32.
193. Knapp P, Baranowski M, Knapp M, Zabielski P, Błachnio-Zabielska AU, Górski J. Altered sphingolipid metabolism in human endometrial cancer. *Prostaglandins Other Lipid Mediat.* 2010;92(1-4):62-6.
194. Knapp M, Baranowski M, Lisowska A, Musiał W. Decreased free sphingoid base concentration in the plasma of patients with chronic systolic heart failure. *Adv Med Sci.* 2012;57(1):100-5.
195. Knapp M, Lisowska A, Zabielski P, Musiał W, Baranowski M. Sustained decrease in plasma sphingosine-1-phosphate concentration and its accumulation in blood cells in acute myocardial infarction. *Prostaglandins Other Lipid Mediat.* 2013;106:53-61.
196. Knapp M, Lisowska A, Knapp P, Baranowski M. Dose-dependent effect of aspirin on the level of sphingolipids in human blood. *Adv Med Sci.* 2013;58(2):274-81.
197. Baranowski M, Charmas M, Długolecka B, Górski J. Exercise increases plasma levels of sphingoid base-1 phosphates in humans. *Acta Physiol (Oxf).* 2011;203(3):373-80.

198. Baranowski M, Górski J, Klapcinska B, Waskiewicz Z, Sadowska-Krepa E. Ultramarathon run markedly reduces plasma sphingosine-1-phosphate concentration. *Int J Sport Nutr Exerc Metab.* 2014;24(2):148-56.
199. Karuna R, Park R, Othman A, Holleboom AG, Motazacker MM, Sutter I, et al. Plasma levels of sphingosine-1-phosphate and apolipoprotein M in patients with monogenic disorders of HDL metabolism. *Atherosclerosis.* 2011;219(2):855-63.
200. Hammad SM, Al Gadban MM, Semler AJ, Klein RL. Sphingosine 1-phosphate distribution in human plasma: associations with lipid profiles. *J Lipids.* 2012;2012:180705.
201. Kontush A, Therond P, Zerrad A, Couturier M, Nègre-Salvayre A, De Souza JA, et al. Preferential sphingosine-1-phosphate enrichment and sphingomyelin depletion are key features of small dense HDL3 particles: Relevance to antiapoptotic and antioxidative activities. *Arteriosclerosis, Thrombosis, and Vascular Biology.* 2007;27(8):1843-9.
202. Lee MH, Hammad SM, Semler AJ, Luttrell LM, Lopes-Virella MF, Klein RL. HDL3, but not HDL2, stimulates plasminogen activator inhibitor-1 release from adipocytes: The role of sphingosine-1-phosphate. *Journal of Lipid Research.* 2010;51(9):2619-28.
203. Levkau B. HDL-S1P: cardiovascular functions, disease-associated alterations, and therapeutic applications. *Front Pharmacol.* 2015;6:243-.
204. Walsh SW, Reep DT, Alam SMK, Washington SL, Al Dulaimi M, Lee SM, et al. Placental Production of Eicosanoids and Sphingolipids in Women Who Developed Preeclampsia on Low-Dose Aspirin. *Reproductive Sciences.* 2020;27(12):2158-69.
205. Picot M, Croyal M, Duparc T, Combes G, Vayssière C, Perret B, et al. Preeclampsia is associated with changes in the composition and dysfunction of high-density lipoproteins. *Archives of Cardiovascular Diseases Supplements.* 2019;11(3, Supplement):e354.

206. Wilkerson BA, Grass GD, Wing SB, Argraves WS, Argraves KM. Sphingosine 1-phosphate (S1P) carrier-dependent regulation of endothelial barrier: high density lipoprotein (HDL)-S1P prolongs endothelial barrier enhancement as compared with albumin-S1P via effects on levels, trafficking, and signaling of S1P1. *J Biol Chem*. 2012;287(53):44645-53.
207. Adamson RH, Clark JF, Radeva M, Kheirrolomoom A, Ferrara KW, Curry FE. Albumin modulates S1P delivery from red blood cells in perfused microvessels: mechanism of the protein effect. *Am J Physiol Heart Circ Physiol*. 2014;306(7):H1011-H7.
208. Winkler MS, März KB, Nierhaus A, Daum G, Schwedhelm E, Kluge S, et al. Loss of sphingosine 1-phosphate (S1P) in septic shock is predominantly caused by decreased levels of high-density lipoproteins (HDL). *Journal of Intensive Care*. 2019;7(1):23.
209. Książek M, Chacińska M, Chabowski A, Baranowski M. Sources, metabolism, and regulation of circulating sphingosine-1-phosphate. *Journal of lipid research*. 2015;56(7):1271-81.
210. Zhao Y, Kalari SK, Usatyuk PV, Gorshkova I, He D, Watkins T, et al. Intracellular generation of sphingosine 1-phosphate in human lung endothelial cells: role of lipid phosphate phosphatase-1 and sphingosine kinase 1. *J Biol Chem*. 2007;282(19):14165-77.
211. Alvarez SE, Harikumar KB, Hait NC, Allegood J, Strub GM, Kim EY, et al. Sphingosine-1-phosphate is a missing cofactor for the E3 ubiquitin ligase TRAF2. *Nature*. 2010;465(7301):1084-8.
212. Zemann B, Urtz N, Reuschel R, Mechtcheriakova D, Bornancin F, Badegruber R, et al. Normal neutrophil functions in sphingosine kinase type 1 and 2 knockout mice. *Immunology Letters*. 2007;109(1):56-63.

213. Sukocheva O, Wadham C, Holmes A, Albanese N, Verrier E, Feng F, et al. Estrogen transactivates EGFR via the sphingosine 1-phosphate receptor Edg-3: the role of sphingosine kinase-1. *The Journal of Cell Biology*. 2006;173(2):301-10.
214. Frisz JF, Lou K, Klitzing HA, Hanafin WP, Lizunov V, Wilson RL, et al. Direct chemical evidence for sphingolipid domains in the plasma membranes of fibroblasts. *Proc Natl Acad Sci U S A*. 2013;110(8):E613-E22.
215. Sutherland CM, Moretti PAB, Hewitt NM, Bagley CJ, Vadas MA, Pitson SM. The Calmodulin-binding Site of Sphingosine Kinase and Its Role in Agonist-dependent Translocation of Sphingosine Kinase 1 to the Plasma Membrane. *Journal of Biological Chemistry*. 2006;281(17):11693-701.
216. Venkataraman K, Thangada S, Michaud J, Oo Myat L, Ai Y, Lee Y-M, et al. Extracellular export of sphingosine kinase-1a contributes to the vascular S1P gradient. *Biochemical Journal*. 2006;397(Pt 3):461-71.
217. Takabe K, Paugh SW, Milstien S, Spiegel S. "Inside-out" signaling of sphingosine-1-phosphate: therapeutic targets. *Pharmacol Rev*. 2008;60(2):181-95.
218. Ancellin N, Colmont C, Su J, Li Q, Mittereder N, Chae SS, et al. Extracellular export of sphingosine kinase-1 enzyme. Sphingosine 1-phosphate generation and the induction of angiogenic vascular maturation. *J Biol Chem*. 2002;277(8):6667-75.
219. Kobayashi N, Nishi T, Hirata T, Kihara A, Sano T, Igarashi Y, et al. Sphingosine 1-phosphate is released from the cytosol of rat platelets in a carrier-mediated manner. *Journal of Lipid Research*. 2006;47(3):614-21.

220. Mitra P, Oskeritzian CA, Payne SG, Beaven MA, Milstien S, Spiegel S. Role of ABCC1 in export of sphingosine-1-phosphate from mast cells. *Proceedings of the National Academy of Sciences of the United States of America*. 2006;103(44):16394-9.
221. Hisano Y, Kobayashi N, Yamaguchi A, Nishi T. Mouse SPNS2 Functions as a Sphingosine-1-Phosphate Transporter in Vascular Endothelial Cells. *PLoS One*. 2012;7(6):e38941.
222. Guan H, Song L, Cai J, Huang Y, Wu J, Yuan J, et al. Sphingosine Kinase 1 Regulates the Akt/FOXO3a/Bim Pathway and Contributes to Apoptosis Resistance in Glioma Cells. *PLOS ONE*. 2011;6(5):e19946.
223. Song L, Xiong H, Li J, Liao W, Wang L, Wu J, et al. Sphingosine Kinase-1 Enhances Resistance to Apoptosis through Activation of PI3K/Akt/NF- κ B Pathway in Human Non-Small Cell Lung Cancer. *Clinical Cancer Research*. 2011;17(7):1839.
224. You B, Ren A, Yan G, Sun J. Activation of Sphingosine Kinase-1 Mediates Inhibition of Vascular Smooth Muscle Cell Apoptosis by Hyperglycemia. *Diabetes*. 2007;56(5):1445.
225. Chakraborty G, Saito M, Shah R, Mao RF, Vadasz C. Ethanol triggers sphingosine 1-phosphate elevation along with neuroapoptosis in the developing mouse brain. *J Neurochem*. 2012;121(5):806-17.
226. Min J, Mesika A, Sivaguru M, Van Veldhoven PP, Alexander H, Futerman AH, et al. (Dihydro)ceramide Synthase 1-Regulated Sensitivity to Cisplatin Is Associated with the Activation of p38 Mitogen-Activated Protein Kinase and Is Abrogated by Sphingosine Kinase 1. *Molecular Cancer Research*. 2007;5(8):801.

227. Liu H, Toman RE, Goparaju SK, Maceyka M, Nava VE, Sankala H, et al. Sphingosine kinase type 2 is a putative BH3-only protein that induces apoptosis. *J Biol Chem.* 2003;278(41):40330-6.
228. Okada T, Ding G, Sonoda H, Kajimoto T, Haga Y, Khosrowbeygi A, et al. Involvement of N-terminal-extended Form of Sphingosine Kinase 2 in Serum-dependent Regulation of Cell Proliferation and Apoptosis. *Journal of Biological Chemistry.* 2005;280(43):36318-25.
229. Yamamoto Y, Olson DM, Bennekou Mv, Brindley DN, Hemmings DG. Increased Expression of Enzymes for Sphingosine 1-Phosphate Turnover and Signaling in Human Decidua During Late Pregnancy¹. *Biology of Reproduction.* 2010;82(3):628-35.
230. Dunlap KA, Kwak H-i, Burghardt RC, Bazer FW, Magness RR, Johnson GA, et al. The Sphingosine 1-Phosphate (S1P) Signaling Pathway Is Regulated During Pregnancy in Sheep¹. *Biology of Reproduction.* 2010;82(5):876-87.
231. Mizugishi K, Li C, Olivera A, Bielawski J, Bielawska A, Deng CX, et al. Maternal disturbance in activated sphingolipid metabolism causes pregnancy loss in mice. *J Clin Invest.* 2007;117(10):2993-3006.
232. Jeng Y-J, Suarez VR, Izban MG, Wang H-Q, Soloff MS. Progesterone-induced sphingosine kinase-1 expression in the rat uterus during pregnancy and signaling consequences. *American Journal of Physiology-Endocrinology and Metabolism.* 2007;292(4):E1110-E21.
233. Kaneko-Tarui T, Zhang L, Austin KJ, Henkes LE, Johnson J, Hansen TR, et al. Maternal and Embryonic Control of Uterine Sphingolipid-Metabolizing Enzymes During Murine Embryo Implantation¹. *Biology of Reproduction.* 2007;77(4):658-65.

234. Dobierzewska A, Palominos M, Sanchez M, Dyhr M, Helgert K, Venegas-Araneda P, et al. Impairment of Angiogenic Sphingosine Kinase-1/Sphingosine-1-Phosphate Receptors Pathway in Preeclampsia. *PLoS One*. 2016;11(6):e0157221.
235. Taha TA, Kitatani K, Bielawski J, Cho W, Hannun YA, Obeid LM. Tumor necrosis factor induces the loss of sphingosine kinase-1 by a cathepsin B-dependent mechanism. *J Biol Chem*. 2005;280(17):17196-202.
236. Pchejetski D, Kunduzova O, Dayon A, Calise D, Seguelas MH, Leducq N, et al. Oxidative stress-dependent sphingosine kinase-1 inhibition mediates monoamine oxidase A-associated cardiac cell apoptosis. *Circ Res*. 2007;100(1):41-9.
237. Van Veldhoven PP, Gijssbers S, Mannaerts GP, Vermeesch JR, Brys V. Human sphingosine-1-phosphate lyase: cDNA cloning, functional expression studies and mapping to chromosome 10q22.1 DNA sequence was deposited in the EMBL database (AJ011304). *Biochimica et Biophysica Acta (BBA) - Molecular and Cell Biology of Lipids*. 2000;1487(2):128-34.
238. Ikeda M, Kihara A, Igarashi Y. Sphingosine-1-phosphate lyase SPL is an endoplasmic reticulum-resident, integral membrane protein with the pyridoxal 5'-phosphate binding domain exposed to the cytosol. *Biochemical and Biophysical Research Communications*. 2004;325(1):338-43.
239. Saba JD. Fifty years of lyase and a moment of truth: sphingosine phosphate lyase from discovery to disease. *J Lipid Res*. 2019;60(3):456-63.
240. Schmahl J, Raymond CS, Soriano P. PDGF signaling specificity is mediated through multiple immediate early genes. *Nature Genetics*. 2007;39(1):52-60.

241. Newbigging S, Zhang M, Saba JD. Immunohistochemical analysis of sphingosine phosphate lyase expression during murine development. *Gene expression patterns : GEP.* 2013;13(1-2):21-9.
242. Tanaka M, Gertsenstein M, Rossant J, Nagy A. Mash2 acts cell autonomously in mouse spongiotrophoblast development. *Dev Biol.* 1997;190(1):55-65.
243. Iwatsuki K, Shinozaki M, Sun W, Yagi S, Tanaka S, Shiota K. A Novel Secretory Protein Produced by Rat Spongiotrophoblast1. *Biology of reproduction.* 2000;62(5):1352-9.
244. Ogawa C, Kihara A, Gokoh M, Igarashi Y. Identification and Characterization of a Novel Human Sphingosine-1-phosphate Phosphohydrolase, hSPP2. *Journal of Biological Chemistry.* 2003;278(2):1268-72.
245. Le Stunff H, Peterson C, Thornton R, Milstien S, Mandala SM, Spiegel S. Characterization of murine sphingosine-1-phosphate phosphohydrolase. *J Biol Chem.* 2002;277(11):8920-7.
246. Mandala SM, Thornton R, Galve-Roperh I, Poulton S, Peterson C, Olivera A, et al. Molecular cloning and characterization of a lipid phosphohydrolase that degrades sphingosine-1-phosphate and induces cell death. *Proc Natl Acad Sci U S A.* 2000;97(14):7859-64.
247. Johnson KR, Johnson KY, Becker KP, Bielawski J, Mao C, Obeid LM. Role of human sphingosine-1-phosphate phosphatase 1 in the regulation of intra- and extracellular sphingosine-1-phosphate levels and cell viability. *J Biol Chem.* 2003;278(36):34541-7.
248. López-Juárez A, Morales-Lázaro S, Sánchez-Sánchez R, Sunkara M, Lomelí H, Velasco I, et al. Expression of LPP3 in Bergmann glia is required for proper cerebellar sphingosine-1-phosphate metabolism/signaling and development. *Glia.* 2011;59(4):577-89.

249. Tang X, Benesch MG, Dewald J, Zhao YY, Patwardhan N, Santos WL, et al. Lipid phosphate phosphatase-1 expression in cancer cells attenuates tumor growth and metastasis in mice. *J Lipid Res.* 2014;55(11):2389-400.
250. Bréart B, Ramos-Perez WD, Mendoza A, Salous AK, Gobert M, Huang Y, et al. Lipid phosphate phosphatase 3 enables efficient thymic egress. *J Exp Med.* 2011;208(6):1267-78.
251. Tang X, Zhao YY, Dewald J, Curtis JM, Brindley DN. Tetracyclines increase lipid phosphate phosphatase expression on plasma membranes and turnover of plasma lysophosphatidate. *Journal of lipid research.* 2016;57(4):597-606.
252. Wijaya JC, Khanabdali R, Georgiou HM, Kokkinos MI, James PF, Brennecke SP, et al. Functional changes in decidual mesenchymal stem/stromal cells are associated with spontaneous onset of labour. *Molecular Human Reproduction.* 2020;26(8):636-51.
253. Dobierzewska A, Soman S, Illanes SE, Morris AJ. Plasma cross-gestational sphingolipidomic analyses reveal potential first trimester biomarkers of preeclampsia. *PLoS One.* 2017;12(4):e0175118.
254. Li Q, Pan Z, Wang X, Gao Z, Ren C, Yang W. miR-125b-1-3p inhibits trophoblast cell invasion by targeting sphingosine-1-phosphate receptor 1 in preeclampsia. *Biochem Biophys Res Commun.* 2014;453(1):57-63.
255. Artal-Sanz M, Tavernarakis N. Prohibitin and mitochondrial biology. *Trends Endocrinol Metab.* 2009;20(8):394-401.
256. Hait NC, Allegood J, Maceyka M, Strub GM, Harikumar KB, Singh SK, et al. Regulation of histone acetylation in the nucleus by sphingosine-1-phosphate. *Science.* 2009;325(5945):1254-7.

257. Ishii I, Friedman B, Ye X, Kawamura S, McGiffert C, Contos JJ, et al. Selective loss of sphingosine 1-phosphate signaling with no obvious phenotypic abnormality in mice lacking its G protein-coupled receptor, LP(B3)/EDG-3. *J Biol Chem*. 2001;276(36):33697-704.
258. Kimura A, Ohmori T, Ohkawa R, Madoiwa S, Mimuro J, Murakami T, et al. Essential roles of sphingosine 1-phosphate/S1P1 receptor axis in the migration of neural stem cells toward a site of spinal cord injury. *Stem Cells*. 2007;25(1):115-24.
259. Sanna MG, Liao J, Jo E, Alfonso C, Ahn M-Y, Peterson MS, et al. Sphingosine 1-Phosphate (S1P) Receptor Subtypes S1P1 and S1P3, Respectively, Regulate Lymphocyte Recirculation and Heart Rate. *Journal of Biological Chemistry*. 2004;279(14):13839-48.
260. Matloubian M, Lo CG, Cinamon G, Lesneski MJ, Xu Y, Brinkmann V, et al. Lymphocyte egress from thymus and peripheral lymphoid organs is dependent on S1P receptor 1. *Nature*. 2004;427:355.
261. Maeda Y, Matsuyuki H, Shimano K, Kataoka H, Sugahara K, Chiba K. Migration of CD4 T Cells and Dendritic Cells toward Sphingosine 1-Phosphate (S1P) Is Mediated by Different Receptor Subtypes: S1P Regulates the Functions of Murine Mature Dendritic Cells via S1P Receptor Type 3. *The Journal of Immunology*. 2007;178(6):3437.
262. Liu Y, Wada R, Yamashita T, Mi Y, Deng C-X, Hobson JP, et al. Edg-1, the G protein-coupled receptor for sphingosine-1-phosphate, is essential for vascular maturation. *The Journal of Clinical Investigation*. 2000;106(8):951-61.
263. Murakami K, Kohno M, Kadoya M, Nagahara H, Fujii W, Seno T, et al. Knock Out of S1P3 Receptor Signaling Attenuates Inflammation and Fibrosis in Bleomycin-Induced Lung Injury Mice Model. *PLOS ONE*. 2014;9(9):e106792.

264. MacLennan AJ, Carney PR, Zhu WJ, Chaves AH, Garcia J, Grimes JR, et al. An essential role for the H218/AGR16/Edg-5/LPB2 sphingosine 1-phosphate receptor in neuronal excitability. *European Journal of Neuroscience*. 2001;14(2):203-9.
265. Gräler MH, Bernhardt G, Lipp M. EDG6, a Novel G-Protein-Coupled Receptor Related to Receptors for Bioactive Lysophospholipids, Is Specifically Expressed in Lymphoid Tissue. *Genomics*. 1998;53(2):164-9.
266. Walzer T, Chiossone L, Chaix J, Calver A, Carozzo C, Garrigue-Antar L, et al. Natural killer cell trafficking in vivo requires a dedicated sphingosine 1-phosphate receptor. *Nat Immunol*. 2007;8(12):1337-44.
267. Schulze T, Golfier S, Tabeling C, Räbel K, Gräler MH, Witzenrath M, et al. Sphingosine-1-phosphate receptor 4 (S1P4) deficiency profoundly affects dendritic cell function and TH17-cell differentiation in a murine model. *The FASEB Journal*. 2011;25(11):4024-36.
268. Novgorodov AS, El-Alwani M, Bielawski J, Obeid LM, Gudz TI. Activation of sphingosine-1-phosphate receptor S1P5 inhibits oligodendrocyte progenitor migration. *The FASEB Journal*. 2007;21(7):1503-14.
269. Blaho VA, Hla T. An update on the biology of sphingosine 1-phosphate receptors. *Journal of lipid research*. 2014;55(8):1596-608.
270. Blaho VA, Hla T. Regulation of mammalian physiology, development, and disease by the sphingosine 1-phosphate and lysophosphatidic acid receptors. *Chem Rev*. 2011;111(10):6299-320.
271. Rosenberg AJ, Liu H, Tu Z. A practical process for the preparation of [(32)P]S1P and binding assay for S1P receptor ligands. *Appl Radiat Isot*. 2015;102:5-9.

272. Skaznik-Wikiel ME, Kaneko-Tarui T, Kashiwagi A, Pru JK. Sphingosine-1-Phosphate Receptor Expression and Signaling Correlate with Uterine Prostaglandin-Endoperoxide Synthase 2 Expression and Angiogenesis During Early Pregnancy¹. *Biology of Reproduction*. 2006;74(3):569-76.
273. Westwood M, Al-Saghir K, Finn-Sell S, Tan C, Cowley E, Berneau S, et al. Vitamin D attenuates sphingosine-1-phosphate (S1P)-mediated inhibition of extravillous trophoblast migration. *Placenta*. 2017;60:1-8.
274. Goyal P, Brunnert D, Ehrhardt J, Bredow M, Piccenini S, Zygmunt M. Cytokine IL-6 secretion by trophoblasts regulated via sphingosine-1-phosphate receptor 2 involving Rho/Rho-kinase and Rac1 signaling pathways. *Molecular Human Reproduction*. 2013;19(8):528-38.
275. Chauvin S, Yinon Y, Xu J, Ermini L, Sallais J, Tagliaferro A, et al. Aberrant TGF β Signalling Contributes to Dysregulation of Sphingolipid Metabolism in Intrauterine Growth Restriction. *J Clin Endocrinol Metab*. 2015;100(7):E986-96.
276. Fugio LB, Coeli-Lacchini FB, Leopoldino AM. Sphingolipids and Mitochondrial Dynamic. *Cells*. 2020;9(3):581.
277. Bailey LJ, Alahari S, Tagliaferro A, Post M, Caniggia I. Augmented trophoblast cell death in preeclampsia can proceed via ceramide-mediated necroptosis. *Cell Death & Disease*. 2017;8(2):e2590-e.
278. Bartho LA, Fisher JJ, Cuffe JSM, Perkins AV. Mitochondrial transformations in the aging human placenta. *American Journal of Physiology-Endocrinology and Metabolism*. 2020;319(6):E981-E94.
279. Vangrieken P, Al-Nasiry S, Bast A, Leermakers PA, Tulen CBM, Schiffers PMH, et al. Placental Mitochondrial Abnormalities in Preeclampsia. *Reproductive Sciences*. 2021.

280. Ausman J, Abbade J, Ermini L, Farrell A, Tagliaferro A, Post M, et al. Ceramide-induced BOK promotes mitochondrial fission in preeclampsia. *Cell Death & Disease*. 2018;9(3):298.
281. Westermann B. Mitochondrial fusion and fission in cell life and death. *Nature Reviews Molecular Cell Biology*. 2010;11(12):872-84.
282. Zhang J, Dunk CE, Lye SJ. Sphingosine signalling regulates decidual NK cell angiogenic phenotype and trophoblast migration. *Human reproduction (Oxford, England)*. 2013;28(11):3026-37.
283. Paugh SW, Payne SG, Barbour SE, Milstien S, Spiegel S. The immunosuppressant FTY720 is phosphorylated by sphingosine kinase type 2. *FEBS Letters*. 2003;554(1-2):189-93.
284. Sykes DA, Riddy DM, Stamp C, Bradley ME, McGuinness N, Sattikar A, et al. Investigating the molecular mechanisms through which FTY 720-P causes persistent S1P1 receptor internalization. *British journal of pharmacology*. 2014;171(21):4797-807.
285. Kovarik JM, Schmouder RL, Slade AJ. Overview of FTY720 clinical pharmacokinetics and pharmacology. *Therapeutic drug monitoring*. 2004;26(6):585-7.
286. Brunnert D, Piccenini S, Ehrhardt J, Zygmunt M, Goyal P. Sphingosine 1-phosphate regulates IL-8 expression and secretion via S1PR1 and S1PR2 receptors-mediated signaling in extravillous trophoblast derived HTR-8/SVneo cells. *Placenta*. 2015;36(10):1115-21.
287. Yang W, Li Q, Pan Z. Sphingosine-1-phosphate promotes extravillous trophoblast cell invasion by activating MEK/ERK/MMP-2 signaling pathways via S1P/S1PR1 axis activation. *PLoS One*. 2014;9(9):e106725.
288. Uhlén M, Fagerberg L, Hallström BM, Lindskog C, Oksvold P, Mardinoglu A, et al. Tissue-based map of the human proteome. *Science*. 2015;347(6220):1260419.

289. Johnstone ED, Mackova M, Das S, Payne SG, Lowen B, Sibley CP, et al. Multiple anti-apoptotic pathways stimulated by EGF in cytotrophoblasts. *Placenta*. 2005;26(7):548-55.
290. Payne SG, Brindley DN, Guilbert LJ. Epidermal growth factor inhibits ceramide-induced apoptosis and lowers ceramide levels in primary placental trophoblasts. *Journal of Cellular Physiology*. 1999;180(2):263-70.
291. Singh AT, Dharmarajan A, Aye ILMH, Keelan JA. Ceramide biosynthesis and metabolism in trophoblast syncytialization. *Molecular and Cellular Endocrinology*. 2012;362(1):48-59.
292. Evseenko DA, Murthi P, Paxton JW, Reid G, Emerald BS, Mohankumar KM, et al. The ABC transporter BCRP/ABCG2 is a placental survival factor, and its expression is reduced in idiopathic human fetal growth restriction. *The FASEB Journal*. 2007;21(13):3592-605.
293. Johnstone ED, Chan G, Sibley CP, Davidge ST, Lowen B, Guilbert LJ. Sphingosine-1-phosphate inhibition of placental trophoblast differentiation through a Gi-coupled receptor response. *Journal of Lipid Research*. 2005;46(9):1833-9.
294. Vyas V, Ashby CR, Jr., Olgun NS, Sundaram S, Salami O, Munnangi S, et al. Inhibition of sphingosine kinase prevents lipopolysaccharide-induced preterm birth and suppresses proinflammatory responses in a murine model. *Am J Pathol*. 2015;185(3):862-9.
295. Qiao Y, Hu R, Wang Q, Qi J, Yang Y, Kijlstra A, et al. Sphingosine 1-Phosphate Elicits Proinflammatory Responses in ARPE-19 Cells. *Investigative Ophthalmology & Visual Science*. 2012;53(13):8200-7.
296. Escalante-Alcalde D, Hernandez L, Le Stunff H, Maeda R, Lee HS, Jr Gang C, et al. The lipid phosphatase LPP3 regulates extra-embryonic vasculogenesis and axis patterning. *Development*. 2003;130(19):4623-37.

297. Del Gaudio I, Hendrix S, Christoffersen C, Wadsack C. Neonatal HDL Counteracts Placental Vascular Inflammation via S1P-S1PR1 Axis. *Int J Mol Sci.* 2020;21(3):789.
298. Smith S, Francis R, Guilbert L, Baker PN. Growth factor rescue of cytokine mediated trophoblast apoptosis. *Placenta.* 2002;23(4):322-30.
299. Straszewski-Chavez SL, Visintin IP, Karassina N, Los G, Liston P, Halaban R, et al. XAF1 mediates tumor necrosis factor-alpha-induced apoptosis and X-linked inhibitor of apoptosis cleavage by acting through the mitochondrial pathway. *J Biol Chem.* 2007;282(17):13059-72.
300. Park ES, Choi S, Shin B, Yu J, Hwang JM, Yun H, et al. Tumor necrosis factor (TNF) receptor-associated factor (TRAF)-interacting protein (TRIP) negatively regulates the TRAF2 ubiquitin-dependent pathway by suppressing the TRAF2-sphingosine 1-phosphate (S1P) interaction. *J Biol Chem.* 2015;290(15):9660-73.
301. Eisenhoffer GT, Rosenblatt J. Bringing balance by force: live cell extrusion controls epithelial cell numbers. *Trends Cell Biol.* 2013;23(4):185-92.
302. Eisenhoffer GT, Loftus PD, Yoshigi M, Otsuna H, Chien CB, Morcos PA, et al. Crowding induces live cell extrusion to maintain homeostatic cell numbers in epithelia. *Nature.* 2012;484(7395):546-9.
303. Hennes A, Held K, Boretto M, De Clercq K, Van den Eynde C, Vanhie A, et al. Functional expression of the mechanosensitive PIEZO1 channel in primary endometrial epithelial cells and endometrial organoids. *Scientific reports.* 2019;9(1):1-14.
304. Xiao B. Levering Mechanically Activated Piezo Channels for Potential Pharmacological Intervention. *Annu Rev Pharmacol Toxicol.* 2020;60:195-218.

305. Wang S, Chennupati R, Kaur H, Iring A, Wettschureck N, Offermanns S. Endothelial cation channel PIEZO1 controls blood pressure by mediating flow-induced ATP release. *The Journal of Clinical Investigation*. 2016;126(12):4527-36.
306. Paz NGd, Frangos JA. Rapid flow-induced activation of Gαq/11 is independent of Piezo1 activation. *American Journal of Physiology-Cell Physiology*. 2019;316(5):C741-C52.
307. Lin Y-C, Guo YR, Miyagi A, Levring J, MacKinnon R, Scheuring S. Force-induced conformational changes in PIEZO1. *Nature*. 2019;573(7773):230-4.
308. Ridone P, Vassalli M, Martinac B. Piezo1 mechanosensitive channels: what are they and why are they important. *Biophys Rev*. 2019;11(5):795-805.
309. Gudipaty SA, Lindblom J, Loftus PD, Redd MJ, Edes K, Davey CF, et al. Mechanical stretch triggers rapid epithelial cell division through Piezo1. *Nature*. 2017;543(7643):118-21.
310. Langbein M, Strick R, Strissel PL, Vogt N, Parsch H, Beckmann MW, et al. Impaired cytotrophoblast cell–cell fusion is associated with reduced Syncytin and increased apoptosis in patients with placental dysfunction. *Molecular Reproduction and Development: Incorporating Gamete Research*. 2008;75(1):175-83.
311. Sugimoto A, Miyazaki A, Kawarabayashi K, Shono M, Akazawa Y, Hasegawa T, et al. Piezo type mechanosensitive ion channel component 1 functions as a regulator of the cell fate determination of mesenchymal stem cells. *Scientific Reports*. 2017;7(1):17696.
312. John L, Ko NL, Gokin A, Gokina N, Mandalà M, Osol G. The Piezo1 cation channel mediates uterine artery shear stress mechanotransduction and vasodilation during rat pregnancy. *American Journal of Physiology-Heart and Circulatory Physiology*. 2018;315(4):H1019-H26.

313. Morley LC, Shi J, Gaunt HJ, Hyman AJ, Webster PJ, Williams C, et al. Piezo1 channels are mechanosensors in human fetoplacental endothelial cells. *Mol Hum Reprod.* 2018;24(10):510-20.
314. Morley LC, Beech DJ, Walker JJ, Simpson NAB. Emerging concepts of shear stress in placental development and function. *Mol Hum Reprod.* 2019;25(6):329-39.
315. Li J, Hou B, Tumova S, Muraki K, Bruns A, Ludlow MJ, et al. Piezo1 integration of vascular architecture with physiological force. *Nature.* 2014;515(7526):279-82.
316. Miura S, Sato K, Kato-Negishi M, Teshima T, Takeuchi S. Fluid shear triggers microvilli formation via mechanosensitive activation of TRPV6. *Nature Communications.* 2015;6(1):8871.
317. Lecarpentier E, Atallah A, Guibourdenche J, Hebert-Schuster M, Vieillefosse S, Chissey A, et al. Fluid Shear Stress Promotes Placental Growth Factor Upregulation in Human Syncytiotrophoblast Through the cAMP/PKA Signaling Pathway. *Hypertension.* 2016;68(6):1438-46.
318. Sanz G, Daniel N, Aubrière MC, Archilla C, Jouneau L, Jaszczyszyn Y, et al. Differentiation of derived rabbit trophoblast stem cells under fluid shear stress to mimic the trophoblastic barrier. *Biochim Biophys Acta Gen Subj.* 2019;1863(10):1608-18.
319. Piddini E. Epithelial Homeostasis: A Piezo of the Puzzle. *Current Biology.* 2017;27(6):R232-R4.
320. Carotenuto AR, Lunghi L, Piccolo V, Babaei M, Dayal K, Pugno N, et al. Mechanobiology predicts raft formations triggered by ligand-receptor activity across the cell membrane. *Journal of the Mechanics and Physics of Solids.* 2020;141:103974.

321. Weng ZP, Wang XM, Qi H, Tao H, Zhang SP, Ji XH. [Effects of transient receptor potential V6 silence on proliferation and apoptosis of trophoblasts]. *Zhonghua Fu Chan Ke Za Zhi*. 2012;47(10):777-80.
322. Costa MA, Fonseca BM, Keating E, Teixeira NA, Correia-da-Silva G. Transient receptor potential vanilloid 1 is expressed in human cytotrophoblasts: Induction of cell apoptosis and impairment of syncytialization. *The International Journal of Biochemistry & Cell Biology*. 2014;57:177-85.
323. Zhao C, Sun Q, Tang L, Cao Y, Nourse JL, Pathak MM, et al. Mechanosensitive Ion Channel Piezo1 Regulates Diet-Induced Adipose Inflammation and Systemic Insulin Resistance. *Front Endocrinol (Lausanne)*. 2019;10:373-.
324. Albarrán-Juárez J, Iring A, Wang S, Joseph S, Grimm M, Strilic B, et al. Piezo1 and G(q)/G(11) promote endothelial inflammation depending on flow pattern and integrin activation. *J Exp Med*. 2018;215(10):2655-72.
325. Williams ER. PIEZO1 promotes inflammation. *Science signaling*. 2019;12(598):eaaz4154.
326. Lee W, Leddy H, McNulty A, Guilak F, Liedtke W. Inflammatory Cytokine Il-1 α Up-Regulates Piezo1 and Hyper-Sensitizes Chondrocytes to Compression. *Biophysical Journal*. 2016;110(3):349a.
327. Martinac B, Poole K. Mechanically activated ion channels. *Int J Biochem Cell Biol*. 2018;97:104-7.
328. Osawa Y, Banno Y, Nagaki M, Brenner DA, Naiki T, Nozawa Y, et al. TNF-alpha-induced sphingosine 1-phosphate inhibits apoptosis through a phosphatidylinositol 3-kinase/Akt

pathway in human hepatocytes. *Journal of immunology* (Baltimore, Md : 1950).

2001;167(1):173-80.

329. Pettus BJ, Bielawski J, Porcelli AM, Reames DL, Johnson KR, Morrow J, et al. The sphingosine kinase 1/sphingosine-1-phosphate pathway mediates COX-2 induction and PGE2 production in response to TNF-alpha. *FASEB J.* 2003;17(11):1411-21.

330. Scherer EQ, Yang J, Canis M, Reimann K, Ivanov K, Diehl CD, et al. Tumor necrosis factor-alpha enhances microvascular tone and reduces blood flow in the cochlea via enhanced sphingosine-1-phosphate signaling. *Stroke.* 2010;41(11):2618-24.

331. Niwa M, Kozawa O, Matsuno H, Kanamori Y, Hara A, Uematsu T. Tumor necrosis factor-alpha-mediated signal transduction in human neutrophils: involvement of sphingomyelin metabolites in the priming effect of TNF-alpha on the fMLP-stimulated superoxide production. *Life Sci.* 2000;66(3):245-56.

332. Du J, Zeng C, Li Q, Chen B, Liu H, Huang X, et al. LPS and TNF-alpha induce expression of sphingosine-1-phosphate receptor-2 in human microvascular endothelial cells. *Pathology, research and practice.* 2012;208(2):82-8.

333. Zhao C, Fernandes MJ, Turgeon M, Tancrede S, Di Battista J, Poubelle PE, et al. Specific and overlapping sphingosine-1-phosphate receptor functions in human synoviocytes: impact of TNF-alpha. *J Lipid Res.* 2008;49(11):2323-37.

334. Brugger BA, Guettler J, Gauster M. Go with the Flow-Trophoblasts in Flow Culture. *Int J Mol Sci.* 2020;21(13):4666.

335. Raja H, Matteson EL, Michet CJ, Smith JR, Pulido JS. Safety of Tumor Necrosis Factor Inhibitors during Pregnancy and Breastfeeding. *Translational Vision Science & Technology.* 2012;1(2):6-.

336. Simán CM, Sibley CP, Jones CJ, Turner MA, Greenwood SL. The functional regeneration of syncytiotrophoblast in cultured explants of term placenta. *Am J Physiol Regul Integr Comp Physiol*. 2001;280(4):R1116-22.
337. Trowell OA. A modified technique for organ culture in vitro. *Experimental Cell Research*. 1954;6(1):246-8.
338. Robbins Jennifer R, Zeldovich Varvara B, Poukchanski A, Boothroyd John C, Bakardjiev Anna I, Adams JH. Tissue Barriers of the Human Placenta to Infection with *Toxoplasma gondii*. *Infection and Immunity*. 2012;80(1):418-28.
339. Jia Z, Bao K, Wei P, Yu X, Zhang Y, Wang X, et al. EGFR activation-induced decreases in claudin1 promote MUC5AC expression and exacerbate asthma in mice. *Mucosal Immunology*. 2021;14(1):125-34.
340. Alexis C, Nicolas J, Yohann D, Hakim O-H, Julien D, Corinne G, et al. PIEZO1 activation delays erythroid differentiation of normal and hereditary xerocytosis-derived human progenitor cells. *Haematologica*. 2020;105(3):610-22.
341. Schnute Mark E, McReynolds Matthew D, Kasten T, Yates M, Jerome G, Rains John W, et al. Modulation of cellular S1P levels with a novel, potent and specific inhibitor of sphingosine kinase-1. *Biochemical Journal*. 2012;444(1):79-88.
342. Yui J, Garcia-Lloret M, Brown AJ, Berdan RC, Morrish DW, Wegmann TG, et al. Functional, long-term cultures of human term trophoblasts purified by column-elimination of CD9 expressing cells. *Placenta*. 1994;15(3):231-46.
343. Tang X, Benesch MG, Brindley DN. Lipid phosphate phosphatases and their roles in mammalian physiology and pathology. *Journal of Lipid Research*. 2015;56(11):2048-60.

344. Peter BF, Lidington D, Harada A, Bolz HJ, Vogel L, Heximer S, et al. Role of sphingosine-1-phosphate phosphohydrolase 1 in the regulation of resistance artery tone. *Circulation research*. 2008;103(3):315-24.
345. Estrada-Bernal A, Lawler S, Nowicki M, Ray-Chaudhury A, Brocklyn J. The role of sphingosine kinase-1 in EGFRvIII-regulated growth and survival of glioblastoma cells. *Journal of neuro-oncology*. 2010;102:353-66.
346. Francy JM, Nag A, Conroy EJ, Hengst JA, Yun JK. Sphingosine kinase 1 expression is regulated by signaling through PI3K, AKT2, and mTOR in human coronary artery smooth muscle cells. *Biochimica et Biophysica Acta (BBA) - Gene Structure and Expression*. 2007;1769(4):253-65.
347. Mechtcheriakova D, Wlachos A, Sobanov J, Kopp T, Reuschel R, Bornancin F, et al. Sphingosine 1-phosphate phosphatase 2 is induced during inflammatory responses. *Cellular Signalling*. 2007;19(4):748-60.
348. Ge J, Chang N, Zhao Z, Tian L, Duan X, Yang L, et al. Essential Roles of RNA-binding Protein HuR in Activation of Hepatic Stellate Cells Induced by Transforming Growth Factor- β 1. *Scientific reports*. 2016;6(1):22141.
349. Wadgaonkar R, Patel V, Grinkina N, Romano C, Liu J, Zhao Y, et al. Differential regulation of sphingosine kinases 1 and 2 in lung injury. *American Journal of Physiology-Lung Cellular and Molecular Physiology*. 2009;296(4):L603-L13.
350. Huang WC, Liang J, Nagahashi M, Avni D, Yamada A, Maceyka M, et al. Sphingosine-1-phosphate phosphatase 2 promotes disruption of mucosal integrity, and contributes to ulcerative colitis in mice and humans. *FASEB journal : official publication of the Federation of American Societies for Experimental Biology*. 2016;30(8):2945-58.

351. Lyu Y, Xu X, Yun J, Yi J, Li X, Liu X, et al. TNF- α regulates the proliferation of human breast cancer cells via regulation of ceramide content. *Xi bao yu fen zi Mian yi xue za zhi*= Chinese Journal of Cellular and Molecular Immunology. 2017;33(10):1303-9.
352. Hod T, Cerdeira AS, Karumanchi SA. Molecular Mechanisms of Preeclampsia. *Cold Spring Harb Perspect Med*. 2015;5(10).
353. Liao J, Zheng Y, Hu M, Xu P, Lin L, Liu X, et al. Impaired Sphingosine-1-Phosphate Synthesis Induces Preeclampsia by Deactivating Trophoblastic YAP (Yes-Associated Protein) Through S1PR2 (Sphingosine-1-Phosphate Receptor-2)-Induced Actin Polymerizations. *Hypertension*. 2021:HYPERTENSIONAHA. 121.18363.
354. Nava VE, Hobson JP, Murthy S, Milstien S, Spiegel S. Sphingosine kinase type 1 promotes estrogen-dependent tumorigenesis of breast cancer MCF-7 cells. *Exp Cell Res*. 2002;281(1):115-27.
355. Chen XL, Grey JY, Thomas S, Qiu FH, Medford RM, Wasserman MA, et al. Sphingosine kinase-1 mediates TNF-alpha-induced MCP-1 gene expression in endothelial cells: upregulation by oscillatory flow. *Am J Physiol Heart Circ Physiol*. 2004;287(4):H1452-8.
356. Yu HM, Li Q, Perelman JM, Kolosov VP, Zhou XD. [Regulation of sphingosine kinase 1 in the TNF-alpha-induced expression of MUC5AC in airway epithelial cells]. *Zhonghua yi xue za zhi*. 2011;91(6):391-5.
357. Benton SJ, Leavey K, Grynspan D, Cox BJ, Bainbridge SA. The clinical heterogeneity of preeclampsia is related to both placental gene expression and placental histopathology. *American Journal of Obstetrics and Gynecology*. 2018;219(6):604.e1-.e25.

358. Bajwa SK, Bajwa SJS, Mohan P, Singh A. Management of prolactinoma with cabergoline treatment in a pregnant woman during her entire pregnancy. *Indian Journal of Endocrinology and Metabolism*. 2011;15(Suppl3).
359. Taha TA, Kitatani K, Bielawski J, Cho W, Hannun YA, Obeid LM. Tumor Necrosis Factor Induces the Loss of Sphingosine Kinase-1 by a Cathepsin B-dependent Mechanism *. *Journal of Biological Chemistry*. 2005;280(17):17196-202.
360. Shida D, Takabe K, Kapitonov D, Milstien S, Spiegel S. Targeting SphK1 as a new strategy against cancer. *Current drug targets*. 2008;9 8:662-73.
361. Thoms HC, Loveridge CJ, Simpson J, Clipson A, Reinhardt K, Dunlop MG, et al. Nucleolar Targeting of RelA(p65) Is Regulated by COMMD1-Dependent Ubiquitination. *Cancer Research*. 2010;70(1):139-49.
362. Venkataraman K, Thangada S, Michaud J, Oo ML, Ai Y, Lee Y-M, et al. Extracellular export of sphingosine kinase-1a contributes to the vascular S1P gradient. *Biochem J*. 2006;397(3):461-71.
363. Wick SM, Duniec J. Effects of various fixatives on the reactivity of plant cell tubulin and calmodulin in immunofluorescence microscopy. *Protoplasma*. 1986;133(1):1-18.
364. Billich A, Ettmayer P. Fluorescence-based assay of sphingosine kinases. *Analytical biochemistry*. 2004;326(1):114-9.
365. Yamamoto Y, Olson DM, van Bennekom M, Brindley DN, Hemmings DG. Increased expression of enzymes for sphingosine 1-phosphate turnover and signaling in human decidua during late pregnancy. *Biol Reprod*. 2010;82(3):628-35.

366. Liu H, Toman RE, Goparaju SK, Maceyka M, Nava VE, Sankala H, et al. Sphingosine Kinase Type 2 Is a Putative BH3-only Protein That Induces Apoptosis *. *Journal of Biological Chemistry*. 2003;278(41):40330-6.
367. Petrusca DN, Mulcrone PL, Macar DA, Bishop RT, Berdyshev E, Suvannasankha A, et al. GFI1-Dependent Repression of SGPP1 Increases Multiple Myeloma Cell Survival. *Cancers (Basel)*. 2022;14(3):772.
368. Schwiebs A, Thomas D, Kleuser B, Pfeilschifter JM, Radeke HH. Nuclear Translocation of SGPP-1 and Decrease of SGPL-1 Activity Contribute to Sphingolipid Rheostat Regulation of Inflammatory Dendritic Cells. *Mediators of Inflammation*. 2017;2017:5187368.
369. ZHANG Q-X, PILQUIL CS, DEWALD J, BERTHIAUME LG, BRINDLEY DN. Identification of structurally important domains of lipid phosphate phosphatase-1: implications for its sites of action. *Biochemical Journal*. 2000;345(2):181-4.
370. Chandra M, Escalante-Alcalde D, Bhuiyan MS, Orr AW, Kevil C, Morris AJ, et al. Cardiac-specific inactivation of LPP3 in mice leads to myocardial dysfunction and heart failure. *Redox Biol*. 2018;14:261-71.
371. Fakhr Y, Koshti S, Habibyan YB, Webster K, Hemmings DG. Tumor Necrosis Factor- α ; Induces a Preeclamptic-like Phenotype in Placental Villi via Sphingosine Kinase 1 Activation. *Int J Mol Sci*. 2022;23(7):3750.
372. Lok CAR, Van der Post JAM, Sturk A, Sargent IL, Nieuwland R. The functions of microparticles in preeclampsia. *Pregnancy Hypertension: An International Journal of Women's Cardiovascular Health*. 2011;1(1):59-65.

373. Tannetta DS, Dragovic RA, Gardiner C, Redman CW, Sargent IL. Characterisation of syncytiotrophoblast vesicles in normal pregnancy and pre-eclampsia: expression of Flt-1 and endoglin. *PLoS One*. 2013;8(2):e56754.
374. Yui J, Hemmings D, Garcia-Lloret M, Guilbert LJ. Expression of the human p55 and p75 tumor necrosis factor receptors in primary villous trophoblasts and their role in cytotoxic signal transduction. *Biol Reprod*. 1996;55(2):400-9.
375. Etemadi N, Chopin M, Anderton H, Tanzer MC, Rickard JA, Abeysekera W, et al. TRAF2 regulates TNF and NF-kappaB signalling to suppress apoptosis and skin inflammation independently of Sphingosine kinase 1. *Elife*. 2015;4.
376. Pettus BJ, Bielawski J, Porcelli AM, Reames DL, Johnson KR, Morrow J, et al. The sphingosine kinase 1/sphingosine-1-phosphate pathway mediates COX-2 induction and PGE2 production in response to TNF- α . *The FASEB Journal*. 2003;17(11):1411-21.
377. Pchejetski D, Nunes J, Coughlan K, Lall H, Pitson SM, Waxman J, et al. The involvement of sphingosine kinase 1 in LPS-induced Toll-like receptor 4-mediated accumulation of HIF-1 α protein, activation of ASK1 and production of the pro-inflammatory cytokine IL-6. *Immunology & Cell Biology*. 2011;89(2):268-74.
378. Snider AJ, Alexa Orr Gandy K, Obeid LM. Sphingosine kinase: Role in regulation of bioactive sphingolipid mediators in inflammation. *Biochimie*. 2010;92(6):707-15.
379. Hung TH, Charnock-Jones DS, Skepper JN, Burton GJ. Secretion of tumor necrosis factor-alpha from human placental tissues induced by hypoxia-reoxygenation causes endothelial cell activation in vitro: a potential mediator of the inflammatory response in preeclampsia. *Am J Pathol*. 2004;164(3):1049-61.

380. Knofler M, Mosl B, Bauer S, Griesinger G, Husslein P. TNF-alpha/TNFR1 in primary and immortalized first trimester cytotrophoblasts. *Placenta*. 2000;21(5-6):525-35.
381. Kim J-W, Kim Y-W, Inagaki Y, Hwang Y-A, Mitsutake S, Ryu Y-W, et al. Synthesis and evaluation of sphingoid analogs as inhibitors of sphingosine kinases. *Bioorganic & Medicinal Chemistry*. 2005;13(10):3475-85.
382. Schnute ME, McReynolds MD, Kasten T, Yates M, Jerome G, Rains JW, et al. Modulation of cellular SIP levels with a novel, potent and specific inhibitor of sphingosine kinase-1. *Biochemical Journal*. 2012;444(1):79-88.
383. Green DR, Llambi F. Cell Death Signaling. *Cold Spring Harb Perspect Biol*. 2015;7(12).
384. Luhr M, Szalai P, Engedal N. The Lactate Dehydrogenase Sequestration Assay - A Simple and Reliable Method to Determine Bulk Autophagic Sequestration Activity in Mammalian Cells. *J Vis Exp*. 2018(137).
385. Yoshii SR, Mizushima N. Monitoring and Measuring Autophagy. *Int J Mol Sci*. 2017;18(9).
386. Urbańska K, Orzechowski A. Unappreciated Role of LDHA and LDHB to Control Apoptosis and Autophagy in Tumor Cells. *Int J Mol Sci*. 2019;20(9):2085.
387. Oh S-y, Roh C-R. Autophagy in the placenta. *Obstet Gynecol Sci*. 2017;60(3):241-59.
388. Xu C, Zhang W, Liu S, Wu W, Qin M, Huang J. Activation of the SphK1/ERK/p-ERK pathway promotes autophagy in colon cancer cells. *Oncol Lett*. 2018;15(6):9719-24.
389. Stefan B, Susanne EU, Horst-Dieter R, Myriam R, Mathias B, Heinrich HDM, et al. Comparison of the Effects of Early Pregnancy with Human Interferon, Alpha 2 (IFNA2), on Gene Expression in Bovine Endometrium. *Biology of Reproduction*. 2011;86(2).

390. Elias KM, Harvey RA, Hasselblatt KT, Seckl MJ, Berkowitz RS. Type I interferons modulate methotrexate resistance in gestational trophoblastic neoplasia. *American Journal of Reproductive Immunology*. 2017;77(6):e12666.
391. Wallace AE, Cartwright JE, Begum R, Laing K, Thilaganathan B, Whitley GS. Trophoblast-Induced Changes in C-X-C Motif Chemokine 10 Expression Contribute to Vascular Smooth Muscle Cell Dedifferentiation During Spiral Artery Remodeling. *Arteriosclerosis, thrombosis, and vascular biology*. 2013;33(3):e93-e101.
392. Jiang Y, Huang F, Chai X, Yuan W, Ding H, Wu X. The role of IP-10 and its receptor CXCR3 in early pregnancy. *Molecular Immunology*. 2021;140:59-69.
393. Luo J, Qiao F, Yin X. Hypoxia Induces FGF2 Production by Vascular Endothelial Cells and Alters MMP9 and TIMP1 Expression in Extravillous Trophoblasts and Their Invasiveness in a Cocultured Model. *Journal of Reproduction and Development*. 2011;57(1):84-91.
394. Holleran G. The role of angiopoietins and their mediators in symptomatic small bowel angiodysplasia; identifying novel diagnostic and therapeutic targets in chronic anaemia and obscure gastrointestinal bleeding. 2021.
395. Aggarwal R, Jain AK, Mittal P, Kohli M, Jawanjal P, Rath G. Association of pro-and anti-inflammatory cytokines in preeclampsia. *Journal of clinical laboratory analysis*. 2019;33(4):e22834.
396. Kalkunte S, Nevers T, Norris WE, Sharma S. Vascular IL-10: a protective role in preeclampsia. *Journal of Reproductive Immunology*. 2011;88(2):165-9.
397. Cohen NA, Rubin DT. New targets in inflammatory bowel disease therapy: 2021. *Curr Opin Gastroenterol*. 2021;37(4):357-63.

398. Issa R, Xie S, Lee K-Y, Stanbridge RD, Bhavsar P, Sukkar MB, et al. GRO- α regulation in airway smooth muscle by IL-1 β and TNF- α : role of NF- κ B and MAP kinases. *American Journal of Physiology-Lung Cellular and Molecular Physiology*. 2006;291(1):L66-L74.
399. Lo H-m, Lai T-h, Li C-h, Wu W-b. TNF- α induces CXCL1 chemokine expression and release in human vascular endothelial cells in vitro via two distinct signaling pathways. *Acta Pharmacologica Sinica*. 2014;35(3):339-50.
400. Cubitt CL, Lausch RN, Oakes JE. Differential induction of GRO alpha gene expression in human corneal epithelial cells and keratocytes exposed to proinflammatory cytokines. *Investigative Ophthalmology & Visual Science*. 1997;38(6):1149-58.
401. Bechara C, Chai H, Lin PH, Yao Q, Chen C. Growth related oncogene-alpha (GRO-alpha): roles in atherosclerosis, angiogenesis and other inflammatory conditions. *Med Sci Monit*. 2007;13(6):Ra87-90.
402. Mulla MJ, Brosens JJ, Chamley LW, Giles I, Pericleous C, Rahman A, et al. ORIGINAL ARTICLE: Antiphospholipid Antibodies Induce a Pro-Inflammatory Response in First Trimester Trophoblast Via the TLR4/MyD88 Pathway. *American Journal of Reproductive Immunology*. 2009;62(2):96-111.
403. Fu P, Usatyuk PV, Ebenezer DL, Natarajan V. ID: 111: The S1p Transporter, Spns2, Mediates Hgf-Induced Lamellipodia Formation and Migration Of Human Lung Endothelial Cells. *Journal of Investigative Medicine*. 2016;64(4):964.
404. León Y, Magariños M, Varela-Nieto I. Ceramide Kinase Inhibition Blocks IGF-1-Mediated Survival of Otic Neurosensory Progenitors by Impairing AKT Phosphorylation. *Frontiers in Cell and Developmental Biology*. 2021;9.

405. Ji Y, Lisabeth EM, Neubig RR. Transforming Growth Factor beta 1 Increases Expression of Contractile Genes in Human Pulmonary Arterial Smooth Muscle Cells by Potentiating Sphingosine-1-Phosphate Signaling. *Molecular Pharmacology*. 2021;100(2):83.
406. Drexler Y, Molina J, Mitrofanova A, Fornoni A, Merscher S. Sphingosine-1-Phosphate Metabolism and Signaling in Kidney Diseases. *Journal of the American Society of Nephrology*. 2021;32(1):9.
407. Maceyka M, Sankala H, Hait NC, Le Stunff H, Liu H, Toman R, et al. SphK1 and SphK2, Sphingosine Kinase Isoenzymes with Opposing Functions in Sphingolipid Metabolism *. *Journal of Biological Chemistry*. 2005;280(44):37118-29.
408. Amaral LM, Wallace K, Owens M, LaMarca B. Pathophysiology and current clinical management of preeclampsia. *Current hypertension reports*. 2017;19(8):1-6.
409. Bu Y, Wu H, Deng R, Wang Y. Therapeutic Potential of SphK1 Inhibitors Based on Abnormal Expression of SphK1 in Inflammatory Immune Related-Diseases. *Front Pharmacol*. 2021;12(2872).
410. Liu H, Peng H, Chen S, Liu Y, Xiang H, Chen R, et al. S1PR2 antagonist protects endothelial cells against high glucose-induced mitochondrial apoptosis through the Akt/GSK-3beta signaling pathway. *Biochem Biophys Res Commun*. 2017;490(3):1119-24.
411. Webster CR, Anwer MS. Hydrophobic bile acid apoptosis is regulated by sphingosine-1-phosphate receptor 2 in rat hepatocytes and human hepatocellular carcinoma cells. *Am J Physiol Gastrointest Liver Physiol*. 2016;310(10):G865-73.
412. Rothbauer M, Patel N, Gondola H, Siwetz M, Huppertz B, Ertl P. A comparative study of five physiological key parameters between four different human trophoblast-derived cell lines. *Scientific reports*. 2017;7(1):5892.

413. Maceyka M, Harikumar KB, Milstien S, Spiegel S. Sphingosine-1-phosphate signaling and its role in disease. *Trends Cell Biol.* 2012;22(1):50-60.
414. Goyal P, Brunnert D, Ehrhardt J, Bredow M, Piccenini S, Zygmunt M. Cytokine IL-6 secretion by trophoblasts regulated via sphingosine-1-phosphate receptor 2 involving Rho/Rho-kinase and Rac1 signaling pathways. *Mol Hum Reprod.* 2013;19(8):528-38.
415. Pitman MR, Lewis AC, Davies LT, Moretti PAB, Anderson D, Creek DJ, et al. The sphingosine 1-phosphate receptor 2/4 antagonist JTE-013 elicits off-target effects on sphingolipid metabolism. *Scientific reports.* 2022;12(1):454.
416. Mammoliti O, Palisse A, Joannesse C, El Bkassiny S, Allart B, Jaunet A, et al. Discovery of the S1P2 Antagonist GLPG2938 (1-[2-Ethoxy-6-(trifluoromethyl)-4-pyridyl]-3-[[5-methyl-6-[1-methyl-3-(trifluoromethyl)pyrazol-4-yl]pyridazin-3-yl]methyl]urea), a Preclinical Candidate for the Treatment of Idiopathic Pulmonary Fibrosis. *Journal of Medicinal Chemistry.* 2021;64(9):6037-58.
417. Hochberg Ze, Perlman R, Bick T. Intracellular Regulation Of Placental Lactogen (hPL) Secretion By Cultured Human Trophoblast. *Pediatric Research.* 1986;20:1180-.
418. Benyo DF, Smarason A, Redman CW, Sims C, Conrad KP. Expression of inflammatory cytokines in placentas from women with preeclampsia. *J Clin Endocrinol Metab.* 2001;86(6):2505-12.
419. Spence T, Allsopp PJ, Yeates AJ, Mulhern MS, Strain JJ, McSorley EM. Maternal Serum Cytokine Concentrations in Healthy Pregnancy and Preeclampsia. *Journal of Pregnancy.* 2021;2021:6649608.

420. Wang M, Luo GH, Liu H, Zhang YP, Wang B, Di DM, et al. Apolipoprotein M induces inhibition of inflammatory responses via the S1PR1 and DHCR24 pathways. *Mol Med Rep.* 2019;19(2):1272-83.
421. Janssen S, Schlegel C, Gudi V, Prajeeth CK, Skripuletz T, Trebst C, et al. Effect of FTY720-phosphate on the expression of inflammation-associated molecules in astrocytes in vitro. *Mol Med Rep.* 2015;12(4):6171-7.
422. Weber M, Weise A, Vasheghani F, Göhner C, Fitzgerald JS, Liehr T, et al. Cytogenomics of six human trophoblastic cell lines. *Placenta.* 2021;103:72-5.
423. Sheppard DM, Fisher RA, Lawler SD. Karyotypic analysis and chromosome polymorphisms in four choriocarcinoma cell lines. *Cancer Genetics and Cytogenetics.* 1985;16(3):251-8.
424. Liao A-H, Muyayalo KP. Chapter 14 - Toll-like receptors and NOD-like receptors at the implantation site. In: Mor G, editor. *Reproductive Immunology: Academic Press*; 2021. p. 277-94.
425. Sun L, Mao D, Cai Y, Tan W, Hao Y, Li L, et al. Association between higher expression of interleukin-8 (IL-8) and haplotype -353A/-251A/+678T of IL-8 gene with preeclampsia: A case-control study. *Medicine.* 2016;95(52):e5537-e.
426. Tsui K-H, Chen L-Y, Shieh M-L, Chang S-P, Yuan C-C, Li H-Y. Interleukin-8 can stimulate progesterone secretion from a human trophoblast cell line, BeWo. *In Vitro Cellular & Developmental Biology-Animal.* 2004;40(10):331-6.
427. Turco MY, Moffett A. Development of the human placenta. *Development.* 2019;146(22).
428. Gude NM, Roberts CT, Kalionis B, King RG. Growth and function of the normal human placenta. *Thromb Res.* 2004;114(5-6):397-407.

429. Fakhr Y, Saadat S, Webster K, Hemmings DG, editors. Sphingosine 1-Phosphate as a Mediator of Tumour Necrosis Factor-alpha (TNF-alpha) Signaling in Syncytialization. Reproductive Sciences; 2020: Springer Heidelberg Tiergartenstrasse 17, D-69121 Heidelberg, Germany.
430. Martínez N, Abán CE, Leguizamón GF, Damiano AE, Farina MG. TPRV-1 expression in human preeclamptic placenta. *Placenta*. 2016;40:25-8.
431. Romac JMJ, Shahid RA, Swain SM, Vigna SR, Liddle RA. Piezo1 is a mechanically activated ion channel and mediates pressure induced pancreatitis. *Nature Communications*. 2018;9(1):1715.
432. El Shahaway AA, Abd Elhady RR, Abdelrhman AA, Yahia S. Role of maternal serum interleukin 17 in preeclampsia: diagnosis and prognosis. *J Inflamm Res*. 2019;12:175-80.
433. Bellos I, Karageorgiou V, Kapnias D, Karamanli KE, Siristatidis C. The role of interleukins in preeclampsia: a comprehensive review. *American Journal of Reproductive Immunology*. 2018;80(6):e13055.
434. Sun Y, Liu S, Hu R, Zhou Q, Li X. Decreased placental IL9 and IL9R in preeclampsia impair trophoblast cell proliferation, invasion, and angiogenesis. *Hypertension in Pregnancy*. 2020;39(3):228-35.
435. Johnstone ED, Speake PF, Sibley CP. Epidermal growth factor and sphingosine-1-phosphate stimulate Na⁺/H⁺ exchanger activity in the human placental syncytiotrophoblast. *Am J Physiol Regul Integr Comp Physiol*. 2007;293(6):R2290-4.
436. Goodwin V, Sato T, Mitchell M, Keelan J. Anti-inflammatory Effects of Interleukin-4, Interleukin-10, and Transforming Growth Factor-β on Human Placental Cells In Vitro. *American Journal of Reproductive Immunology*. 1998;40(5):319-25.

437. Cottrell JN, Amaral LM, Harmon A, Cornelius DC, Jr. MWC, Vaka VR, et al. Interleukin-4 supplementation improves the pathophysiology of hypertension in response to placental ischemia in RUPP rats. *American Journal of Physiology-Regulatory, Integrative and Comparative Physiology*. 2019;316(2):R165-R71.
438. Williams MA, Mahomed K, Farrand A, Woelk GB, Mudzamiri S, Madzime S, et al. Plasma tumor necrosis factor- α soluble receptor p55 (sTNFp55) concentrations in eclamptic, preeclamptic and normotensive pregnant Zimbabwean women. *Journal of reproductive immunology*. 1998;40(2):159-73.
439. Zhu J, Jin M, Wang J, Zhang H, Wu Y, Li D, et al. TNF α induces Ca²⁺ influx to accelerate extrinsic apoptosis in hepatocellular carcinoma cells. *Journal of Experimental & Clinical Cancer Research*. 2018;37(1):43.
440. Kupper N, Pritz E, Siwetz M, Guettler J, Huppertz B. Placental Villous Explant Culture 2.0: Flow Culture Allows Studies Closer to the In Vivo Situation. *Int J Mol Sci*. 2021;22(14):7464.
441. Bae C, Sachs F, Gottlieb PA. The mechanosensitive ion channel Piezo1 is inhibited by the peptide GsMTx4. *Biochemistry*. 2011;50(29):6295-300.
442. Bourne GW, Trifaró JM. The gadolinium ion: A potent blocker of calcium channels and catecholamine release from cultured chromaffin cells. *Neuroscience*. 1982;7(7):1615-22.
443. Tapia R, Velasco I. Ruthenium red as a tool to study calcium channels, neuronal death and the function of neural pathways. *Neurochemistry International*. 1997;30(2):137-47.
444. Kalantar F, Rajaei S, Heidari AB, Mansouri R, Rashidi N, Izad MH, et al. Serum levels of tumor necrosis factor-alpha, interleukin-15 and interleukin-10 in patients with pre-eclampsia

in comparison with normotensive pregnant women. *Iran J Nurs Midwifery Res.* 2013;18(6):463-6.

445. Wang Y, Walsh SW. TNF alpha concentrations and mRNA expression are increased in preeclamptic placentas. *J Reprod Immunol.* 1996;32(2):157-69.

446. Yu J, Jia J, Guo X, Chen R, Feng L. Modulating circulating sFlt1 in an animal model of preeclampsia using PAMAM nanoparticles for siRNA delivery. *Placenta.* 2017;58:1-8.

447. Nielsen OH, Loftus EV, Jr., Jess T. Safety of TNF-alpha inhibitors during IBD pregnancy: a systematic review. *BMC Med.* 2013;11:174.

448. Holder BS, Tower CL, Jones CJP, Aplin JD, Abrahams VM. Heightened Pro-Inflammatory Effect of Preeclamptic Placental Microvesicles on Peripheral Blood Immune Cells in Humans¹. *Biology of Reproduction.* 2012;86(4).

449. Ma Y, Ye Y, Zhang J, Ruan C-C, Gao P-J. Immune imbalance is associated with the development of preeclampsia. *Medicine.* 2019;98(14).

450. Azzam HAG, Abousamra NK, Goda H, El-Shouky R, El-Gilany A-H. The expression and concentration of CD40 ligand in normal pregnancy, preeclampsia, and hemolytic anemia, elevated liver enzymes and low platelet count (HELLP) syndrome. *Blood Coagulation & Fibrinolysis.* 2013;24(1).

451. Zhou C, Zou Q-Y, Jiang Y-Z, Zheng J. Role of oxygen in fetoplacental endothelial responses: hypoxia, physiological normoxia, or hyperoxia? *American journal of physiology Cell physiology.* 2020;318(5):C943-C53.

452. Depoix CL, Haegeman F, Debiève F, Hubinont C. Is 8% O₂ more normoxic than 21% O₂ for long-term in vitro cultures of human primary term cytotrophoblasts? *Molecular Human Reproduction.* 2018;24(4):211-20.

453. Lo CH, Schaaf TM, Grant BD, Lim CK-W, Bawaskar P, Aldrich CC, et al. Noncompetitive inhibitors of TNFR1 probe conformational activation states. *Science signaling*. 2019;12(592):eaav5637.
454. Han P, Li D-x, Lei Y, Liu J-m, Ding X-m, Wang H, et al. A Potential Model for Detecting Crowding-induced Epithelial Cell and Cancer Cell Extrusion. *Current Medical Science*. 2019;39(3):391-5.
455. Kharel Y, Mathews TP, Kennedy AJ, Houck JD, Macdonald TL, Lynch KR. A rapid assay for assessment of sphingosine kinase inhibitors and substrates. *Anal Biochem*. 2011;411(2):230-5.
456. Reynolds GM, Visentin B, Sabbadini R. Immunohistochemical detection of sphingosine-1-phosphate and sphingosine kinase-1 in human tissue samples and cell lines. *Sphingosine-1-Phosphate*: Springer; 2017. p. 43-56.
457. O'Brien N, Jones ST, Williams DG, Cunningham HB, Moreno K, Visentin B, et al. Production and characterization of monoclonal anti-sphingosine-1-phosphate antibodies 1. *Journal of Lipid Research*. 2009;50(11):2245-57.
458. Pérez-Jeldres T, Alvarez-Lobos M, Rivera-Nieves J. Targeting Sphingosine-1-Phosphate Signaling in Immune-Mediated Diseases: Beyond Multiple Sclerosis. *Drugs*. 2021;81(9):985-1002.
459. Müller-Deile J, Schiffer M. Preeclampsia from a renal point of view: Insides into disease models, biomarkers and therapy. *World journal of nephrology*. 2014;3(4):169.
460. Balli S, Kibar AE, Ece İ, Oflaz MB, Yilmaz O. Assessment of Fetal Cardiac Function in Mild Preeclampsia. *Pediatric Cardiology*. 2013;34(7):1674-9.

Appendices

Appendix A

ELSEVIER LICENSE TERMS AND CONDITIONS

May 11, 2022

This Agreement between University of Alberta -- Yuliya Fakhr ("You") and Elsevier ("Elsevier") consists of your license details and the terms and conditions provided by Elsevier and Copyright Clearance Center.

License Number	5304561138865
License date	May 08, 2022
Licensed Content Publisher	Elsevier
Licensed Content Publication	The International Journal of Biochemistry & Cell Biology
Licensed Content Title	Mechanically activated ion channels
Licensed Content Author	Boris Martinac, Kate Poole
Licensed Content Date	Apr 1, 2018
Licensed Content Volume	97
Licensed Content Issue	n/a

Article Title	Phospholipid Mediators of Inflammatory Signaling in Placental Dysfunction	Expected presentation date	2022-06-16
http://markspack.copyright.com/m-a-web/mp/license/535f928c-29ba-4e43-a7ec-56677648074/balboa01-a87a-4e15-a904-95c9cc37d08f			

1/5

Licensed Content Pages	4
Start Page	104
End Page	107
Type of Use	reuse in a thesis/dissertation
Portion	figures/tables/illustrations
Number of figures/tables/illustrations	1
Format	both print and electronic
Are you the author of this Elsevier article?	No
Will you be translating?	No
Title	Mechanosensory and Sphingolipid Mediators of Inflammatory Signaling in Placental Dysfunction
Institution name	University of Alberta
Expected presentation date	Jun 2022
Portions	I would like to use Figure 1 in my thesis. thank you

Requestor Location	University of Alberta 10883 Saskatchewan Drive Northwest 202 Edmonton, AB t6e1v5 Canada Attn: University of Alberta
Publisher Tax ID	GB 494 6272 12
Total	0.00 CAD
Terms and Conditions	

Appendix B

5/10/22, 10:18 PM <https://marketplace.copyright.com/ip-ai-web/mp/license/535928c-29ba-4c43-a7ec-566177d48074/babb011-4d7a-4e15-a904-f6c9cc37d8b6/>

Instructor name Yulya Fakhr

ADDITIONAL DETAILS

Order reference number	N/A	The requesting person / organization to appear on the license	yulya fakhr
------------------------	-----	---	-------------

REUSE CONTENT DETAILS

Title, description or numeric reference of the portion(s)	I am requesting to use figure 1 in my thesis.	Title of the article/chapter the portion is from	Tissue barriers of the human placenta to infection with <i>Toxoplasma gondii</i> .
Editor of portion(s)	Robbins, Jennifer R; Zeldovich, Varvara B; Poukchanski, Anna; Boothroyd, John C; Bakardjiev, Anna I	Author of portion(s)	Robbins, Jennifer R; Zeldovich, Varvara B; Poukchanski, Anna; Boothroyd, John C; Bakardjiev, Anna I
Volume of serial or monograph	80	Issue, if republishing an article from a serial	1
Page or page range of portion	418-428	Publication date of portion	2011-12-31

RIGHTSHOLDER TERMS AND CONDITIONS

We ask that you review the copyright information associated with the article that you are interested in, as some articles in the ASM Journals are covered by creative commons licenses that would permit free reuse with attribution. Please note that ASM cannot grant permission to reuse figures or images that are credited to publications other than ASM journals. For images credited to non-ASM journal publications, you will need to obtain permission from the journal referenced in the figure or table legend or credit line before making any use of the image(s) or table(s). ASM is unable to grant permission to reuse supplemental material as copyright for the supplemental material remains with the author. This journal title may publish some Open Access articles, which provide specific user rights for reuse. Please refer to the article copyright line to determine whether the content you wish to use is Open Access. For Open Access content, permission to reuse is granted subject to the terms of the License under which the work was published. Please check the License conditions for the work which you wish to reuse. Full and appropriate attribution must be given. This permission does not cover any third party copyrighted material which may appear in the work requested. Please contact the publisher with any questions.

CCC Terms and Conditions

1. Description of Service; Defined Terms. This Republication License enables the User to obtain licenses for republication of one or more copyrighted works as described in detail on the relevant Order Confirmation (the "Work(s)"). Copyright Clearance Center, Inc. ("CCC") grants licenses through the Service on behalf of the rightsholder identified on the Order Confirmation (the "Rightsholder"). "Republishing", as used herein, generally means the inclusion of a Work, in whole or in part, in a new work or works, also as described on the Order Confirmation. "User", as used herein, means the person or entity making such republication.
2. The terms set forth in the relevant Order Confirmation, and any terms set by the Rightsholder with respect to a particular Work, govern the terms of use of Works in connection with the Service. By using the Service, the person transacting for a republication license on behalf of the User represents and warrants that he/she/it (a) has been duly authorized by the User to accept, and hereby does accept, all such terms and conditions on behalf of User, and (b) shall inform User of all such terms and conditions. In the event such person is a "freelancer" or other third party independent of User and CCC, such party shall be deemed jointly a "User" for purposes of these terms and

<https://marketplace.copyright.com/ip-ai-web/mp/license/535928c-29ba-4c43-a7ec-566177d48074/babb011-4d7a-4e15-a904-f6c9cc37d8b6/>

2/5

conditions. In any event, User shall be deemed to have accepted and agreed to all such terms and conditions if User republishes the Work in any fashion.

3. Scope of License; Limitations and Obligations.

- 3.1. All Works and all rights therein, including copyright rights, remain the sole and exclusive property of the Rightsholder. The license created by the exchange of an Order Confirmation (and/or any invoice) and payment by User of the full amount set forth on that document includes only those rights expressly set forth in the Order Confirmation and in these terms and conditions, and conveys no other rights in the Work(s) to User. All rights not expressly granted are hereby reserved.
- 3.2. General Payment Terms: You may pay by credit card or through an account with us payable at the end of the month. If you and we agree that you may establish a standing account with CCC, then the following terms apply: Remit Payment to: Copyright Clearance Center, 29118 Network Place, Chicago, IL 60673-1291. Payments Due: Invoices are payable upon their delivery to you (or upon our notice to you that they are available to you for downloading). After 30 days, outstanding amounts will be subject to a service charge of 1-1/2% per month or, if less, the maximum rate allowed by applicable law. Unless otherwise specifically set forth in the Order Confirmation or in a separate written agreement signed by CCC, invoices are due and payable on "net 30" terms. While User may exercise the rights licensed immediately upon issuance of the Order Confirmation, the license is automatically revoked and is null and void, as if it had never been issued, if complete payment for the license is not received on a timely basis either from User directly or through a payment agent, such as a credit card company.
- 3.3. Unless otherwise provided in the Order Confirmation, any grant of rights to User (i) is "one-time" (including the editions and product family specified in the license), (ii) is non-exclusive and non-transferable and (iii) is subject to any and all limitations and restrictions (such as, but not limited to, limitations on duration of use or circulation) included in the Order Confirmation or invoice and/or in these terms and conditions. Upon completion of the licensed use, User shall either secure a new permission for further use of the Work(s) or immediately cease any new use of the Work(s) and shall render inaccessible (such as by deleting or by removing or severing links or other locators) any further copies of the Work (except for copies printed on paper in accordance with this license and still in User's stock at the end of such period).
- 3.4. In the event that the material for which a republication license is sought includes third party materials (such as photographs, illustrations, graphs, inserts and similar materials) which are identified in such material as having been used by permission, User is responsible for identifying, and seeking separate licenses (under this Service or otherwise) for, any of such third party materials; without a separate license, such third party materials may not be used.
- 3.5. Use of proper copyright notice for a Work is required as a condition of any license granted under the Service. Unless otherwise provided in the Order Confirmation, a proper copyright notice will read substantially as follows: "Republished with permission of [Rightsholder's name], from [Work's title, author, volume, edition number and year of copyright]; permission conveyed through Copyright Clearance Center, Inc." Such notice must be provided in a reasonably legible font size and must be placed either immediately adjacent to the Work as used (for example, as part of a by-line or footnote but not as a separate electronic link) or in the place where substantially all other credits or notices for the new work containing the republished Work are located. Failure to include the required notice results in loss to the Rightsholder and CCC, and the User shall be liable to pay liquidated damages for each such failure equal to twice the use fee specified in the Order Confirmation, in addition to the use fee itself and any other fees and charges specified.
- 3.6. User may only make alterations to the Work if and as expressly set forth in the Order Confirmation. No Work may be used in any way that is defamatory, violates the rights of third parties (including such third parties' rights of copyright, privacy, publicity, or other tangible or intangible property), or is otherwise illegal, sexually explicit or obscene. In addition, User may not conjoin a Work with any other material that may result in damage to the reputation of the Rightsholder. User agrees to inform CCC if it becomes aware of any infringement of any rights in a Work and to cooperate with any reasonable request of CCC or the Rightsholder in connection therewith.

4. Indemnity. User hereby indemnifies and agrees to defend the Rightsholder and CCC, and their respective employees and directors, against all claims, liability, damages, costs and expenses, including legal fees and expenses, arising out of any use of a Work beyond the scope of the rights granted herein, or any use of a Work which has been altered in any unauthorized way by User, including claims of defamation or infringement of rights of copyright, publicity, privacy or other tangible or intangible property.
5. Limitation of Liability. UNDER NO CIRCUMSTANCES WILL CCC OR THE RIGHTSHOLDER BE LIABLE FOR ANY DIRECT, INDIRECT, CONSEQUENTIAL OR INCIDENTAL DAMAGES (INCLUDING WITHOUT LIMITATION DAMAGES FOR LOSS OF BUSINESS PROFITS OR INFORMATION, OR FOR BUSINESS INTERRUPTION) ARISING OUT OF THE USE OR INABILITY TO USE A WORK, EVEN IF ONE OF THEM HAS BEEN ADVISED OF THE POSSIBILITY OF SUCH DAMAGES. In any event, the total liability of the Rightsholder and CCC (including their respective employees and directors) shall not exceed the total amount actually paid by User for this license. User assumes full liability for the actions and omissions of its principals, employees, agents, affiliates, successors and assigns.
6. Limited Warranties. THE WORK(S) AND RIGHT(S) ARE PROVIDED "AS IS". CCC HAS THE RIGHT TO GRANT TO USER THE RIGHTS GRANTED IN THE ORDER CONFIRMATION DOCUMENT. CCC AND THE RIGHTSHOLDER DISCLAIM ALL OTHER WARRANTIES RELATING TO THE WORK(S) AND RIGHT(S), EITHER EXPRESS OR IMPLIED, INCLUDING WITHOUT LIMITATION IMPLIED WARRANTIES OF MERCHANTABILITY OR FITNESS FOR A PARTICULAR PURPOSE. ADDITIONAL RIGHTS MAY BE REQUIRED TO USE ILLUSTRATIONS, GRAPHS, PHOTOGRAPHS, ABSTRACTS, INSERTS OR OTHER PORTIONS OF THE WORK (AS OPPOSED TO THE ENTIRE WORK) IN A MANNER CONTEMPLATED BY USER; USER UNDERSTANDS AND AGREES THAT NEITHER CCC NOR THE RIGHTSHOLDER MAY HAVE SUCH ADDITIONAL RIGHTS TO GRANT.
7. Effect of Breach. Any failure by User to pay any amount when due, or any use by User of a Work beyond the scope of the license set forth in the Order Confirmation and/or these terms and conditions, shall be a material breach of the license created by the Order Confirmation and these terms and conditions. Any breach not cured within 30 days of written notice thereof shall result in immediate termination of such license without further notice. Any unauthorized (but licensable) use of a Work that is terminated immediately upon notice thereof may be liquidated by payment of the Rightsholder's ordinary license price therefor; any unauthorized (and unlicensable) use that is not terminated immediately for any reason (including, for example, because materials containing the Work cannot reasonably be recalled) will be subject to all remedies available at law or in equity, but in no event to a payment of less than three times the Rightsholder's ordinary license price for the most closely analogous licensable use plus Rightsholder's and/or CCC's costs and expenses incurred in collecting such payment.
8. Miscellaneous.
- 8.1. User acknowledges that CCC may, from time to time, make changes or additions to the Service or to these terms and conditions, and CCC reserves the right to send notice to the User by electronic mail or otherwise for the purposes of notifying User of such changes or additions; provided that any such changes or additions shall not apply to permissions already secured and paid for.
- 8.2. Use of User-related information collected through the Service is governed by CCC's privacy policy, available online here: <https://marketplace.copyright.com/rs-ai-web/mp/privacy-policy>
- 8.3. The licensing transaction described in the Order Confirmation is personal to User. Therefore, User may not assign or transfer to any other person (whether a natural person or an organization of any kind) the license created by the Order Confirmation and these terms and conditions or any rights granted hereunder; provided, however, that User may assign such license in its entirety on written notice to CCC in the event of a transfer of all or substantially all of User's rights in the new material which includes the Work(s) licensed under this Service.
- 8.4. No amendment or waiver of any terms is binding unless set forth in writing and signed by the parties. The Rightsholder and CCC hereby object to any terms contained in any writing prepared by the User or its principals, employees, agents or affiliates and purporting to govern or otherwise relate to the licensing

5/10/22, 10:18 PM

<https://marketplace.copyright.com/ip-ai-web/mp/license/535928c-29ba-4c43-a7ec-566177648074/babbca11-a07a-4e15-a904-f5c9cc37d88f>

transaction described in the Order Confirmation, which terms are in any way inconsistent with any terms set forth in the Order Confirmation and/or in these terms and conditions or CCC's standard operating procedures, whether such writing is prepared prior to, simultaneously with or subsequent to the Order Confirmation, and whether such writing appears on a copy of the Order Confirmation or in a separate instrument.

- 8.5. The licensing transaction described in the Order Confirmation document shall be governed by and construed under the law of the State of New York, USA, without regard to the principles thereof of conflicts of law. Any case, controversy, suit, action, or proceeding arising out of, in connection with, or related to such licensing transaction shall be brought, at CCC's sole discretion, in any federal or state court located in the County of New York, State of New York, USA, or in any federal or state court whose geographical jurisdiction covers the location of the Rightsholder set forth in the Order Confirmation. The parties expressly submit to the personal jurisdiction and venue of each such federal or state court. If you have any comments or questions about the Service or Copyright Clearance Center, please contact us at 978-750-8400 or send an e-mail to support@copyright.com.

v 1.1